MOLECULAR CHARACTERIZATION OF BOVINE ADENOVIRUS-3 IVA2 PROTEIN

A Thesis Submitted to the

College of Graduate and Postdoctoral Studies

in Partial Fulfillment of the Requirements for the

Degree of Doctor of Philosophy

in the

Department of Veterinary Microbiology

University of Saskatchewan

Saskatoon

By

Tekeleselassie Ayalew Woldemariam

PERMISSION TO USE

In presenting this thesis in partial fulfillment of the requirements for a postgraduate degree from the University of Saskatchewan, I agree that the libraries of this university may make it freely available for inspection. I further agree that permission for copying of this thesis in any manner, whole or in part, for scholarly purposes may be granted by the professors who supervised my thesis work or in their absence, the Head of the Department or the Dean of the college in which my thesis work was done. It is understood that any copying or publication or use of this thesis or parts thereof for financial gain shall not be allowed without any written permission. It is also understood that due recognition shall be given to me and to the University of Saskatchewan in any scholarly use which may be made of any material in my thesis.

Request for permission to copy or to make other use of material in this thesis in whole or part should be addressed to:

Head of the Department of Veterinary Microbiology

University of Saskatchewan,

Saskatoon, Saskatchewan, S7N 5B4

OR

Dean

College of Graduate and Postdoctoral Studies

University of Saskatchewan

116 Thorvaldson Building, 110 Science Place

Saskatoon, Saskatchewan S7N 5C9

Canada

ABSTRACT

Adenovirus is a naked icosahedral viral particle enclosing a double stranded DNA genome. Adenoviral genes are classified as early, intermediate and late based on their duration of expression. Adenoviruses encode two intermediate gene products, pIX and IVa2. Adenovirus IVa2 is one of the conserved proteins encoded by members of the family of *Adenoviridae*. Prior studies indicate that IVa2 localizes to the nucleus\nucleolus and, is involved in adenovirus genome packaging and activation of major late promoter (MLP) thus enhancing the expression of late adenoviral proteins. Moreover, IVa2 has been suggested to perform multiple functions by interacting with different viral proteins including 33K and DBP (DNA binding protein), 52K and pVIII.

Positional homologs encoded by members of *Mastadenovirus* genus are different in structure and function. Since Bovine adenovirus (BAdV) -3 IVa2 displays limited homology compared with homologs encoded by other members of *Mastadenovirus* genus, the present study was undertaken to characterize IVa2 of BAdV-3, to identify viral protein interacting with IVa2 and to determine the role of IVa2 in the virus life cycle.

As part of characterization, BAdV-IVa2, detected as a 50kDa protein in BAdV-3 infected cells (12-18 hrs post infection) and plasmid DNA transfected cells (48 hrs post transfection). Although IVa2 could be detected both in the nucleus and nucleolus of virus infected or DNA transfected cells, IVa2 appeared predominantly located in the nucleolus. Analysis of IVa2 by cNLS mapper program predicted the nuclear localization signals (NLSs) of IVa2 interacting with importin. Analysis of mutant IVa2 suggested that N- terminus amino acids 4-18 appear essential for the nuclear localization of IVa2. Several lines of evidence suggest that IVa2 N-terminus amino acids 1-25 appear to contain functional NLS. First, IVa2 N-terminus amino acids 4-18 are

not sufficient to translocate a cytoplasmic fusion protein GFP/β gal to the nucleus of transfected cells. Secondly, GST pull-down assay suggested that amino acid 4-18 does not bind to importin α-1. Thirdly, N-terminus 25 amino acids bind to importin α-1 and translocate GFP/β gal to the nucleus of the transfected cells. Analysis of mutant IVa2 proteins also suggested that C-terminal amino acids 373-448 appear essential for the nucleolar localization of IVa2 in transfected cells. While amino acids 373-448 appear to contain multiple nucleolar localization signals (NoLSs), the NLS and NoLS of IVa2 does not appear to be overlapping.

The identified nuclear localization signal of IVa2 contains clusters of basic amino acids, (^{6}RRK^{8}), similar to that of classical nuclear localization signal. The substitution of arginine or lysine residues to glycine did not alter the nuclear localization of IVa2 in DNA transfected cells or mutant BAdV-3 infected cells indicating that ^{6}RRK$^{8)}$ residues are not essential for nuclear localization of BAdV-3 IVa2.

To identify the viral proteins interacting with IVa2, initially we attempted to use affinity tag purification method. However, repeated attempts to isolate recombinant BAdV-3 expressing IVa2 containing Step Tag were not successful. Instead, using Bi molecular Fluorescence Complementation (BiFC) assay, we identified several viral proteins including pV that interact with IVa2. Mass spectrometry also indicated that pV interacts with IVa2. Finally, the interaction of IVa2 with pV was confirmed by co-immunoprecipitation (Co-IP) assay in DNA transfected and BAdV-3 infected cells. Further analysis identified IVa2 amino acids 121-140 as the domain involved in the interaction with pV.

Several lines of evidences suggest that IVa2 protein is sensitive to any addition \deletion. To assess the role of IVa2 in the virus life cycle, we attempted to isolate IVa2 deleted BAdV-3 in non-IVa2 complementing cells. First, transfection of cells with full-length BAdV-3 genomic

clone containing deletion of IVa2 region overlapping polymerase region did not result in the isolation of viable virus. Second, transfection of cells with full-length BAdV-3 genomic clone containing addition of Cre recombinase recognition loxP sequence in-frame to IVa2 coding sequence did not result in the rescue of viable virus. Third, transfection of cells with individual full length BAdV-3 genomic clone containing insertion of Strep tag at amino acids 146,242 or 448 did not result in the isolation of viable virus. However, transient expression of BAdV-3 IVa2 complemented the defect of IVa2 in BAV304a.dIVa2 in cotton rat lung (CRL) cells suggesting that IVa2 is essential for replication of BAdV-3.

ACKNOWLEDGEMENTS

In the first place, I would like to express my heartfelt appreciation to my supervisor Dr. Suresh Kumar Tikoo. From the day accepting me to work in his lab till the present time, I have been receiving his inspirational mentorship and unreserved all-rounded support.

I also like to extend my acknowledgment to members of my advisory committee Dr. Janet Hill (Head of the Department of Veterinary Microbiology and graduate chair), Dr. Joyce Wilson, Dr. Yan Zhou and Dr. Alexander Zakhartchouk for their continuous encouragements, comments and suggestions during my study period.

I am also indebted to the staff of VIDO-InterVac, as well as Department of Veterinary microbiology for the follow-up, technical and administrative support.

My special thanks also go to Dr. Lisanework Eshetu, Dr. Amit Gaba and Dr. Abdelrahman Said for the recommendation, suggestions, and help.

I am also grateful to the present and past members of Dr. Tikoo's lab: Shermila, Vinoth, Maria, Niraj, Mingjie, Zhao, Jeeva, Sugandhika, Vani, Pankaj, Azhar, Kyle, Andrea, Wenxiu, Chenyi, Fang, Vani, and Sanjeev for valuable suggestions and discussions.

My sincere gratitude also goes to my Mom, Abozen and Dad, Ayalew as well as my brothers and sisters for the continuous encouragement and support.

Finally, I wish to express my deepest gratitude to my wife Meseret for your love, support and patience and as well as my lovely boys Nathnaiel and Surafel for providing me the joy and laughter in life.

TABLE OF CONTENTS

LIST OF TABLES

LIST OF FIGURES

ABBREVIATIONS USED IN THIS WORK

Ad	Adenovirus
Ad-pol	Adenovirus polymerase
ADP	Adenovirus death protein
Arf	Alternative reading frame
BAdV-3	Bovine adenovirus -3
BAK	BCL2-antagonist/killer
BAX	Bcl-2-associated X protein
Bcl-2	B-cell lymphoma 2
BiFC	Bi molecular fluorescence complementation assay
Bop1	Block of Proliferation 1
BoPSAP/BoMtch1	Bovine presenilin-1-associated protein/mitochondrial carrier
CAR	Coxcakie adenovirus receptor
CBP	CREB binding protein
CD	Cluster of differentiation
cNLS	Classical nuclear localization signal
Co-IP	Co-immunoprecipitation
CPE	Cytopathic effect
CRL	Cotton rat lung
CsCl	Cesium chloride
CTBP1	C-Terminal Binding Protein 1
DAPI	4', 6-diamidino-2-phenylindole
DBP	DNA binding protein

DCAF7	DDB1- and CUL4-associated factor 7
dCMP	Deoxycytidine monophosphate
DDR	DNA damage response
DDX3	Dead box family of RNA helicases 3
DFC	Dense fibrillar centered granular center
DMEM	Dulbecco's minimal essential medium
DYNLT1	Dynein light chain 1
DYRIKA	Dual-specificity tyrosine (Y)-phosphorylation regulated kinase A
E	Early
eIF4G	Eukaryotic translation initiation factor 4 G
eIF6	Eukaryotic initiation factor 6
ERK	Extracellular signal-regulated kinases
ET	Electron tomography
E2F1	E2F Transcription Factor 1
FBS	Fetal bovine serum
FBW7	F-box and WD repeat domain-containing 7
FC	Fibrillar center
FG	Phenylalanine-glycine
FOXK1	Forkhead box protein K
FUBP1	Far upstream element-binding protein 1
GADD	Growth arrest and DNA damage-inducible protein
GC	Granular center
GFP/β gal	Green fluorescent /beta-galactosidase

GST	Glutathione s-transferase
HAdV	Human adenovirus
HDM2	Human double minute 2
HIPK2	Homeodomain interacting protein kinase 2
ITR	Inverted terminal repeats
ITSs	Internal transcribed spacers
Kbps	Kilo base pairs
kDa	Kilo Dalton
L	Late
LC-MS/MS	Liquid chromatography mass spectroscopy
LDV	Leucine -aspartic acid-valine
MDV	Methionine-aspartic acid -valine
MDBK	Madin Darby bovine kidney
MDM2	Mouse double minute 2 homolog
MED23	Mediator of RNA polymerase II transcription subunit 23
MEM	Minimal essential medium
MLP	Major late promoter
MLTU	Major late transcription unit
MOI	Multiplicity of infection
mRNA	Messenger RNA
NEAA	Nonessential amino acids
NFBP	NF-kB-binding protein
NFBP	NFB-binding protein

NFI	Nuclear factor I
NLSs	Nuclear localization signal
NoLSs	Nucleolar localization signal
NPC	Nuclear pore complex
NTF2	Nuclear transport factor 2
NUP	Nucleoporin
Oct1	Octamer-binding protein 1
ORFs	Open reading frames
PABP	Poly (A)-binding protein
PCAF	p300/CBP-associated factor
PEG-LiAc	Polyethylene glycol –Lithium acetate
PC	Phase contrast
PKA	protein kinase A
PML	Promyelocytic leukemia
Pol	Polymerase
pRB	Retinoblastoma protein
pre-rRNA	Precursor ribosomal RNA
pTP	Pre terminal protein
pV	Protein V
rDNA	Ribosomal DNA
RGD	Arginine-glycine-aspartic acid
RP	Ribosomal protein
RPA	Replication protein A

rRNA	Ribosomal RNA
SCF	Skp, Cullin, F-box
SDS-PAGE	Sodium dodecyl sulphate polyacrylamide gels
SP1	Specificity protein 1
SPOC1	Survival-time associated PHD protein in ovarian cancer 1
TNF	Tumor necrosis factor
TP	Terminal protein
TPL	Tripartite leader
WSAdV-1	White sturgeon AdV-1
YPDA	Yeast peptone dextrose adenine broth
βTrCP	β-transducing repeat-containing protein

1.0 LITERATURE REVIEW

The literature review comprises four sections: adenovirus, nuclear pore complex and nucleoporins, nuclear import of protein, and nucleolus and its functions. The adenovirus section describes the classification of adenoviruses, structure of adenovirus virion as well as adenovirus life cycle using well-studied adenovirus type A2 and adenovirus type C of the human adenoviruses. This section also deals with further classification and genome organization of human as well as bovine adenoviruses. Function/functional interaction of human, as well as bovine adenoviral proteins, also summarized. In the nuclear pore complex and nucleoporins section, the role of the nuclear pore complex and organization of nucleoporins described in detail. The section that talks about the nuclear import of protein discuss the mechanism of nuclear import of protein across the nuclear pore complex. The last part describes the nucleolus and its functions, the nucleolus structure and function; in particular, the role of nucleolus in ribosome biogenesis is discussed.

1.1. Introduction to adenovirus

Adenoviruses are medium-sized, naked icosahedral viruses with a double-strand DNA genome (Harrach, 2014). They acquired their name from the original tissue (adenoid) where the virus was isolated (Enders et al., 1956; Hilleman and Werner, 1954; Rowe et al., 1953). Adenoviruses are mostly isolated from different animals and humans with ailments such as respiratory infection, conjunctivitis, or encephalitis. Except in fowl (Schachner et al., 2018) and deer (Woods et al., 2014), adenoviruses do not lead to severe disease outcomes in most of the farm animals (Maclachlan et al., 2017). However, in humans specifically, in young and immunocompromised individuals, adenoviruses are important disease-causing agents (Lion,

2014). Though not observed in humans, adenoviruses are also known to induce malignancies in different animal models (Hohlweg et al., 2004; Javier, 1994). Compared to its role as a disease-causing agent, adenoviruses are known for being a model organism in molecular virology as well as viral vectors (Greber et al., 2013). For the last two decades, adenovirus has been serving as a viral vector platform for vaccination as well as gene therapy (Alonso-Padilla et al., 2016; Singh et al., 2019; Wold and Toth, 2013; Zhang and Zhou, 2016).

1.1.1 Classification of Adenoviruses

The family of *Adenoviridae* comprises more than 100 adenovirus serotypes (Greber et al., 2013). They are classified based on host origin and constitution of the DNA under the genus *Mastadenovirus, Atadenovirus, Aviadenovirus, Siadenovirus, Ichtadenovirus*, and the recently proposed genus *Testadenovirus* (Davison et al., 2003; Harrach, 2014; Harrach et al., 2012).

The genus *Mastadenovirus* is the largest genus of the family of *Adenoviridae,* known to include 1/3 of the adenovirus species infecting only mammals (Harrach et al., 2012). Their genome size ranges between 30.5-37.8 Kbps with GC content that varies from 43.6 to 63.9%. The genus also characterized by having complex inverted terminal repeats that range from 93 to 371bp. In addition, viral protein V, IX, and most of the proteins encoded by early viral mRNA (E1A, E1B, E3, and E4) are unique to the genus (Harrach, 2014).

Members of *Aviadenovirus* genus only infect birds and are cause diseases in birds, including hydro-pericardium syndrome, inclusion body hepatitis, edema, pulmonary congestion, and gizzard erosion (Grgic, et al., 2014; Harrach, 2014). They possess a large genome size (25-40% greater) than members of the *Mastadenovirus* genus (Harrach et al.,

2012). Despite a bigger genome size, the ITR region is relatively shorter than the members of *Mastadenovirus.* Moreover, genes encoding protein V and IX, as well as those encoded by E1 and E3 region of *Mastadenovirus*, are absent in members of the *Aviadenovirus* genus (Harrach et al., 2012). Except for some members of the Aviadenovirus genus (Grgic, et al., 2011), most of the members of *Aviadenovirus* contain two fibers that extend from the penton base (Chiocca et al., 1996; Griffin and Nagy, 2011; Kajan et al., 2012; Kajan et al., 2010; Marek et al., 2012).

Members of the *Atadenovirus* genus include adenoviruses isolated from a wider host range, including reptiles, birds, ruminants, and marsupials (Berk, 2013; Davison et al., 2003). The genome size of adenovirus in the *Atadenovirus* genus ranges from 29.5 to 33.2 kbps with relatively low GC content and high AT content (Harrach et al., 2012). Unlike members of *Mastadenovirus*, protein V and IX are absent in members of this genus (Davison et al., 2003; Gorman et al., 2005). Moreover, there is a marked difference regarding the right and left extremities of the genome between members of Atadenovirus and *Mastadenovirus* (Both, 2011; Harrach, 2014). Among the unique genes, p32K (Elo et al., 2003) and LH3 (Gorman et al., 2005) are conserved at the genus level and serve as viral structural components. Due to some similarities in their sequence, it has been assumed that LH3 as a homolog of *Mastadenovirus* E1B 55K protein. However, they are functionally distinct as E2B 55K serve as an anti-apoptotic protein in infected cells (Gorman et al., 2005).

Members of the *Siadenovirus* genus comprise adenovirus isolated from amphibians and birds (Harrach et al., 2012). The genus acquires its name in relation to a unique protein sialidase encoded by the members of the genus (Davison et al., 2003). Some members of the genus are characterized by having the shortest genome size (26.1 to 26.2kbps). The members of this genus also contain short ITRs (29-39bps) (Harrach et al., 2012; Kovacs and Benko, 2009).

While members of *Siadenovirus* encode five proteins that are unique (Harrach et al., 2012), the homologs of proteins V and IX and proteins encoded by E1, E3, and E4 regions of members of the Mastadenovirus are absent (Harrach et al., 2012). Only a single adenovirus isolate, white sturgeon AdV-1 (WSAdV-1), belongs to this genus (Benko et al., 2002). WSAdV-1 possesses the adenoviral genome of 48,395bp (Harrach, 2014). Although there is a similarity with members of non-Mastadenovirus genus regarding the organization of the middle part of the genome, there is a marked difference in terms of hexon and protease sequences (Kovacs et al., 2003). In addition, the right part of the genome of WSAdV-1 encodes multiple novel genes (Harrach, 2014). Adenovirus infection in different chelonians (Turtles and Tortoise) species has been reported (Doszpoly et al., 2013; Farkas & Gal, 2009; Rivera et al., 2009; Schumacher et al., 2012). Though isolation of adenovirus from the various chelonians was not successful, partial sequence analysis using hexon as well as viral DNA polymerase genes indicate that the putative adenovirus is distinct genetically from the five officially accepted genera of *Adenoviridae* (Doszpoly et al., 2013). As a result, a sixth genus" Testadenovirus" is proposed for the novel adenovirus of chelonians in the superfamily *Testudinoidea* (Doszpoly et al., 2013; Harrach, 2014).

1.1.2 Structure of adenoviral virion (viral particle)

Structurally, adenoviral particle is composed of an outer capsid and inner core structure (Fig 1.1). The capsid structure besides protecting the viral genome interacts with the host cell structure to deliver the viral genome (Roos et al., 2007). Composition wise, the adenoviral capsid is consists of major and minor proteins. The major proteins include hexon, penton base and fiber (Liu et al., 2010; Russell, 2009).

While 240 trimeric hexon organized to form the surface of the icosahedron, pentameric penton base (capsomeres) held to occupy the vertices of the icosahedron, with a protruding fiber at each vertex of the icosahedron (Berk, 2013).

Minor adenoviral capsid protein includes proteins IIIa, VI, VIII, and IX. Although minor capsid proteins serve as cement to strengthen the capsid structure, some are involved in linking the core structure to the capsid and also play a role in viral entry (Flatt and Butcher, 2019; Reddy and Nemerow, 2014; Vellinga et al., 2005).

The core of adenovirus consists of linear double-stranded DNA (genome) and associated proteins, including protein VII, V, X, Mu terminal protein (TP), and viral protease (San Martin, 2012). Most of the core proteins are composed of basic amino acids that enable them to interact and condense the viral genome (Perez-Berna et al., 2015). Besides, some core proteins link the core to the capsid components (structure) (Liu et al., 2010). Moreover, core protein, such as TP, is involved in the replication of the viral genome (de Jong et al., 2003).

1.1.3 Adenovirus life cycle

The adenovirus life cycle is a coordinated process that involves both viral and cellular components (Pied and Wodrich, 2019). The host cell nucleus is the site of adenovirus replication or major events in the virus life cycle, including gene expression, viral DNA replication, assembly, packaging, and maturation (Pied and Wodrich, 2019). As a result, adenoviral particle undergoes pre-nuclear steps, including attachment and entry, uncoating, and transport to the host cell nucleus (Cassany et al., 2015; Flatt and Butcher, 2019; Greber and Flatt, 2019).

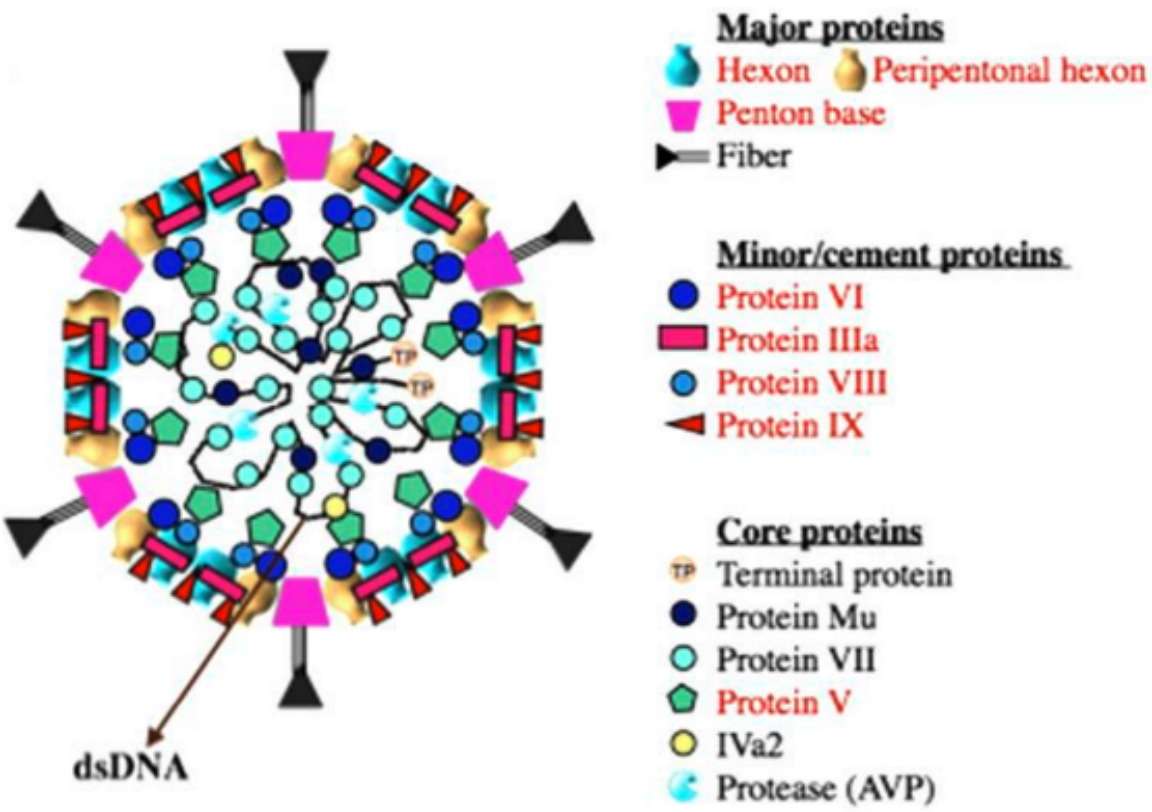

Fig. 1.1 A schematic illustration of human adenoviral particle showing capsid and core structural components. Re printed from Reddy and Numerow, 2014. Proc Natl Acad Sci, 111(32): 11715-20 (Publisher PNAS)

1.1.3.1 Attachment and entry

Adenovirus life cycle (Fig. 1.2) starts with the entry of the virus into the target cell, which is initiated by the primary attachment of fiber to the cell surface receptor. Coxcakie adenovirus receptor (CAR) is used as a primary receptor by most adenovirus spices except group D adenoviruses (Bergelson et al., 1997; Roelvink et al., 1998). In addition to CAR, different human adenoviruses use receptors such as desmoglein (Wang et al., 2011), heparin sulfate (Dechecchi et al., 2001), CD 46 (Gaggar et al., 2003; Marttila et al., 2005), sialic acid (Arnberg et al., 2000; Lenman et al., 2018). Following primary attachment, virus entry commences by the secondary interaction of the RGD motif of adenovirus penton base with cellular integrin receptors (Wolfrum and Greber, 2013). Integrin penton base interaction results in the release of fiber and also initiates a signalling cascade that ends up in uptake of virus particle via clathrin-mediated endocytosis (Meier and Greber, 2004). Uptake of adenoviruses also involves alternatively via micropinocytosis (Meier et al., 2002).

Adenoviral particle escapes from the endosomal compartment using membrane lytic protein pVI (Wiethoff et al., 2005). Also, a signalling cascade initiated at the time of attachment helps the process of viral escape via inducing a membrane drift (Burckhardt et al., 2011; Wolfrum and Greber, 2013). Prior reports indicates that exposure of adenoviral particle to low pH induces a conformation change in the adenoviral particle that leads to destabilization of the endosomal membrane (Greber et al., 1993). However, recent studies indicate that endosomal membrane penetration is pH independent (Suomalainen et al., 2013).

After the endosomal escape, partially uncoated capsid (capsid without fiber, penton base and VI) joins the cytoplasm where hexon mediated interaction with microtubule dynein motor directs the movement of partially uncoated capsid to the nucleus (Bremner et al., 2009; Leopold

et al., 2000). Final capsids disassembly occurs at the nuclear pore complex (NPC) where partially disassembled capsids dock at the NPC through the interaction of hexon with NUP 214 of the NPC (Cassany et al., 2015).

Further disassembly of the viral capsid is achieved via the coordinated interaction involving kinesin light and heavy chains with pIX of docked adenovirus and nup358, respectively (Strunze et al., 2011).

After the process of uncoating, pVII of the viral protein, which strongly associates and condenses the viral genome mediate interaction with soluble receptors to use the nuclear import machinery and deliver the viral genome to the nucleus (Wodrich et al., 2006). In addition to facilitating the entrance of adenoviral genome via NPC by dismantling the viral capsid structure, interaction or docking the partially disassembled capsid is associated with displacement of nup214, nup62 and nup358 resulting in a transient increase in permeability of the NPC and translocation of the viral genome (Strunze et al., 2011; Strunze et al., 2005).

1.1.3.2 Human adenovirus genome organization

Human adenoviruses belong to the genus Mastadenovirus (Harrach, 2014). Like other adenoviruses, human adenoviruses contain a single linear double-stranded genome that ranges in size from 26–46 kbps (Ghebremedhin, 2014). The viral genome organized as early, intermediate, and late transcription units based on their duration of expression (Berk, 2013) (Fig 1.3).

1.1.3.2. 1 Early gene expression

The early (E) regions include E1-E4 (E1A, E1B, E2, E3, and E4) (Berk, 2013).

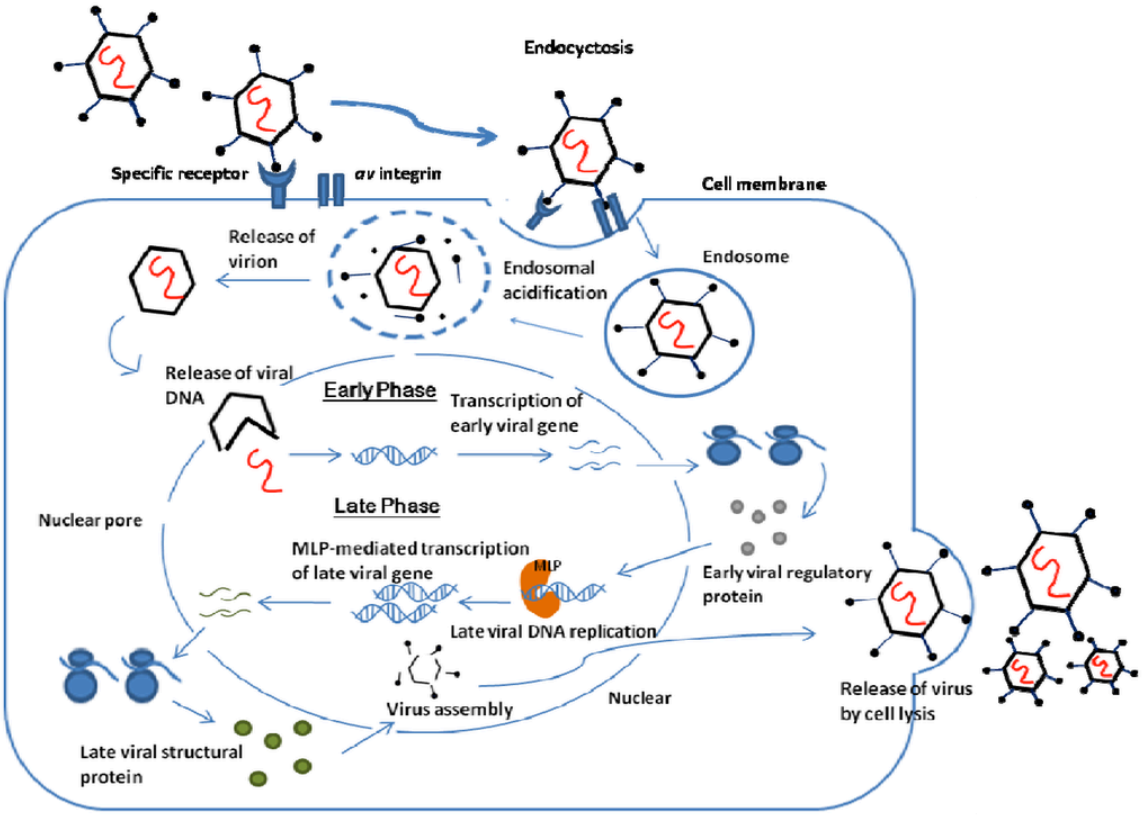

Fig. 1.2 Schematic illustration of human adenovirus life cycle. Re printed from Waye and Sing, 2010, Pharmaceuticals (Basel). 2010 Oct; 3(10): 3343–3354 (2 (Publisher MDPI).

After the localization of the viral genome to the nucleus, the first gene to be transcribed is E1A. As a result, it is also called an immediate early gene (Zhao et al., 2014). Initial E1A pre-mRNA transcript, produces several mRNA transcripts including 13S, 12S, 11S, and 9S via alternate splicing that has the potential to encode proteins of 289, 243, 217, 117, and 55 residues, respectively (Stephens and Harlow, 1987; Ulfendahl et al., 1987).

While the 13S and 12S mRNA transcripts are abundant during early times, the rest of the mRNA transcript predominates at a later time (Zhao et al., 2014). Most of the function of E1A is attributed to 13S and 12S translation products, while the rest of the transcripts play a minor role and are dispensable for lytic infection (Radko et al., 2015). E1A involves several protein-protein interactions that play a role in the transcriptional activation of other viral gene products, protection of infected cells from host antiviral response, control of cell cycle, and apoptosis (King et al., 2018b) (Table 1.1). Adenoviral E1B encodes E155K and E1 19K proteins, both of which prevent cellular apoptosis. Besides, E1B 55K undergoes a variety of protein-protein interactions with viral as well as cellular proteins (Hung and Flint, 2017) intending to protect infected cells from antiviral mechanisms launched by the host (Table 1.2).

Adenovirus E2 region produces mRNAs that encode DNA binding protein (DBP), precursor terminal protein (pTP), and adenovirus polymerase (Ad-pol), which are involved in viral DNA replication (de Jong et al., 2003) (Table 1.3).

Adenovirus E3 region of human adenovirus produces seven mRNA transcripts from its precursor mRNA (Wold et al., 1995; Zhao et al., 2014) the translation products of which play a

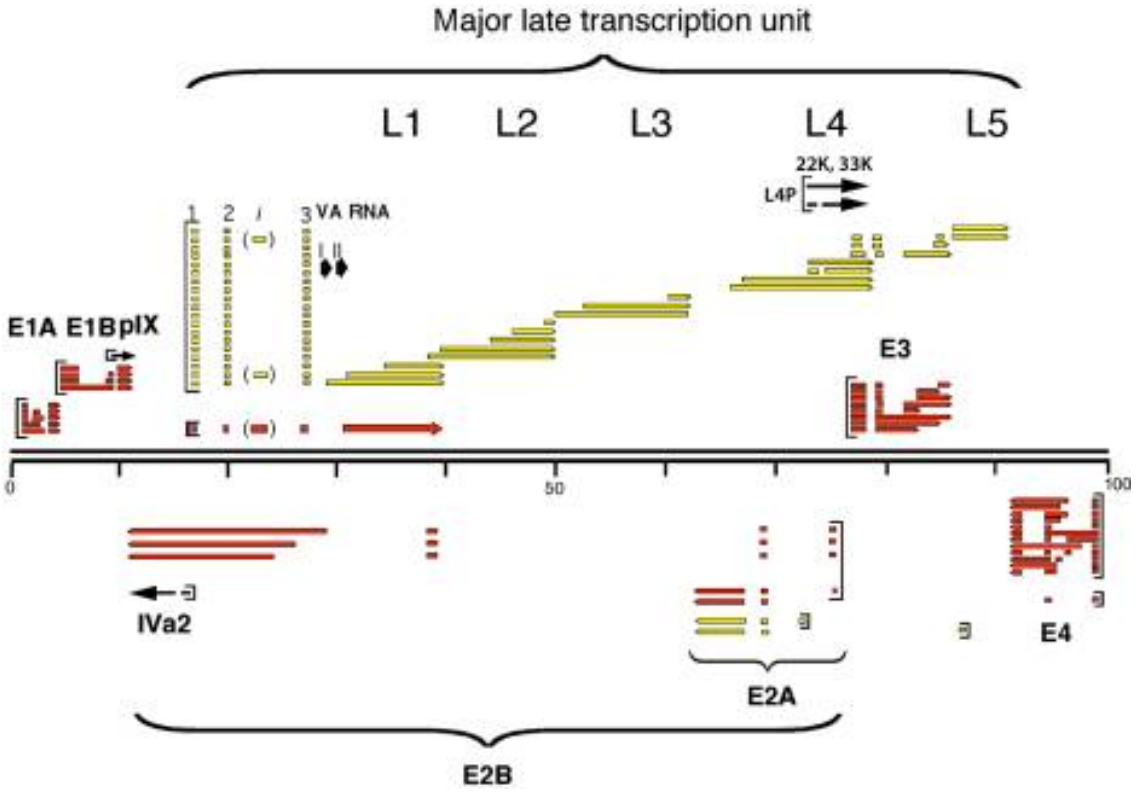

Fig. 1.3 Schematic diagram of the Ad5 transcription map. Transcripts shown in red and yellow color represent early and late transcripts respectively. Re printed from Biasiotto and Akusjarvi, 2015. Int J Mol Sci.; 16(2): 2893–2912 (Publisher MDPI).

Table 1.1 Role of adenovirus E1A in the virus life cycle

Function /Functional interaction of Adenovirus E1A	Reference
E1A locates to nucleus by interacting with cellular soluble transport receptors using its classical or non-consensus nuclear localization signal(s)	(Cohen et al., 2014; Marshall et al., 2014)
E1A interacts with an adaptor protein DECAF 7 and manipulate localization and activity of cellular kinases DYRIKA, DYRIKB and HIPK2 involved in cellular transformation, proliferation or transcription.	(Glenewinkel et al., 2016; Miyata and Nishida, 2011; Ritterhoff et al., 2010)
E1A interacts with PKA; sequester PKA to the nucleus and favor viral replication cycle.	(Fax et al., 2001; King et al., 2016; King et al., 2018; Taylor et al., 2013)
E1A bind competitively with cellular transcriptional co-repressors CtBP1 and CtBP2 to relieve host gene transcription involved in cell growth and apoptosis.	(Chinnadurai, 2009; Subramanian et al., 2013)
E1A interact with MED23 or pfa1 in elongation of adenovirus transcripts. In addition, E1A recruiting other components of super elongation complexes elongate adenovirus transcripts.	(Fonseca et al., 2014; Fonseca et al., 2013; Vijayalingam and Chinnadurai, 2013)
E1A via association with FOXK1/2, DCAF7 and CtBP suppress activation of interferon-stimulated genes.	(Zemke and Berk, 2017)
E1A p300/CBP, PCAF, Bre1, GCN5, p400 and BS69 control transcription from specific loci that stimulate cell cycle or interfere with host defense mechanism.	(Ablack et al., 2012; Fonseca et al., 2013; Lang and Hearing, 2003; Pelka et al., 2009; Zhang et al., 2018; Zhao et al., 2017)
E1A interact with UBC9 and interfere its SUMOylation role affecting the reorganization of nuclear PML bodies.	(Yousef et al., 2010)
E1A interacts with pRB and prevents its SUMOylation counteracting its role in cell cycle control.	(Ledl et al., 2005)
E1Ainteracts an antiviral DREF and delocalize it away from adenoviral replication center.	(Radko et al., 2014)
E1A interact with BS69 and prevent degradation of E1A.	(Isobe et al., 2006)
E1A interact with a tumor suppressor protein and Fbw7, and increase the stability of Fbw7 recognized cellular targets involved in cellular proliferation.	(Isobe et al., 2009)
E1A through up regulation of ubiquitin ligase SCF (β-TrCP), enhance the degradation of tumor suppressor protein RESET thereby enhancing cell proliferation.	(Guan and Ricciardi, 2012)
E1A bound with pRB enhance cellular proliferation. E1A interact with DP-1 recruit E2F/DP-1 complex to E2F-regulated promoters and activate cell cycle gene.	(Bayley and Mymryk, 1994; Pelka et al., 2011)
E1A interacts with Nek9 and down regulate expression of GADD45A involved in cell cycle arrest.	(Jung et al., 2016; Pelka et al., 2007)
E1A interact with FUBP1 and prevent p53 mediated antiviral response.	(Frost et al., 2018)

role in the protection of infected cells from the host defense mechanism (Horwitz, 2004; Lichtenstein et al., 2004) (Table 1.4).

Adenovirus E4 region undergoes complex splicing process that encodes products with multiple functions, including RNA splicing, nucleo-cytoplasmic transport, and translation of mRNA as well as transcriptional activation (Berk, 2013).

Generally, early gene products create a favorable environment for viral replication via activation of viral genes, inducing host cell to synthesis phase to supply necessary input for viral replication, mediating viral replication, blocking apoptosis, and counteracting host antiviral defense mechanism (Table 1.1- 1.4).

1.1.3.2. 2 Replication of the adenoviral genome

Once early gene products create a favorable environment, the process of viral replication commences (Radko et al., 2015). Both cellular and viral proteins take part in the process of replication. Cellular proteins NFI and OctI via binding of TP and viral polymerase respectively, recruit the TP–polymerase heterodimer to the origin of replication and by doing so increase the replication by 200 fold (de Jong et al., 2003; Hoeben and Uil, 2013; Mysiak et al., 2004). E2A product DNA binding protein (DBP) also plays a role in the attachment of TP-Pol to the replication origin via manipulating the double-strand DNA (de Jong et al., 2003).

The process of viral DNA replication initiated with the formation of a covalent linkage between hydroxyl groups of pTP to the terminal dCMP of the GAGA template of the viral DNA catalyzed by viral polymerase (Hoeben and Uil, 2013). After initiation of replication, pTP-trinucleotide (pTP-CAT) jumps back to base-pair with a template base.

Table 1.2. Role of adenovirus E1B in the virus life cycle

Protein	Function/Functional interactions	Reference
E1B 55K	Through direct binding with p53, as well as disruption of p53 interaction with cellular factors involved in its acetylation and activation, E1B 55K inhibit p53-induced transcription of apoptotic factors.	(Blackford and Grand, 2009)
	Through its involvement in the porteasomal degradation of proapoptotic cellular factor Daxx, E1B 55K inhibit the transcription factors that act as cell cycle checkpoints.	(Schreiner et al., 2010; Wimmer et al., 2012)
	Undergoes SUMOylation via SUMO E1 and its SUMOylation thought to be essential for its anti apoptotic functions that involve various approaches.	(Wimmer et al., 2012)
E1B 19K	Inhibit apoptosis through TNF-α and Fas ligand pathways by influencing downstream mediators BAX and BAK.	(Debbas and White, 1993; Sundararajan et al., 2001)
	In a similar fashion with cellular anti apoptotic BCL2, it bind and inactivate proapoptotic proteins BAX and BAK.	(Cuconati et al., 2002; White, 2006)

Table 1.3. Role of adenovirus E2 in the virus life cycle

Protein	Function/Functional interaction	
E2 DBP	Helps in the formation of initiation through assisting the binding of cellular NFI to the origin of replication.	(de Jong et al., 2003; Hoeben and Uil, 2013)
	Helps to protect the viral polymerase from nucleases.	(Hoeben and Uil, 2013)
	It has a role in unwinding double strand of viral DNA and during elongation step of viral replication.	(de Jong et al., 2003; Dekker et al., 1997)
E2 pTP	Interacts with viral polymerase and involve in the formation of initiation complex and serve as a primer for viral DNA replication. It also interacts with cellular protein Oct-1 for its recruitment to the origin of replication.	(de Jong et al., 2003) Mysiak et al.,2004,van Breukelen et al., 2003
E2 Ad-pol	Initiate Viral DNA replication via coupling dCTP to pTP. It also interacts cellular NFI for its recruitment to the origin of replication.	(de Jong et al., 2003)

Table 1.4. Role of adenovirus intermediate region in the virus life cycle

Protein	Function/functional interaction	Reference
IVa2	IVa2 binds with packaging domain of viral DNA and involves in packaging viral genome.	(Ostapchuk et al., 2005; Perez-Romero et al., 2005; Tyler et al., 2007; Zhang and Imperiale, 2000)
	IVa2 possesses a conserved ATPase motif; bind with ATP and occupy a single vertex of icosahedron. Mutation in its ATPase motif known to interfere with packaging of viral genome.	(Ahi et al., 2013; Christensen et al., 2008; Ostapchuk et al., 2011; Ostapchuk and Hearing, 2008)
	IVa2 interacts with 33K and DBP. Interaction of IVa2 with 33K shown to activate its ATPase activity suggesting that IVa2 might serve as a motor protein for stuffing of viral DNA.	(Ahi et al., 2015; Ahi et al., 2013)
	Adenovirus IVa2 interacts with L1 52/55 kDa protein and may play role in recruiting 52/55 kDa to the viral DNA packaging domain.	(Gustin et al., 1996; Wu et al., 2012)
	IVa2 acts as a trans-acting factor to activate the major late promoter (MLP) via binding downstream region of MLP.	(Lutz and Kedinger, 1996)
pIX	Involve in stabilization of capsid via cementing groups of hexon.	(Furcinitti et al., 1989; Reddy and Nemerow, 2014; Rosa-Calatrava et al., 2001)
	It also acts as a transcriptional activator of TATA containing viral promoters.	(Lutz et al., 1997; Rosa-Calatrava et al., 2001)
	Through sequestration of antiviral PML pIX involve in efficient replication of adenovirus.	(Rosa-Calatrava et al., 2003)

While pTP dissociates from the complex, the viral polymerase undertakes the elongation step (Hoeben and Uil, 2013). Through its involvement in unwinding the double helix structure, DBP assists the process of elongation. Besides, DBP plays a role in the stabilization of single-strand DNA via binding and protecting it from degradation (de Jong et al., 2003). A cellular protein named topoisomerase also known to play a role in the production of genome length products (de Jong et al., 2003).

1.1.3.2. 3 Expression of late genes

Late (L) adenoviral gene expression is detected mostly after the onset of viral DNA replication (Zhao et al., 2014). The late gene of adenovirus isexpressed from the MLP that produces a single transcriptional unit called MLTU (Akusjarvi, 2008). The primary transcript undergoes differential polyadenylation providing five different mRNA transcripts with similar 3' ends (Akusjarvi, 2008; Biasiotto and Akusjarvi, 2015). Each of mRNAs (L1-L5) undergoes differential splicing producing at least 20 mRNA (Zhao et al., 2014). Each of the late mRNA transcripts acquires a non-coding region called tripartite leader sequence (TPL), which is known to enhance translation of the late mRNA products. The role of late adenoviral proteins summarized in Table 1.5.

1.1.3.2. 4. Genome encapsidation

Following viral DNA replication, most of the proteins involved in capsid formation and genome encapsidation are produced in the cytoplasm and transported to the nucleus where assembly and packaging take place (Ding et al., 2010; Li et al., 2019; Tessier et al., 2019). Major capsid protein, hexon undergoes trimerization in the cytoplasm with the help of 100K

protein (Hong et al., 2005). Another late adenoviral protein, pVI, mediates the nuclear import of hexon (Wodrich et al., 2003). Similarly, the penton base and fiber protein join to form a complex before nuclear entry (Hunter, 2012). In addition to major capsid proteins, minor capsid protein pIIIa, pVI, pVIII, IX also take part in the process of capsid formation (Vellinga et al., 2005). Viral genome condensed with core adenovirus proteins interacts with packaging protein IVa2, 22K, 33K, and 52K to affect packaging. Currently, two models try to explain adenovirus morphogenesis (Ahi and Mittal, 2016; Condezo and San Martin, 2017; Ostapchuk et al., 2011).

According to the concerted model, capsid formation and genome encapsidation is a coupled process. Initiation of capsid formation and genome packing occurs in a separate pool, and L1 52K tethers the two pools, and capsid formation continues around the genome via the addition of capsomeres (Condezo and San Martin, 2017). In support of this model, a thermo-conditional mutation on DNA binding affects the synthesis of viral DNA and the reduction of virus particle production (D'Halluin et al., 1978). Also, the presence of L1 52/55 kDa in genome-less adenovirus particle together with the ability of this protein to interact *in vivo* with packaging domain and protein IIIa *in vitro* is indicative of the role of L1 52/55 kDa in tethering the core structures with capsid fragments signifying that packaging in adenovirus is of concerted type (Condezo et al., 2015; Condezo and San Martin, 2017; Ma and Hearing, 2011).

According to the sequential packaging of the adenovirus model, an empty capsid formed first, and viral genome packaging follows as a result of the interaction of packaging proteins with the packaging sequence located close to the left end of the viral genome (Ahi and Mittal, 2016). It has been reported that the adenovirus IVa2 displays ATPase activity, binds with ATP and occupy a single vertex of an icosahedron (Christensen et al., 2008; Ostapchuk and Hearing, 2008).

Table 1.5. Role of adenovirus late region in the virus life cycle

Protein	Function/functional interaction	Reference
52/55K	Involved in encapsidation of viral DNA by interacting with genome packaging domain.	(Perez-Romero et al., 2005)
	Interacts with IVa2 possibly for its recruitment of the packaging domain.	(Gustin et al., 1996; Wu et al., 2012)
	Interacts with and cleaved by viral protease.	(Perez-Berna et al., 2014)
	Interacts with IIIa connecting core with capsid structures.	(Condezo and San Martin, 2017; Ma and Hearing, 2011)
	It is also found in empty capsid indicating its potential role in capsid formation.	(Condezo et al., 2015)
IIIa	Stabilize capsid by connecting group of hexon and interacting with minor protein pVIII.	(Reddy and Nemerow, 2014; San Martin, 2012)
	Interact with 52K and viral packaging sequence: a role in genome packaging	(Crosby and Barry, 2014; Ma and Hearing, 2011)
pX	High proportion of basic residues and it bind and condense viral genome.	(Perez-Berna et al., 2015)
pIII	Penton base, a major capsid component involved in capsid formation.	(Russell, 2009)
	Penton base interact with integrin receptor facilitating adenovirus internalization	(Russell, 2009)
pVII	pVII interacts with transport receptors and incoming viral DNA and translocate viral DNA across the NPC to the nucleus.	(Hindley et al., 2007; Wodrich et al., 2006)
	pVII protect adenoviral DNA from detector system of the DDR; interacts with SPOC1, involved in detection of Double Strand Break.	(Karen and Hearing, 2011; Schreiner et al., 2013)
	pVII interacts with viral DNA, condenses DNA and also acts as a transcriptional suppressor.	(Johnson et al., 2004)
	pVII play role a role in early stage of adenoviral infection via adenoviral endosomal escape.	(Ostapchuk et al., 2017)
pV	pV interacts with pVI and pVII, and links core with capsid structure.	(Chatterjee et al., 1985; Matthews Russell, 1998).
	pV translocate B23.1 to viral replication center and enhance viral replication.	(Ugai et al., 2012)
	pV interacts p32, which might play a role in the nuclear import of adenoviral DNA.	(Matthews and Russell, 1998)

Table 1.5 ------Continued

Protein	Function /Functional interaction	References
pVI	pVI help in transport of hexon to nucleus. And stabilization of capsid structure.	(Wodrich et al., 2003)
	Interaction of pVI pV and pVIII link the capsid structure with Virion core structure.	(Reddy and Nemerow, 2014)
	pVI serve as a cofactor for activation of adenoviral proteinase activity.	(Mangel et al., 1993)
	pVI as a membrane lytic protein involved in endosomal membrane disruption and escape of viral particle from endosome.	(Maier et al., 2010; Wiethoff et al., 2005)
	pVI interact with Daxx, and enhance E1A transcription activation function.	(Schreiner et al., 2012)
Protease	Cleavage adenoviral proteins before Virion maturation of progeny Virion.	(Mangel and San Martin, 2014)
Hexon	Interact with minor capsid components to stabilize capsid structure.	(Liu et al., 2010; Reddy and Nemerow, 2014; San Martin,2012)
	Interacts with 100K and pVI for hexon trimer formation and transport into the nucleus, respectively.	(Hong et al., 2005 Wodrich et al., 2003)
pVIII	A minor capsid protein located in the interior aspect of the viral capsid. It associates with pVI and stabilize capsid and links the capsid with core structure.	(Reddy and Nemerow, 2014; Vellinga et al., 2005)
Fiber	Structural protein used as the mediator of viral entry to host cell.	(Arnberg, 2012)

Table 1.5 Continued

33K	33K bind to MLP and activate transcription	(Ali et al., 2007; Wu et al., 2013)
	33K involve in early late switch in the temporal pattern of viral gene expression.	(Farley et al., 2004; Tormanen et al., 2006)
	33K interact with IVa2 and DBP and occupy a single vertex of an icosahedron. Involve in viral genome encapsidation and appears essential for the virus lifecycle.	(Ahi et al., 2013; Fessler and Young, 1999; Finnen et al., 2001; Wu et al., 2013)
	33K interacts with PKA and DNA-PK enhancing and inhibiting its splicing function	(Tormanen Persson et al., 2012)
22K	22K protein binds to the viral packaging domain in the presence of IVa2 and involve in packaging of adenoviral genome	(Guimet and Hearing, 2013; Ostapchuk et al., 2006; Wu et al., 2012)
	22K also interact with DE elements of adenovirus MLP and activate transcription of MLTU.	(Backstrom et al., 2010; Guimet and Hearing, 2013; Morris and Leppard, 2009; Wu et al., 2012)
	22K also enhance late gene expression from MLTU post-transcriptionally.	(Guimet and Hearing, 2013)
	22K involved in virus induced cell lysis by regulation of adenovirus death protein (ADP)	(Wu et al., 2012)
100K	100K interact with hexon and assist in hexon trimer formation.	Hong et al., 2005 (Hong et al., 2005; Koyuncu and Dobner, 2009; Morin and Boulanger, 1986)
	100K interact with eIF4G and PABP, recruit 40S ribosome, favoring viral mRNA translation via ribosome shunting while inhibiting cap mediated cellular mRNA translation	(Cuesta et al., 2004; Hayes et al., 1990; Xi et al., 2004
	100K via interacting and stabilizing granzyme B it prevents infected cell from cytotoxic T cell mediated destruction.	(Andrage et al., 2001, 2003)

These observations indicate that adenovirus contains a packaging component similar to those that use a sequential genome packaging approach (Ahi and Mittal, 2016). Another evidence in support of this model is the detection of low-density viral particles (empty capsids) during adenovirus purification as well as accumulation of empty capsids as a result of encapsidation failure in cells infected with mutant viruses containing mutation in the viral proteins that interact with the packaging sequence (Ahi et al., 2013; Ostapchuk et al., 2011; Stilwell et al., 2003; Wu et al., 2013; Wu et al., 2012).

Lack of portal protein is one of the weaknesses attributed to the sequential model of adenovirus packaging; however, a recent report indicates that adenovirus E4 34K displays a higher degree of similarity with a portal protein of bacteriophages that are known to package their genome in a preformed capsid. The presence of the protein in a single vertex of the icosahedron and its interaction with packaging proteins indicate that E4 34K may be acting as a portal protein of adenoviruses strengthening the sequential model of adenovirus packaging (Ahi et al., 2017).

1.1. 4 Bovine adenovirus

Bovine adenovirus isolated for the first time in the year 1959 (Klein et al., 1959). Since then, the virus isolated from apparently healthy as well as cattle with respiratory and enteric aliments (Graham et al., 2005; Smyth et al., 1996; Thomson, 1994). Experimental studies indicate that infection with bovine adenoviruses results in from inapparent to mild/moderate clinical manifestation (Caswell and Williams 2016; Lehmkuhl et al., 1975; Mittal et al., 1999).

1.1.4.1 Classification

Since the first report, a total of 14 bovine adenovirus serotypes reported so far (Lehmkuhl and Hobbs, 2008; Sibley et al., 2011). Historically, based on sharing common complement-fixing antigen or not and based on growth characteristics in tissue culture, bovine adenoviruses were classified into two groups group I and group II (Bartha, 1969). According to the current nomenclature, on the basis of genome organization or phylogenetic analysis, bovine adenovirus serotypes fall under either *Mastadenovirus* or *Atadenovirus* genus (Harrach et al., 2012; Harrach, 2014).

1.1.4.2 Genome organization of bovine adenovirus -3

Bovine adenovirus (BAdV)-3 classified within the genus of Mastadenovirus (Davison et al., 2003; Harrach, 2014). BAdV-3 was isolated from healthy cattle as well as from cattle manifesting or having respiratory or enteric infections (Darbyshire et al., 1965). However, no significant clinical manifestation observed upon experimental infection (Lehmkuhl et al., 1975; Mittal et al., 1999).

BAdV-3 contains a double-strand linear DNA genome of 34446 bp (Reddy et al., 1998). The double-strand viral DNA is flanked by an inverted terminal repeat (ITR), which is longer than human adenovirus (HAdV)-2 and -5 (Reddy et al., 1998). BAdV-3 ITR contains E1A transcriptional control elements and also plays a role in the packaging of the viral genome (Xing and Tikoo, 2007). Similar to other adenoviruses, gene expression patterns in BAdV-3, is temporally regulated (Fig. 1.4), where early genes transcribed first, followed by intermediate and late genes (Reddy et al., 1998).

1.1.4.2.1 Early genes of bovine adenovirus -3

Early (E) region of BAdV-3 divided into four regions (E1-E4) (Baxi et al., 1998; Idamakanti et al., 1999; Reddy et al., 1999a). Similar to HAdV-5, E1 region of BAdV-3 divided into E1A and E1B (Reddy et al., 1999a). However, unlike HAdV-5, E1A, and E1B regions, BAdV-3 E1A and E1B are obtained from overlapping transcriptional units (Reddy et al., 1999a) controlled by separate promoters and share the same polyA sites (Reddy et al., 1999a).

The E1A region produces 211, 115, and 100R mRNA transcripts detected as 43, 57, and 65 kDa protein respectively from BAdV-3 infected cells, all of which sharing N terminus 93 amino acids (Reddy et al., 1999a). While the 43kDa expressed as early as 6 hr, the rest of the E1A protein expression starts from 24 hours onwards (Reddy et al., 1999a). Function wise E1A involve in transactivation of other BAdV-3 early genes (Zhou and Tikoo, 2001). Moreover, E1A is indispensable for BAdV-3 life cycle (Reddy et al., 1999b; Zhou and Tikoo, 2001). Though the significance of phosphorylation is not studied, E1A of BAdV-3 appeared to be phosphorylated (Reddy et al., 1999a; Reddy et al., 1998). E1B of BAdV-3 encodes one small (157R) and one large (420R) protein that encode 19kDa and 48 kDa proteins, respectively (Reddy et al., 1999a; van Olphen et al., 2002). Their expression kinetics indicates that the 19kDa protein expressed earlier than the 48kDa protein. E1B proteins of BAdV-3 are highly phosphorylated (Reddy et al., 1999a). While 19kDa is not essential for the replication of BAdV-3, the 48 kDa E1B protein appears to be necessary for BAdV-3 life cycle (Reddy et al., 1999b; Zhou and Tikoo, 2001). The E2A region of BAdV-3 divided into two regions: E2A and E2B that encode protein involved in viral replication (Reddy et al., 1998). E2A encodes for DBP, a 423 amino acid long protein displaying less than 50% similarity with the homologous protein encoded by HAdV-5. The conserved C-terminus region is involved in DNA binding

and viral replication (Kitchingman, 1985; Reddy et al., 1998). The protein also contain cluster of basic amino acids as well as serine and arginine repeats that may potentially serve as nuclear localization signal and phosphorylation sites, respectively (Reddy et al., 1998).

The E2B of BAdV-3 produces precursor terminal protein (pTP) and viral DNA polymerase (pol) mRNAs that are 3' co-terminal (Baxi et al., 1998; Reddy et al., 1998). BAdV-3 pTP and pol encodes 649 and 1023 amino acid long protein, respectively, with significant homology with homologs encoded by other adenoviruses (Baxi et al., 1998; Reddy et al., 1998). BAdV-3 pTP contains a conserved amino acid sequence (YSRLVYR), which contains amino acids involved in initiation complex formation (Hsieh et al., 1990). In addition to the conserved sequence involved in the initial stage of adenoviral DNA replication, BAdV-3 pTP contains a partially conserved sequence used as a nuclear localization signal in HAdV-5 pTP (Zhao and Padmanabhan, 1988). Moreover, among the three potential pTP cleavage sites of HAdV-5 pTP, two of them are conserved in BAdV3-pTP (Baxi et al., 1998; Zhao and Padmanabhan, 1988). The E3 region of BAdV-3 encodes for 284, 121, 86, and 82R proteins (Idamakanti et al., 1999; Reddy et al., 1998). Among the four proteins, 121R, expressed as 14.5kDa in infected cells, show limited homology with HAdV-5 14.7kDa protein (Idamakanti et al., 1999; Zakhartchouk et al., 2001) while 284R appeared to be unique to BAdV-3 (Idamakanti et al., 1999). Similar to HAdV-5 E3 14.7 kDa protein, 121R of BAdV-3 displays serological similarity and prevent TNF-α mediated cell lysis (Zakhartchouk et al., 2001). The E3 region of BAdV-3 is dispensable for the propagation of the virus in tissue culture (Mittal et al., 1993; Zakhartchouk et al., 1998).

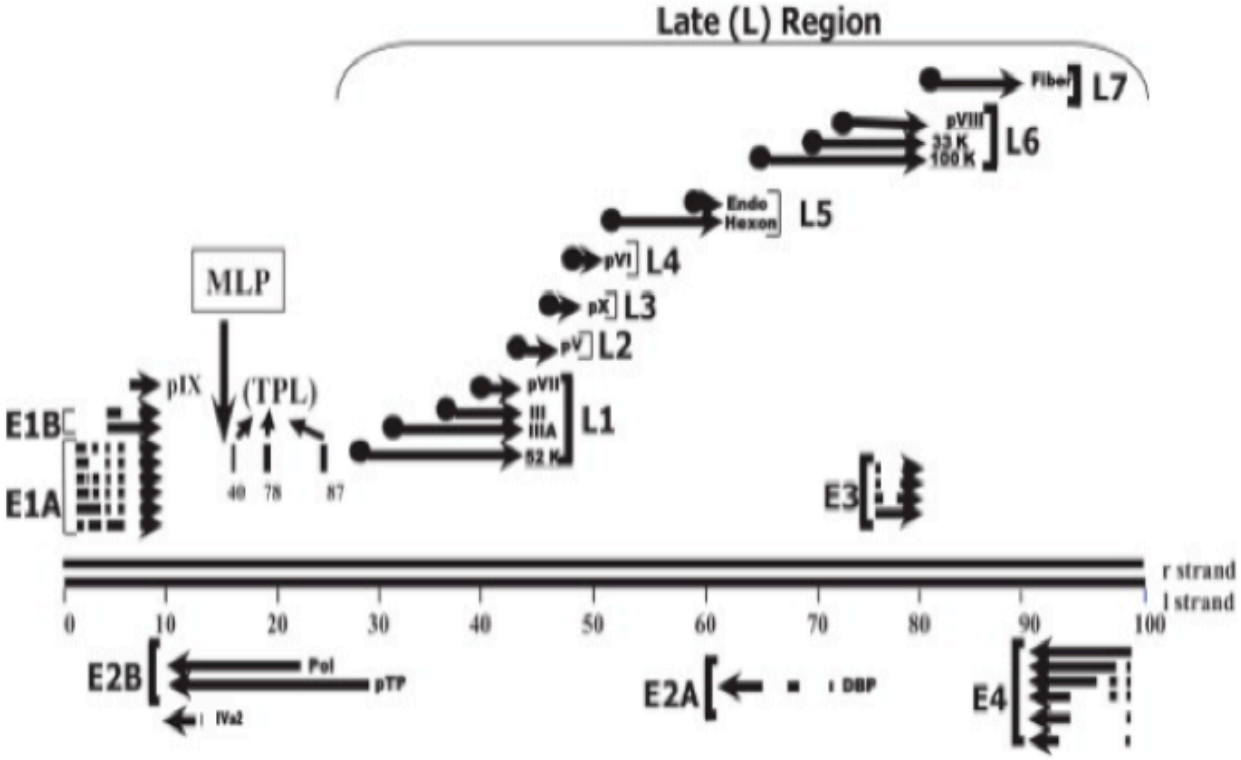

Fig. 1.4 Transcriptional map of BAdV-3.

The double line represent double stranded DNA genome and the arrows indicate transcripts from both strands. Major late promoter (MLP), a promoter where late mRNA transcript are driven. Tripartite leader (TPL) sequence, none coding regions where late mRNA transcripts acquire it via alternate splicing Horizontal arrows represent direction of transcription. Re printed from Ayalew et al., 2015. Vaccine, 15; 33(4):493-9 (with permission from Elsivier)

The E4 region of BAdV-3 located in the right end of the genome, transcribed from the complementary (l) strand and has a potential to encode five different transcripts that encode proteins with amino acid length of 143, 69, 289, 143 and 219, respectively (Lee et al., 1998; Reddy et al., 1998). While BAdV-3 E4 Orf 3 and 5 show partial homology with HAdV-2 34K protein (Lee et al., 1998), the remaining Orfs are unique to the BAdV-3 (Lee et al., 1998). Though deletion of individual Orf 1, 2, 3, or 4 showed no effect on BAdV-3, deletion of E4 Orf 5, orf1-3 or orf3-5 region affected BAdV-3 replication (Baxi et al., 2001).

1.1.4.2.2 Intermediate genes bovine adenovirus -3

Similar to other adenoviruses in the genus Mastadenovirus, BAdV-3 encodes two intermediate genes, pIX and IVa2 (Baxi et al., 1998; Reddy et al., 1999a). Like the E2 and E4 genes, IVa2 transcribed from the complementary strand. Reports indicate that BAdV-3 IVa2 encodes 376 amino acids long protein with its C-terminus 22 amino acids overlapping with N-terminus of the viral polymerase (Baxi et al., 1998). However, further analysis of reported BAdV-3 genome sequence indicates that 80 amino acids of IVa2 overlap with the polymerase region, and 13 nucleotides of IVa2 obtained via alternate splicing from the polymerase coding region (Davison et al., 2003). BAdV-3 pIX is 125 amino acid long protein, and its transcripts overlap with E1 region (Baxi et al., 1998; Zheng et al., 1994). The protein has the potential to accommodate foreign genes as recombinant BAdV-3 containing EYFP or RGD motif fused to C-terminus of pIX could be successfully rescued, indicating that its potential as a site of insertion of foreign genes (Zakhartchouk et al., 2004).

1.1.4.2.3 Late genes of bovine adenovirus -3

The late (L) genes of adenovirus, in general, encode structural components of the viral capsid and non-structural proteins involved in the formation of capsids. The late genes transcribed from the major late promoter, the activation of which produce a major late transcription unit that undergoes alternate spicing and polyadenylation to produce multiple transcripts (Berk, 2013). Unlike the HAd-5 major late transcriptional unit (MLTU), which produces five transcripts (L1-L5), BAdV-3 MLTU produces seven transcripts L1-L7. Each of the transcripts acquires a tripartite leader (TPL) sequence via alternate splicing from three exon regions (Reddy et al., 1998).The L1 region of BAdV-3 encodes for two structural (pIIIa and pIII), one core (pVII), and one non-structural (52K) protein (Reddy et al., 1998). The pIII is 568 amino acids long protein with 25-57 % homology with pIIIa encoded by other adenoviruses and has a consensus protease cleavage site (Reddy et al., 1998). The pIII (penton base) is 482 amino acid long protein with 44-64% homology with a penton base encoded by other adenoviruses (Reddy et al., 1998). Unlike conserved RGD and LDV motifs involved in the secondary interaction of penton base with integrin family of receptors in HAdV-5, BAdV-3 penton known to have MDV motif that may have a role in the entry of the virus into target cells (Komoriya et al., 1991; Reddy et al., 1998). Moreover, BAdV-3 pIII possesses a conserved sequence used by other members of adenoviruses in the interaction of penton base with fiber (Reddy et al., 1998). The pVII of BAdV-3 is 171 amino acids and shows 33.3% to 53.2% homology with pVII encoded by other adenoviruses (Reddy et al., 1998). The pVII contains a mitochondrial localization signal, localizes to mitochondria, and prevents infected cells from mitochondrial-mediated apoptosis (Anand et al., 2014). The BAdV-3 pVII also shown to interact with viral protein 52K (Paterson, 2010).

The 52K protein of BAdV-3 consists of 370 amino acids and show homology of 56.8% to 61.6 % with 52K encoded by other adenoviruses (Reddy et al., 1998). The 52K detected as a 40 kDa protein in infected as well as transfected cells (Paterson et al., 2012). The 52K contains a bipartite nuclear localization signal, which interacts with α-3 importin for nuclear transport of 52K (Paterson et al., 2012). The 52K protein interacts with cellular protein NF-kB binding protein (NFBP) (Paterson, 2010) and viral proteins pVII (Paterson, 2010), 33K, and 22K (Said et al., 2018a) in BAdV-3 infected cells.

The L2 region encodes a single protein pV, which contains a high content of basic amino acids (Reddy et al., 1998). BAdV-3 pV is 423 amino acid long protein-containing nuclear and nucleolar localization signals (Zhao and Tikoo, 2016). The protein displays three nucleolar localization signals with redundant function as the deletion of the entire nucleolar localization signal rather than individual nucleolar localization signals affected viral replication (Zhao, 2016). The protein interacts with cellular transport receptor importin α-3 to cross the nuclear pore complex towards the nucleus. Moreover, pV interacts with viral protein 100K and cellular protein nucleolin (Zhao, 2016). BAdV-3 pV appears to be essential for BAdV-3 replication as its deletion affects virus assembly, reduced late adenoviral protein expression, and reduced thermostability (Zhao and Tikoo, 2016).

The L3 region of BAdV-3 encodes 80 amino acid long, basic proteins, pX (Reddy et al., 1998). The protein shows 38-64 % homology with pX of other adenoviruses (Reddy et al., 1998). The protein also displays sequences potentially involved in protease cleavage and nuclear localization of pX, indicated by its conserved nature among similar sequences present in pX encoded by other adenoviruses (Anderson et al., 1989; Reddy et al., 1998)

The L4 region of BAdV-3 encodes pVI protein showing 15-38% homology with pVI encoded by other adenoviruses (Reddy et al., 1998). BAdV-3 pVI displays significant homology with C-terminus of HAdV- 2 counterpart suggesting potential functional similarity (Reddy et al., 1998). Moreover, pVI of BAdV-3 contains consensus protease cleavage sites (Reddy et al., 1998).

The L5 region of BAdV-3 encodes a structural protein, hexon (Reddy et al., 1998). It is a major structural protein of 910 amino acids, detected with a molecular weight of 98kDa protein in mature virus (Kulshreshtha et al., 2004). The protein shows 45 to 70% homology with hexon encoded by other adenoviruses (Reddy et al., 1998). BAdV-3 L5 region also encodes protease of 204 amino acid long that shows significant homology with proteases encoded by other adenoviruses (Reddy et al., 1998). BAdV-3 precursor proteins pIIIa, pVI, pVII, pIX and pTP contain conserved consensus protease cleavage site(s) (Reddy et al., 1998). Recent, report shows that BAdV- 3 protease cleave pVIII (Gaba et al., 2017) and non-structural protein 100K (Makadiya et al., 2015).

The L6 region of BAdV-3 encodes three non-structural (22K, 33K,100K) and one structural (pVIII) protein (Reddy et al., 1998). BAdV-3 100K, a non-structural protein, is detected as 130 kDa protein at early and late times post-infection (Makadiya et al., 2015). The 100K localizes both in the nucleus and cytoplasm in the infected cells. The 100K protein interacts with viral protein pV and cellular protein dynein light chain 1 (DYNLT1) (Makadiya, 2013). The 100K protein contains two consensus protease cleavage sites, which are cleaved by BAdV-3 protease. The cleaved C-terminus of 100K utilizes NLS (amino acid 789-811) to localize to the nucleus (Makadiya et al., 2015). However, cleavage of 100K appears to be dispensable for the replication of BAdV-3 (Makadiya et al., 2015). Two other non-structural proteins encoded by

L6 region of BAdV-3 include 22K and 33K, which are encoded by an un-spliced transcript and spliced 33K transcript, respectively (Kulshreshtha, 2009; Reddy et al., 1998). The BAdV-3 33K and 22K share the N-terminus region of 138 amino acids (Kulshreshtha and Tikoo, 2008). The 22K is 274 amino acids long, expressed as 42kDa and 37 kDa proteins in infected cells (Kulshreshtha et al., 2015). BAdV-3 22K localize to the nucleus by interacting with cellular transport proteins, importin α-5 and α-7 (Said et al., 2018a). Amino acids 238-241 are essential for nuclear localization of 22K, which appears necessary for the replication of BAdV-3 (Said et al., 2018a). Besides, amino acid 35-65 of BAdV-3 22K interacts with BAdV-3 52K (Said et al., 2018a).

The 33K of BAdV-3 is 279 amino acids long and expressed as 42 kDa, 38 kDa, and 33 kDa proteins in infected cells (Kulshreshtha et al., 2015). The conserved C-terminus of BAdV-3 33K contains leucine residues, which appear to bind with the downstream element of the MLP and stimulate transcription activity from the MLP (Kulshreshtha et al., 2015). The conserved C-terminus of BAdV-3 also contains RS (Arginine, Serine) repeats, which bind to the transportin receptor and localize 33K to the nucleus (Kulshreshtha et al., 2014). Besides, BAdV-3 33K appears to interact with viral protein 52K (Said et al., 2018a) and cellular proteins importin α-5 (Kulshreshtha et al., 2014) and bovine presenilin-1-associated protein (BoPSAP) (Kulshrestha, 2009). Additionally, BAdV-3 33K appears to be indispensable for virus replication (Kulshreshtha et al., 2004; 2008; Kulshreshtha, 2009).

The pVIII is a structural protein encoded by L6 region of BAdV-3 (Reddy et al., 1998). The protein consists of 216 amino acids, detected as 24 kDa and 8kDa proteins in infected cells (Ayalew et al., 2014). BAdV-3 pVIII displays two consensus protease cleavage sites with redundant function (Gaba et al., 2017). Although mutation of single-site produces thermolabile

progeny virus, mutation of both sites is lethal for progeny virus production (Gaba et al., 2017). Earlier, we demonstrated that pVIII interacts with cellular dead box family of RNA helicases (DDX3) and interfere translation of capped mRNA (Ayalew et al., 2016). Recently, we reported that pVIII interacts with eukaryotic initiation factor 6 (eIF6) and delays the joining of 60S ribosomes to 40S ribosome to form a mature 80S ribosome (Gaba et al., 2018).

BAdV-3 fiber is the only protein encoded by the L7 region of BAdV-3. The protein is 976 amino acid long with lower degree of homology with the fiber of other adenoviruses (Reddy et al., 1998). BAdV-3 fiber detected as 102 kDa glycoprotein in the infected cell (Wu et al., 2004a). It is localized in the nucleus using basic amino acid located in the N-terminus 41 amino acids (Wu et al., 2004a). BAdV-3 fiber protein is involved in the initial viral interaction with host cell sialic acid receptors (Li et al., 2009). Moreover, the replacement of the cell receptor-binding region of BAdV-3 with cell receptor binding region of HAdV-5 fiber alters the tropism of BAdV-3 (Wu and Tikoo, 2004b).

1.1.4.2.4 Protein-protein interaction in bovine adenovirus -3

Viruses undergo viral-viral or viral-cellular protein-protein interaction at different stages of their life cycle (Cook et al., 2018). As they have limited genetic information, viral-cellular protein-protein interactions are crucial for tapping cellular resources (Halehalli and Nagarajaram, 2015). In this regard, knowledge of viral protein-protein interactions increases our understanding of virus biology (Cook et al., 2018). Present knowledge regarding protein-protein interactions in BAdV-3 summarized below in Table 1.6 (a)(b (Paterson, 2010).

Table 1.6 BAdV-3 interactions with viral\cellular proteins. (a) Interaction of non structural proteins of BAdV-3 with viral\cellular proteins.

Protein	Viral\cellular interacting proteins	Reference
52K	Viral proteins: 22K, pVII Cellular protein: Importin α-3, NF-kB-binding protein (NFBP)	Paterson, 2010; Paterson et al., 2012; Said et al., 2018a
100K	Viral protein: 33K Cellular protein: Importin α-3, Dynin (DYNLT1) light chain1;	Makadiya, 2013. Makadiya et al., 2015
22K	Viral protein: 52K. Cellular protein: Importin α-5; importin α-7	Said et al., 2018a
33K	Viral protein: 100K, pV, 52K Cellular protein: Importin α-5; Transportin; bovine presenilin-1-associated protein / mitochondrial carrier homolog (BoPSAP/BoMtch1)	Kulshreshtha and Tikoo, 2008; Kulshrestha, 2009; Said et al., 2018a

(b). BAdV-3 structural proteins interaction with viral\cellular proteins

pVIII	Viral protein: Cellular protein: Importin α-3; DDX3; eIF-6	Ayalew et al., 2016; Gaba et al., 2018
pV	Viral protein:33K Cellular protein: Nucleolin,	Zhao, 2016
pVII	Viral protein: 52K	Paterson , 2010
Fiber	Cellular protein: sialic acid receptors	(Li et al., 2009)

1.1.5 **Adenovirus IVa2**

Adenovirus IVa2 is one of the conserved viral proteins of adenoviruses, transcribed from the complementary viral DNA (Davison et al., 2003). It is a product of the intermediate region the expression of which is suppressed by an unknown cellular factor (Davison et al., 2003; Huang et al., 2003; Iftode and Flint, 2004). Earlier reports indicated that IVa2 displays a nucleolar and nucleoplasmic distribution (Lutz et al., 1996). Studies in human adenovirus IVa2 shown that the viral protein is involved in the transcriptional activation of late adenoviral proteins involved in the formation of viral capsid via associating with the viral major late promoter region (Lutz and Kedinger, 1996; Pardo-Mateos and Young, 2004; Tribouley et al., 1994). Besides, IVa2 is involved in the packaging of the viral genome via sequence-specific interaction of the viral protein with the packaging domain located at the left end of the adenoviral sequence (Hammarskjold and Winberg, 1980; Ostapchuk and Hearing, 2005). The viral protein IVa2 localizes at the unique vertex of the icosahedron (Christensen et al., 2008) and has conserved ATPase motifs with an essential role in the virus life cycle (Ostapchuk and Hearing, 2008). Recent findings are also in support of the hypothesis where IVa2 localize at a unique vertex of the icosahedral capsid, forming a complex with other viral proteins (Ahi et al., 2013).

Previous reports have shown that human adenovirus IVa2 cooperatively with 22K protein interacts with viral packaging sequence for efficient packaging of the viral genome (Ewing et al., 2007; Ostapchuk et al., 2006; Yang and Maluf, 2012). Similarly, interactions of IVa2 with 33K as well as 52K proteins, which have known to be involved in enhancing gene expression and packaging of adenovirus respectively, have been documented (Ali et al., 2007; Gustin and Imperiale, 1998; Gustin et al., 1996). Recently, via in vivo crosslinking approach IVa2 protein

shown to associate with 22K, 33K and DNA binding protein with localization of the complex at a single vertex of adenoviral capsid further indicating that IVa2 carries out its function via forming a functional association with other adenoviral proteins (Ahi et al., 2013).

1.2 Nuclear pore complex and nucleoporins

One of the characteristic features of eukaryotic cells is the presence of a membrane-bound nucleus that creates a controlled environment for activities taking place in the nuclear and cytosolic compartments (Anderson and Hetzer, 2007). However, the bidirectional transport of materials between the nucleus and cytoplasm is essential for coordinated cellular function. For instance, transcription products, as well as other macromolecules that are essential for cytosolic translation of messenger RNA, need to get access to the cytoplasm, and proteins required for nuclear function have to transverse the nuclear membrane to reach the nucleus (Nakielny and Dreyfuss, 1999).

The nuclear pore complex (NPC) mediates the movement of materials between the nucleus and cytoplasm (Wente and Rout, 2010). NPC is a macromolecular protein assembly embedded within the nuclear envelope. Multiple copies of about 34 nucleoporins (nups) involved in the formation of functional units of the NPC (Hoelz et al., 2011). As revealed by cryo-ET studies, NPC consists of an asymmetric core (comprising cytoplasmic, inner and nuclear rings), and asymmetric cytoplasmic filaments and nuclear basket (Fig. 1.5). Nuceolporins are named using a three-letter Nup followed by a number that indicates the molecular protein weight (Schwartz, 2016). Based on their location, within the nuclear pore complex, nucleoporins are classified as coat nucleoporins (nups) transmembrane nups, adaptor nups, channel nups, cytoplasmic filament nups, and basket nucleoporins (Hoelz et al., 2011; Hsia et al., 2007) (Fig. 1.5).

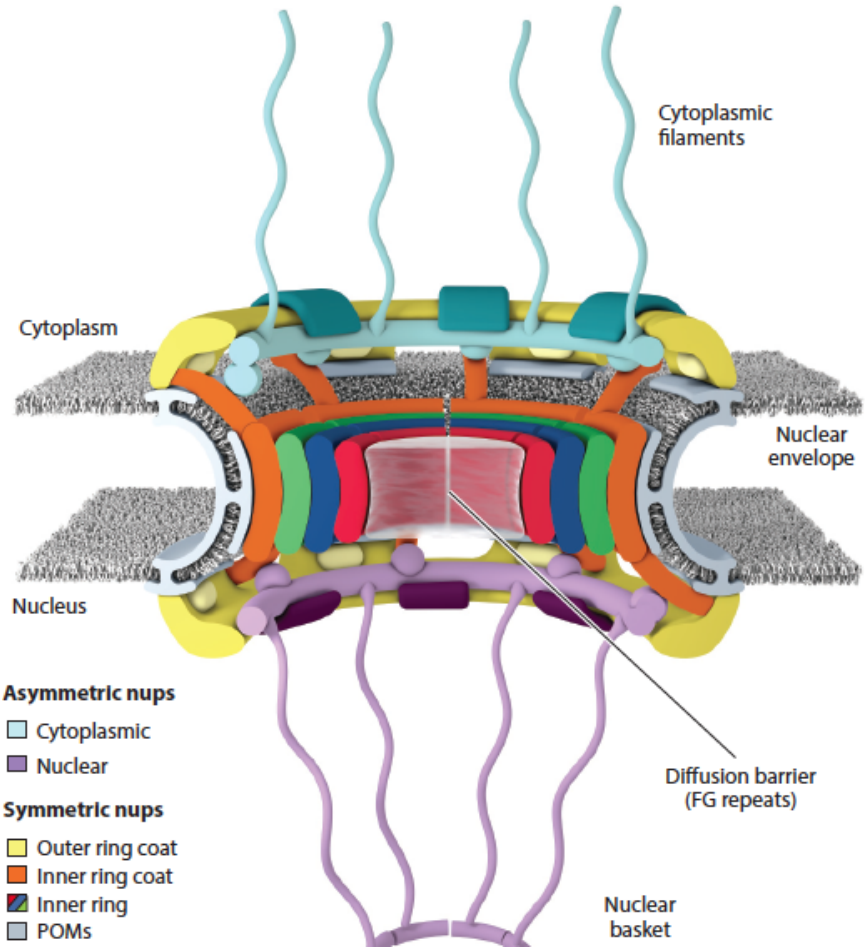

Fig 1.5 Schematic representation of the nuclear pore complex. Re printed from Lin and Hoelz, 2019 Annu Rev Biochem. 20; 88: 725–783. (With permission from Annual Review)

Nucleoporins consist of a structural domain, including β-propellers, α-helical solenoid, and phenylalanine-glycine (FG) repeats (Hoelz et al., 2011; Lin and Hoelz, 2019). While all the nucleoporins consist of FG repeats, nucleoporins that form the symmetric core of the NPC mainly consist of α- helical regions and β-propellers (Lin and Hoelz, 2019). Nucleoporins are known to organize themselves as subcomplexes dictated by the stability of protein interaction, which eventually joined each other to form the nuclear pore complex. So far, four nucleoporins subcomplexes have been reported (Lin and Hoelz, 2019). The first one is the coat nucleoporins subcomplex, also known as the Y complex, and it is a major constituent of the outer ring (Hoelz et al., 2011). In humans, the Y complex is known to comprise (Sec13, Seh1, Nup96, Nup75, Nup107, Nup160, Nup133, Nup37, Nup43, and ELYS (Lin and Hoelz, 2019). The second subcomplex is known as the inner ring subcomplex, also called the nup93 subcomplexes. Unlike the coat nucleoporins subcomplex, the inner ring subcomplex displays different conformation (Lin and Hoelz, 2019; Stuwe et al., 2015). The subcomplex includes Nup53, Nup93, Nup155, Nup205, Nup188, Nup98. In addition to these nucleoporins, the inner ring subcomplex consists of Nup54, Nup58, and Nup62, which contribute FG repeats that form a molecular sieve structure within the central channel (Lin and Hoelz, 2019). The third group of subcomplex is nucleoporins that form the cytoplasmic filaments. Nucleoporins that form the cytoplasmic filaments include Nup214, Nup88, Nup62, Gle1, Nup42, Rae1, and Nup98 (D'Angelo and Hetzer, 2008; Hoelz et al., 2011). These nucleoporins are characterized by having long flexible extension that protrudes into the cytoplasm (Jarnik and Aebi, 1991). Cytoplasmic filament nucleoporins, in particular, FG repeats within these nucleoporins, serve as attachment sites with transport receptors. Cytoplasmic filament nucleoporins play a role in the control of mRNA export (Bonnet and Palancade, 2014). Another nucleoporins sub-complex

that forms the asymmetric portion of the NPC is the nups that form the nuclear basket of the NPC (Umlauf et al., 2013). Basket Nucleoporins include nucleoporins that form the nuclear face of the nuclear pore complex. In humans, the components include Nup50, Nup153, and Tpr (Meszaros et al., 2015; Schwartz, 2016). The nuclear basket nucleoporins beside their role in the nucleocytoplasmic transport of mRNA; they are involved in transcriptional regulation (Kohler and Hurt, 2010).

1.3 Nuclear import of proteins

The nuclear pore complex (NPC) allows passive transport of small molecules less than 40kDa, whereas the transport of macromolecules across the NPC involves an active transport system known as the nuclear transport system (Christie et al., 2016). (Fig.1.6). The components of the system include a protein Ran (create a gradient which in turn determines the directionality of transport), cargo molecule displaying a stretch of recognition sequence called localization signals, and soluble transport receptors (Christie et al., 2016). A small GTPase, Ran, has ATP and GDP bound forms (RanGTP and RanGDP) (Gorlich et al., 1996). There is high concentration gradient of RanGTP in the nucleus, which is achieved by a combined action of RanGAP (RanGTPase activating protein) that is present only in the cytoplasm and converts RanGTP to RanGDP where the latter is transported into the nucleus using cellular protein NTF2 (Bischoff et al., 1995; Ribbeck et al., 1998). In the nucleus using a protein present only in the nucleus, Ran guanine exchange factor 1, also called regulator of chromosome condensation 1 (RCC1), facilitates the reconstituting RanGTP (Bischoff et al., 1995). For instance, for the transport of the protein to the nucleus across the NPC, cargo protein using its nuclear localization signal interacts with soluble transport receptors (karyopherins). Interaction

can be mediated by adaptor transport protein such as importin-α or directly via interaction of cargo with karyopherins-β (Gorlich et al., 1995; Xu et al., 2010). Importin α consists of three conserved structural domains (Miyamoto et al., 2016; Oka and Yoneda, 2018). The first is the N terminus part, also called the importin β binding domain, involved in the interaction with importin β1 (Lott and Cingolani, 2011; Miyamoto et al., 2016). The middle portions is involved in the interaction with the NLS of cargo protein (Miyamoto et al., 2016; Xu et al., 2010). In a majority of the cases, importin α binds with classical NLS, NLS containing clusters of basic amino acids that can be of monopartite (consisting single clusters of basic amino acids) or bipartite (containing two stretches of basic amino acids separated by a linker (Lange et al., 2007). The last domain of importin α is the C terminus part, the domain of importin α that serves as a binding site for the exportin, cellular apoptosis susceptibility protein (CAS) (Goldfarb et al., 2004; Stewart, 2006). The middle and C terminus portions of importin α are made of armadillo (ARM) repeats, each of which consists of 42-43 amino acids (Oka and Yoneda, 2018). Although importin α serves as a receptor for protein with classical nuclear localization signals, a protein with a non-classical nuclear localization signal has shown to utilize the adaptor protein (Nakada et al., 2015). Proteins with monopartite NLS usually bind to the major groove of the helical structure of importin α (middle portion of importin α containing 2-4 of the ARM repeats), and protein with bipartite classical NLS binds to both major and minor groove of importin α (the part made from 6-8 ARM repeats)(Kosugi et al., 2009b). Nuclear import of many proteins with non-classical nuclear localization signals is mediated by direct interaction with importin β2 (Xu et al., 2010). Protein that interacts with importin β2 though they lack conserved consensus motif unlike classical NLS, it has been shown that these proteins contain proline and tyrosine residues at the end of their sequence (Lange et al., 2008).

Ternary complex consisting of cargo protein, importin-α and karyopherin-β1 or cargo protein karyopherin-β2 complex docks at the nuclear pore complex via interaction of karyopherin-β with nucleoporins residing on the cytoplasmic side of the NPC. After the complex traverse, the NPC, disassembly of cargo achieved by the binding of RanGTP (Moroianu et al., 1996; Rexach and Blobel, 1995). The RanGTP bound soluble transporter transported back into the cytoplasm (Arnold et al., 2006). The principle of nuclear export of protein is the same except the cargo displaying nuclear export signal is recognized by a different class of transporter called exportin and the fact that binding of cargo with nuclear export receptors requires the binding of Ran GTP (Matsuura, 2016). Exportin docks cargo complex to the nuclear basket of the nuclear complex, and the whole complex translocated to the cytoplasm (Matsuura, 2016). In the cytoplasm, RanGAP act on RanGTP to be converted into its GDP form for dissociation of the complex and RanGDP transported back to the nucleus to maintain high RanGTP concentration gradient (Christie et al., 2016).

1.4 Nucleolus

The nucleolus is a membrane-less structure organized around a tandem array of ribosomal DNA (rDNA) genes (Hernandez-Verdun et al., 2010). Electron microscopic observation revealed three distinct subcompartments named as a fibrillar center (FC), dense fibrillar centered (DFC), and granular center (GC) (Boisvert et al., 2007; Hernandez-Verdun et al., 2010). Though several non-canonical functions of nucleolus come into to picture, historically, the nucleolus is associated with the biogenesis of protein, translating machinery called ribosomes (Boisvert et al., 2007).

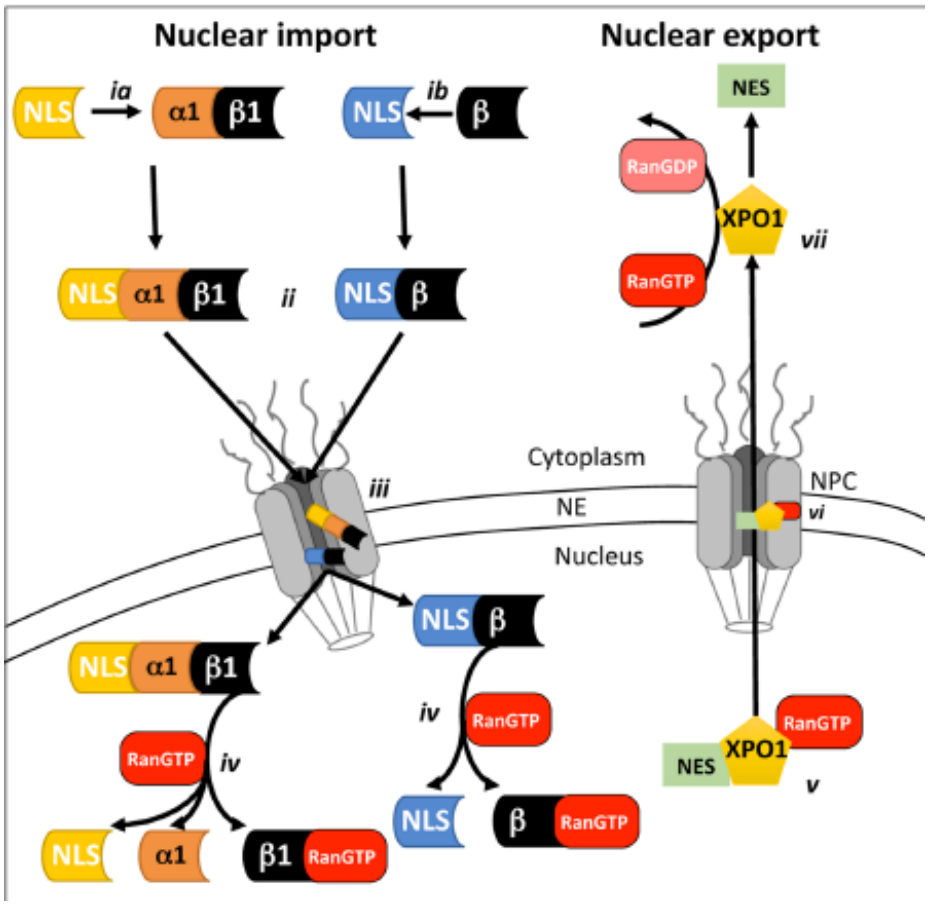

Fig. 1.6 Schematic illustration of the cellular nucleocytoplasmic transport. Re printed from Caly et al., 2015 Front Microbiol. 14;6:848. (Publisher MDPI).

1.4.1 Nucleolus and ribosome biogenesis

The process of ribosome biogenesis involves coordinated activities of RNA polymerase I , RNA polymerase II, and RNA polymerase III (Ciganda and Williams, 2011; Martin et al., 2006). In addition to the three RNA polymerases, many transacting factors, such as small nucleolar RNA and non-ribosomal proteins, are involved in the process fig. 1.7 (Matera et al., 2007). Ribosome biogenesis starts with the transcription of 47S precursor ribosomal RNA (pre-rRNA) from ribosomal DNA (rDNA) using RNA polymerase I and associated transcription factors in the nucleolus. Concurrent to transcription or post-transcriptionally two important nucleotide modifications, namely 2'-O-ribose methylation and pseudouridylation carried out on selected nucleotide bases using conserved small nucleolar ribonucleoprotein containing methyltransferases and pseudouridylase respectively. The pre-rRNA transcript, in addition to the coding sequences of the mature rRNAs, consists of two external transcribed spacers at the 3' and 5' end and an internal transcribed spacer 1 and 2 (ITS1 and ITS2) flanked by the 5.8S rRNA. Besides base modification, 47S pre-rRNA undergoes processing, which involves the removal of internal and external transcribed spacer sequences resulting in the production of 28S, 18S, and 5.8S mature ribosomal RNAs. Ribosomal RNA encoding messenger RNA and 5S ribosomal RNA are transcribed in the nucleus using RNA polymerase II and RNA polymerase III, respectively. Ribosomal protein-encoding mRNA exported to the cytoplasm and translated products (ribosomal proteins) imported back to the nucleus and incorporated with rRNAs to form ribosomal subunits (Henras et al., 2015; Matera et al., 2017). In mammals, the ribosome comprises 40S (small) and 60S (large) ribosomal subunits. While 28S, 5.8S, 5S together with ribosomal protein form the 60S subunit, 18S rRNA, and its protein form the 40S subunits.

Generally, most of the process of ribosome biogenesis takes place in the nucleolus. While transcription of polycistronic RNA takes place at the junction of FC and DFC, modification, processing, and assembly processes take place in DFC and GC region of the nucleolus. Finally, the two subunits leave the nucleolus and exported to the cytoplasm, where it undergoes further maturation and formation of the 80S subunit (Boulon et al., 2010; Henras et al., 2015; Matera et al., 2007). Proteomic analysis of nucleolus indicates nucleolus possess more than 4500 resident proteins, of which only 30% of them linked with ribosome biogenesis role (Ahmad et al., 2009). Although reports indicate the involvement of nucleolus in various cellular processes (Boisvert et al., 2007), the role of the nucleolus as a sensor of nucleolar stress and its relationship in cell cycle control is well established (Boulon et al., 2010).

1.4.2 **Role of nucleolus as the sensor of nucleolar stress and cell cycle control**

The concept of nucleolar stress started since 2001, where Pestov and colleagues found that mutation in a nucleolar protein block of proliferation 1 (Bop1) interferes with the process of ribosome biogenesis. From that observation, they proposed that defects in ribosome biogenesis results in nucleolar stress leading to p53 dependent cell cycle arrest (Pestov et al., 2001). Later, Rubbi and miller undertook several studies and strengthened the concept of nucleolar stress (Rubbi and Milner, 2003). It is now well established that stress factors such as radiation, toxic agents that inflict DNA damage, nutrient depletion, hypoxia, and heat shock interfere with the process of ribosome biogenesis resulting in nucleolar stress (Boulon et al., 2010; Rubbi and Milner, 2003). The outcome in response to nucleolar stress can be DNA repair, cell cycle arrest or apoptosis which depend on the magnitude of damage (Chen, 2016), and the response can be mediated with or without the involvement of p53 (James et al., 2014).

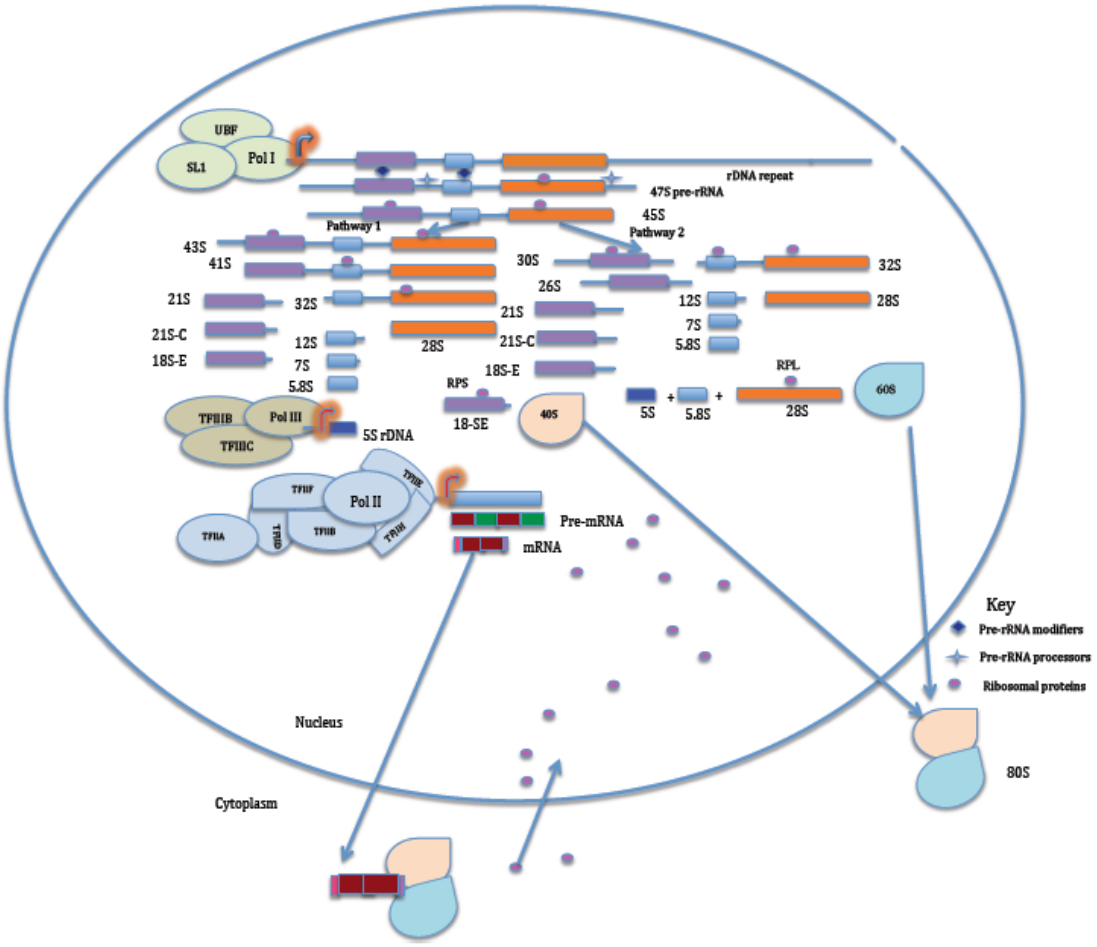

Fig. 1.7 |Schematic illustration of the process of ribosome biogenesis.

1.4.2.1 **Nucleolar stress and the role of p53 in the process**

P53, the guardian of the cell, plays a role in the protection of the cellular DNA (Lane, 1992). Under normal condition, the level of p53 is kept at low level by the action of mouse/human double minute 2 (MDM2/HDM2) protein which bind and facilitate its degradation by the proteasomal degradation system (Haupt et al., 1997; Kubbutat et al., 1997) as well as via binding and shielding its transcriptional activation function (Oliner et al., 1993). However, at times of stress, various players involved in the process of p53 activation, including protein-protein interaction that relief the suppressive action of its negative regulator MDM2 through mechanisms that allow selective translation of p53's mRNA as well as via posttranslational modification based enhancement of p53 activity. (Hafner et al., 2019).

The major players in protein-protein interaction-based activation of p53 are ribosomal proteins (Liu et al., 2016). During nucleolar stress, ribosomal proteins translocate from the nucleolus to the nucleoplasm, where they bind with MDM2 and increase free form of p53 where the later increase the translation of genes activated by p21 leading to cell cycle arrest or apoptosis (Deisenroth and Zhang, 2010; Zhang and Lu, 2009). Although the significance of interaction was not well established, the interaction of the ribosomal protein (RP) with MDM2 dates back in 1994 (Marechal et al., 1994). Currently, there is a growing list of ribosomal proteins involved in p53 activation via interacting with MDM2; however, most of them are targeted by the proteasomal degradation system (Kim et al., 2014; Lam et al., 2007). Among the ribosomal proteins RP5, RP11 alone or, more importantly as a complex with 5S RNA proven to have a significant effect in activating the p53 signalling pathway in response to nucleolar stress (Donati et al., 2013; Nicolas et al., 2016; Sloan et al., 2013). In agreement with this, unlike RP5 and RP11, depletion of most of the ribosomal proteins did not affect the

activity of p53 indicating the significant role of RPL5 and RPL 11 as mediators of p53 mediated nucleolar stress signalling pathway (Bursac et al., 2012). In addition to ribosomal proteins, other nucleolar proteins are known to translocate and activate p53 (Daniely et al., 2002; Yang et al., 2016).

One of the nucleolar proteins is a tumor-suppressive protein alternative reading frame (Arf), a protein normally sequestrated in the nucleolus via its interaction with another nucleolar protein nucleophosmin (Bertwistle et al., 2004). Arf transcription increases in response to oncogenes and release to the nucleoplasm and interact with MDM2, thereby stabilizing p53 (Palmero et al., 1998; Weber et al., 1999). Another nucleolar protein known to act as a mediator of nucleolar stress is nucleophosmin (Avitabile et al., 2011). Nucleophosmin is a multifunctional protein that involves in the various steps of ribosome biogenesis (Lindstrom, 2011). The protein directly interacts with p53 resulting in its stabilization and enhancing its transcriptional activity (Colombo et al., 2002). Besides to its direct action on p53, nucleophosmin interacts with MDM2 and counteracts its inhibitory action on p53 (Kurki et al., 2004). Similarly, nucleolin and nucleostemin, nucleolar proteins involved in the process of ribosome biogenesis (Romanova et al., 2009; Tajrishi et al., 2011), interact with MDM2/HDM2 and activate p53 (Dai et al., 2008; Saxena et al., 2006). In addition to MDM2 mediated activation of p53, ribosomal protein, such as RPL26, enhances the activity of p53 through a selective translation of p53 mRNA vial binding to its 5'-terminal oligopyrimidine tracts mRNA (Takagi et al., 2005). Another mechanism that influences p53 activity involves posttranslational modifications (Liu et al., 2019).

During stress, p53 undergoes posttranslational modification, including phosphorylation, acetylation, ubiquitination, SUMOylation, and NEDDylation (Kruse and Gu, 2008; Liu et al.,

2019; Meek and Anderson, 2009). Ubiquitination has an inhibitory role in p53 activity where mono and polyubiquitination involve in nuclear export and degradation of p53, respectively (Li et al., 2003). In response to genotoxic damage by radiation, p53 undergoes phosphorylation at multiple sites in particular in its N terminus region reviewed in (Moll and Petrenko, 2003). Such phosphorylation was shown to stabilize and enhance p53 transcriptional activity via weakening its interaction with MDM2 (Moll and Petrenko, 2003). Another posttranslational modification that enhances p53 activity is acetylation (Reed and Quelle, 2014). Acetylation via competitive occupation of the ubiquitination site as well as through interfering p53 association with MDM2 prevents p53 degradation (Li et al., 2002). In addition, acetylation also increases p53 activity by facilitating its transcription (Barlev et al., 2001). On the other hand, the effect of methylation on p53 activity is determined by the site of modification (Chuikov et al., 2004). Two ubiquitination-like modifications, SUMOylation and NEEDylation, reported modifying p53 activity (Kruse and Gu, 2008). Though NEDDylation shown to positively regulate p53, the effect of SUMOylation on p53 activity is not conclusively established (Abida et al., 2007).

1.4.2.2 **Nucleolar stress-mediated independent of p53**

Although most of the outcomes of nucleolar stress are mediated mainly involving p53, there are reports where nucleolar stress outcomes managed independently of p53 (James et al., 2014). It has been shown that in p53 silenced cells, interference with pol I transcription machinery end up in cell cycle arrest, mediated by phosphorylation of pRB and down-regulation of genes activated by E2F transcription factor 1 (E2f1) (Donati et al., 2011). In cells treated with 5-fluorouracil, extracellular signal-regulated kinases (ERK)-mediated phosphorylation of RPL3

and specificity protein 1 (SP1) enhance their binding to p21 promoter activating expression of p21, leading to cell cycle arrest and apoptosis without involving p53 (Pagliara et al., 2016).

2.0 Hypothesis and objectives

2.1 The rationale of the hypothesis

Bovine adenovirus-3 (BAdV-3) is one of the potential viral vectors for use in human as well as veterinary vaccination. The development of an efficient BAdV-3 viral vector needs detailed knowledge about the biology of BAdV-3. For better understanding of the basic biology of BAdV-3, we and others have begun to determine the protein-protein interaction involving both BAdV-3 non-structural and structural proteins, and its biological significance in BAdV-3 life cycle (Ayalew et al., 2016; Gaba et al., 2018; Kulshreshtha et al., 2004; Kulshreshtha and Tikoo, 2008; Makadiya, 2013; Makadiya et al., 2015; Paterson, 2010; Paterson et al., 2012; Said et al., 2018a; Zhao, 2016). Despite having a similar genomic organization, BAdV-3 exhibits distinct features compared to human adenoviruses (Reddy et al., 1998; Li et al., 2009). The present study focuses on BAdV-3 IVa2 that would potentially contribute to the better understating of the viral biology and hence to the design of better viral vector.

2.2. Hypothesis

Given the conserved nature IVa2 in the family of Adenoviridae and its multifunctional role in human adenoviruses, we hypothesize that IVa2 of BAdV-3 is indispensable for the BAdV-3 life cycle and involves protein-protein interaction to accomplish its role.

2.3 Objectives

The objectives of this study are:

1. To characterize of IVa2 of BAdV-3
2. To identify other BAdV-3 proteins that interact with IVa2
3. To determine significance of IVa2 in the BAdV-3 lifecycle.

3.0 NUCLEAR AND NUCLEOLAR LOCALIZATION OF BOVINE ADENOVIRUS-3 IVA2

3.1 Introduction

Bovine adenovirus-3 (BAdV-3), a non-enveloped icosahedral virus, contains a double-stranded DNA genome of 34446 bp (Reddy et al., 1998). Despite having similar genomic organization into early, intermediate and late regions, the BAdV-3 late transcriptional unit organized into seven (L1-L7) regions (Reddy et al., 1998) instead of five (L1-L5) regions reported in human adenovirus (HAdV)-5, In addition, several unique features reported for other regions of BAdV-3 including E3 region, E4 region, location of cis-acting packaging signals and E1A promoter (Bangari and Mittal, 2006; Idamakanti et al., 1999; Reddy et al., 1998; Xing and Tikoo, 2006, 2007; Xing et al., 2003).

Since assembly of progeny adenovirus occurs in the nucleus of cell and involves encapsidation of viral genome into capsids (Cassany et al., 2015; Condezo and San Martin, 2017), the formation of viral capsids in the nucleus require transport of newly synthesized adenovirus proteins from cytoplasm to the nucleus of infected cells (Ding et al., 2010; Tessier et al., 2019). Transport of macromolecules including viral proteins between cytoplasm and nucleus requires viral proteins to pass through nuclear pore complex (NPC), which acts as a gatekeeper for import or export of macromolecules including proteins from the nucleus (Lin and Hoelz, 2019). Transport of proteins to the nucleus can occur passively or actively depending upon the size of the protein and presence\absence of NLS (Lin and Hoelz, 2019). Although surface characteristics of protein including introduction of hydrophobic residues can help larger proteins (70 kDa-110 kDa) devoid of nuclear localization signal (NLS) to cross

NPC passively (Frey et al., 2018; Naim et al., 2009), usually proteins larger than 40 kDa and devoid of NLS cannot passively diffuse in the nucleus (Samudram et al., 2016).

While active nuclear localization of viral proteins require interaction of nuclear localization signals (NLSs) of transported protein with importins and transportin 3 receptors in the cell, the translocation of viral proteins to nucleolus require the interaction of nucleolar localization signals (NoLSs) of a protein with bonafide nucleolar protein(s) or rRNA so that viral protein retained in the nucleolus of the cell (Reed et al., 2006).

The intermediate region of HAdV-5 encodes structural proteins pIX and IVa2 (Parks, 2005). Protein IVa2 presented as few copies per virion (Russell, 2009) and expressed as 50 kDa and 40 kDa protein in virus-infected cells (Pardo-Mateos and Young, 2004), and contains Walker A and B motifs required for binding ATP (Ostapchuk and Hearing, 2008). Although the role of HAdV-5 IVa2 in adenovirus DNA packaging is not clear, it may act as adenovirus packaging ATPase (Ostapchuk et al., 2011). In addition, IVa2 appears to act as a transcriptional activator of the HAdV-5 major late promoter (Lutz and Kedinger, 1996). Although viral protein homologs are present in all members of Mastadenovirus genomes, they appear be less conserved in protein function, use of protein domains\]motifs for subcellular localization and interaction with other viral\cellular proteins (Blanchette et al., 2013; Cheng et al., 2013; Stracker et al., 2005). Since BAdV-3 IVa2 shows 29 to 69% homology with IVa2 encoded by other members of Mastadenovirus (Reddy et al., 1998), we sought to characterize BAdV-3 IVa2, a protein of 448 amino acids. Here, we report the identification of BAdV-3 IVa2 domain(s) involved in nuclear \ nucleolar localization.

3.2 Materials and Methods

3.2.1 Cell lines and Viruses

Madin-Darby bovine kidney (MDBK) (ATCC CCL22), cotton rat lung (CRL), (Papp et al., 1997) and VIDO DT1 (CRL cells expressing endonuclease I-SceI) cells were propagated at 37°C in minimal essential medium (MEM; Sigma) with 5% CO_2. The HEK 293T (ATCC CRL-11268) and African green monkey kidney (Vero) (ATCC CCL-81) cells cultured using Dulbecco's modified minimal essential medium (DMEM; Sigma). All the cell lines supplemented with heat-inactivated 10% fetal bovine serum (FBS; SAFC industries, Sigma), 0.1mM nonessential amino acids (NEAA; Gibco), and 10mM HEPES (Gibco) and 50ug/ml gentamicin (Bio Basics). Wild type and recombinant BAdV-3 viruses propagated as described previously (Reddy et al., 1998).

3.2.2 Antibodies

Anti-replication protein A (RPA) MAb (sc-48425) purchased from Santa Cruz. Anti-HA antibody (A1978) and anti-actin β antibody (H9658) obtained from Sigma. Alexa 488 goat anti-mouse antibody (catalog # 115-545-003) and Cy3 conjugated goat-anti mouse antibody (# 115-165-146) and alkaline phosphatase-conjugated goat anti-rabbit (111-055-003) antibody bought from Jackson Immune Research. Rabbit anti-GST antibody (ab19256) and Alexa Fluor 647-conjugated goat anti-rabbit IgG were also obtained from Abcam and Invitrogen, respectively.

3.2.3. Sequence analysis of BAdV-3 IVa2

Initially, to assess the extent of sequence similarity between BAdV-3 IVa2 protein and IVa2 protein of adenoviruses isolated from different domestic animals and humans, multiple sequence alignment were carried out using Clone manager version 9.3 (BLOSUM 62). Besides, the presence of potential nuclear localization signal/s of IVa2 was assessed using cNLS mapper (Kosugi et al., 2009a).

3.2.4 Production of BAdV-3 IVa2 serum

The GST.IVa2 fusion produced and characterized as described earlier (Kulshreshtha and Tikoo, 2008; Said et al., 2018b). Briefly, a 1363 bp DNA fragment containing BAdV-3 IVa2 coding sequence amplified by PCR (using forward EcoRI FP and XhoI RP primers and plasmid pC.Va2 DNA as a template, appendix 1). The PCR product digested with *EcoRI* - *XhoI* and ligated to *EcoRI* - *XhoI* digested plasmid pGEX-5x-1 (GE Healthcare) DNA creating plasmid pGEX-IVa2. The junction of IVa2 and Glutathione-S-transferase (GST) fusion protein confirmed by DNA sequencing. For the production of GST IVa2 fusion production, *E. coli* (BL-21) transformed with pGEX-IVa2 DNA and plated out in Luria-Bertani (LB) plate containing 100ug/µl of ampicillin (Sigma). A single colony of BL21 cell transformed with pGEX-IVa2 inoculated in 14 mL culture tube containing 3mL of LB broth added with 50µg/µl kanamycin and 100ug/µl of ampicillin (Sigma). After overnight incubation, the 3 mL culture used to inoculate 500mL LB broth in the presence of the kanamycin and ampicillin as described. The culture allowed to grow at 37°C on a rotary shaker until the OD600 value reaches 0.6. Then, Fusion protein expression induced with the addition of 0.5mM isopropyl-β-D-thiogalactopyranoside (IPTG; Sigma). After 2hr incubation, cells were pelleted by

centrifugation at 6,000 RPM for 15 min. The cell pellet was then resuspended in 30mL of Glutathione S-transferase (GST) binding buffer in the presence of protease inhibitor cocktail (Roche) transferred into a 50mL disposable tubes and sonicated three times for 30 seconds under cold condition. The Sonicated sample was transferred into 50mL Nalgene polycarbonate tube and centrifuged at 12,000 RPM for 15 min at 4^0C. The supernatant was further centrifuged under the same condition after being transferred into similar tubes. Finally, 200ul of prewashed GST beads (GE health care) added to the supernatant, and the mixture was incubated overnight on a nutator at 4^0C. After overnight incubation, beads were washed 4X (10 min each) using GST binding buffer and pelleted at 1000 RPM for 2 min. After the final wash, beads were transferred into 1.5 mL Eppendorf tube, and protein was eluted by incubating beads for 20min with the addition of 200ul of elution buffer. Elution was repeated using a similar volume of buffer. In the end, the protein concentration of eluted protein measured by Bradford assay (Bio-Rad) and Libra S22UV/Vis Spectrophotometer (Biochrom). Expression of GST IVa2 fusion protein was confirmed via coomassie brilliant blue G250 (Bio-Rad) staining and through western blotting using Rabbit anti-GST antibody.

Rabbit immunized intradermally with 500ug of purified GST.IVa2 fusion protein emulsified with Freund's complete adjuvant (Sigma). The immunized rabbits boosted twice with 300ug GST.IVa2 fusion protein emulsified in Freund's incomplete adjuvant (Sigma) subcutaneously at 21 and 35 days post-primary immunization. Two weeks after the last immunization, serum was collected, aliquoted, and stored at -80^0C.

3.2.5 Plasmid construction

Plasmids used to study a) the subcellular localization of IVa2 and map regions of IVa2 involved in the nuclear and nucleolar localization of IVa2, b) the effect of amino acid substitution on the localization of IVa2 and c) the nuclear import pathway of IVa2 were constructed using standard molecular techniques as described earlier (Sambrook and. Russell, 2000) and are described in Appendix 1.

Construction of plasmids containing full length BAdV-3 genomic DNA. The primers sequences used to construct plasmids are described in Table 1, Appendix 1.

pMCS.3821. Initially, a 7162 bp *Aar*I DNA fragment containing the IVa2 coding sequence was isolated by the digestion of plasmid pUC304a+ DNA with *AarI*. Finally, a 3821 bp *Sph*I-*Sac*II DNA fragment (containing IVa2 coding sequence flanked by 1463 bps and 1022 bp) of 7162 bp DNA fragment was isolated and ligated to *Sph*I - *Sac*II digested plasmid pMCS (Thanbichler et al., 2007) DNA creating a plasmid pMCS.3821.

pUC304a.dIVA2SbfI. Using *Sph*I FP and IRPΔIVa2 primers (Table 1), and plasmid pMCS.3821 DNA, as a template, a 1501 bp DNA fragment (P1), was amplified by PCR. Similarly, using primers IFPΔIVa2 and SacII RP (Table 1), and plasmid pMCS.3821 DNA as a template, a 1286 bp DNA fragment (P2) was amplified by PCR. The P1 and P2 DNA fragments were annealed, and a, 2635 bp DNA fragment was amplified by PCR using SphI FP and SacII RP as primers (Table 1). The 2635 bp DNA fragment was digested with *Sph*I -*Sac*II and ligated to *Sph*I-*Sac*II digested plasmid pMCS DNA, creating plasmid pMCS.3821.dIVA2SbfI *(Sbf*I restriction site introduced). A 1240 bp *Sbf*I DNA fragment of plasmid pUKC4K (Taylor and Rose, 1988) containing Kanamycin resistant gene was isolated

and ligated to *Sbf*I linearized plasmid pMCS.3821dIVA2*Sbf*I DNA creating plasmid pMCS.3821.dIVA2Kan.

Homologous recombination in *Escherichia coli* BJ5183 (Chartier et al., 1996) between 3860 bp *Sph*I - *Sac*II DNA fragment of plasmid pMCS.3821dIVA2Kan and pUC304a+ (Du and Tikoo, 2010) DNA resulted in creating plasmid pUC304a.dIVA2Kan which could grow in LB plates containing ampicillin and kanamycin. The plasmid pUC304a.dIVA2Kan was digested with *Sbf*I, and the large fragment was religated, resulting in creating plasmid pUC304a.dIVA2SbfI (*plasmid pUC304a+ containing unique SbfI site in IVa2).*

pUC304aM1. Using primers SphI FP and IRP6M (Table 1), and plasmid pMCS.3821 DNA as a template, a 2814 bp DNA fragment (P1) was amplified by PCR. Similarly, using primers IFP 6M and SacII RP, and plasmid pMCS.3821 DNA as a template, a1064 bp DNA fragment (P2) was amplified by PCR. The P1 and P2 DNA fragments were annealed, and a 3836 bp DNA fragment was amplified by PCR using primers SphI FP and SacII RP (Table 1). The 3836 bp DNA fragment was digested with *Sph*I-*Sac*II and ligated to *Sph*I-*Sac*II digested plasmid pMCS DNA creating plasmid pMCS.3821.RM (*containing a substitution of 6th amino acid of IVa2 from R to G).*

Escherichia coli BJ5183 based homologous recombination between 3821 bp *Sph*I-*Sac*II DNA fragment of plasmid pMCS.3821.RM and *Sbf*I digested plasmid pUC304a.dIVA2.SbfI (described above) resulted in the isolation of plasmid pUC304aM1 (*pUC304a+ containing a substitution of 6th amino acid of IVa2 from R.to G).*

pUC304aM2. Using primers SphI FP and IRP7M (Table 1), and plasmid pMCS.3821 DNA as a template, a 2831 bp DNA fragment (P1), was amplified by PCR. Similarly, using primers IFP7M and SacII RP (Table 1), and plasmid pMCS.3821 DNA as a template, a 1052 bp DNA

fragment (P2), was amplified by PCR. The P1 and P2 DNA fragments were annealed and a 3836 bp DNA fragment was amplified by PCR using primers *Sph*I FP and *Sac*II RP (Table 1). The 3836 bp DNA fragment was digested with *Sph*I-*Sac*II and ligated to *Sph*I-*Sac*II digested plasmid pMCS DNA creating plasmid pMCS.3821.R2M *(containing a substitution of 7th amino acid of IVa2 from R to G).*

Escherichia coli BJ5183 based homologous recombination between 3821 bp *Sph*I-*Sac*II DNA fragment of plasmid pMCS.3821.R2M and *Sbf*I linearized plasmid pUC304a.dIVA2.SbfI (described above) DNA resulted in the isolation of plasmid pUC304aM2 (*pUC304a+ containing a substitution of 7th amino acid of IVa2 from R to G).*

pUC304aM3. Using primers SphI FP and IRP8M (Table 1), plasmid pMCS.3821 DNA as a template, a 2831 bp DNA fragment (P1), was amplified by PCR. Similarly, using primers IFP8M and SacII RP (Table 1), and plasmid pMCS.3821 DNA as a template, a 1052 bp DNA fragment (P2), was amplified by PCR. The P1 and P2 DNA fragments were annealed, and a 3836 bp DNA fragment was amplified by PCR using primers SphI FP and SacII RP (Table 1). The 3836 bp DNA fragment was digested with and ligated to *Sph*I-*Sac*II digested plasmid pMCS DNA, creating a plasmid pMCS.3821.KM (*containing a substitution of 8th amino acid of IVa2 from K to G).*

Escherichia coli BJ5183 based homologous recombination between 3821 bp *Sph*I-*Sac*II DNA fragment of plasmid pMCS.3821.KM and *Sbf*I linearized plasmid pUC304a.dIVA2SbfI (described above) DNA resulted in isolating plasmid pUC304aM3 (*pUC304a+ containing substitution of 8th amino acid of IVa2 from K to G)*

pUC304aM4. Using primers SphI FP and IRP6-8M (Table 1), and plasmid pMCS.3821 DNA as a template, a 2831 bp DNA fragment (P1), was amplified by PCR. Similarly, using

IFP6-8M and SacII RP (Table 1), and plasmid pMCS.3821 DNA as a template, a 1052 bp DNA fragment (P2) was amplified by PCR. Using primers SphI FP and SacII RP, and The P1 and P2 DNA fragments were annealed, and a 3836 bp DNA fragment was amplified using primers SphI FP and SacII RP (Table 1). The 3836 bp DNA fragment was digested with *Sph*I-*Sac*II and ligated to *Sph*I-*Sac*II digested plasmid pMCS DNA creating plasmids pMCS.3821.RRK *(containing a substitution of 6th, 7th & 8th amino acid of IVa2 from RRK to GGG).*

Escherichia coli BJ5183 based homologous recombination between 3821 bp *Sph*I-*Sac*II DNA fragment of plasmid pMCS.3821.RRK and *SbfI* linearized pUC304a.dIVA2SbfI (described above) DNA resulted in the isolation of plasmid pUC304aM4 *(pUC304a+ containing a substitution of 6th, 7th & 8th amino acid of IVa2 from RRK to GGG).*

***pMCS.loxpIVa2 448*.** Using primers SphI FP and IRP loxp448, and template DNA pMCS-3821 1508 bp PCR product (P1) amplified. Similarly, using primers IFPloxp448 and SacII RP, and template DNA pMCS.3821 2134 bp PCR product (P2) generated. Using primers SphI FP and SacII RP, and P1 and P2 DNA mix as a template 3606 bp PCR product (P3) generated. SphI-SacII digested P3 ligated into SphI-SacII digested pMCS, creating a plasmid pMCS.loxpIVa2448 (loxp sequence introduced at the end of IVa2).

pUC304A.loxpIVa2C.75. Using primers SphI FP and IRP loxp373, and plasmid pMCS-loxpIVa2448 DNA as a template, *a* 1777 bp DNA fragment (P1) was amplified by PCR. Similarly, using primers IFP loxp373 and SacII RP, and plasmid pMCS.loxpIVa2 448 DNA as a template, a 2171 bp DNA fragment (P2) was amplified by PCR. The P1 and P2 DNA fragments were annealed and a 3912 bp DNA fragment was amplified by PCR using primers SphI FP and SacII RP (Table 1). The 3912 bp DNA fragment was digested with *Sph*I-*Sac*II and

ligated to *Sph*I-*Sac*II digested plasmid pMCS, creating a plasmid pMCS.3821loxp.IVa2C.75 (*loxP flanked IVa2 nucleolar localization signal).*

Escherichia coli BJ5183 based homologous recombination between 3896 bp *Sph*I-*Sac*II fragment of plasmid pMCS.loxpIVa2C.75 and *Sbf*I linearized plasmid pUC304a.dIVA2SbfI DNA resulted in isolation of plasmid pUC304a.loxpIVa2C.75 (*pUC304a+ containing loxP flanked IVa2 nucleolar localization signal).*

3.2.6 Transfection

For transfection of cells plasmid DNA of interest or full-length genomic clones, an appropriate amount of DNA diluted with the corresponding amount of optimum in one tube. Similarly, the recommended volume of lipofectamine 2000 diluted with the corresponding amount of optimum in another tube. Diluted DNA sample mixed with lipofectamine solution and incubated for five to ten minutes. After incubation, the DNA lipofectamine mixture added into a culture dish or slides in a dropwise manner. Based on the sensitivity of cells for lipofectamine, the transfection medium replaced with culture medium after 4 to 8 hrs.

3.2.7 Isolation of recombinant BAdV-3 viruses

Isolation of recombinant BAdV-3 carried out in VIDODT1 cells (Du and Tikoo, 2010) or CRL cells as described earlier in (Zhao and Tikoo, 2016). VIDODT1 cells grown in 6 well tissue culture dish transfected with 5ug of indicated plasmid DNA using lipofectamine 2000. Alternatively, CRL cells grown in 6 well culture dishes transfected with *PacI* digested indicated plasmid DNA using lipofectamine 2000. After 4 hrs of transfection, the transfection medium was replaced with MEM containing 5% fetal bovine serum and the cells were

incubated at 37^0C in the presence of 5% CO_2. The medium was replaced with MEM containing 2% fetal bovine serum) every 48 hrs and the cells were observed for the appearance of cytopathic effect.

3.2.8. Western blotting

Western blotting was carried out as described in (Kulshreshtha et al., 2004) with slight modification. At indicated times post infection or transfection, the cells were rinsed with ice-cold PBS, collected and lysed after the addition of the appropriate amount of radioimmunoprecipitation assay (RIPA) buffer in the presence of protease inhibitor cocktail (Roche) for 30 min at 4^0C. The cell lysate was then separated by centrifugation at 12000 revolutions per minute (RPM) for 15 minutes. The supernatant was collected, mixed with sodium dodecyl sulfate (SDS) loading buffer containing 10 % β-mercaptoethanol and boiled for 5 minutes. The proteins in the mixture were resolved using 12% sodium dodecyl sulfate polyacrylamide gel electrophoresis (SDS-PAGE) and transferred to nitrocellulose membranes (Bio-Rad). The membrane was blocked with 5% skim milk in 1x tris buffered saline containing 1% tween 20 (TBST) for 1hr. Following blocking, the membranes were rinsed with 1x TBST and incubated with anti primary antibody of interest for 2hrs on a shaker at room temperature or overnight at 4 ^{0}C. Following a repeated wash with 1x TBST, the membranes further incubated with appropriate secondary antibody conjugated alkaline phosphatase for 1.5 hrs After washing, the membranes were developed using BCIP/NBT solution (Sigma) to visualize protein bands.

3.2.9. Immunofluorescence assay

Direct immunofluorescence. About $1X10^5$cells transfected grown in 4-well chamber slides, Thermo Scientific (Cat #, 1256517) transfected with individual plasmid DNA using LipofectamineTM 2000 [Invitrogen]) as per manufacturer's instructions. After 36 hrs post-transfection, the cells fixed with a 3.7% formaldehyde solution in 0.1M PBS and mounted using mounting media (Vectashield) containing 4', 6-diamidino-2-phenylindole (DAPI) and examined using Zeiss LSM 5 Laser scanning confocal microscope.

Indirect immunofluorescence assay. The protocol in virus-infected or plasmid transfected cells described earlier (Ayalew et al., 2014). Briefly, MDBK cells infected with BAdV-3 (MOI of 2) or Vero cells transfected with individual plasmid DNA using LipofectamineTM 2000 [Invitrogen]) as per manufacturer's instructions and incubated for 36 hrs. Thirty-six hrs post-infection or transfection, growth medium removed, cells rinsed with PBS and fixed with 3.7% paraformaldehyde for 15 minutes. After fixation, cells rinsed with PBS and permeablized with 0.25% Triton X-100 for 10 minutes at room temperature. After permeabilization, cells rinsed with PBS and incubated with 5% goat serum for an hour to block non-specific binding of antibodies. Following blocking, cells incubated with a primary antibody of interest for two hours. After 3x wash (10 minutes each) with PBS, cells further incubated with corresponding secondary antibody for 1.5 hrs At last, after repeated wash with PBS, slides allotted to dry, and coverslips then mounted on glass slides with VectaShield mounting medium containing 4', 6-diamidino-2-phenylindole (DAPI) as a nuclear counterstaining. Finally, images visualized using a Leica confocal microscope.

3.2.10. *In-vitro* nuclear import assay

In vitro nuclear import assay was carried out as described earlier (Wu and Tikoo, 2004). Briefly, Vero cells in two well chamber slides were transfected with the control plasmid (pCMVGFP/βgal) DNA, plasmid pGFP/bgal1.NLS (GFP/Bgal fused with N-terminus 1-25 amino acids of IVa2) DNA or plasmid pGFP/bgal1.NLS1 (GFP/Bgal fused with N-terminus 4-18 amino acids of IVa2) DNA (Appendix1). Twenty-four hrs post-transfection, the slides were processed for direct confocal microscopic observation.

3.2.11 GST pull-down assay

The GST pull-down assay performed as described previously (Paterson et al., 2012; Said et al., 2018a; Zhou and Tikoo, 2001) to assess the interaction of BAdV-3 IVa2 with nuclear transport proteins. GST fusions of importin α1, α3, α5, α7 and importin β were obtained from Dr. M. Köhler and described in (Depping et al., 2008). GST-transportin phusion plasmid also a gift from Dr. Woan-Yuh Tarn and described in (Lai et al., 2001). The production of GST or GST fusion protein carried out as described elsewhere (Said et al., 2018a). Invitro transcribed, translated and radiolabeled full–length IVa2, IVa2 with N-terminus 25 amino acid, GFP/Bgal containing inframe fusion of N-terminus 25 or N terminus 4-18 amino acid of IVa2 or protein produced by in-vitro transcription and translation of plasmid pC.IVa2 DNA using TNT T7 Coupled Reticulocyte Lysate System (Promega) in the presence of [35S]-methionine (Perkin Elmer). Fifteen μgs of purified GST or GST fusions (GST fused to importin- α-1, α-3, α-5, α-7, β1 or transportin-3) were incubated individually with 20μl of prewashed glutathione sepharose beads plus 10μl of in-vitro synthesized IVa2. The mixture was incubated overnight at + 4^0C on a nutator. The beads were washed three times (10 min each) with GST binding buffer, boiled

for 5 min in the presence of boiled in 2x SDS loading buffer containing 5% β-mercaptoethanol and the radiolabeled proteins resolved using 12% SDS-PAGE. Subsequently, the gel was fixed in fixative solution (methanol, acetic acid, and water mixed in 50:10:40 ratio respectively) for 30min, dried onto filter paper at 80^0C for 2hrs and visualized using F-X Molecular Imager (Bio-Rad).

3.2.1.2 Virus purification

The recombinant BAdV-3s were purified by CsCl gradient centrifugation as described earlier (Gaba et al., 2018). Briefly, freshly confluent monolayers of MDBK cells in multiple T-150 flasks were infected individually with BAV304a or mutant virus at MOI of 5. After 48 hrs of infection, the cells were collected and resuspended in 10 ml of culture medium. After repeated (4X) freeze thawing, the supernatant was collected, loaded on top of pollyallomer tube containing CsCl density gradient and subjected to ultracentrifugation at 35 000 rpm for 1 hr at 4^0C. The bands containing viruses were collected, and subjected to a second round of CsCl density gradient centrifugation at 35 000 rpm for 16 hrs at 4^0C. Finally, the virus band was collected, dialyzed and stored in small aliquots at -80°C.

3.2.13 Virus growth kinetic determination

Gowth kinetics of recombinant BAdV-3 was determined as described earlier (Kulshreshtha et al., 2004, Gaba et al., 2017). Briefly, MDBK cells were infected with individual virus at 2 MOI. At different times (0, 6, 12, 24, 36 and 48) post infection, the infected cell lysates were collected, freeze thawed and virus was titrated on MDBK cells in 96 well culture plates. After 5-7 days post infection, the cells were observed for the appearance of fluorescent foci. The data obtained was used to determine the viral titer using $TCID_{50}$ (Reed and Muench, 1938).

3.3 Results

3.3.1 Sequence analysis of IVa2

Multiple sequence alignment of BAdV-3 IVa2 protein sequence with its homologs encoded by different adenoviruses carried out as indicated in Fig. 3.1a. Except the highly conserved middle portion of IVa2, which corresponds to the different ATPase motifs (Ostapchuk and Hearing, 2008), N- and C- terminus of IVa2 shows a lower degree of similarity with the IVa2 encoded by members of Mastadenovirus genus. Secondly, analysis of BAdV-3 IVa2 protein sequence by cNLS mapper program predicted the presence of potential nuclear localization signals (NLSs) located at amino acid 6-35 and amino acids 64-73 Fig. 3.1b).

3.3.2 Expression of BAdV-3 IVa2

To characterize BAdV-3 pC.IVa2 protein, affinity-purified GST-IVa2 fusion protein (Fig. 3.2, panel a, b) expressing 448 amino acids of IVa2 used to produce anti-IVa2 serum in rabbits. The specificity of the sera (designated as IVa2gst sera) collected and analyzed after the last boost. Infected MDBK cells (MOI 2) also analyzed by Western blot using IVa2gst sera. As seen in Fig. 3.2 (panel c), IVa2gst serum detected a protein of 50 kDa in BAdV-3 infected cells. No such protein could be detected in mock-infected cells. Moreover, the expression of IVa2 could be detected at 24-48 hrs post-infection but not at 18 hrs post-infection (Fig.3.2, panel d).

a)

```
  1  MDTR-GRRK--VRHQQAQPEALAGQQTDASAALHGHRDDPGEDAQALERPHPAGHRPSPSRPLQQQPPQP  BAdV-3
  1  MEQRAGEPA--LSHQPPEFKTDPRYEPKQRGPVHSHRNNFNAHSEALERQDPCRHRRPPPDALLEKQPKP  OAdV-A
  1  METK-ARKRH-LQHQPPQPQEDPGHRAAPDRPLHRHRDHPHAGPPALEGPDPPPARRPPPRSVLTQQPQP  PAdV-3
  1  MEEKAGLGR--LQNQQDEPAQDPHQRAGPRATFHSDRNHPNKEAEAMEGQNPACSRHASSHSIQPQASKP  CAdV-A
  1  METR-GRRPAALQHQQDQPQAHPGQRAARSAPLHRDPDYADEDPAPVERHDPGPSGRAPTTAVQRKPPQP  HAdV-2
  1  METR-GRRPAALQHQQDQPQAHPGQRAARSAPLHRDPDYADEDPAPVERHDPGPSGRAPTTAVQRKPPQP  HAdV-5

 68  KKQRAMLDGDVLDHVSELWDKCALMQQCLESMPMAEGLKPLRHFSSLDELLAMGGATLLNALSDYNQAIR  BAdV-3
 69  KKQRCMLDDTAVEHVKELWDKLSVLNKSLKAMPYSEGLKPLECFSSFDHLMSLAGQSLLQSLARDNVVIR  OAdV-A
 69  EKQPDLLEDDTVGHVTELWERMRVLHQALQDMPYAEGLKPLKAFASLSHLLSLGGRHLLQDLVQENRNLR  PAdV-3
 69  KKHRNYLDGAAVDDLKSLWDRLQTLQQSLTNMPYAEGLKPLKNFASFEELLSMGGDSLLNDLLDIQDSIT  CAdV-A
 70  AKRGDMLDRDAVEHVTELWDRLELLGQTLKSMPTADGLKPLKNFASLQELLSLGGERLLAHLVRENMQVR  HAdV-2
 70  AKRGDMLDRDAVEQVTELWDRLELLGQTLKSMPTADGLKPLKNFASLQELLSLGGERLLADLVRENMRVR  HAdV-5

138  DAMNATMPYLRPDGSCKSLNFTMQPVIGVVYGPTGCGKSQLLRNLMSTGLIQPPPETVFFIVPQVDMIPP  BAdV-3
139  DMLNKCSPYLTQQGSCKSINFQMQPVIGVVYGPTGCGKSQLLRNIISTQLLTPPPETVFFIVPQIDMIPP  OAdV-A
139  DTLNACMPFLTPAGTCRSLNYQVQPVIAVIYGPTGSGKSQLLRNLISSQLLSPPPETVFFITPQVDMIPP  PAdV-3
139  QCCMKVSKYLNKDGSCASLNYYKQPFIAAVYGPTGCGKSQLLRNLMSAQLIVPAPETVFFITPQVDMIPP  CAdV-A
140  DMLNEVAPLLRDDGSCSSLNYQLQPVIGVIYGPTGCGKSQLLRNLLSSQLISPTPETVFFIAPQVDMIPP  HAdV-2
140  DMLNEVAPLLRDDGSCSSLNYQLHPVIGVIYGPTGCGKSQLLRNLLSSQLISPTPETVFFIAPQVDMIPP  HAdV-5

208  QELLAWETQICEGNYTPGPTGTLVPQSSTLKPAFKIMSYEDLTMDYNYDVAHPQNVFAQAAKTGPIAIIM  BAdV-3
209  QEMSAWETQICEGNYVIGEQGTLIPQSGSLLPEFIKMSYADLTQEFNYDLSDPRNVFAKAASKGPIAIIL  OAdV-A
209  QEVVAWETQICEGNYRSGPDHTLIPQTATLMPDFVRMSYQDLMQEHNYDVTDSRNVFARAAARGPIAIVL  PAdV-3
209  QEIAAWETQICEGNFLAGPENTVVPQSGSIMPKFVQMSYAELTNEANYDVTNPTNVFARAASKGPLAIVM  CAdV-A
210  SELKAWEMQICEGNYAPGPDGTIIPQSGTLRPRFVKMAYDDLILEHNYDVSDPRNIFAQAAARGPIAIIM  HAdV-2
210  SELKAWEMQICEGNYAPGPDGTIIPQSGTLRPRFVKMAYDDLILEHNYDVSDPRNIFAQAAARGPIAIIM  HAdV-5

278  DECMEDLGRHKAISKFFHAFPSKLHDKFPKCTGYSVFVVLHNMNPRKDLGGNIANLKIQAKLHLISPRMH  BAdV-3
279  DECMEDMGNHKGIAKFFHAFPSKLHDRFPKCTGYAVLVVLHNMNPRKDHAGNISNLKIQAKLHIISPKMQ  OAdV-A
279  DECMEDLGGHKGVAKFFHAFPSKLHARFPRCTGYAVLVVLHNMNPRRDQSGNISNLKIQAKYHIMSPLMQ  PAdV-3
279  DECMEDLGGNRGIAKFFHAFPSKLLDRFPKCTGYSVIVVLHNMNPRRDQGGNIANLKIQAKMHIISPKVH  CAdV-A
280  DECMENLGGHKGVSKFFHAFPSKLHDKFPKCTGYTVLVVLHNMNPRRDMAGNIANLKIQSKMHLISPRMH  HAdV-2
280  DECMENLGGHKGVSKFFHAFPSKLHDKFPKCTGYTVLVVLHNMNPRRDMAGNIANLKIQSKMHLISPRMH  HAdV-5

348  PSQLNRFINTYTKSLPLPITLLLKDIFSFHAQHSQYDWIIYNTLPPHESLQWLYLNPSEGLMPMYLNIHA  BAdV-3
349  PSQLNRFINSYTKGLPLPISLLLKDIFNYHKTHSQYDWIVYNTCPEVEAFQWSYLHPTEGLVPMYLNVQC  OAdV-A
349  PAQVNRFINAYTKGLPTAISLLLKDIFNHHRNQNAYDWIIYCTCPPHPALQWLYLHPAEGVMPMYFNVQH  PAdV-3
349  PSQLNRFINIYTKGQPTAISLLLKDIFNYHRLNTNFDWIVYNTEPIDNCMHWLYLSPDEGLIPMYLNIQA  CAdV-A
350  PSQLNRFVNTYTKGLPLAISLLLKDIFRHHAQRSCYDWIIYNTTPQHEALQWCYLHPRDGLMPMYLNIQS  HAdV-2
350  PSQLNRFVNTYTKGLPLAISLLLKDIFRHHAQRSCYDWIIYNTTPQHEALQWCYLHPRDGLMPMYLNIQS  HAdV-5

418  MVYEALLRMHRTLIDRARWTRYYH-RKNKEFY                                        BAdV-3
419  KLYAILEKIHKVISDRQRWTKYYH-SKK----                                        OAdV-A
419  QVYRCLEKIHKTLQDRERWTRYYR-SKHP---                                        PAdV-3
419  KVYQAMERIHRTITDRQRWTRYYH-SKKK---                                        CAdV-A
420  HLYHVLEKIHRTLNDRDRWSRAYRARKTPK--                                        HAdV-2
420  HLYHVLEKIHRTLNDRDRWSRAYRARKTPK--                                        HAdV-5
```

Fig. 3.1 Analysis of BAdV-3 IVa2 amino acid sequence (a) *Amino acid sequence homology of BAdV-3 IVa2.* Alignment of amino acid sequences of BAdV-3 IVa2 (GenBank Accession # (AP_000025.1) with homologs encoded by ovine adenovirus (OAV)-A (AP_000005.1), porcine adenovirus (PAdV)-3 (YP_009200.1), canine adenovirus (CAdV)-2 IVa2 (AP_000612.1), human adenovirus (HAdV)-2 IVa2 (AP_000165.1) and HAdV-55 IVa2 (AP_000201.1). The identical amino acids are marked yellow.

b)

MDTRG**RRKVRHQQAQPEALAGQQTDASAALHGHRD**DPGEDAQALERPH PAGHRPSPSRPLQQQ**PPQ** 66

PKKQRAMLDGDVLDHVSELWDKCALMQQCLESMP MAEGLKPLRHFSSLDELLAMGGATLLNALSDY 132

NQAIRDAMNATMPYLRPD GSCKSLNFTMQPVIGVVYGPTGCGKSQLLRNLMSTGLIQPPPE TVFFI VP 200

QVDMIPPQELLAWETQICEGNYTPGPTGTLVPQSSTLKPAFKIMSYEDLTMD YNYDVAHPQ NVFAQAA 268

KTGPIAIIMDECMEDLGRHKAISKFFHAFPSKLHDKFPKCTGYSVFVVLHNMNPRKDLGGNIANLKIQA 337

KLHLISPRMHPSQ LNRFINTYTKSLPLPITLLLKDIFSFHAQHSQYDWIIYNTL PPHESLQWLYLNPSEGL 408

MPMYLNIHAMVYEALLRMHRTLIDRARWTRYYHRKNKEFY 448

Fig. 3.1 Analysis of BAdV-3 IVa2 amino acid sequence (b) *Identification of potential BAdV-3 IVa2 nuclear localization signal (NLS).* Potential NLS is shown in bold and underlined.

3.3.3 Sub cellular localization of IVa2

To assess the subcellular localization of IVa2, mock-infected, or BAdV-3 infected cells were analyzed at 36 hrs post-infection by indirect immunofluorescence using IVa2gst serum. As seen in Fig. 3.2e, BAdV-3 IVa2 localized in the nucleus of the infected cells (panels a1-a3). No such fluorescence could be detected in mock-infected cells (panels, b1-b3). To determine if IVa2 localized in the nucleolus of infected cells, MDBK cells were infected with BAdV-3 and analyzed by dual-label immunofluorescence using IVa2gst serum and anti- replication protein A (RPA) serum. As seen in Fig. 3.2e, IVa2 co-localized with nucleolar protein RPA in the nucleolus of BAdV-3 infected cells (panels c1-c4). No IVa2 protein could be detected in mock-infected cells (panels, d1-d4).

To exclude the possibility of involvement of other BAdV-3 proteins in the sub cellular localization of IVa2, Vero cells transfected with plasmid pDR.IVa2 (IVa2 coding sequence fused in frame with DsRed) and analyzed by direct immunofluorescence. As seen in Fig. 3.3, IVa2 localized to the nucleus\nucleolus of plasmid pDR.IVa2 DNA transfected cells (panels, a1-a3). In contrast, DsRed protein localized to both cytoplasm and nucleus of plasmid pDR DNA transfected cells (panel c1-c3). No such protein could be localized in pcDNA3-transfected cells (panels, b1-b3). Similarly, dual-label immunofluorescence using IVa2gst serum and anti- replication protein A (RPA) serum detected IVa2 co-localized with nucleolar RPA protein in the nucleolus of plasmid pDR.IVa2 transfected cells (Fig. 3.3, panels, d1-d4). No IVa2 protein could be detected in pCDNA3 transfected cells (Fig. 3.3, panels, e1-e4).

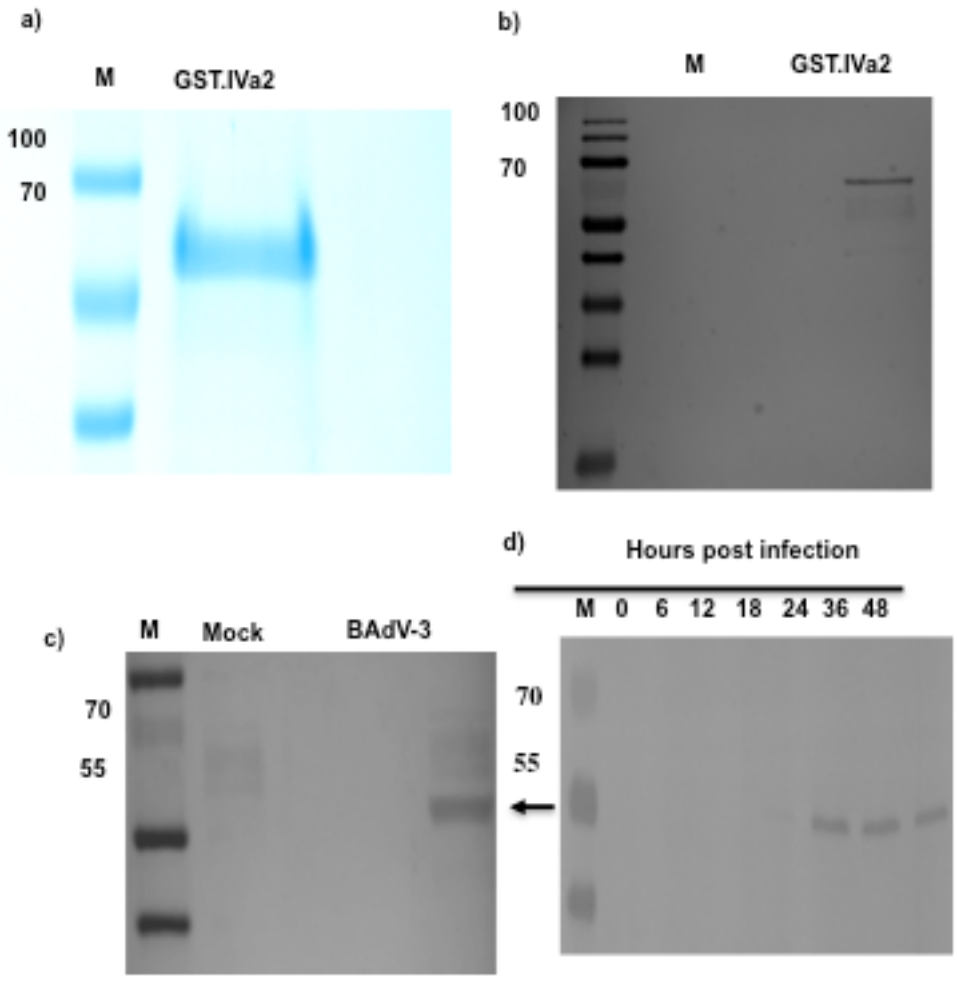

Fig. 3.2. Expression of IVa2 in BAdV-3 infected cells. (a,b,c,d) *Western Blot*. Purified GST.IVa2 fusion proteins were separated by 12% and (a) stained with 0.25% Coomassie blue stain SDS-PAGE or **(b)** transferred to nitrocellulose and analysed in Western blot using Anti-GST serum. Proteins from the lysates of BAdV-3 infected MDBK cells harvested **(c)** at 36 hrs post infection or **(d)** at various times post infection were separated by 12% SDS-PAGE transferred to nitrocellulose and probed in Western blot using IVa2gst serum. The single arrow shows IVa2 protein (panels, c and d). The double arrow shows GST.IVa2 protein (panel, b),

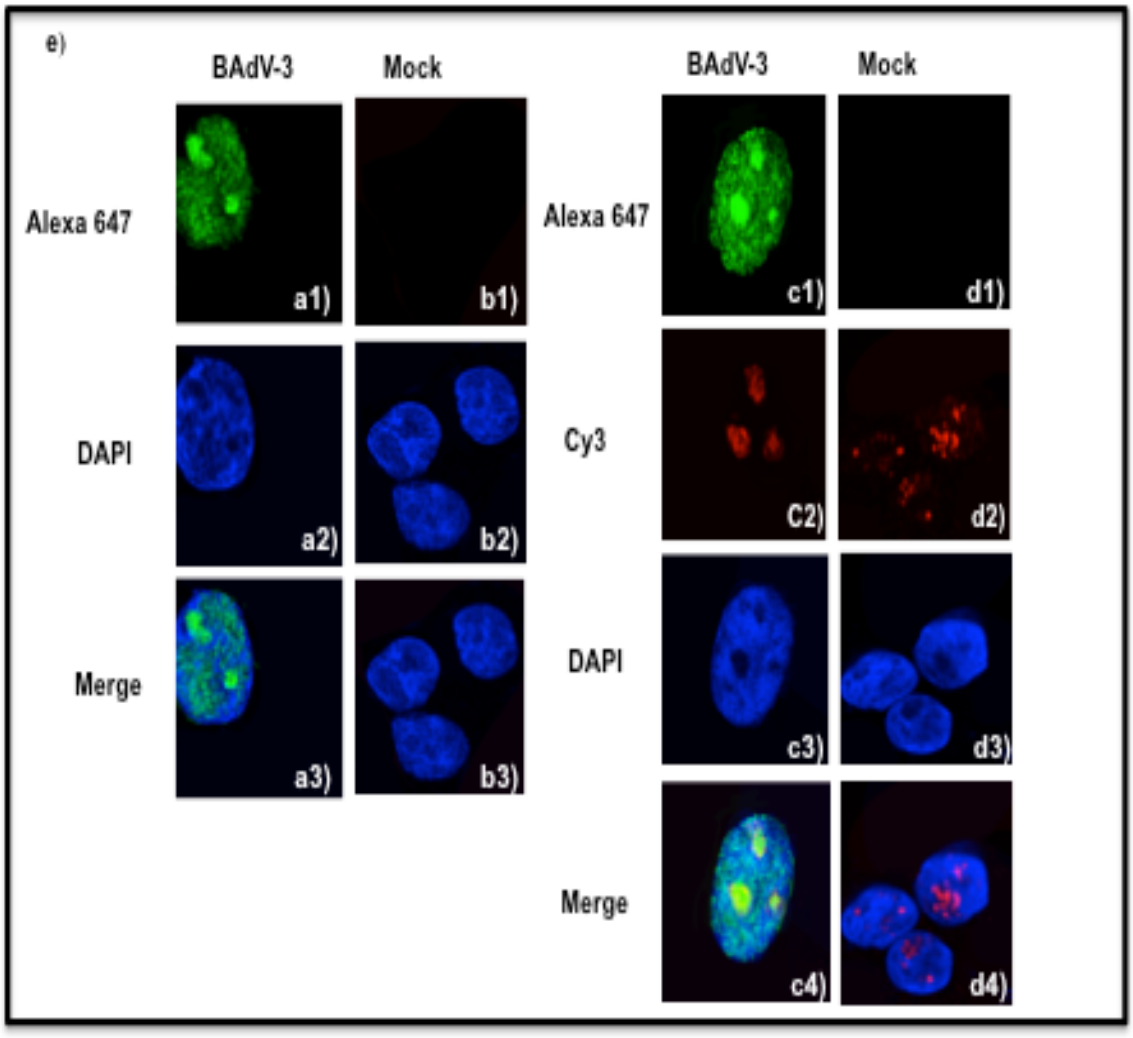

Fig. 3.2. Expression of IVa2 in BAdV-3 infected cells e) Nuclear\nucleolar localization. MDBK cells were infected with BAdV-3 (panels a1-a3; c1-c4) or mock infected (panels b1-b3; d1-d4) and fixed at 36hrs post infection. The subcellular localization of IVa2 was visualized by indirect immunofluorescence using IVa2gst serum. The nuclei were stained with DAPI (panels a2, b2, c3,d3) and nucleoli were visualized by staining with anti-RPA antibody and Cy-3 conjugated goat anti-mouse antibody (panels,c2,d2). A merge of the images is shown in panels a3, b3, c4, d4.

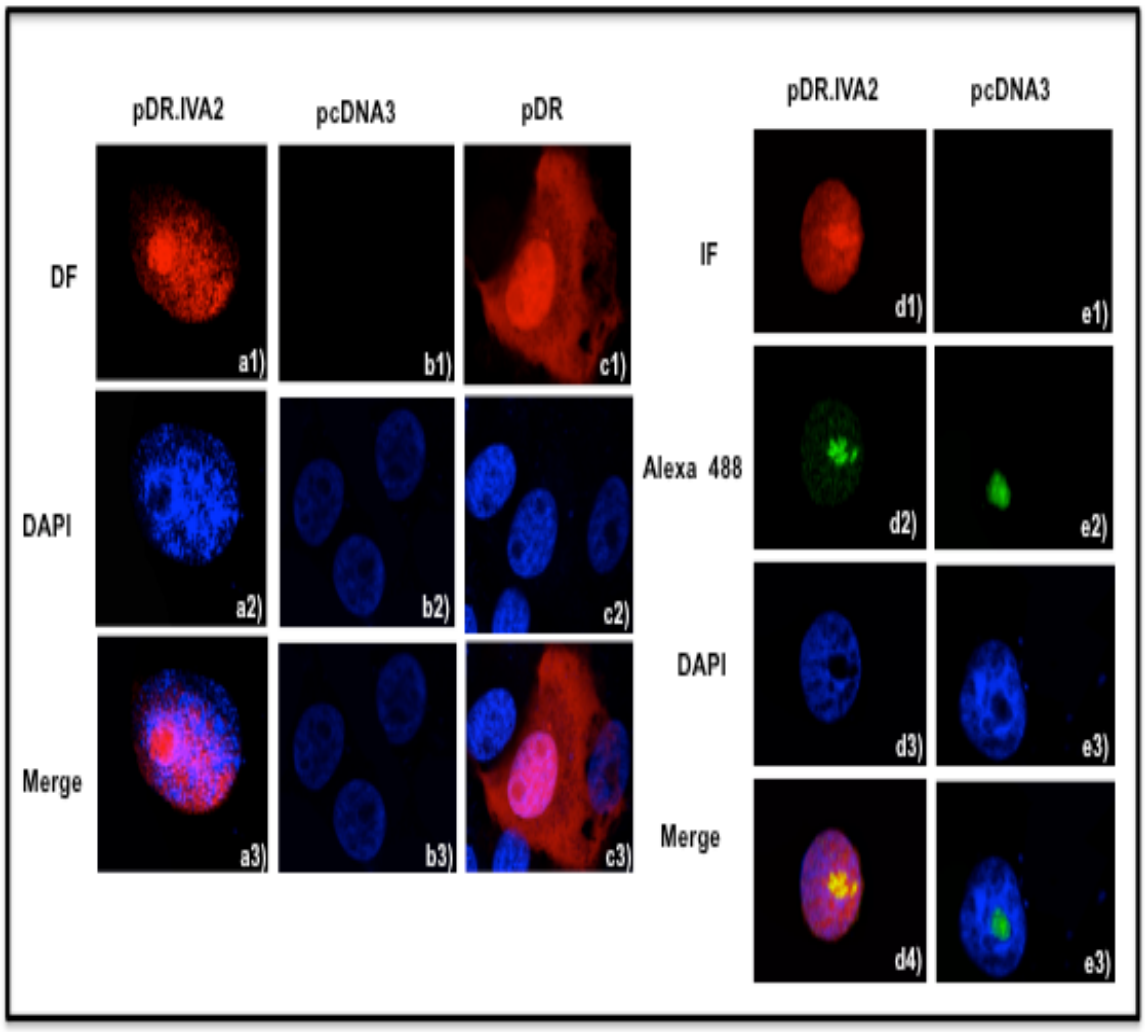

Fig. 3.3 Expression of BAdV-3 IVa2 in transfected cells. *Sub-cellular localization of IVa2*. Vero cells were transfected with plasmid pDR. IVa2 DNA (panels a1-a3; d1-d4), plasmid pcDNA3 DNA (panels b1-b3;e1-e4) or plasmid pDR DNA (panel c1-c3) and sub cellular localization was visualized after 36 hrs post transfection by direct fluorescence using confocal microscope. The nuclei were stained with DAPI (panels a2, b2, c2, d3,e3) and nucleoli were visualized by staining with anti-RPA antibody and Alexa 488 conjugated goat anti-mouse antibody (panels d2,e2). A merge of the images is shown in panels a3, b3, c3, d4 and e4.

3.3.4 Mapping IVa2 nuclear localization signal

To map nuclear localization signal (NLS) of IVa2, plasmids expressing truncated or deleted mutant IVa2 were constructed and individually fused to gene encoding DsRed. Based on the analysis of nuclear localization domain(s) of HAdV-5 IVa2 (Lutz and Kedinger, 1996) and computer program predicted NLS of BAdV-3, we constructed plasmids (Fig. 3.4a) containing C-terminus truncations (amino acids 424-448 or 398-448) and two N-terminus truncations (amino acids 2-25 and 2-75). Vero cells were transfected with individual plasmid DNA and examined by direct immunofluorescence. As seen in Fig. 3.4b, wild-type IVa2 expressed in the cells transfected with plasmid pDR.IVa2 (panels, a1-a3) localized to the nucleus of the transfected cells. Similarly, mutant IVa2 expressed in cells transfected with plasmid pDR.IVa2d1 DNA (panels, b1-b3) as well as pDR.IVa2d2 DNA (panels, c1-c3) localized to the nucleus of the transfected cells. In contrast, mutant IVa2 expressed in the cells transfected with either plasmid pDR.IVa2.d3 DNA (panels, d1-d3) or plasmid pDR.IVa2d4 DNA (panels, e1-e3) localized to the cytoplasm of the transfected cells.

To confirm if N-terminus 25 amino acids are sufficient to localize IVa2 to the nucleus, plasmid pGFP/βgal.NLS containing N-terminus 25 amino acids of IVa2 fused in frame with a heterologous cytoplasmic green fluorescent protein-beta galactosidase (GFP/βGal) fusion protein (Fig. 3.4c) constructed. Vero cells transfected with either of pCMVGFP/βgal or pGFP/βgal.NLS plasmid DNA and analyzed by direct immunofluorescence. As expected, GFP/βGal protein expressed in the cells transfected with plasmid pCMVGFP/βgal DNA localized predominantly in the cytoplasm of transfected cells (Fig. 3.4d, panels a1-a3.)

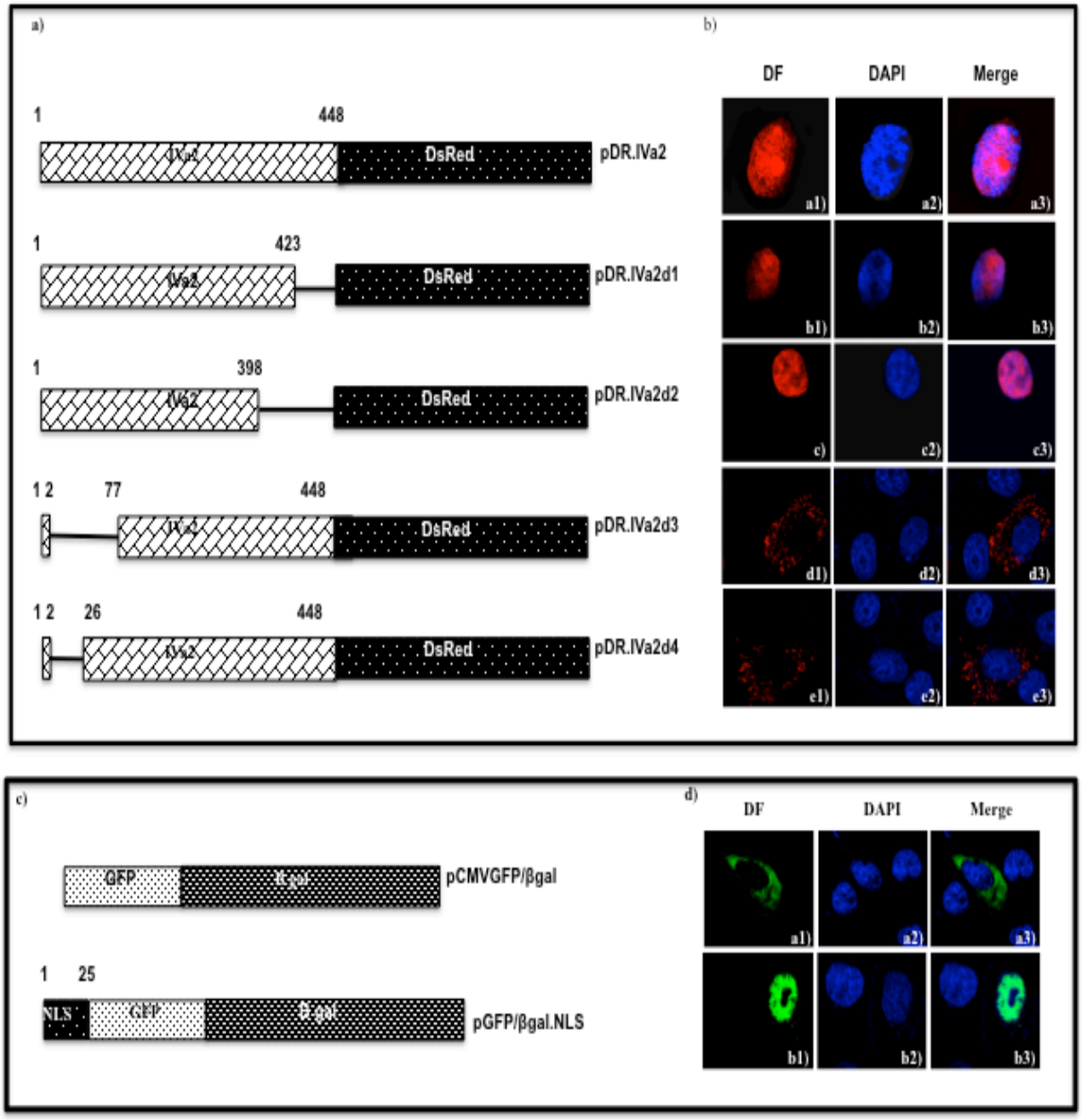

Fig. 3.4 Sub-cellular localization of mutant IVa2 in transfected cells. (a) *Schematic diagram of plasmid DNAs.* Amino acid numbers are depicted. The name of the plasmids is depicted on the right of the panel. The thick black line represents deleted region (s) of IVa2. **(b).** *Direct immunofluorescence.* Vero cells were transfected with indicated plasmid DNA. At 36 hrs post transfection, the cells were fixed and the subcellular localization of IVa2 was observed by direct fluorescence using confocal microscope. DF (direct fluorescence). **(c).** *Schematic diagram of plasmid DNAs.* The name of the plasmid is depicted on the right. Amino acid numbers are depicted on top of schematic diagram. NLS (nuclear localization signal) of IVa2; GFP (green fluorescent protein). **(d).** *Direct Immunofluorescence*. Vero cells were transfected with indicated plasmid DNA. At 36 hrs post transfection, the cells were fixed and analysed by direct immunofluorescence using confocal microscope.

In contrast, fusion protein (containing N-terminus 25 amino acids of IVa2 fused to GFP/βGal) expressed in the cells transfected with plasmid pGFP/βgal.NLS DNA and localized predominantly to the nucleus of the transfected cells (Fig. 3.4d, panels b1-b3).

To further narrow down the amino acid sequence involved in the translocation of IVa2 to the nucleus, plasmids expressing mutant IVa2 proteins (containing internal deletions within N-terminus amino acids 1-25 of IVa2) fused in-frame to DsRed were constructed (Fig. 3.5a). Vero cells were transfected with individual plasmid DNA and analyzed by direct immunofluorescence. The mutant protein expressed in the cells transfected with plasmid pDR.IVa2d3.1 DNA (Fig. 3.5b, panels a1-a3) or plasmid pDR.IVa2d3.2 DNA (Fig. 3.5b, panels, b1-b3) localized predominantly in the nucleus\nucleolus of the transfected cells. The mutant protein expressed in cells transfected with plasmid pDR.IVa2d3.3 DNA localized in both nucleus\nucleolus and cytoplasm of the transfected cells (Fig. 3.5b, panels, c1-c3). The mutant protein expressed in the cells transfected with plasmid pDR.IVa2d3.4 DNA localized in the cytoplasm (predominantly) and in the nucleus\nucleolus of the transfected cells (Fig. 3.5b, panels d1-d3). In contrast, a mutant protein expressed in cells transfected with plasmid pDR.IVa2d3.5 DNA appears to localize predominantly in the cytoplasm of the transfected cells (Fig. 3.5b, panels, e1-e3).

To determine influence of amino acid substitution with in IVa2 NLS on its localization, initially, we constructed plasmids expressing mutant IVa2 containing a substitution of a cluster (^{6}RRK^{8}) of basic residues (arginine or lysine) to glycines (Fig. 3.5c). As seen in Fig. 3.5d, mutant IVa2 encoded by plasmid pDR.IVa2M1 (panel b1-b3), plasmid pDR.IVa2M2 (panels c1-c3), plasmid pDR.IVa2M3 (panels d1 to d3) and plasmid pDR.IVa2.M4 (panels e1-e3) localized predominantly in the nucleolus of transfected cells. Since the substitution to glycine

residues may influence recognition of protein by transport proteins, sequential substitution of IVa2 NLS with poly alanine sequences carried out (Fig 3.5e). Vero cells were transfected with individual mutant plasmid DNA and analyzed by direct fluorescence. As seen in Fig. 3.5f, mutant IVa2 containing a substitution of amino acid 6-8 (RRK to AAA) encoded by plasmid pDR.IVa2d3.1a (Fig. 3.5f, panels b1-b3) or substitution of amino acids 4-8 (RGRRK to AAAAA) encoded by plasmid pDR.IVa2d3.2a (Fig. 3.5f, panels c1-c3) localized to the nucleus of the transfected cells. Mutant IVa2 protein-containing substitution of amino acids 4-11 (RGRRKVRH to AAAAAAAA) encoded by plasmid pDR.IVa2d3.3a was localized both in the nucleus and cytoplasm of the transfected cells (Fig. 3.5f, panels d1-d3). Mutant IVa2 protein-containing substitution of amino acid 4-15 (RGRRKVRHQQAQ to AAAAAAAAAAA A) encoded by plasmid pDR.IVa2d3.4a localized both in the nucleus (predominantly) and cytoplasm of the transfected cells (Fig. 3.5f, panels e1-e3). Mutant IVa2 protein-containing substitution of amino acids 4-18 (RGRRKVRHQQAQPEA to AAAAAAA AAAAAAAA) encoded by plasmid pDR.IVa2d3.5a
was localized predominantly in the cytoplasm of the transfected cells (Fig. 3.5f, panels f1-f3).

To determine if amino acids 4-18 were sufficient for nuclear localization of IVa2, plasmid pGFP/βgal.NLS1 containing N-terminus 4-18 amino acids of IVa2 fused in frame with a heterologous cytoplasmic green fluorescent protein-beta galactosidase (GFP/βGal) fusion protein (Fig. 3.5g). Vero cells transfected with plasmid pGFP/βgal.NLS DNA and analyzed by direct immunofluorescence. As expected, GFP/βGal protein expressed in the cells transfected with plasmid pCMV.GFP/βgal DNA localized predominantly in the cytoplasm of transfected cells (Fig. 3.5h, panels a1-a3). The fusion protein (containing N-terminus 25 amino acids of IVa2 fused to GFP/βGal) expressed in the cells transfected with plasmid pGFP/βgal.NLS DNA

localized predominantly to the nucleus of the transfected cells panels (Fig. 3.5h, panels b1-b3). In contrast, fusion protein (containing N-terminus 4-18 amino acids of IVa2 fused to GFP/βGal) expressed in the cells transfected with plasmid pGFP/βgal.NLS1 DNA localized predominantly to the cytoplasm of the transfected cells (Fig. 3.5h, panels c1-c3).

3.3.5 Interaction of IVa2 with protein transport receptors

To determine which of the import receptor (s) are involved in the transport of IVa2 across the nuclear pore complex, GST pull-down assay carried out. In-vitro transcribed/translated [^{35}S] methionine labelled IVa2 (plasmid.pC.IVa2) was incubated with purified GST or GST fused to importin α-1, α-3, α-5, α-7, β-1 or TRN-SR2 (Fig. 3.6ab). Bound proteins were separated by 12% SDS-PAGE and visualized by autoradiography using FX molecular imager. As seen in Fig. 3.6c, radiolabeled proteins appear to interact with importin α-1 (lane 3). No such interaction could be observed when radiolabeled IVa2 pulled down using purified GST fused to (lane 2), α-3 (lane 4), α-5 (lane 5), α-7 (lane 6), β-1 (lane 7) or TRN-SR2 (lane 8). Radiolabelled full-length IVa2 (Fig. 3.6c,d) lane 1 and or N terminus 25 amino acid truncated IVa2 (Fig. 3.8d) lane 4 were used as input control.

To determine the domain of IVa2 involved in the interaction with importin receptor α-1, the GST pull-down assay was performed using radiolabeled mutant IVa2 (containing a deletion of amino acids1-25) and purified GST-importin α-1 fusion protein (Fig. 3.6a, b). As expected, radiolabeled IVa2 interacted with purified GST-importin α-1 fusion protein (Fig. 3.6c, lane 3) but not with purified GST alone (Fig. 3.6c, lane 2). Radiolabeled mutant IVad25 did not interact with either GST (Fig. 3.6d, lane 5) or GST-importin α-1 fusion protein (Fig. 3.6d, lane 6).

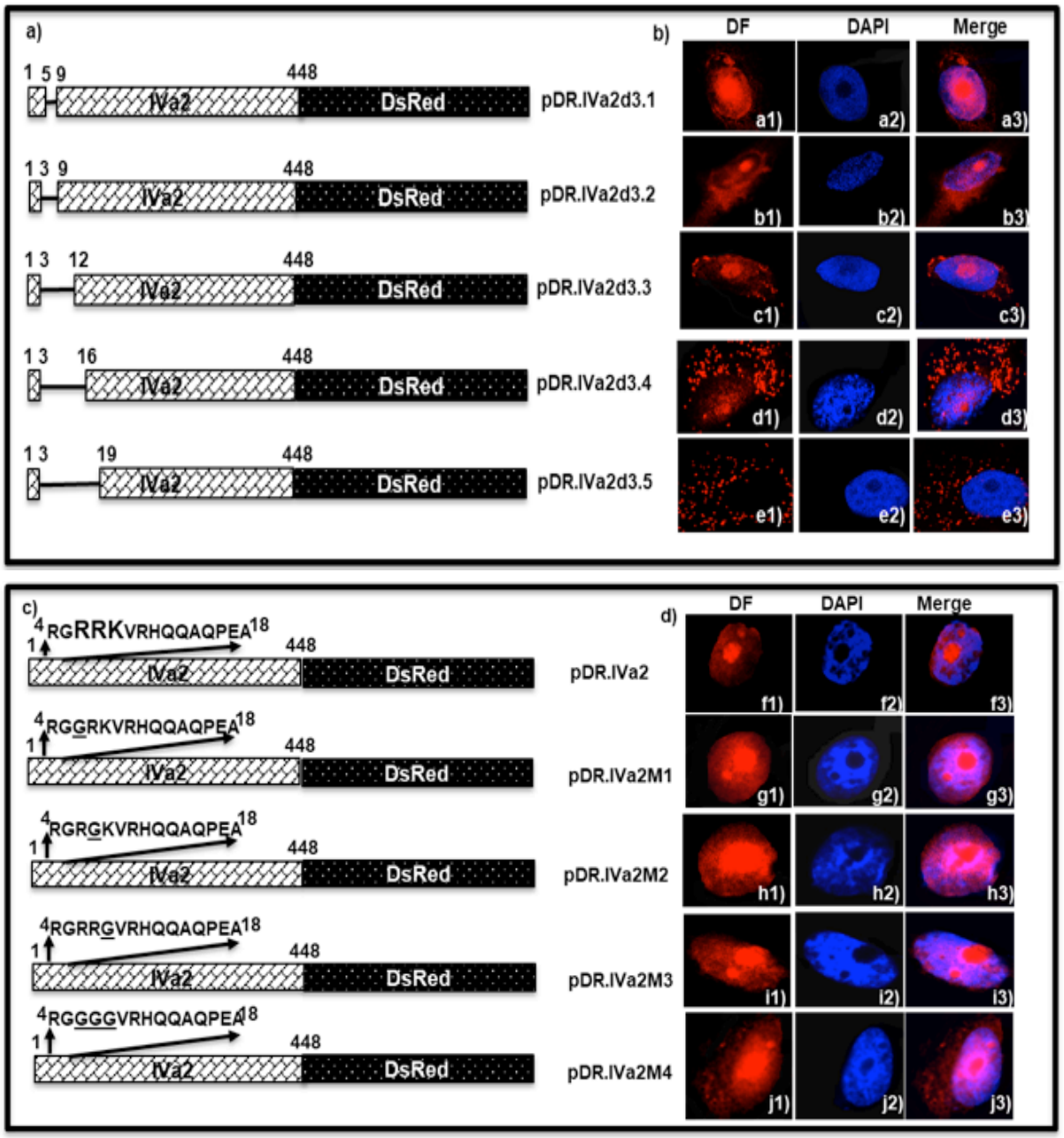

Fig. 3.5. Sub-cellular localization of mutant IVa2 containing small deletions\ substitutions. (a). *Schematic diagram of plasmid DNAs.* Amino acid numbers are depicted. The name of the plasmid is depicted on the right of the panel. The thick line represents the deleted region(s). **(b).** *Sub-cellular localization.* Vero cells were transfected with indicated plasmid DNA. At 36 hrs post transfection, the cells were fixed and the subcellular localization of IVa2 was observed by direct fluorescence using confocal microscope. DF (direct fluorescence). **(c).** *Schematic diagram of plasmid DNAs.* The name of the plasmid is depicted on the right of the panel. Amino acid numbers are depicted. The Basic residues RRK are shown in bold. The substituted amino acids of BAdV-3 IVa2 are underlined. **(d).** *Sub-cellular localization*. Vero cells were transfected with indicated plasmid DNA. At 36 hrs post transfection, the cells were fixed and analysed by direct fluorescence using confocal microscope.

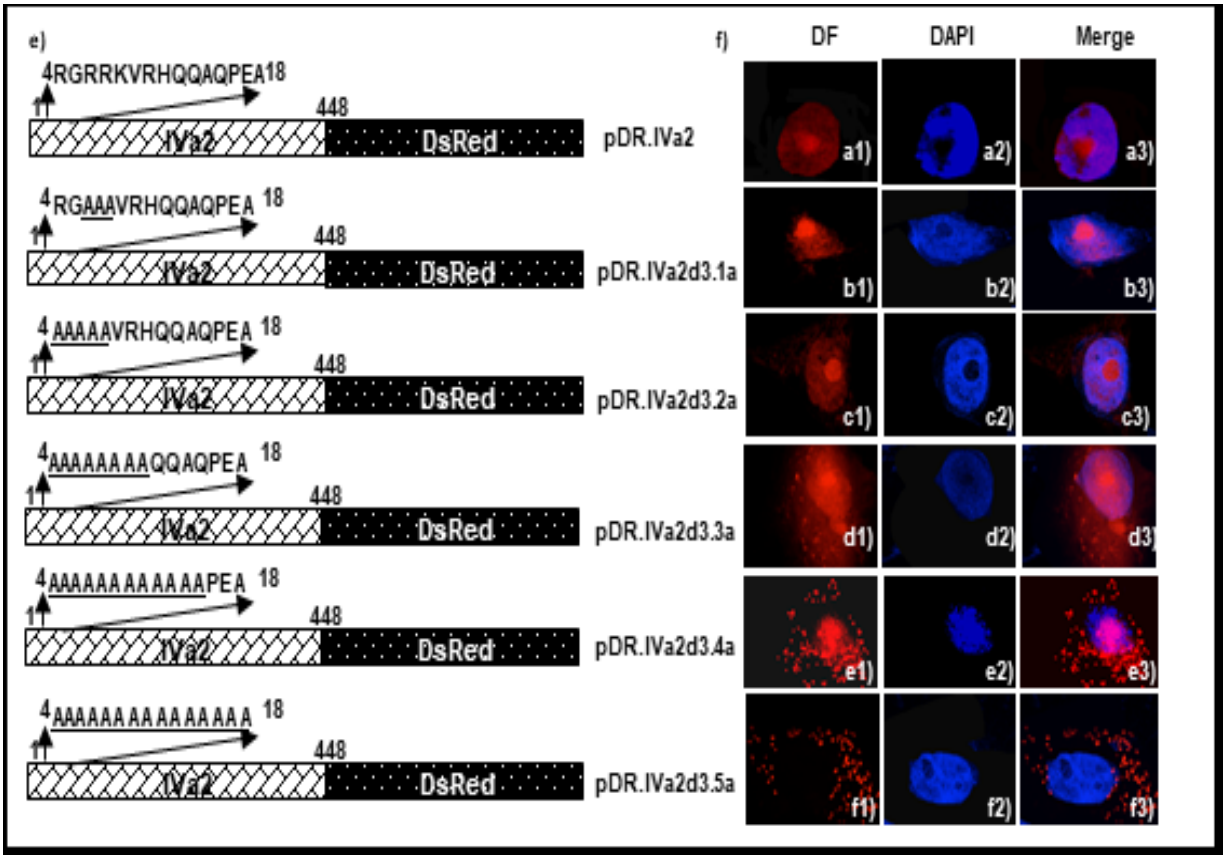

Fig. 3.5. Sub-cellular localization of mutant IVa2 containing small deletions\ substitutions. (e). *Schematic diagram of plasmid DNAs.* The name of the plasmid is depicted on the right of the panel. Amino acid numbers are depicted. The substituted amino acids of BAdV-3 IVa2 are underlined. **(f).** *Sub-cellular localization*. Vero cells were transfected with indicated plasmid DNA. At 36 hrs post transfection, the cells were fixed and analysed by direct fluorescence using confocal microscope. DF (direct fluorescence).

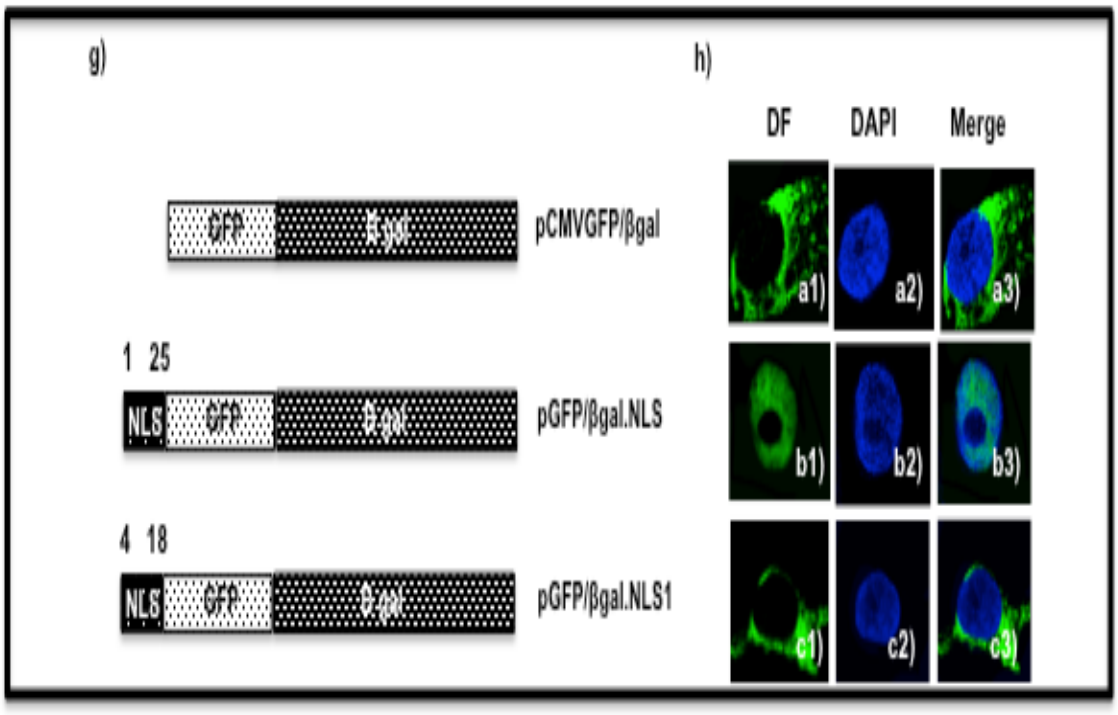

Fig. 3.5. Sub-cellular localization of mutant IVa2 containing small deletions\ substitutions.g) *Schematic diagram of plasmid DNAs.* The name of the plasmid is depicted on the right of the panel. Amino acid numbers are depicted. The substituted amino acids of BAdV-3 IVa2 are underlined. NLS (nuclear localization signal) of IVa2; GFP (green fluorescent protein). **(H).** *Sub-cellular localization*. Vero cells were transfected with indicated plasmid DNA. At 36 hrs post transfection, the cells were fixed and analysed by direct immunofluorescence using confocal microscope. DF (direct fluorescence).

Radiolabelled IVa2 (Fig. 3.6d, lane 1) and IVa2d25 (Fig. 3.6d, lane 4) were used as input control. Similarly, radiolabeled GFP/βgal.NLS1 did not interact with either GST-importin α-1 fusion protein (Fig. 3.6e, lane 3) or GST (Fig. 3.6e, lane 4). In contrast, radiolabeled GFP/βgal.NLS interacted with GST-importin α-1 fusion protein (Fig. 3.6e, lane 2) but not with GST (Fig. 3.6e, lane 6). Radiolabeled GFP/βgal.NLS (Fig. 3.6e, lane 1) and GFP/βgal.NLS1 (Fig. 3.6e, lane 5) was used as input control.

3.3.6 Mapping of IVa2 nucleolar localization signal

To map nucleolar localization signal (NoLS) of IVa2, plasmids expressing truncated or deleted mutant IVa2 were constructed and individually fused to gene encoding DsRed (Fig. 3.10a). Since mutant protein expressed in plasmid pDR.IVa2d2 DNA (Fig. 3.4b, panels c1-c3) transfected cell showed altered nucleolar localization; we constructed plasmids containing C-terminal deletions\truncation (Fig. 3.7a). Vero cells transfected with individual plasmid DNA were analyzed by direct immunofluorescence. As seen in Fig. 3.7b, wild-type IVa2 expressed in cells transfected with plasmid pDR.IVa2 DNA localized to the nucleolus\nucleus of the transfected cells (panels, a1-a4). Mutant IVa2 protein expressed in cells transfected with plasmid pDR.IVa2d2 DNA showed altered nucleolar localization without affecting the nuclear localization (panels, b1-b4). In contrast, a mutant protein expressed in the cells transfected with plasmid pDR.IVa2d5 localized predominantly in the nucleus of the transfected cells (panels, c1- c4). Mutant proteins expressed in cells transfected with plasmid pDR.IVa2d5.1 DNA (panels, d1-d4), plasmid pDR.IVa2d5.2 DNA (panels, e1-e4), plasmid DNA pDR.IVa2d5.3 DNA (panels f1-f4), plasmid pDR.IVa2d5.4 DNA (panels, g1-g4), plasmid

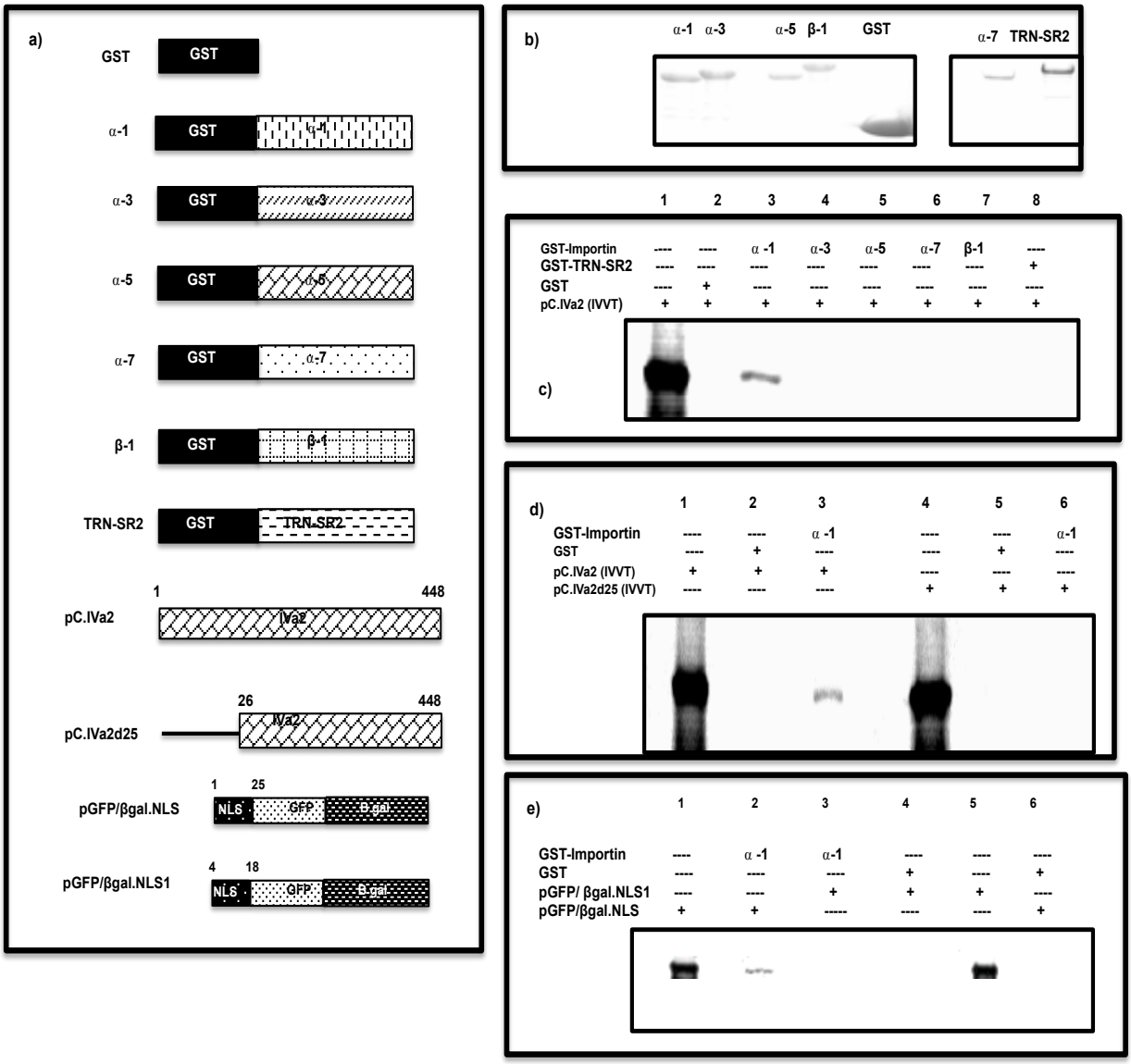

Fig. 3.6. Interaction of IVa2 with nuclear transport receptors (a). *Schematic diagram of plasmid DNAs.* The amino acid numbers of IVa2 are depicted. The name of the protein is depicted on left of the panel. The name of the plasmid is depicted on the right of the panel. GST (glutathione S-transferase); TRN-SR2 (transportin). **(b).** *Commassie blue staining.* Purified GST-transport receptor proteins were separated by 12% SDS-PAGE and the gels were stained with 0.25% Commassie blue. **(c, d).** *GST pull-down assay*. **(c).** *In-vitro* synthesized [^{35}S]-labeled BAdV-3 IVa2 was incubated with either purified individual GST fusion proteins (GST fused with importin α1, α3, α5, α7, β1, or TRN-SR2 or GST and pulled down with glutathione sepharose beads II. **(d).** *In - vitro* synthesized [^{35}S]-labeled BAdV-3 IVa2 or IVa2d25 was incubated individually with either purified individual GST- importin α1 fusion protein or GST alone, and pulled down with glutathione sepharose beads II. (e) *In - vitro* synthesized [^{35}S]-labeled GFP/βgal.NLS or GFP/βgal.NLS1 was incubated individually with either purified individual GST- importin α1 fusion protein or GST alone, and pulled down with glutathione sepharose beads II. The samples from (c), (d) and (e) were separated by 12% SDS-PAGE and visualized using phosphor screen.

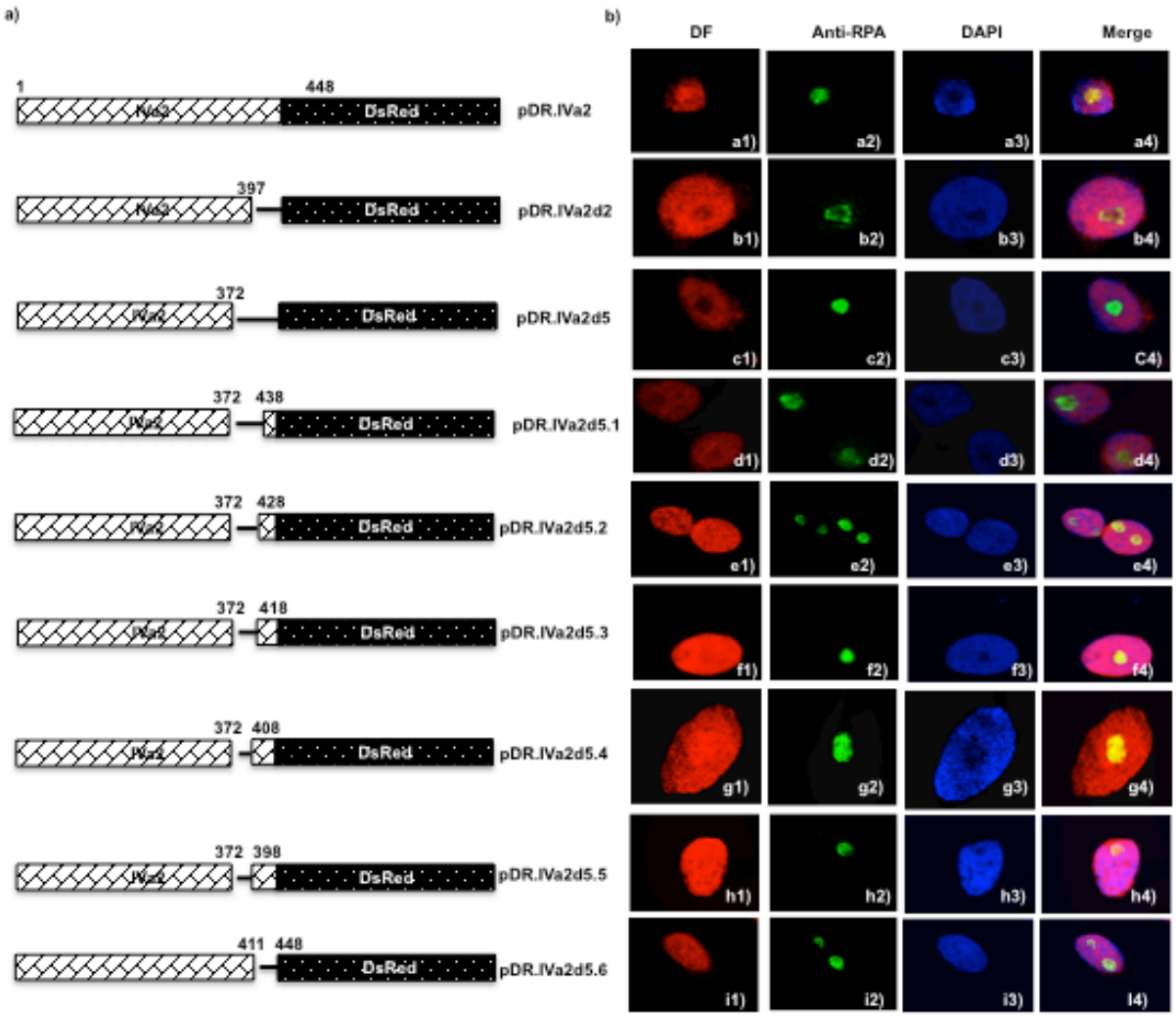

Fig. 3.7 Mapping of IVa2 nucleolar localization signal. (a) *Schematic diagram of plasmid DNAs*. The amino acid numbers of IVa2 protein are depicted. The name of the plasmid is depicted on the right of the panel. The thick line depicts deleted region(s). **(b).** *Sub-cellular localization*. Vero cells were transfected with indicated plasmid DNA. At thirty-six hrs post transfection, the slides were fixed, permeabilized, blocked and probed using anti-RPA antibodies followed by Alexa 633 conjugated goat anti- mouse antibodies. The nuclei were stained with DAPI. The sub-cellular localization was visualized by confocal microscope. Direct fluorescence (DF).

pDR.IVa2d5.5 DNA (panels, h1-h4) and plasmid pDR.IVa2d5.6 DNA (i1-i4) localized to the nucleolus of the transfected cells.

3.3.7 Isolation of recombinant BAdV-3 expressing IVa2 containing nucleolar localization signal flanked by loxP sequence

To conditionally knockdown BAdV-3 IVa2 nucleolar localization sequence, we constructed a full-length plasmid pUC304a.loxIVa2C.75 (appendix 1) expressing BAdV-3 IVa2 containing loxP sequence inserted in-frame at amino acid 373 and amino acid 448. The CRL cells were transfected with 5 ug of PacI digested plasmid pUC304a.loxIVa2C.75 DNA and monitored for the detection of EYFP expressing cells and the development of cytopathic effects. Although GFP expressing cells observed in cells transfected with plasmid pUC304a.loxIVa2C.75 DNA (data not shown), repeated transfections did not induce the development of cytopathic effects.

3.3.8 Isolation and characterization of recombinant BAdV-3 expressing mutant IVa2

To determine if a stretch of basic residues (^{6}RRK^{9}) in IVa2 NLS affect replication of BAdV-3, we constructed full-length BAdV-3 genomic clones expressing mutant IVa2 containing a substitution of basic amino acids with glycine in NLS (Fig. 3.8a). Transfection of VIDO DT1 cells (DU and Tikoo, 2010) with individual full-length plasmid DNAs lead to the detection of green fluorescent cells and cytopathic effects in 15 days (Fig. 3.8b). The infected cells were collected, freeze-thawed and recombinant viruses were purified by CsCl density gradient. The proper introduction of the desired mutation was confirmed by DNA sequencing of mutant viral DNA. The ability of recombinant BAdV-3 to express IVa2 was confirmed by Western blot using IVa2gst serum.

As seen in Fig.3.8, proteins of expected molecular weight could be detected in lysates of cells infected with mutant viruses (panel c).

To assess the effect of amino acid substitutions on the nuclear location of IVa2, the cells infected with individual recombinant BAdV-3 were analyzed by immunofluorescence using a Confocal microscope. As seen in Fig. 3.8e, mutant IVa2 appears to be localized predominantly in the nucleoli of infected cells.

To determine if amino acid substitution affected the replication of BAdV-3, we compared the growth kinetics of recombinant BAdV-3 in MDBK cells. As seen in Fig. 3.8d, there was no detectable difference in the titer of BAV304AM1, BAV304aM2, BAV304aM3, and BAV304a. In contrast, recombinant BAV304aM4 grew about 1 log less compared to other BAdV-3s.

3.4 Discussion

The different steps involved in the efficient production of progeny adenovirus, including nuclear translocation of individual adenovirus protein to produce stable adenovirus capsids, involve the interaction of adenovirus proteins with cellular and/ viral proteins (Flatt and Butcher, 2019). Recently, we reported that nuclear localization of some structural and non-structural proteins encoded by L1-L7 regions of late transcriptional unit of BAdV-3 genome requires interaction with different importins\ transportin 3 receptors (Ayalew et al., 2014; Kulshreshtha et al., 2014; Paterson et al., 2012; Said et al., 2018a).

Adenovirus IVa2, a multifunctional core protein, interacts with 52K (Gustin et al., 1996) and pVIII (Singh et al., 2005). Moreover, protein IVa2 encoded by HAdV-5 localizes to both nucleus and nucleolus in infected cells using amino acid 432-449 and amino acids 50-136 as nuclear and nucleolar localization signals respectively (Lutz et al., 1996). Since the structure \

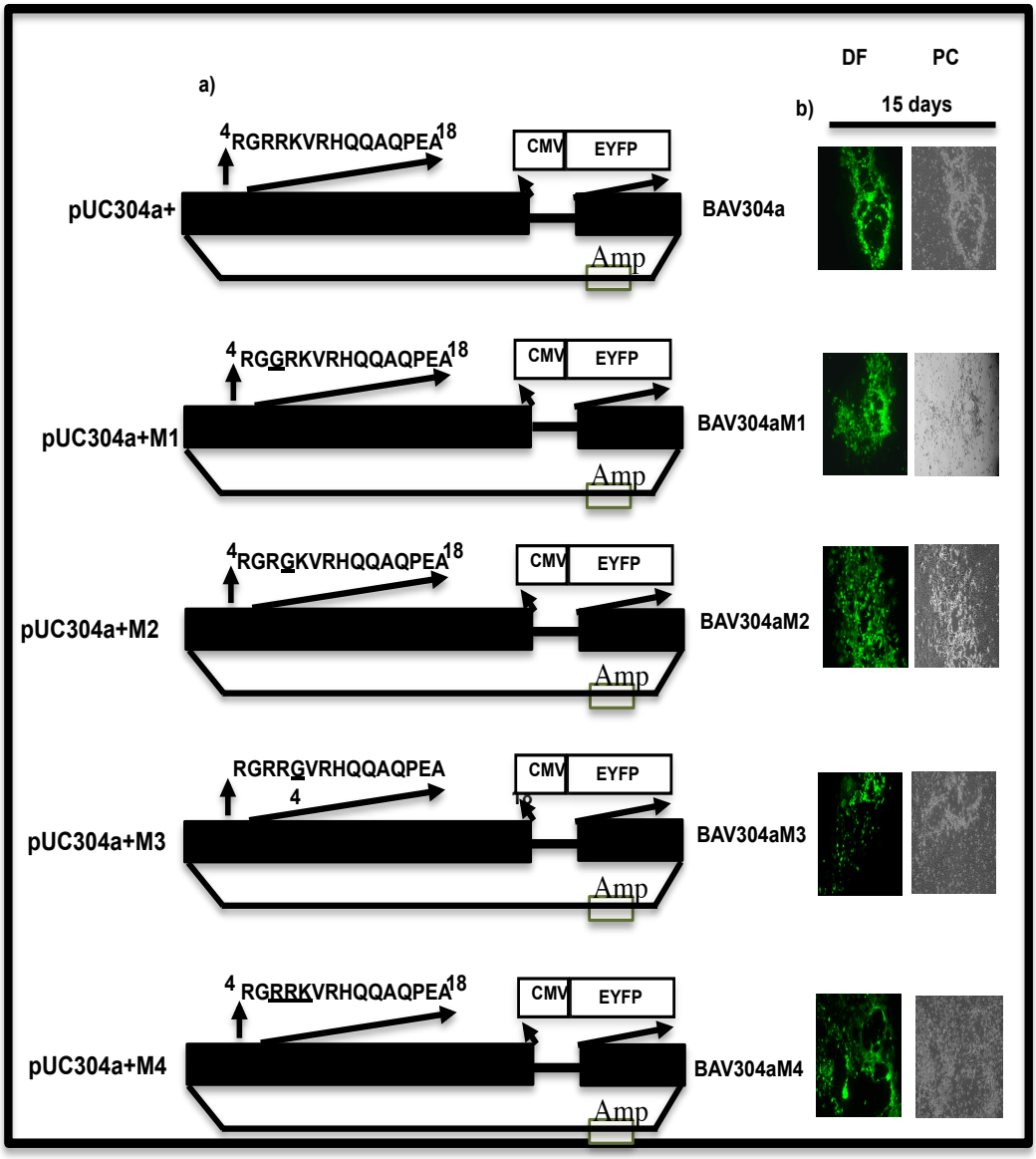

Fig. 3.8 Isolation and characterization of mutant BAdV-3. (a). *Schematic diagram of plasmid DNAs.* The name of the plasmids is depicted on the right of the panel. The BAdV-3 sequence is represented by filled box. The thin line represents deleted region (E3). The numbers represent the amino acids of BAdV-3 IVa2. The glycines substituted for arginines are underlined. Human cytomegalovirus (CMV) immediate early promoter; Enhanced yellow fluorescent protein (EYFP). **(b).** *Direct Fluorescence.* Monolayers of VIDO DT1 cells were transfected with 5 µg of indicated plasmid DNA and visualized for EYFP expression and development of cytopathic effects using fluorescent microscope TCS SP5 (Leica). Direct fluorescence (DF); Phase contrast (PC).

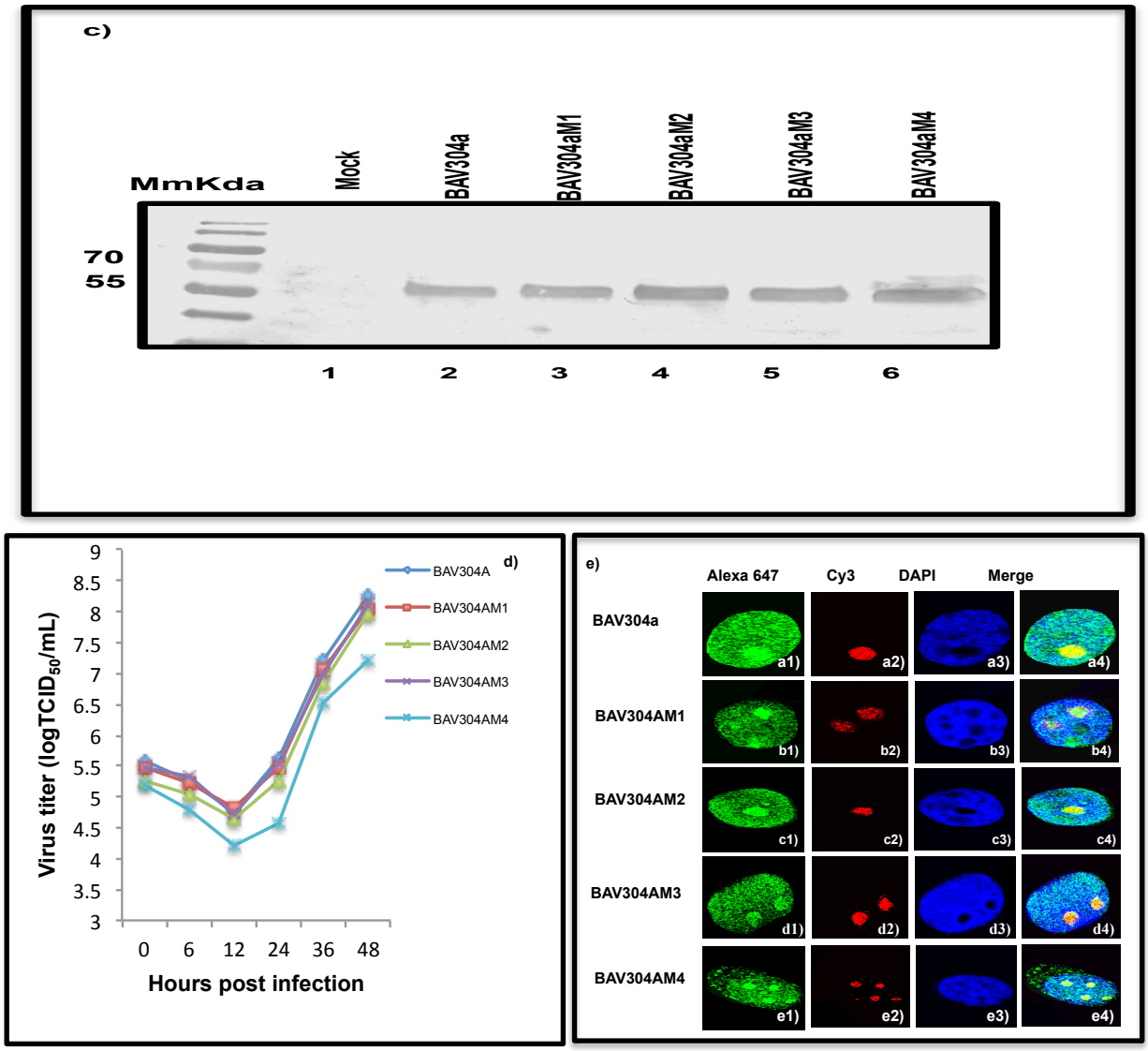

Fig. 3.8 Isolation and characterization of mutant BAdV-3 (c). *Western blot.* Proteins from the lysates of CRL cells individually infected with BAV304a or mutant BAdV-3s were collected at indicated times post infection were separated by 12% SDS-PAGE, transferred to nitrocellulose and analysed by Western blot using IVa2gst serum. Molecular weight markers (M). **(d).** *Determination of viral titer using TCID$_{50}$.* MDBK cells in 24 well plates infected with BAV304a, BAV304aM1, BAV304aM2, and BAV304aM3 or BAV304aM4 virus at MOI of 5. Cell lysates collected at different time points, freeze thawed and used to determine viral titer using TCID$_{50}$. Displayed values are average values of two sepearte experiments. **(e)** *Sub cellular localization of IVa2.* MDBK cells infected with BAV304a (panel a1-a4), BAV304a M1 (panel b1-b4), BAV304aM2 (panel c1-c4), BAV304aM3 (panel d1-d4) or BAV304aM4 (panel e1-e4) with 2 MOI. At 36 hrs post transfection, the cells were fixed and the subcellular localization of IVa2 was visualized by confocal microscope after staining with IVa2gst serum and goat anti-rabbit alexa 647 antibodies..Cells nuclei stained withd DAPI (panels a3,b3,c3,d3,e3) and nucleoli were visualized by staining with anti-RPA antibody and Cy3 conjugated goat anti-mouse antibody (panels a2,b2,c2,d2,e2). A merge of the images is shown in (panels a4, b4, c4, d4 ,e4).

function of colinear proteins in members of the Mastadenvirus genus does not appear to be conserved (Blanchette et al., 2013; Cheng et al., 2013, Makadiya et al., 2015), the present study characterized and identified the functional domains of BAdV-3 IVa2.

The IVa2 mRNA transcribed from the bottom strand of BAdV-3 genome encodes a protein of 448 amino acids, which is detected as 55 kDa protein between 18-24 hrs to 48 hrs post-infection. Similarly, IVa2 specific 55 kDa protein could also be detected in immature and mature virions (Kulshreshtha et al., 2004). The IVa2 protein appears to be localized predominantly to the nucleus and nucleolus of BAdV-3 infected cells. Detection of IVa2 in the nucleus and nucleolus of plasmid DNA transfected cells in the absence of any other viral protein suggest that IVa2 protein may contain non-overlapping NLS \ NoLS, which are located in different domains of the protein (Cheng et al., 2002; Sheng et al., 2004) or overlapping NLS \ NoLS, which are located in the same domain of the protein (Cros et al. 2004).

Active nuclear localization of a protein is regulated by NPC (Lin and Hoelz, 2019) and require an NLS, which can be a classical NLS, a bipartite NLS or a non-classical NLS (Christophe et al., 2000). Analysis of BAdV-3 IVa2 amino acid sequence did not identify any potential classical \ bipartite NLS. However, cNLS Mapper computer program (which predicts NLS specific to importin a\b by calculating NLS scores; (Kosugi et al., 2009a) transport pathway predicted amino acid 5-35 and 64-73 to act as potential NLS. Analysis of mutant BAdV-3 IVa2 proteins containing deletions or substitutions of amino acids suggested that amino acids 4-18 are essential for nuclear localization of BAdV-3 IVa2. However, residues 4-18 of BAdV-3 IVa2 were not sufficient to direct nuclear localization of a fusion protein GFP/βgal, predominantly a cytoplasmic protein. Earlier reports have suggested that residues

upstream or downstream of NLS motif may be involved in the efficient transport of a protein to the nucleus (Seki et al., 1997).

Viral proteins utilize single (Ayalew et al., 2014; Makadiya et al., 2015; Paterson et al., 2012) or multiple (Arnold et al., 2006; Ayalew et al., 2014; Kulshreshtha et al., 2014; Said et al., 2018a; Wodrich et al., 2006) transport receptors for localization to the nucleus, which may depend on the amount of importin available in a particular cell (Arnold et al., 2006). Our results suggest that BAdV-3 IVa2 utilizes importin α-1 as a nuclear receptor for transport to nucleus. Although three importins have been identified as nuclear receptors for translocation of HAdV-5 pVII to nucleus (Wodrich et al., 2006), so far BAdV-3 proteins have been shown to use either single importin α -3 for nuclear transport of 52K (Paterson et al., 2012) 100K (Makadiya et al., 2015) and pV (Zhao and Tikoo, unpublished data) or two importins α -5 and α -7 for nuclear transport of 22K (Said et al., 2018a), and α -5 and transportin -3 for nuclear transport of 33K (Kulshreshtha et al., 2014).

An earlier study suggested that basic residues appeared essential for the nuclear localization of BAdV-3 52K (Paterson et al., 2012). The NLS of BAdV-3 IVa2 contains a cluster of basic residues ^{6}RRK^{8}. Mutant IVa2 proteins containing a substitution of basic residues located predominantly to the nucleolus of the plasmid DNA transfected or recombinant BAdV-3 infected cells suggesting that the cluster of basic residues in potential IVa2 NLS is not essential for the nuclear localization of BAdV-3 IVa2. Moreover, though mutation of a cluster of basic residues ^{6}RRK^{8} to ^{6}GGG^{8} appears to be responsible for a marginal reduction in virus yield of recombinant BAV304aM4, it does not appear to be required for the replication of BAdV-3.

The nucleolar transport of a viral protein requires binding of nucleolar transport signal (NoLS) of a viral protein to nucleolar RNAs \ proteins. The NoLS is rich in basic residues and

is usually at N-terminus or C-terminus of the protein (Reed et al., 2006; Scott et al., 2010). Analysis of BAdV-3 IVa2 truncations\deletion mutants suggested that amino acid 373-448 contains multiple NoLSs, which appear to be functionally redundant. Interestingly, the deletion of IVa2 NoLs does not abrogate nuclear localization of IVa2, suggesting that IVa2 contains non-overlapping NoLS \ NLS. While NoLS appears to be located at the C-terminus of IVa2 protein, NLS appears to be located at N-terminus of the IVa2 protein.

In summary, we have demonstrated that BAdV-3 IVa2 localizes to nucleus and nucleolus utilizing amino acids 4-18 and 373-448, respectively. Moreover, 1-25 and amino acids of BAdV-3 IVa2 interacts with importin α-1 of the nuclear transport receptor.

4.0 Transition from 3.0 to 5.0

By raising antibody against BAdV-3 IVa2 protein, its expression timeline was determined. Additionally, subcellular localization of BAdV-3 IVa2 shown to be predominantly in the nucleolus. Moreover, nuclear and nucleolar localization signals, as well as the mechanism of nuclear import also identified. Further analysis of the effect of basic amino acid in the nuclear localization of IVa2 also examined. Generally, in the course of an adenovirus life cycle, the viral proteins undergo viral- cellular and or viral-viral protein interaction to accomplish their duties. In the present work, we identified intra-viral proteins interaction between IVa2 and late adenoviral proteins.

5. BOVINE ADENOVIRUS (BAdV-3) IVA2 INTERACTS WITH VIRAL PROTEIN pV

5.1 Introduction

Protein IVa2 encoded by intermediate region of HAdV-5 is a protein of 449 amino acids, which is localized in the nucleus and nucleolus of the infected cells (lutz et al., 1996), and unique vertex of purified adenovirus particle (Christensen et al., 2008). Adenovirus IVa2, a multifunctional protein appears to be involved in different steps of viral replication including transactivation of major late promoter (MLP) and adenovirus genome packaging (Ahi and Mittal, 2013), and virion stability (Singh et al., 2005). One way protein IVa2 performs multiple functions is by interacting with different viral proteins including 52/55K for cooperative packaging of viral genome (Gustin et al., 1996; Perez-Romero et al., 2006), with 22K, 33K and DBP (Ahi et al., 2013) and pVIII for virion stability (Singh et al., 2005).

The intermediate region of BAdV-3 encodes structural proteins pIX and IVa2 (Reddy et al., 1998). The BAdV-3 IVa2, a protein of 448 amino acids is detected as a 50kDa protein in virus infected cells (Chapter 3). The IVa2 localizes to the nucleus and the nucleolus using amino acids 4-18 and 373-448, respectively. Moreover, IVa2 interacts with importin α-1 to cross the nuclear membrane (Chapter 3).

Adenovirus genomes contain a positional homolog of BAdV-3 IVa2 (Reddy et al., 1998). Since the positional homologs of adenoviruses differ in structure and function (Blanchette et al., 2013; Cheng et al., 2013;Makadiya et al., 2015; Stracker et al., 2005), we have begun to characterize BAdV-3 IVa2 in detail. Here, we determined the interaction of BAdV-3 IVa2 with other viral proteins.

5.2 Materials and Methods

5.2.1. Cells and viruses

Madin-Darby bovine kidney (MDBK) (ATCC CCL22), cotton rat lung (CRL), (Papp et al., 1997), and and VIDO DT1 cells were propagated at 37°C in minimal essential medium (MEM; Sigma) with 5% CO_2. The HEK 293T (ATCC CRL-11268) cells cultured using Dulbecco's modified minimal essential medium (DMEM; Sigma). All the cell lines supplemented with heat-inactivated 10% fetal bovine serum (FBS; SAFC industries, Sigma), 0.1mM nonessential amino acids (NEAA; Gibco), 10mM HEPES (Gibco) and 50ug/ml gentamicin (Bio Basics). Wild type and recombinant BAdV-3 propagated as described previously (Reddy et al., 1998).

5.2.2 Antibodies.

Anti-IVa2 antiserum (IVa2gst) raised against GST fused full-length IVa2 protein recognizes a protein of 50kDa kDa in BAdV-3 infected cells (section 3.3.2). Production of anti -pV sera has been described (Zhao, 2016). Anti-HA antibody (A1978) obtained from Sigma. Alkaline phosphatase-conjugated goat anti-mouse antibody (115-055-205) and goat anti-rabbit antibody (111-055-003) purchased from Jackson Immuno Research.

5.2.3 Plasmid construction

Plasmids were constructed using standard molecular techniques as described earlier (Sambrook and. Russell, 2000).

PMCS.3821.Initially, a 7162 bp *Aar*I DNA fragment containing IVa2 coding sequence was isolated by digestion of plasmid pUC304a+ DNA with AarI. Finally, a 3821 bp *Sph*I-*Sac*II

DNA fragment (containing IVa2 coding sequence flanked by 1463 bps and 1022 bp) of 7162 bp DNA fragment was isolated and ligated to *Sph*I - *Sac*II digested plasmid pMCS (Thanbichler et al., 2007) DNA creating a plasmid pMCS.3821.

pUC304a.ST146. Using primers AflII FP and IRP146 (Table 2, Appendix 2) and plasmid pMCS.3821 DNA as template, a 595 bp DNA fragment (P1) was amplified by PCR. Similarly, using primers IFP146 and SacI RP (Table 2, Appendix 2), and plasmid pMCS.3821 (described above) DNA as a template, a 1177 bp DNA fragment (P2) was amplified. The P1 and P2 DNA fragments were annealed and a 1748 bp was amplified by PCR using primers AflII FP and SacI RP (Table 2, Appendix 2). The 1748 bp DNA fragment was digested with *Afl*II-*Sac*I and ligated to *Afl*II-*Sac*I digested plasmid pMCS.3821 DNA creating plasmid pMCS.3821.ST146.

Escherichia coli BJ5183 based homologous recombination between 3845 bp *Sph*I-*Sac*II fragment of plasmid pMCS.3821.STIVa2146 and *Sbf*I linearized plasmid pUC304a.dIVA2SbfI (described above) DNA resulted in isolation of plasmid pUC304a.ST146 (*pUC304a+ containing strep tag II (ST-II) sequence after amino acid 146 of IVa2).*

pUCK304a.ST242. Using primers SphI FP and IRP242 (Table 2, Appendix 2), and plasmid pMCS.3821 DNA as a template, a 2116 bp DNA fragment (P1) was amplified by PCR. Similarly, using primers IFP242 and SacII RP (Table 2, Appendix 2), and plasmid pMCS.3821 DNA as a template, a 1768 bp DNA fragment (P2) was amplified by PCR. The P1 and P2 DNA fragments were annealed and a 3860 bp DNA fragment was amplified by PCR using primers SphI FP and SacII RP (Table 2, Appendix 2). The 3860 bp DNA fragment was digested with *Sph*I-*Sac*II and ligated to *Sph*I-*Sac*II digested plasmid pMCS (Thanbichler et al., 2007) DNA creating plasmid pMCS.3821.ST242.

Escherichia coli BJ5183 based homologous recombination between 3845 bp *Sph*I-*Sac*II fragment of plasmid pMCS.3821.ST242 and *Sbf*I linearized plasmid pUC304a.dIVa2SbfI DNA resulted in the isolation of plasmid pUC304a.ST242 (pUC304a+ containing STII sequence after amino acid 242 of IVa2).

pUC304a.ST448. Using primers SphI FP and IRP448 (Table 2, Appendix 2) and plasmid pMCS.3821DNA as a template, a 1498 bp DNA fragment (P1) was amplified by PCR. Similarly, using primers IFP448 and SacII RP (Table 2, Appendix 2), and plasmid pMCS.3821 DNA, a 2386 bp DNA fragment (P2) was amplified. The P1 and P2 DNA fragments were annealed and a 3860 bp DNA fragment was amplified by PCR using primers SphI FP and SacII RP (Table 2, Appendix 2). The 3860 DNA fragment was digested with *Sph*I-*Sac*II and ligated to *Sph*I-*Sac*II digested plasmid pMS (Thanbichler et al., 2007) DNA creating plasmid pMCS.3821.ST448.

Escherichia coli BJ5183 based homologous recombination between 3845 bp *Sph*I-*Sac*II fragment of plasmid pMCS.3821.ST448 and *Sbf*I linearized plasmid pUCK304a.dIVa2*Sbf*I DNA resulted in isolation of plasmid pUC304a.ST448 (*pUC304a+ containing STII sequence IVa2 stop codon).*

5.2.4 Transfection

The transfection of cells with plasmid DNA was performed as described in section 3.2.6.

5.2.5 Isolation of recombinant BAdV-3 viruses

The recombinant BAdV-3s were isolated using plasmid DNA transfection of cells as described in section 3.2.7.

5.2.6 Western blotting

Virus-infected cells, plasmid transfected cells, or purified proteins were analyzed by Western blotting (Kulshreshtha et al., 2004) as described in section 3.2.8 using protein-specific antiserum and alkaline phosphatase-conjugated secondary antibody.

5.2.7. Sequence analysis of BAdV-3 IVa2

To identify specific protein– protein interacting motif within the full-length of IVa2, we analyzed the BAdV-3 IVa2 protein sequence by a coiled-coil program (Lupas et al., 1991).

5.2.8 Bimolecular fluorescence complementation (BiFC) analysis

BiFC assay (Kerppola, 2009) performed as described earlier (Levin et al., 2009; Rosenbluh et al., 2007; Said et al., 2018b). The pGN and pGC plasmids were provided by Dr. Abraham Loyter (The Hebrew University of Jerusalem, Israel). Preparation and transformation of competent S288c cells (yeast competent cells, a gift from Dr. Troy Harkness, University of Saskatchewan) were carried out according to the method outlined in the yeast protocols handbook (Clontech Laboratories 2009). Briefly, several 2-3mm colonies of yeast S288c cells inoculated into 1mL of yeast peptone dextrose adenine broth (YPDA). After dispensing clumps via vortexing, the inoculate was transferred into 50 mL YPDA and incubated at 30^0C for 18 hrs with shaking at 220 RPM until OD 600 value reaches $\geq$ 1.5. The culture was transferred to 300mL of YPDA and further incubated at 30^0C with shaking at 220 RPM for 3hrs When OD 600 value of the culture reached 0.5, the culture was pelleted at 1000 g for 5 min and resuspended in 30mL of sterile double distilled water. The supernatant removed by centrifuging at 1000g for 5 min, and cell pellets again resuspended in 1.5mL of 1X Tris-EDTA /lithium

acetate. Transformation of yeast cells with indicated plasmid DNAs were carried out using polyethylene glycol–Lithium acetate (PEG-LiAc) method (Clontech Laboratories 2009). In a single Eppendorf tube, 0.4ug of each plasmid, 0.1mg of carrier DNA (salmon sperm), 0.1mL of a freshly prepared competent cell, and 0.6mL of PEG-LiAc (40% PEG, 1X TE, 1X LiAc) solution was mixed and incubated for 30 min on a shaker at 200RPM. After incubation, 70ul of dimethyl sulfoxide was added, mixed with gentle inversion before heat shocking for 15 min at 42^0C followed by 2min chilling on ice. The supernatant was removed by centrifuging cells at 14000 RPM for 5min, followed by suspension of cell pellet in 0.5mL of 1X TE. Finally, 100ul of the suspension was used to streak a plate containing selective dropout medium supplemented 2% glucose in the absence of urease and histidine. The streaked plates incubated at 30^0C for 3 days. The colonies were picked, spread, and fixed with 3.7% paraformaldehyde for 15min. The fixed slides were allowed to dry, mounted with mounting medium (Vectashield) containing DAPI examined using Zeiss LSM 5 Laser scanning confocal microscope.

5.2.9 Co-Immunoprecipitation (Co-IP) assay

The co-immunoprecipitation assay was performed as described (Said et al., 2018a). Briefly, forty-eight hr post transfection, the cells were washed with ice-cold PBS, scraped off the culture plate in the presence of NP-40 lysis buffer containing protease inhibitor cocktail (Roche) and further incubated for 30 min at 4^0C on a shaker. After 30 min incubation, the cell lysate was centrifuged at 12000g for 10 min at 4^0C. The clarified lysates were transferred to an Eppendorf tube containing sepharose A beads conjugated to protein specific antibodies and incubated overnight at 4^0C on a rotator. After overnight incubation, the beads were pelleted and washed 4x with lysis buffer. Next, 50ul of 2X SDS sample buffer added to the resin and

protein was denatured by heating at 100^0C for 3 mins. Finally, the proteins were separated by 12% SDS-PAGE, transferred to nitrocellulose and probed in Western blotting carried out using appropriate protein specific primary followed by appropriate secondary antibody. The protein bands were visualized by developing using specific substrate.

Co-immunoprecipitation in the context of virus infection was carried out using (Co-IP) kit from Thermo Scientific as per the instruction of the manufacturer. Generally, the overall protocol involves purification of IgG, immobilization of antibodies with beads, cell lysis, and pre-clearing and actual Co-IP. IgG purification was carried out by passing anti pV antibody or pre-immune sera through an IgG purification column. The purified antibody, coupled with AminoLink Plus Resin beaded agarose, which is reactive towards primary amines (-NH2) found on antibodies. After antibody coupling, actual CO-IP proceeded by clarifying supernatant containing protein sample by incubating with Sepharose A beads and transferring to a spin column containing AminoLink Plus Resin coupled with anti PV IgG or pe immune sera. After overnight incubation, at 4^0C on an orbital shaker, the spin column was centrifuged, and the resin washed 3x with lysis buffer. After the final wash, the protein sample was eluted using a gentle elution buffer mixed with SDS sample buffer. After boiling at 100^0C for 3 min. the proteins in sample were sepatrated by 12% SDS-PAGE and probed in Western blot using an anti IVa2 antibody followed by an alkaline phosphatase-conjugated secondary antibody. Finally, the protein bands were visualized using Pierce™ ECL Western blotting substrate (Thermo Fisher), and the image captured using X-ray films (GE Healthcare).

5.3 Results

5.3.1 Isolation of mutant BAdV-3 containing insertion of Strep-tag

For isolation of recombinant BAdV-3 expressing IVa2 containing Step tag (Trp-Ser-His-Pro-Gln-Phe-Glu-Lys) (Schmidt and Skerra, 2007), full-length plasmids pUC304a.ST146, pUC304a.ST242, and pUC304a.ST448 containing Strep tag sequence inserted in-frame after amino acid 146, 242, and 448, respectively (Fig. 5.1a). The selection of insertion sites was based on prior information in human IVa2 studies and also areas that appear to be less conserved. As seen in Fig. 5.1b (panel a1-a2), expression of EYFP, and development of cytopathic effects observed in cells transfected with plasmid pUC304a+ DNA. Repeated transfection of VIDO DT1 cells with 5ug of mutant individual plasmid DNAs did show expression of EYFP, however cytopathic effects were not visible in the cells transfected with plasmid pUC304a.ST146 (panels, b1-b2) DNA, plasmid pUC304a.242 (panel, c1-c2) DNA or plasmid pUC304a.448 (panels, d1-d2) DNA up to 20 days post-transfection (Fig. 5.1, panel b).

5.3.2 Interaction of IVa2 with BAdV-3 proteins

To determine the interaction of IVa2 with other viral proteins, we performed a BiFC assay. The competent S288c cells were co-transformed with indicated plasmid DNAs. Transformed yeast cells were plated out in a dropout medium devoid of histidine and uracil and incubated for 3 days at 30^0C. Individual colonies were fixed, smeared out in the glass side, stained with DAPI and observed under a confocal microscope. As seen in Fig. 5.2, green fluorescence was observed in yeast cells co-transformed with plasmid pGN.IVa2 +pGC.pV DNAs (panels, a1-a4); pGN.IVa2+ pGC.pVII DNAs (panels, b1-b4); pGN.IVa2 + pGC.pVIII DNAs (panels, c1-c4); pGN.IVa2 + pGC.p22K DNAs (panels, d1-d4); pGN.IVa2 + pGC.52K DNAs (panels, e1-e4); pGN.IVa2 + pGC.Fiber DNAs (panels, f1-f4) and pGN.IVa2 + pGC.hexon DNAs (panels, g1-g4).

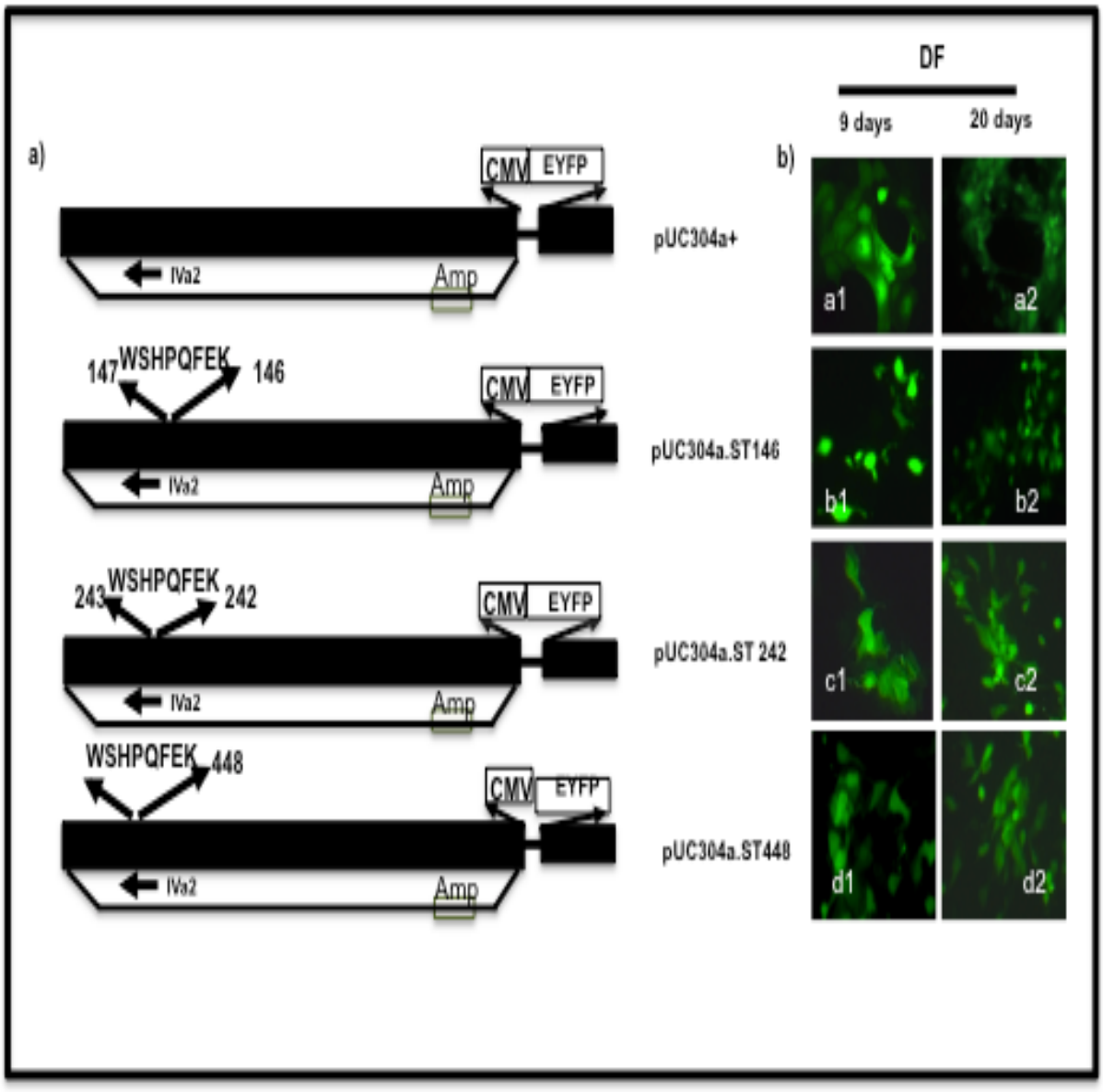

Fig. 5.1 Isolation of mutant BAdV-3. (a). *Schematic diagram of plasmid DNAs.* The name of the plasmids is depicted on the right of the panel. The BAdV-3 sequence is represented by filled box. The thin line represents deleted region (E3). The amino acids of Strep tag II are indicated. The numbers represent the amino acids of BAdV-3 IVa2. Human cytomegalovirus (CMV) immediate early promoter; Enhanced yellow fluorescent protein (EYFP). **(b)** *Direct Fluorescence.* Monolayers of VIDO DT1 cells were transfected with 5 µg indicated plasmid DNA and visualized for EYFP expression and development of cytopathic effects using fluorescent microscope TCS SP5 (Leica). Direct fluorescence (DF).

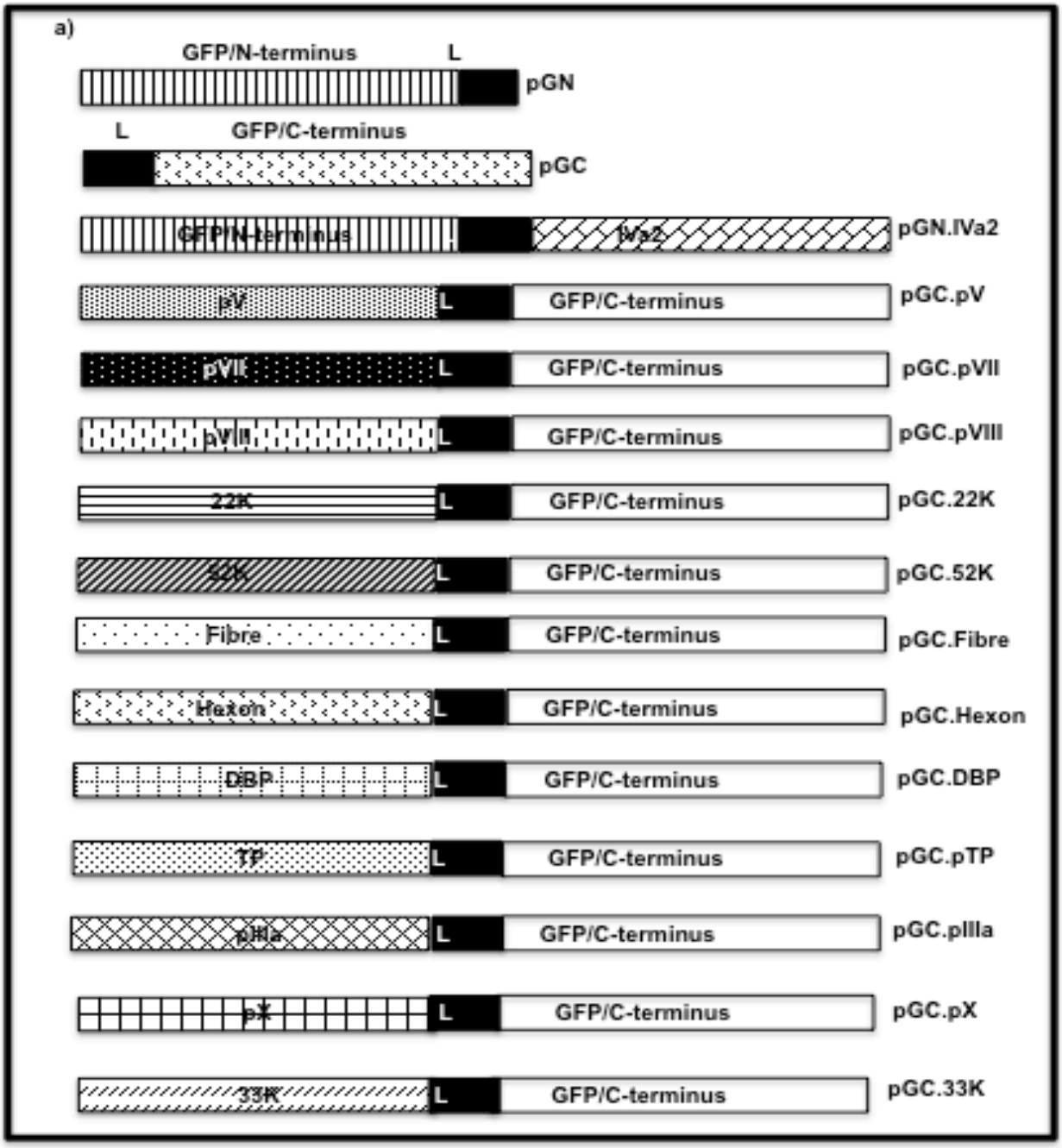

Fig. 5.2 Interaction of IVa2 with BAdV-3 proteins. (a). *Schematic diagram of plasmid DNAs*. The name of the plasmid is depicted on the right of the panel. Linker region (L). Green fluorescent protein N-terminus (GFP/N-terminus), Green fluorescent protein C-terminus (GFP/C-terminus).

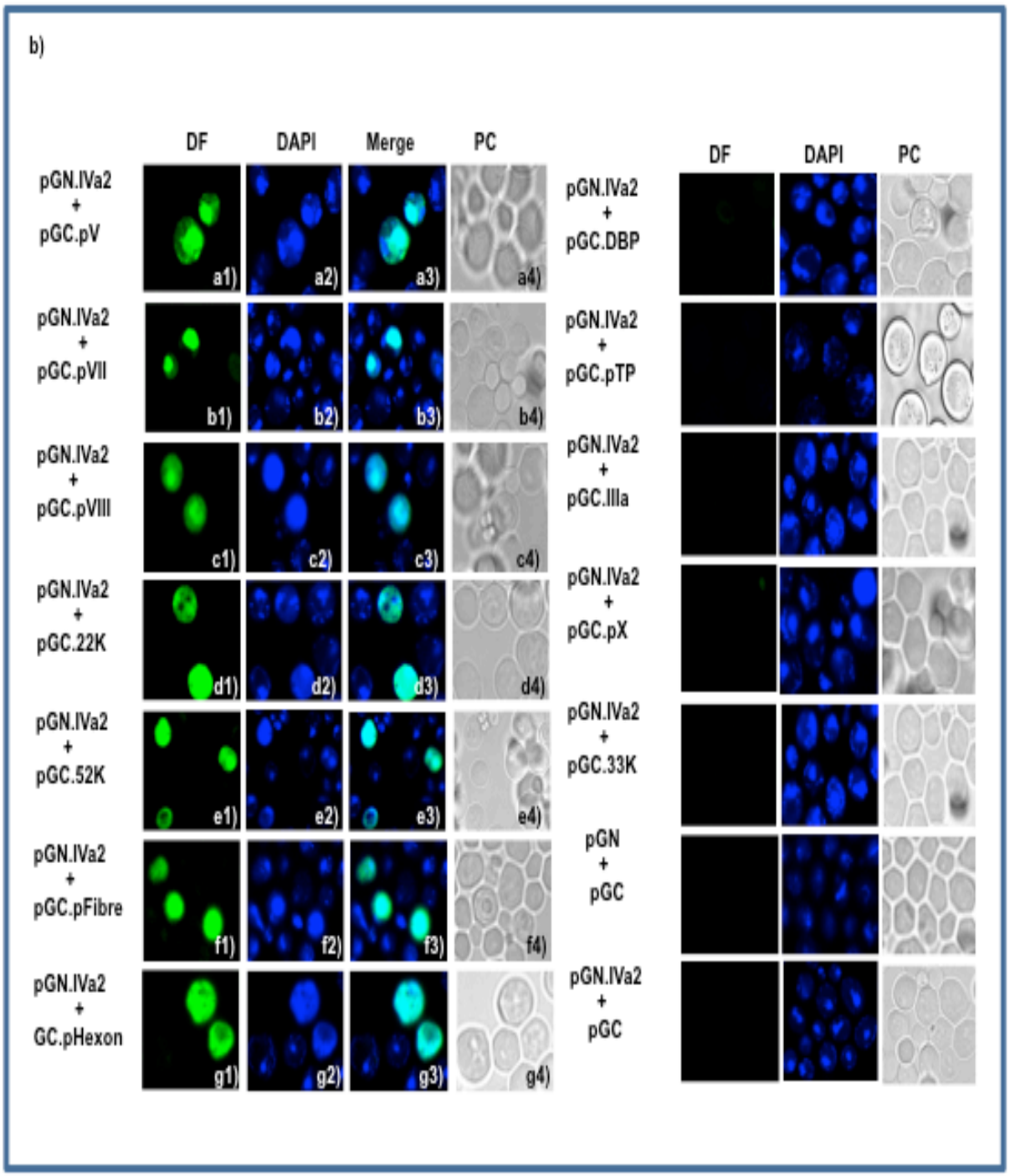

Fig. 5.2 Interaction of IVa2 with BAdV-3 proteins (b). *Biomolecular fluorescence complementation assay (BiFC).* Yeast S288c cells were co-transformed with indicated plasmid DNA, incubated on a selective media and observed under a confocal microscope. Direct fluorescence (DF), Phase contrast (PC).

5.3.3 Interaction of IVa2 with pV

Earlier, mass spectrometry analysis of protein complexes, purified from recombinant BAV ST (pV containing an insertion of Strep Tag sequence) infected cells using Strep-Tactin Sepharose pull-down assay suggested that BAdV-3 IVa2 interacts with pV (Zhao, 2016). To confirm the interaction of IVa2 with pV, initially, we repeated BiFC assay. Yeast competent cells S288c-were co-transformed with plasmid pGN.IVa2 and pGC.pV DNA or plasmid pGN.IVa2 and pGC DNA or plasmid pGN and pGC DNA (Fig. 5.3, panel a,b). Transformed yeast cells plated out in a dropout medium devoid of histidine and uracil and allowed to grow for 3 days at 30^0C. Individual colonies were fixed, smeared out in the glass side, stained with DAPI, and observed under a confocal microscope. As seen in Fig. 5.3 (panel b), green fluorescence was observed in yeast cell co-transformed with plasmid pGC.pV and pGN.IVa2 DNA (panel a1-a3). No such fluorescence could be observed in yeast cells co-transformed with plasmid pGN.IVa2 and pGC DNA (panels, b1-b3) or plasmid pGN and pGC (panels, c1-c3). To further confirm the interaction of IVa2 with pV, a co-immunoprecipitation assay performed.

At 36 hrs post-transfection, the lysates of 293T cells co-transfected with indicated plasmid DNAs as seen in (Fig. 5.4a) were immune-precipitated using anti-HA MAb and co-immunoprecipitated IVa2 protein was detected in Western blot using IVa2gst sera. As Fig. 5.4b IVa2 specific band could be observed in the cells co-transfected with plasmid pC.IVa2 + pC.HApV (Zhao, 2016) DNAs (panel b, lane 2). No such band could be observed in cells transfected with plasmid pC.IVa2 + pC.HA DNAs (panel b, lane 1).

Finally, the interaction of IVa2 with pV was confirmed in BAdV-3 infected cells. The cell lysates from mock or BAdV-3 infected cells were immune-precipitated with anti-pV sera or

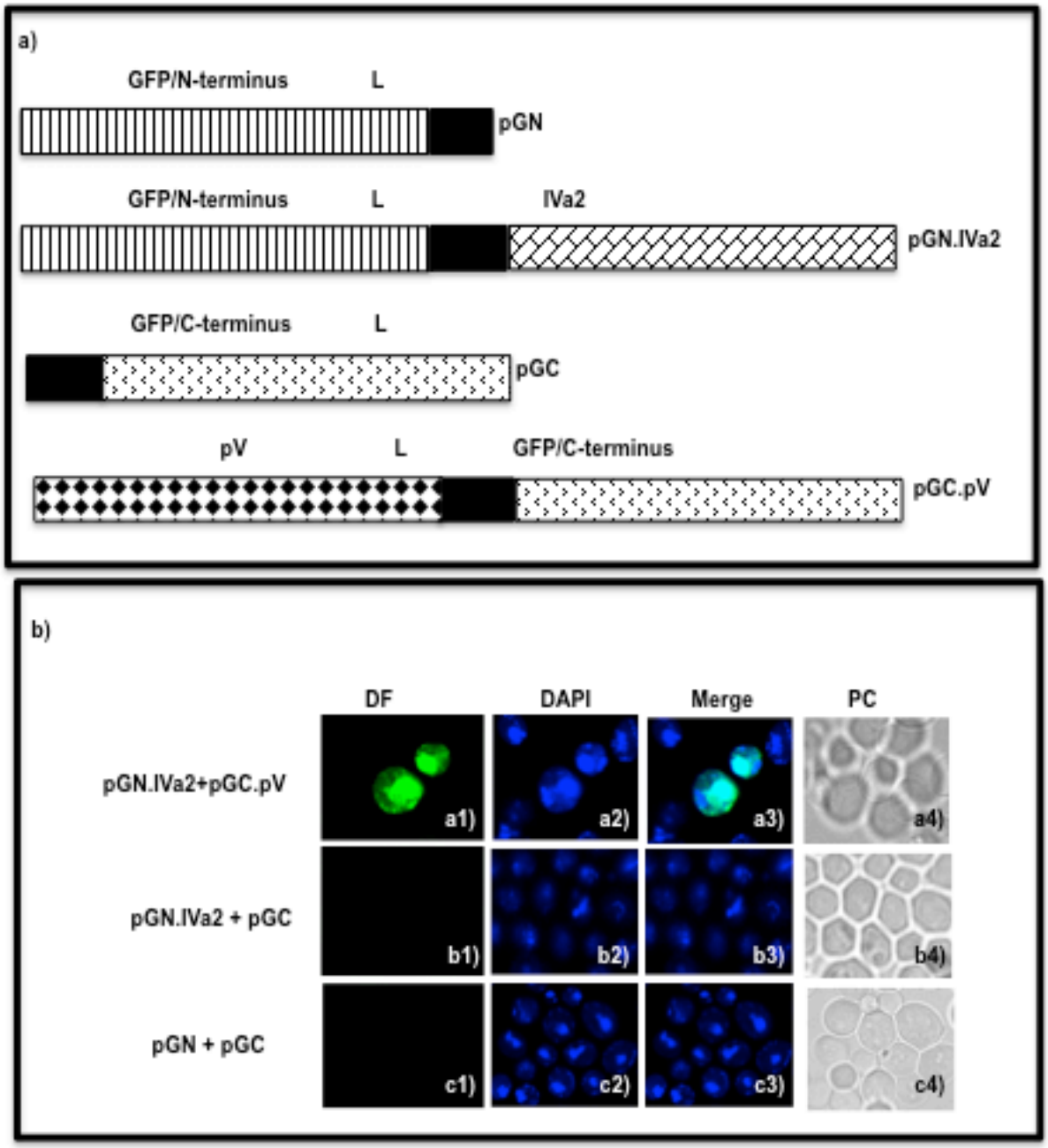

Fig. 5.3 Interaction of IVa2 with BAdV-3 pV. (a). *Schematic diagram of plasmid DNAs*. The name of the plasmid is depicted on the right of the panel. Linker region (L). Green fluorescent protein N-terminus (GFP/N-terminus), Green fluorescent protein C-terminus (GFP/C-terminus). **(b).** *Biomolecular fluorescence complementation assay (BiFC)*. Yeast S288c cells were co-transformed with indicated plasmid DNA, incubated on a selective media and observed under a confocal microscope. Direct fluorescence (DF), Phase contrast (PC).

pre-immune sera and co-immunoprecipitated IVa2 protein detected in Western blot using IVa2gstsera. As seen in Fig. 5.4b, IVa2 specific band could be detected in BAdV-3 infected cells immunoprecipitated with anti-pV sera (panel c, lane 3). No such band could be detected in mock-infected cells with (panel c, lane 4) or without (panel c, lane 6) immunoprecipitation with anti-pV sera. Similarly, no such band could be observed in BAdV-3 infected cells (panel c, lane 2) or mock-infected cells (panel b, lane 5) immunoprecipitated with pre-immune sera. Protein IVa2 detected in BAdV-3 infected cells act as a protein input control (panel c, lane 1).

5.3.4 Mapping interacting region of IVa2 with PV

To identify the domain of IVa2 interacting with pV, BiFC assay was performed using plasmids expressing mutant IVa2 containing truncations\deletions (Fig. 5.5, panel a). Green fluorescence could be observed in yeast cells co-transformed with plasmid pGN.IVa2 + pGC.pV DNA (Fig. 5b, panels, a1-a4). Similarly, green fluorescence could be detected in yeast cells co-transformed with plasmid pGN.IVa2d6 + pGC.pV DNAs (Fig. 5.5b, panels, b1-b4) or plasmid pGN.IVa2d7 + pGC.pV DNAs (Fig. 5.5b, panels, c1-c4). No such fluorescence could be observed in yeast cells co-transformed with plasmid pGN.IVa2d8 DNAs (Fig. 5.5b, panels, d1-d4), or plasmid pGN.IVa2d9 + pGC.pV DNAs (Fig. 5.5b, panels, e1-e4).

To narrow down the domain of IVa2 interacting with pV, plasmids expressing mutant IVa2 protein containing small deletions in amino acids 121-140 were constructed (Fig. 5.5, panel a). However, no fluorescence could be observed in yeast cells co-transformed with plasmid pGN.IVa2d9.1 + pGC.pV DNAs (Fig. 5.5b, panels f1-f4), plasmid pGN.IVa2d9.2 + pGC.pV DNAs (Fig. 5.5b, panels g1-g4) or plasmid pGN.IVa2d9.3 + pGC.pV DNAs (Fig. 5.5b, panel

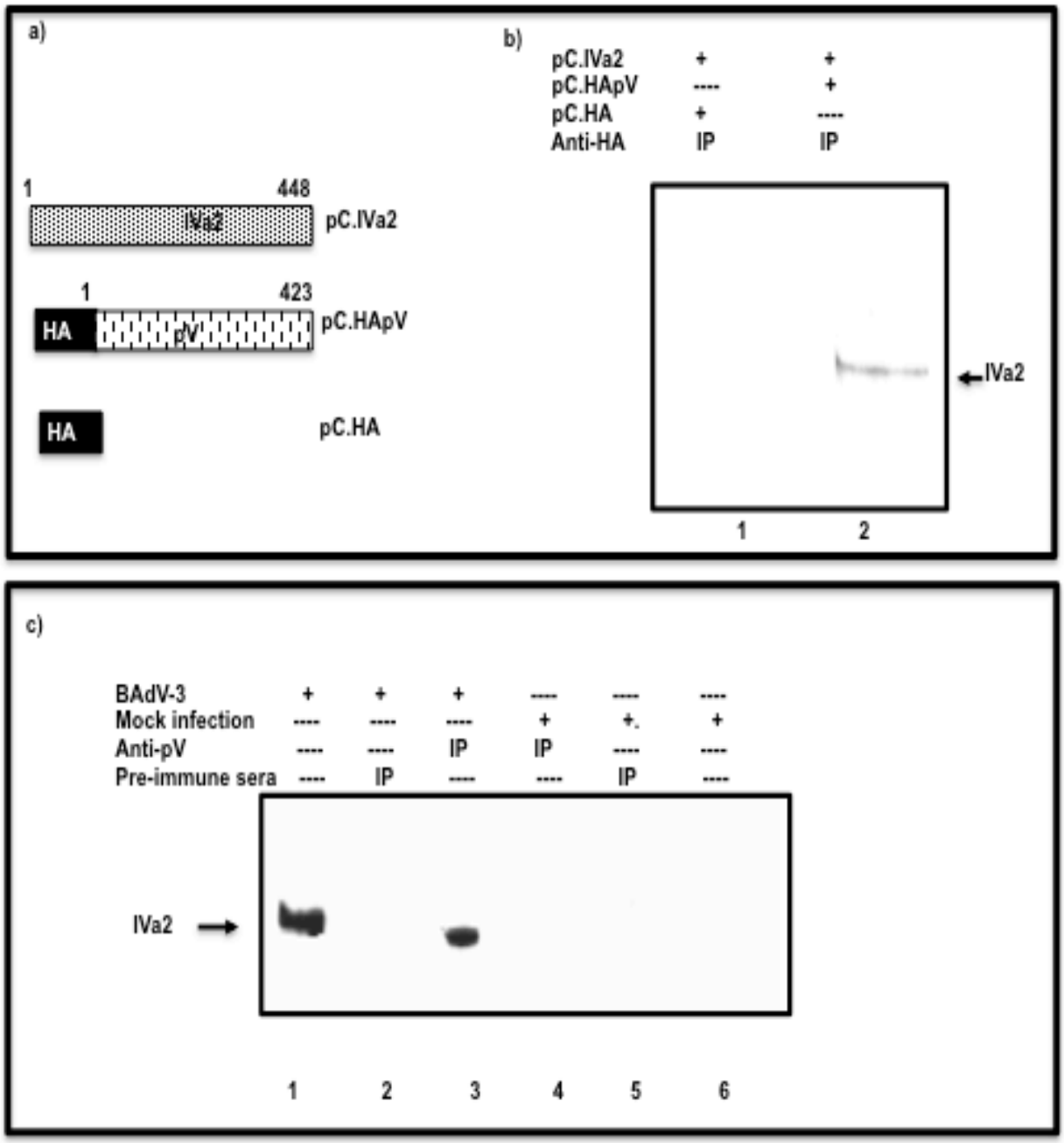

Fig. 5.4 Interaction of IVa2 with pV. (a) *Schematic diagram of plasmid DNAs*. Amino acid numbers are depicted. The name of the plasmid is depicted on the right of the panel. Linker region (L). **(b)** *Co-immunoprecipitation in transfected cells.* Proteins from the lysates of indicated plasmid transfected HEK 293T cells were immunoprecipitated with anti-HA MAb, separated by 12 % SDS-PAGE, transferred to nitrocellulose membrane and analyzed by Western blot using IVa2gst serum. (**c)** *Co-immunoprecipitation in BAdV-3 infected cells*. Proteins from the lysates of BAdV-3 infected cells were immunoprecipitated with anti-pV sera (Zhao, 2016) or pre immune sera, transferred to nitrocellulose and analysed by Western blot using IVa2gst sera.

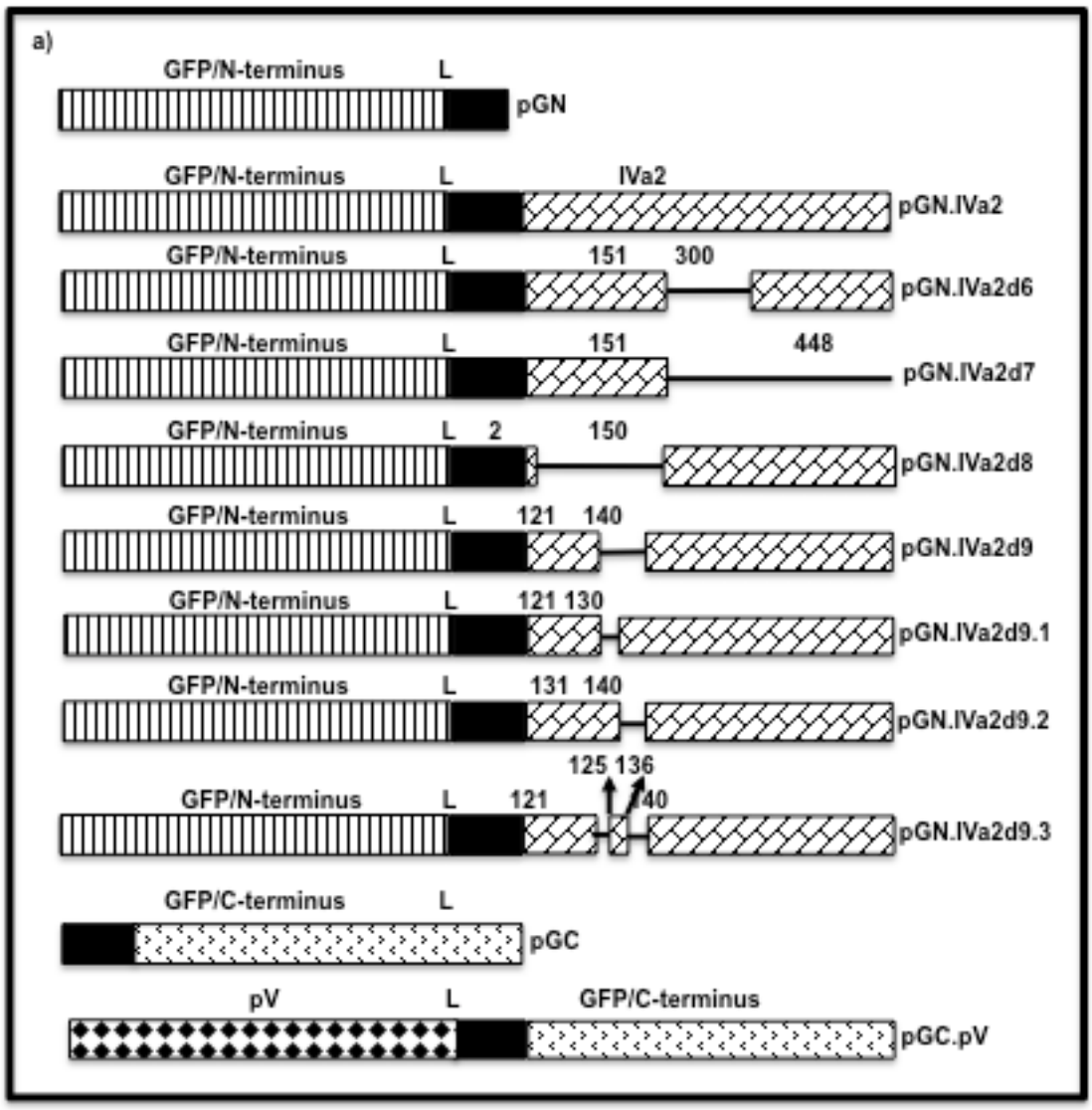

Fig. 5.5 Identification of region of IVa2 interacting with BAdV-3 pV pV. (a). *Schematic diagram of plasmid DNAs*. The name of the plasmid is depicted on the right of the panel. The amino acid numbers of IVa2 are depicted. The thin line represents deleted regions. Linker region (L). Green fluorescent protein N-terminus (GFP/N-terminus), Green fluorescent protein C-terminus (GFP/C-terminus

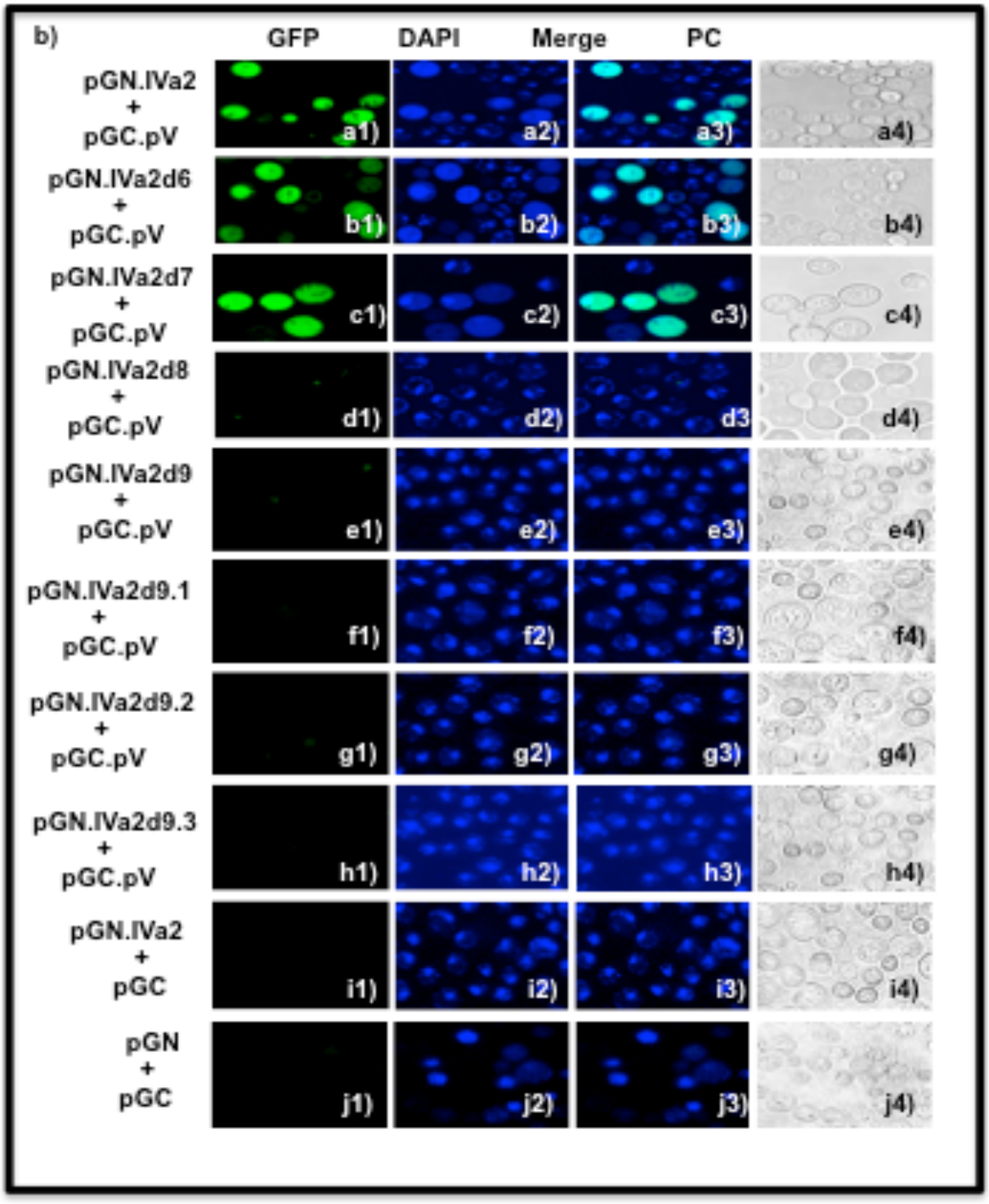

Fig. 5.5 Identification of region of IVa2 interacting with BAdV-3 pV pV. (b). *Biomolecular fluorescence complementation assay (BiFC).* Yeast S288c cells were co-transformed with indicated plasmid DNA, incubated on a selective media and observed under a confocal microscope. Direct fluorescence (DF), Phase contrast (PC).

h1-h4). Similarly, no fluorescence could be observed in yeast cells co-transformed with plasmid pGN.IVa2 + pGC DNAs (Fig. 5.5b, panels, i1-i4) or plasmid pGN + pGC DNAs (Fig. 5.5b, panels, j1-j4).

5.3.5 Sequence analysis of IVa2

Analysis of IVa2 sequence using coiled-coil program, Fig. 5.6, predicted the presence of a coil-coil region between amino acid 129 to 142.

5.4 Discussion

Successful interactions between viral protein-viral DNA, viral-viral proteins, and viral-cellular proteins appear essential for the production of an infectious progeny adenovirus. Several adenoviral proteins have reported interacting with viral (Ma and Hearing, 2011; Perez-Romero et al., 2005; Wohl and Hearing, 2008; Zhang and Imperiale, 2000), cellular proteins (Inturi et al., 2013, Paterson, 2010, Zhao, 2016) and other viral proteins (Ahi et al., 2013, Gustin et al., 1996, Singh et al., 2005, Said et al., 2018b, Tyler et al., 2007) to facilitate virus assembly. An earlier report suggested the involvement of IVa2 in genome packaging, activation of transcription from MLP, and virion stability (Christensen et al., 2012; Pardo-Mateos and Young 2004; Perez-Romero et al., 2006; Ostapchuk et al., 2005; Singh et al., 2005).

The multifunctional role played by IVa2 suggests that IVa2 may interact with other viral\ cellular proteins. Earlier reports have suggested that adenovirus IVa2 interacts with 33K and DBP (Ahi et al., 2013), 52K (Gustin et al., 1996), and pVIII (Singh et al., 2005). Our initial attempts to purify and identify proteins interacting with pC.IVa2 by affinity tag purification of

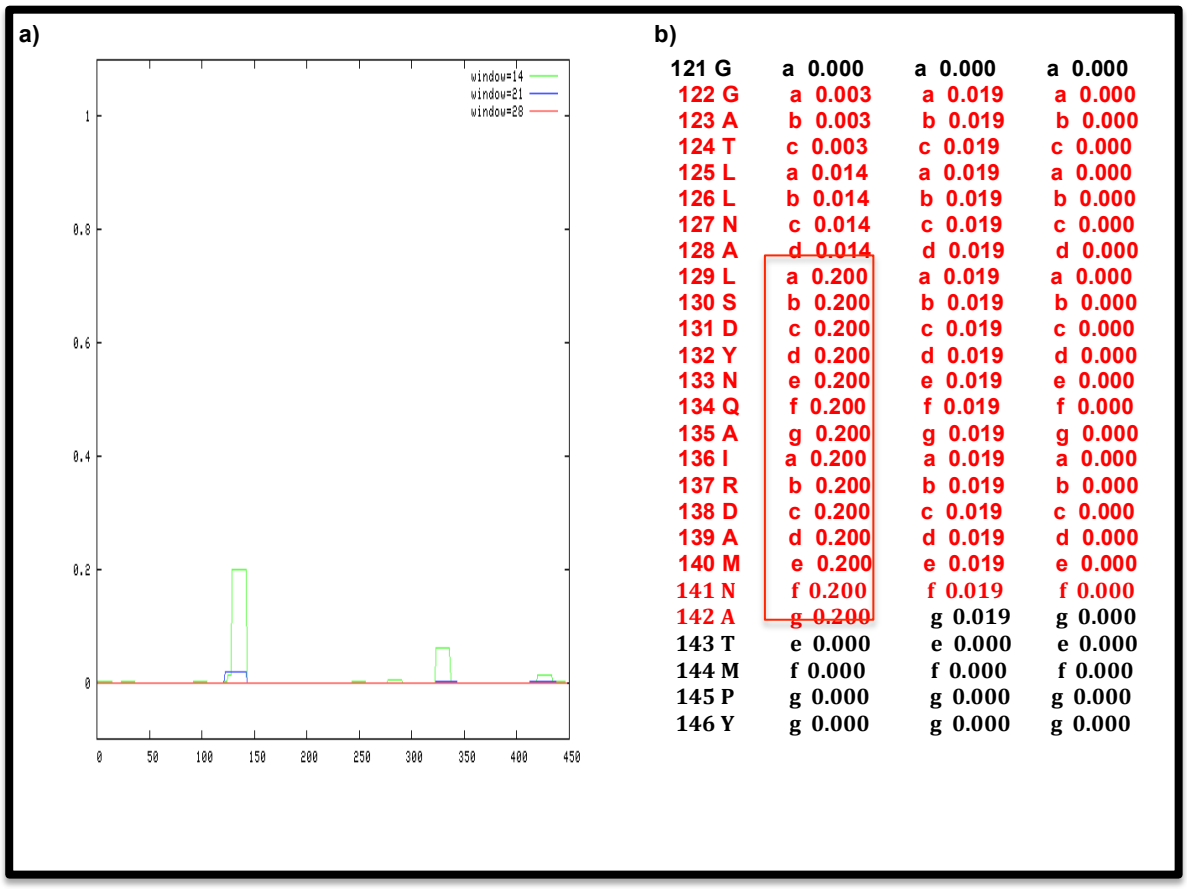

Fig. 5.6 Analysis of IVa2 protein sequence by Coiled-Coil program. Graphic presentation of IVa2 amino acid sequence showing coiled coil region. b) Numeric value of coiled coil region of IVa2 sequence.

protein complexes from recombinant BAdV-3 infected cells were not successful as the insertion of strep tag II in IVa2 proved lethal for the replication of recombinant BAdV-3s. However, the bimolecular fluorescence complementation (BiFC) assay indicated that BAdV-3 IVa2 protein might be interacting with hexon, fiber, pVII, pVIII, 22K, 52K and pV. Earlier, analysis of proteins co-immunoprecipitated with pV by LC-MS/MS also indicated that IVa2 interacts with pV (Zhao, 2016). The specific interaction between BAdV-3 IVa2 and pV was confirmed by co-immunoprecipitation and BAdV-3 infected cells. Earlier observations in human adenovirus have speculated that IVa2 may indirectly interact with pV via other viral proteins (Ahi et al., 2015; Zhang and Arcos, 2005). The Co-immunoprecipitation analysis in plasmid DNA transfected cells confirms that BAdV-3 IVa2 interacts directly with pV protein.

Analysis of mutant IVa2 proteins suggested that amino acids121-140 of BAdV-3 IVa2 interact with pV. Interestingly, analysis of BAdV-3 IVa2 amino acid sequence identified a coiled-coil region (Lupas et al., 1991) located between amino acids 129 to 142, which acts as a protein-protein interaction motif that holds proteins together (Ali et al., 2007). However, the function of IVa2-pV interaction in the production of progeny adenovirus virions is not clear.

DNA binding studies have suggested that binding of pV to DNA still leaves several regions of pV accessible for interaction with other adenoviral proteins (Perez-Vargas et al., 2014).

In fact, studies have suggested that pV interacts with pVI and pVII, which helps to act as a bridge between viral capsid and core (Perez-Vargas et al., 2014). We hypothesize that the interaction of IVa2 with pV further helps to stabilize the bridge between viral core and capsid.

The stability of mature adenovirus virion requires interactions between different adenoviral capsid proteins (Reddy and Nemerow, 2014). The BAdV-3 pV is essential for the production

of infectious progeny virion (Zhao and Tkoo, 2016) as the deletion of pV results in the production of progeny virions with fragile capsids (Zhao and Tikoo 2016). Given the significant role of pV in BAdV-3 life cycle, the interaction of pV and IVa2 could possibly contribute to linking the core with capsid structure or increasing the stability of the capsid structure.

6.0 TRANSITION FROM CHATER 5 TO 7

Using a bimolecular fluorescent complementation assay, we found some late adenoviral proteins, including pV that interact with IVa2. Interaction of BAdV-3 IVa2 with pV confirmed in the context of infection and transfection using co-immunoprecipitation assay. Amino acid 121-140 of IVa2 found to be responsible for its interaction with PV. A recent report on pV of BAdV-3 indicates that the viral protein found to be essential for the virus life cycle (Zhao and Tikoo 2016). Proteins involve viral-viral or viral-cellular protein-protein interaction during the course of virus infection to carry out their duty. In the following section, we demonstrate the role of IVa2 in the BAdV-3 life cycle.

7. BOVINE ADENOVIRUS-3 IVA2 IS ESSENTIAL FOR VIRAL REPLICATION

7.1 Introduction

Adenovirus contains double-stranded DNA genome (26-48 kbp) surrounded by a non-enveloped capsid (Harrach, 2014). The transcription of adenoviral mRNA is temporally regulated as early, intermediate, and late transcripts, which encode 23-46 proteins depending on the characteristics of an adenovirus genus (Ghebremedhin, 2014). Depending upon their function in the production of progeny adenovirus, these proteins designated as capsid protein (structural proteins, core proteins) and non-capsid proteins (non-structural proteins) (Kallsten et al., 2017). The capsids of members of genus Mastadenovirus contain thirteen proteins including major capsid proteins (penton, hexon, fiber), minor capsid proteins (IX, VI, IIIa, VIII,) and core proteins (Mu, V, TP, VII, IVa2, cysteine protease) (Russell, 2009; Vellinga et al., 2005). Earlier reports suggest that human adenovirus -5 (HAdV-5) protein IVa2 detected as a 50 kDa and 40 kDa proteins in infected cells (Pardo-Mateos and Young, 2004). Each purified virion contains 6-8 copies of IVa2 (Christensen et al., 2008). Protein IVa2 appears involved in the transcriptional activation of the adenovirus major late promoter and in adenovirus genome packaging (Lutz and Kedinger, 1996; Ostapchuk et al., 2011).

Bovine adenovirus-3 (BAdV-3), a member of genus Mastadenovirus, contains a double-stranded DNA genome of 34446 bps long, which encodes structural proteins, non -structural proteins and core proteins (Reddy et al., 1998). The core proteins of adenovirus attach to the genome and act as a bridge between viral core, including genome and viral capsid. Earlier, reports have shown that BAdV-3 core protein pVII is expressed as 26 kDa and 24 kDa proteins and localizes to mitochondria altering mitochondrial functions (Anand et al., 2014). Recently,

we detected a 55 kDa BAdV-3 core protein, pV in purified virions, which appears to be essential for the replication of BAdV-3 (Zhao and Tikoo, 2016). In addition, nucleolar localization of BAdV-3 pV appears essential for the replication of BAdV-3 (Zhao, 2016).

The intermediate region of BAdV-3 encodes minor core protein IVa2 of 376 amino acids, which show 29-69% amino acid identity to IVa2 proteins encoded by other adenoviruses (Baxi et al., 1998; Reddy et al., 1998). Earlier, we demonstrated that BAdV-3 IVa2 is a) expressed as 50 kDa protein in BAdV-3 infected cells, b) localized to the nucleus and nucleolus of BAdV-3 infected cells, and c) interacts with importin α-1 and BAdV-3 pV protein. Here, we demonstrate that BAdV-3 IVa2 appears essential for the replication of BAdV-3.

7.2 Materials and Methods

7.2.1 Cell lines and Viruses

Madin-Darby bovine kidney (MDBK) (ATCC CCL22), cotton rat lung (CRL) (Papp, et al., 1997), and CRL.IVa2 (CRL cells expressing BAdV-3 IVa2; in this study) cells were propagated at 37°C in minimal essential medium (MEM; Sigma) with 5% CO_2. The HEK 293T cells cultured using Dulbecco's modified minimal essential medium (DMEM; Sigma). All the cell lines supplemented with heat-inactivated 10% fetal bovine serum (FBS; SAFC industries, Sigma), 0.1mM nonessential amino acids (NEAA; Gibco), and 10mM HEPES (Gibco) and 50 ug/ml gentamicin (Bio Basics). Wild type and recombinant BAdV-3 propagated, as described previously (Reddy et al., 1998).

7.2.2 Antibodies

Anti gstIVa2 antisera described in section 3.3.2, Cy3 conjugated goat-anti rabbit antibody (#111-165-003) and alkaline phosphatase-conjugated goat anti-Rabbit (111-055-003) antibodies bought from Jackson Immune Research.

7.2.3 Plasmid construction

Plasmids were constructed using standard molecular techniques as described earlier (Sambrook and. Russell, 2000).

pTrip-IVa2-Puro. A 1371 bp *XhoI-BamHI* DNA fragment of plasmid pDR-IVa2 (Appendix 1) was ligated to *Xho*I-*Bam*HI digested plasmid pTrip-CMV-Puro (a gift from Dr R. Brownlie) creating a plasmid pTrip-IVa2 Puro.

pMCS.3821. Initially, a 7162 bp *Aar*I DNA fragment containing IVa2 coding sequence was isolated by digestion of plasmid pUC304a+ (Du & Tikoo., 2010) DNA with *AarI*. Finally, a 3821 bp *Sph*I-*Sac*II DNA fragment (containing IVa2 coding sequence flanked by 1463 bps and 1022 bp) of 7162 bp DNA fragment was isolated and ligated to *Sph*I - *Sac*II digested plasmid pMCS (Thanbichler et al., 2007) DNA creating a plasmid pMCS.3821.

pMCS3821.dIVA2SbfI. Using *Sph*I FP and IRPΔIVa2 primers (Table 3, Appendix 3), and plasmid pMCS.3821 DNA as a template, a 1501 bp DNA fragment (P1) was amplified by PCR. Similarly, using primers IFPΔIVa2 and *Sac*II RP (Table 3, Appendix 3), and plasmid pMCS-3821 DNA as a template, a 1286 bp DNA fragment (P2) was amplified by PCR.The P1 and P2 DNA fragments were annealed and a, 2635 bp DNA fragment was amplified by PCR using SphI FP and SacII RP as primers (Table 3, Appendix 3). The 2635 bp DNA fragment was

digested with *Sph*I -*Sac*II and ligated to *Sph*I-*Sac*II digested plasmid pMCS DNA creating plasmid pMCS3821.dIVA2SbfI *(Sbf*I restriction site introduced in deleted region of IVa2).

pUC304a.dIVa2SbfI. A 1240 bp *Sbf*I DNA fragment of plasmid pUC4K (Taylor and Rose, 1988) containing Kanamycin resistant gene was isolated and ligated to *Sbf*I linearized plasmid pMCS.3821.dIVa2*Sbf*I DNA creating plasmid pMCS.3821.dIVa2Kan.

Homologous recombination in *Escherichia coli* BJ5183 (Chartier et al., 1996) between 3860 bp *Sph*I - *Sac*II DNA fragment of plasmid pMCS.3821dIVA2Kan and pUC304a+ DNA resulted in creating plasmid pUC304a.dIVA2Kan which could grow in LB plates containing ampicillin and kanamycin. The plasmid pUC304a.dIVa2Kan was digested with SbfI and large fragment was religated resulting in creating plasmid pUC304a.dIVA 2SbfI (*plasmid pUC304a+ containing unique SbfI site in place of deleted region of IVa2),* which could only grow in LB plates containing ampicillin.

pUC304a.IVa2s. Using primers *Sph*I FP and IRP STC (Table 3, Appendix 3), and plasmid pMCS.3821 DNA as a template, a 2808 bp DNA fragment (P1) was amplified by PCR. Similarly, using primers IFPSTC and SacII RP (Table 3, Appendix 3), and plasmid pMCS-3821 DNA as a template, a 1080 bp DNA fragment (P2) amplified by PCR. The P1 and P2 DNA fragments were annealed and a 3836 bp DNA fragment was amplified by PCR using SphI FP and SacII RP as primers (Table 3, Appendix 3). The 3836 bp DNA fragment was digested by *SphI*-*SacI* and ligated to *Sph*I-*Sac*II digested plasmid pMCS.3821 DNA creating plasmid pMCS.3821.SIVa2 (*pMCS.3821 containing stop codon within IVa2).*

Escherichia coli BJ5183 based homologous recombination between 3821 bp *Sph*I-*Sac*II fragment of plasmid pMCS-SCIVA2 and *Sbf*I linearized plasmid pUC304a.dIVa2SbfI DNA

resulted in isolating plasmid pUC304a.IVa2s (*pUC304a+ containing stop codon within IVa2 sequence).*

pMCSloxpIVa2.448. Using primers SphI FP and IRP loxp448 (Table 3, Appendix 3), and plasmid pMCS.3821 DNA as a template, a 1508 bp DNA fragment (P1) was amplified by PCR. Similarly, using primers IFPloxp448 and *Sac*II RP (Table 3, Appendix 3), and plasmid pMCS.3821 DNA as a template, a 2134 bp DNA fragment (P2) was amplified by PCR. The P1 and P2 DNA fragments were annealed and a 3606 DNA fragment was amplified by PCR using primers SphI FP and SacII RP (Table 3, Appendix 3). The 3606 DNA fragment was digested with *Sph*I-*Sac*II and ligated to *Sph*I-*Sac*II digested plasmid pMCS DNA creating plasmid pMCSloxpIVa2.448 (*loxP sequence introduced at the end of IVa2*).

pUCK304A.loxPIVa2. Using primers *Sph*I FP and IRP loxp79 (Table 3, Appendix 3), and plasmid pMCS-loxpIVa2 448 DNA as a template, a 2591 bp DNA fragment (P1) was amplified by PCR. Similarly, using primers IFPloxp79 and *Sac*II RP (Table 3, Appendix 3), and plasmid pMCS-loxpIVa2448 DNA as a template, a 1292 bp DNA fragment (P2) was amplified by PCR. The P1 and P2 DNA fragments were annealed and a 3915 bp DNA fragment was amplified by PCR using *Sph*I FP and *Sac*II RP as primers (Table 3, Appendix 3). The 3915 bp DNA fragment was digested bu *Sph*I-*Sac*II and ligated to *Sph*I-*Sac*II digested plasmid pMCS creating plasmid pMCS.3821loxpIVa2 (*loxP flanked non polymerase overlapping IVa2*).

Escherichia coli BJ5183 based homologous recombination between 3900 bp *Sph*I-*Sac*II fragment of plasmid pMCS.3821loxpIVa2 and *Sbf*I linearized plasmid pUC304a.dIVa2SbfI DNA resulted in isolation of plasmid pUC304a.loxPIVa2 (*pUCK304a+ containing loxP flanked IVa2).*

7.2.4 Transfection

The transfection of the cells with plasmid DNA was performed as described in 3.2.6.

7.2.5 Transient complementation of IVa2 deleted BAdV-3 genomic clone

For the complementation assay, VIDO DT1 cells were co-transfected using plasmids pC.IVa2 and pUC304a.dIVA2 DNAs or plasmids pCDNA3 and pUC304a.dIVa2 DNAs. After 5 hrs post transfection, the media was replaced with MEM supplemented with 2% FBS. The co-transfected cells were monitored under the fluorescent microscope for the appearance of green fluorescent protein (GFP) positive cells/foci. At day 3 and day 10-post transfection, the GFP positive cells/foci per well were counted. Fluorescent focus units (FFUs) per field were taken from average number of GFP positive cell foci from three independent co-transfection experiments.

7.2.6 Generation of BAdV-3 IVa2 expressing cell line

For the generation of a cell line stably expressing IVa2, second-generation lentivirus system used as described in (Du and Tikoo, 2010). Briefly, HEK293T cells grown to 70-80% confluency in 100mm dish were co-transfected with plasmid pTrip-IVa2-Puro expressing IVa2, plasmid pMD2.G expressing vesicular stomatitis virus G protein and plasmid pSPAX expressing human immunodeficiency virus Gag/Pol proteins. Briefly, the plasmids were diluted with water up to a total volume of 0.5mL followed by the addition of 0.5ml 2x HEPES buffer saline (HBS). Finally, 50µl 2.5M CaCl2 added, the mixture was shaken and kept at room temperature for 30 min. After half an hour incubation, the DNA mixture added in a drop wise manner on to the surface of HEK293T cells. The medium replaced after 16 hrs. After 48 hrs of

incubation, the medium was collected, centrifuged briefly to remove gross materials and filtered with 0.45-micron filter. After centrifugation at 25000 RPM for 2hrs, the pellet containing lentivirus particles (designated Trip.IVa2) reconstituted with 1 ml of sterile water and lentivirus concentration was measured using Lenti-X GoStix Kits (Clontech).

Finally, CRL cells transduced with lentivirus Trip.IVa2 expressing BAdV-3 IVa2 in the presence of 10ug/mL polybrene (Sigma). After 24 hrs post-transduction, the media replaced with MEM containing 5% fetal bovine serum and 10ug/mL of puromycin (Gibco). After 10-15 days post-transduction, the puromycin resistant clones were picked, expanded in media containing puromycin, and tested for the expression of IVa2.

7.2.7 Isolation of Cre recombinase expressing cell line

For isolation of Cre recombinase expressing cell line, a second-generation lentivirus system used as described in (Du and Tikoo, 2010). Initially, lentivirus Trip.Cre was isolated as described above, using plasmid pCre-IRES-PuroR DNA (addgene # 30205). The CRL cells transduced with lentivirus Trip.Cre and grown in the presence of puromycin. The puromycin resistant CRL clones isolated after the transduction of CRL cells with lentivirus Trip.Cre analyzed for the expression of Cre recombinase.

7.2.8 Isolation of recombinant BAdV-3

The recombinant BAdV-3s were isolated using plasmid DNA transfection of cells, as described in section 3.2.7.

7.2.9 Western blotting

Proteins from the cell lysates of IVa2 expressing cell lines were separated by 12 % SDS-PAGE, transferred to nitrocellulose and analyzed by Western blot using IVa2gst sera as described in section 3.2.8.

7.2.10 Immunofluorescence assay

Immunofluorescence assays were performed as described in section 3.2.9.

7.2.11 Transmission electron microscopy

Monolayers of CRL cells in 6 well plates were either infected with BAV304a at MOI of 5 or transfected with 5ug of plasmid pUC304a.dIVa2 DNA. Two or ten days post-infection or transfection, respectively, the cells were rinsed with ice-cold PBS, fixed using cold 2.5% glutaraldehyde containing 0.1M cacodylate buffer at 4^0C . After 5 hrs of fixation, the cells were harvested, centrifuged at 1500 RPM, and suspended in 1% osmium tetroxide (OsO_4). Subsequent to dehydration in a graded ethanol series and propylene oxide, sample embedded using propylene oxide and Epon-812 (Sigma), and polymerized at 60^0C for 24 hrs. Finally, the ultrathin section were obtained with Reichert ultra cut-ultramicrotome, counterstained with alkaline lead citrate, and observed under Philips CM10 transmission electron microscope (TEM).

7.3 Results

7.3.1 Isolation of mutant BAV304.dIVa2 \ BAV304.IVa2s

To determine the role of IVa2 in BAdV-3 lifecycle, initially we constructed a plasmid pUC304a.dIVa2 (Fig. 7.1a) containing full-length BAV304a genomic DNA with deletion of non polymerase overlapping region of IVa2 (amino acid 81-448). VIDO DT1 (Du and Tikoo, 2010) cells transfected with either plasmid pUC304a.dIVa2 DNA or plasmid pUC304a+ DNA observed for the development of cytopathic effects. Although cells transfected with plasmid pUC304a+ DNA showed expression of EYFP and developed cytopathic effects in 7 days post transfection, repeated transfection of cells with plasmid pUC304a.dIVa2 DNA did show expression of EYFP without showing development of any cytopathic effect even 25 days post transfection (Fig. 7.1b).

Next, we constructed a plasmid pUC304a.IVa2s (Fig. 7.1a) containing full-length BAV304a genomic DNA with insertion of stop codon after 12 amino acids of IVa2 without affecting the amino acid sequence of DNA polymerase. However, repeated transfection of VIDO DT1 cells with 5 ug of plasmid pUC304a.IVa2s DNA did show expression of EYFP without showing the development of any detectable cytopathic effects after 25 days post transfection (Fig. 7.1b).

7.3.2 Transient complementation of BAV304.dIVa2

To determine if IVa2 can complement the defect of BAV304a.dIVa2, VIDO DT1 cells were co-transfected using plasmids pC.IVa2 and pUC304a.dIVa2 DNAs or plasmids pCDNA3 and pUC304a.dIVa2 DNAs. As expected, co-transfection of VIDO DT1 cells with plasmid pCDNA3 and pUC304a.dIVa2 DNAs did not produce progeny virus as indicated by the absence of increase of foci of fluorescent cells from 3 day to 10 day post transfection (Fig. 7.2). In contrast, co-transfection of VIDO DT1 cells with plasmids pC. IVa2 and pUC304a.dIVa2

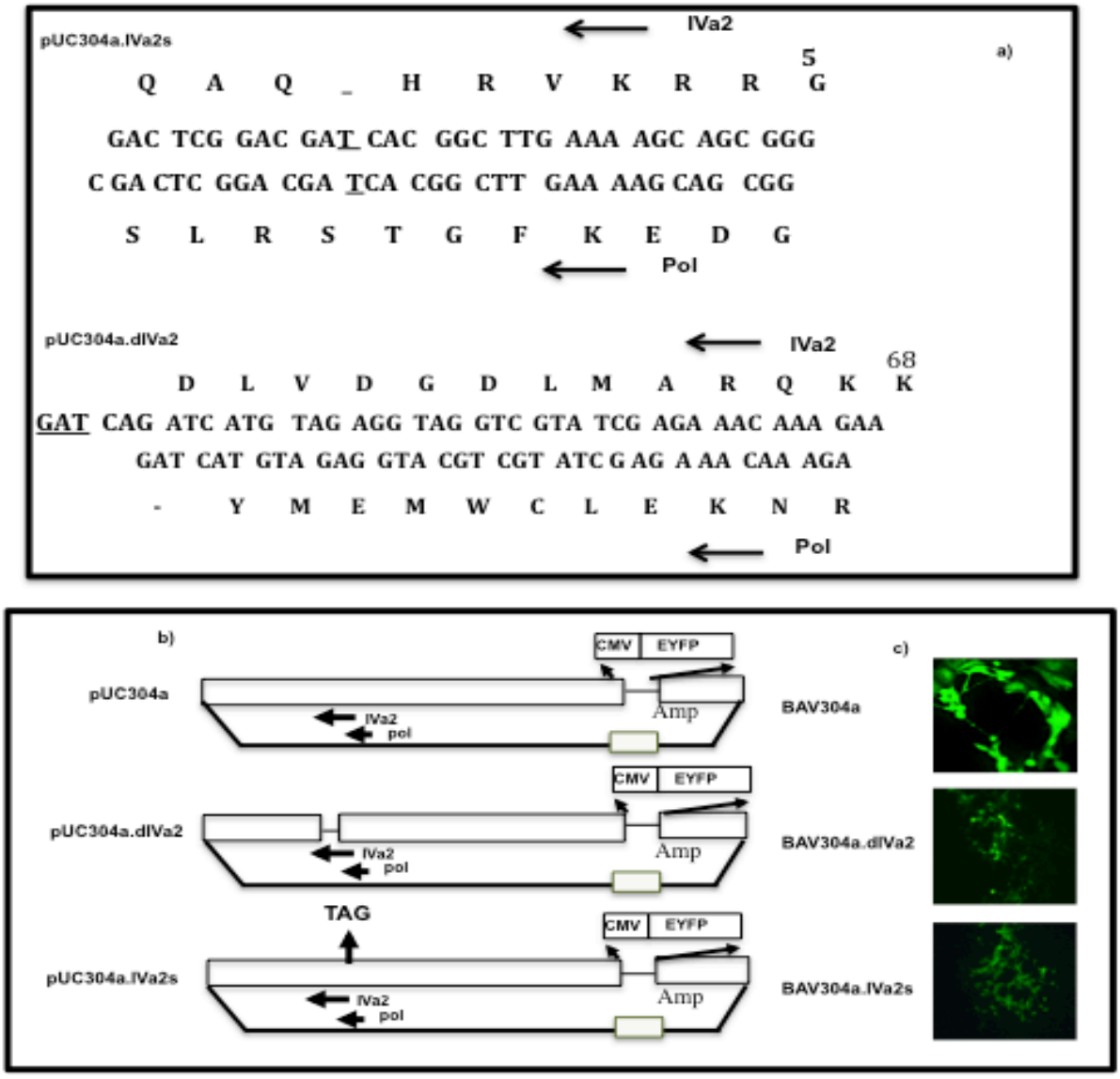

Fig. 7.1 Isolation mutant BAdV-3s. (a) Schematics of BAdV-3 DNA sequence showing introduction of stop codon as well as deletion of non-polymerase overlapping regions of IVa2 without affecting the polymerase (pol). Arrows show the direction of transcription of pol and IVa2 from the complementary DNA strand. **(b).** *Schematic diagram of plasmid DNAs.* The name of the plasmids is depicted on the right of the panel. The name of the recombinant BAdV-3 is depicted on the left of the panel. The BAdV-3 sequence is represented by open box. The thin line represents deleted region (E3). The arrow show the direction of transcription. Human cytomegalovirus (CMV) immediate early promoter; Enhanced yellow fluorescent protein (EYFP). **(c)** *Direct Fluorescence.* Monolayers of VIDO DT1 cells were transfected with indicated plasmid DNA and visualized for EYFP expression and development of cytopathic effects using fluorescent microscope TCS SP5 (Leica). Direct fluorescence (DF). (c,d) Amino acid sequence of IVa2 and polymerase protein. The substituted nucleotides are underlined.

DNAs produced progeny virus as indicated by significant increase in the number of foci of fluorescent cells from 3 day to 10 day post transfection (Fig. 7.2).

7.3.3 Generation of IVa2 expressing cell line

To construct a stable cell line expressing BAdV-3 IVa2 protein, the lentivirus TRIP.IVa2 was constructed (Du and Tikoo, 2010) and used to transduce CRL cells in the presence of 10ug/ml of polybrene (Zhao and Tikoo, 2016). The transduced cells were grown in the presence of 10ug/mL of puromycin (Gibco). The puromycin resistant clones were further propagated and analyzed for the expression of IVa2.

First, Western blotting assay used to detect the expression of IVa2 in CRL.IVa2 cell line. As seen in Fig. 7.3a, IVa2gst sera detected a protein of 50 kDa in BAdV-3 infected cells (lane 1). Similarly, IVa2gst sera detected a protein of 50 kDa in CRL.IVa2 cells (Fig. 7.3a, lane 2). No such protein could be detected in CRL cells (Fig. 7.3a, lane 3). Secondly, indirect immunofluorescence used to determine the localization of recombinant IVa2 in CRL.IVa2 cells. As seen in Fig.7.3b, IVa2 localized to nucleus\nucleolus of the cells infected with BAdV-3 (panels, a1-a3). Similarly, recombinant IVa2 localized to both nucleus and nucleolus of IVa2 expressing CRL.IVa2 cells (panels b1-b3) No such protein could be detected in the nucleus\nucleolus of CRL cells (panels, c1-c3).

7.3.4 Isolation of mutant BAdV-3 in CRL.IVa2 cells

To isolate mutant BAdV-3, CRL.IVa2 cells were transfected with individual plasmid DNAs and observed for the expression of GFP and the development of cytopathic effects. As seen in Fig. 7.4 CRL.IVa2 cells transfected with plasmid pUC304a+ (panel a), pUC304a.dIVa2 (panel

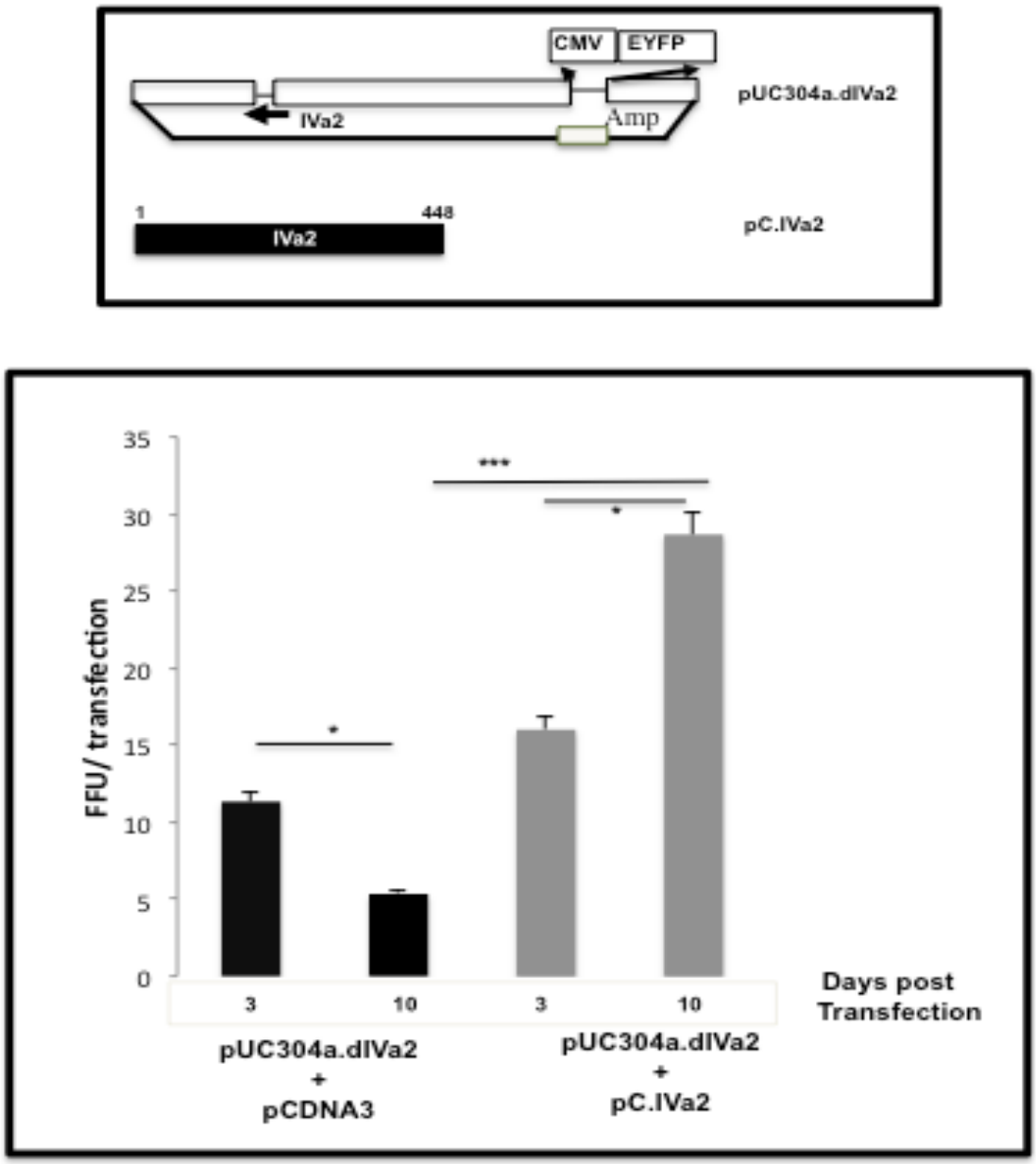

Fig. 7.2 Marker rescue. (a). *Schematic diagram of plasmid DNAs.* The name of the plasmids is depicted on the right of the panel. The name of the recombinant BAdV-3 is depicted on the left of the panel. The BAdV-3 sequence is represented by filled box. The thin line represents deleted region (E3). The arrow show the direction of transcription. Cytomegalovirus (CMV) immediate early promoter; Enhanced yellow fluorescent protein (EYFP). **(b).** *Complementation of pUC304a.dIVa2 genome.* VIDO DT1 cells were co-transfected with indicated plasmid DNAs and the fluorescent foci forming units were counted at indicated times post transfection. The number on X axis denote the days post transfection. The results depict the average of three experiments.

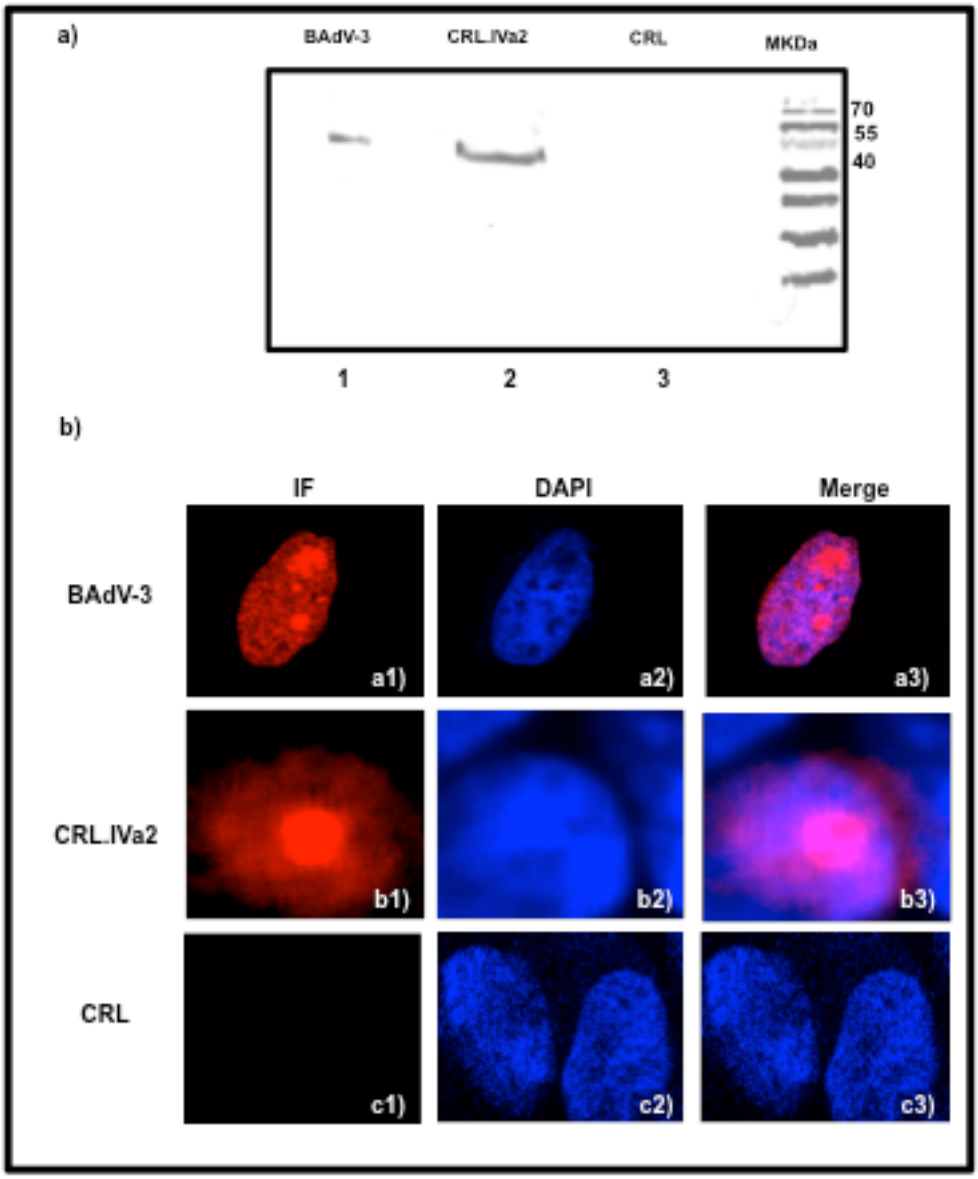

Fig. 7.3 Isolation of BAdV-3 expressing cell line (CRL.IVa2). (a) *Western blot.* Proteins from the lysates of BAdV-3 infected cells (lane 1), CRL.IVa2 cells (lane2) or CRL cells (lane 3) were separated by 12 % SDS-PAGE, transferred to nitrocellulose membrane and analyzed by Western blot using IVa2gst serum and alkaline phosphatase conjugated goat-anti rabbit serum. The position of the molecular weights in kDa is shown on the right. Molecular weight markers (M). **(b).** *Indirect immunofluorescence.* The BAdV-3 infected CRL cells (panels a1-a3), mock infected CRL.IVa2 cells (panels, b1-b3) or mock infected CRL cells (panels, c1-c3) were visualized by indirect immunofluorescence using IVa2gst serum and Cy3 conjugated goat anti-rabbit serum (panels, a1,b1,c1). The nuclei were stained with DAPI (panels, a2, b2, c2).A merge of the images is shown in panels, a3, b3 and c3.

b) or pUC304a.IVa2s (panel c) DNA showed expression of GFP in 15 days post-transfection. As expected, an increase in the intensity of GFP along with detectable development of cytopathic effects could be observed in cells transfected with plasmid pUC304a+ (panel a1) DNA. In contrast, though, the intensity of GFP expression increased in the cells transfected with plasmid pUC304a.dIVa2 (panel b1) or pUC304a+IVa2s (panel c1) DNAs, no typical cytopathic, could be observed in transfected cells.

To determine if transfection of CRL.IVa2 cells with plasmid pUC304a.dIVa2 DNA or plasmid pUC304a.IVa2s DNA leads to the formation of BAdV-3 particles, transfected cells analyzed by transmission electron microscopy (TEM). Monolayers of CRL.IVa2 cells were transfected with individual plasmid DNA or infected with BAV304a at MOI of 2. Two days and fifteen days post-infection and transfection, respectively, the cells were collected and processed for TEM. As seen in fig. Fig. 7.4, the appearance of uniform icosahedral virus particles could be observed in CRL.IVa2 cells (panel a2) infected with BAdV-3. No such particles could be detected in CRL.IVa2 cells transfected with plasmid pUC304a.dIVa2 DNA (panel b2) or plasmid pUC304a.IVa2s DNA (panel c2).

Moreover, the analysis of virus-infected cells by electron microscope detected progeny virions in the cells transfected with plasmid pUC304a+ DNA (panel a). No such virions could be detected in the cells transfected with plasmid pUC304a.dIVa2 (Fig. 7.4, panel b) DNA or plasmid pUC304a.IVa2s (Fig. 7.4, panel c) DNA.

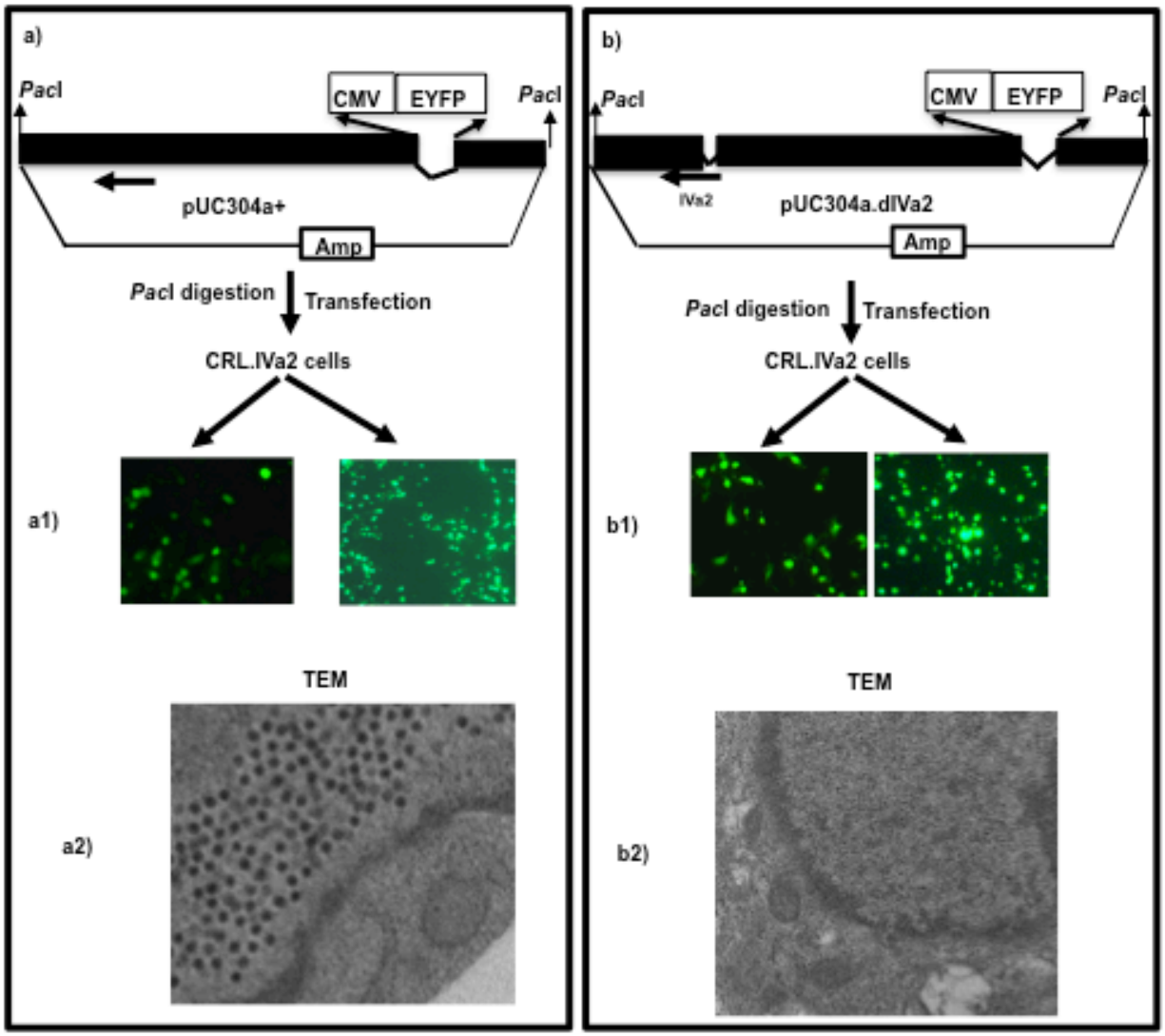

Fig. 7.4 Isolation of mutant BAdV-3 in CRL.IVa2 cells. **(a,b).** *Schematic diagram of plasmid DNAs.* The name of the plasmids is depicted. The BAdV-3 sequence is represented by filled box. The V marked thin represents deleted region. The amino acid numbers of IVa2 are indicated in panel c. The arrow show the direction of transcription. Human cytomegalovirus (CMV) immediate early promoter; Enhanced yellow fluorescent protein (EYFP). Ampicillin (Amp). **(a1, b1)** *Direct Fluorescence.* Monolayers of CRL.IVa2 cells were transfected with indicated plasmid DNA and visualized for EYFP expression and development of cytopathic effects using fluorescent microscope TCS SP5 (Leica). **(a2, b2)** *Electron microscopic analysis.* CRL.IVa2 cells transfected with plasmid pUC304a+ (panel a2) DNA or plasmid pUC304a.dIVa2 (panel b2) DNA are shown at a magnification of X100000 Transmission electron microscopy (TEM).

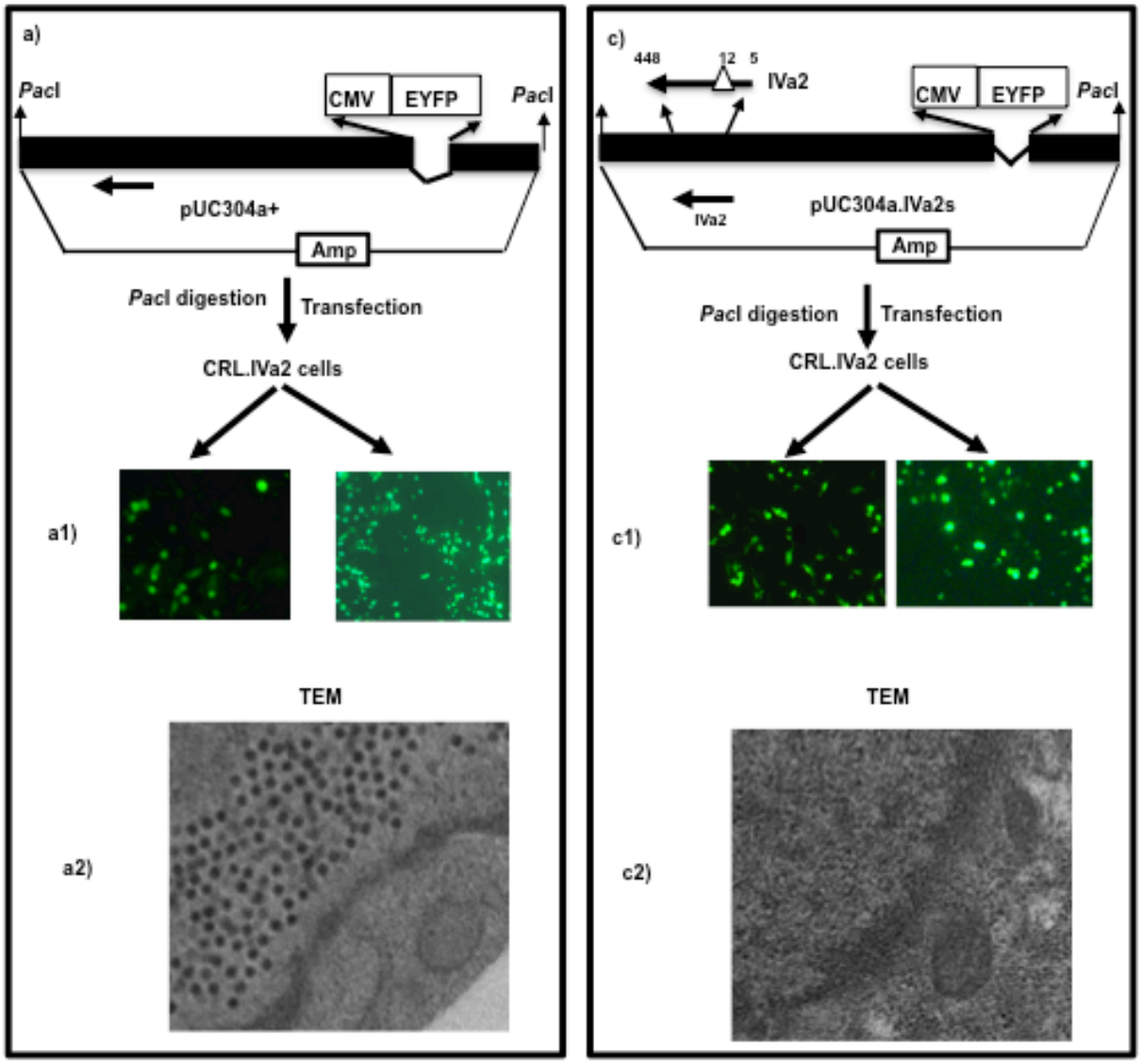

Fig. 7.4 Isolation of mutant BAdV-3 in CRL.IVa2 cells. **(a,c).** *Schematic diagram of plasmid DNAs.* The name of the plasmids is depicted. The BAdV-3 sequence is represented by filled box. The V marked thin lines represents deleted region. The amino acid numbers of IVa2 are indicated in panel c. The arrow show the direction of transcription. Human cytomegalovirus (CMV) immediate early promoter; Enhanced yellow fluorescent protein (EYFP). Ampicillin (Amp). **(a1,c1)** *Direct Fluorescence.* Monolayers of CRL.IVa2 cells were transfected with indicated plasmid DNA and visualized for EYFP expression and development of cytopathic effects using fluorescent microscope TCS SP5 (Leica). **(a2,c2)** *Electron microscopic analysis.* CRL.IVa2 cells transfected with plasmid pUC304a+ (panel a2) DNA, plasmid or plasmid pUC304a.IVa2s (panel c2) DNA are shown at a magnification of X100000. Transmission electron microscopy (TEM).

7.3.5 Generation of Cre expressing cell line

To obtain a cell line expressing Cre recombinase, CRL cells were transduced with lentivirus Trip.Cre expressing Cre recombinase and grown in the media containing puromycin. After 12 days, puromycin resistant clones were analyzed for the expression of Cre recombinase by visualizing the Cre recombinase-dependent inducible expression of GFP in puromycin resistant cells transfected with plasmid pCALNL-GFP DNA expressing GFP Orf containing a transcription stop flanked by loxP sequence. As seen in Fig. 7.5, no GFP could be detected in mock-transfected CRL cells (panel a1-a3). Similarly, no GFP expression could be detected in CRL cell transfected with plasmid pCALNL-GFP DNA (panels, b1-b3). In contrast, expression of GFP could be detected in CRL.Cre cells transfected with plasmid pCALNL-GFP DNA (panels, c1-c3).

7.3.6 Isolation of recombinant BAdV-3 expressing loxP flanked IVa2

Since we could not isolate mutant BAdV-3 containing a deletion of IVa2 in CRL.IVa2 cells, we attempted to conditionally knock out IVa2 in BAdV-3 using the Cre-loxP system (Ostapchuk et al., 2017; Sengupta et al., 2017). Since N-terminus 79 amino acid of BAdV-3 IVa2 overlap with the C-terminus region of the polymerase protein, we constructed a plasmid pUC304a.loxPIVa2 by inserting loxP sequence (34 bp) in- frame after BAdV-3 IVa2 amino acid 79 and 448 amino acids (Fig. 7.6a).

To isolate recombinant BAdV304a containing insertion of loxP sequences in IVa2, CRL cells transfected with *Pac I* digested plasmid pUC304a.loxPIVa2 DNA using lipofectamine 2000 reagent and observed for the expression of EYFP and development of cytopathic effect.

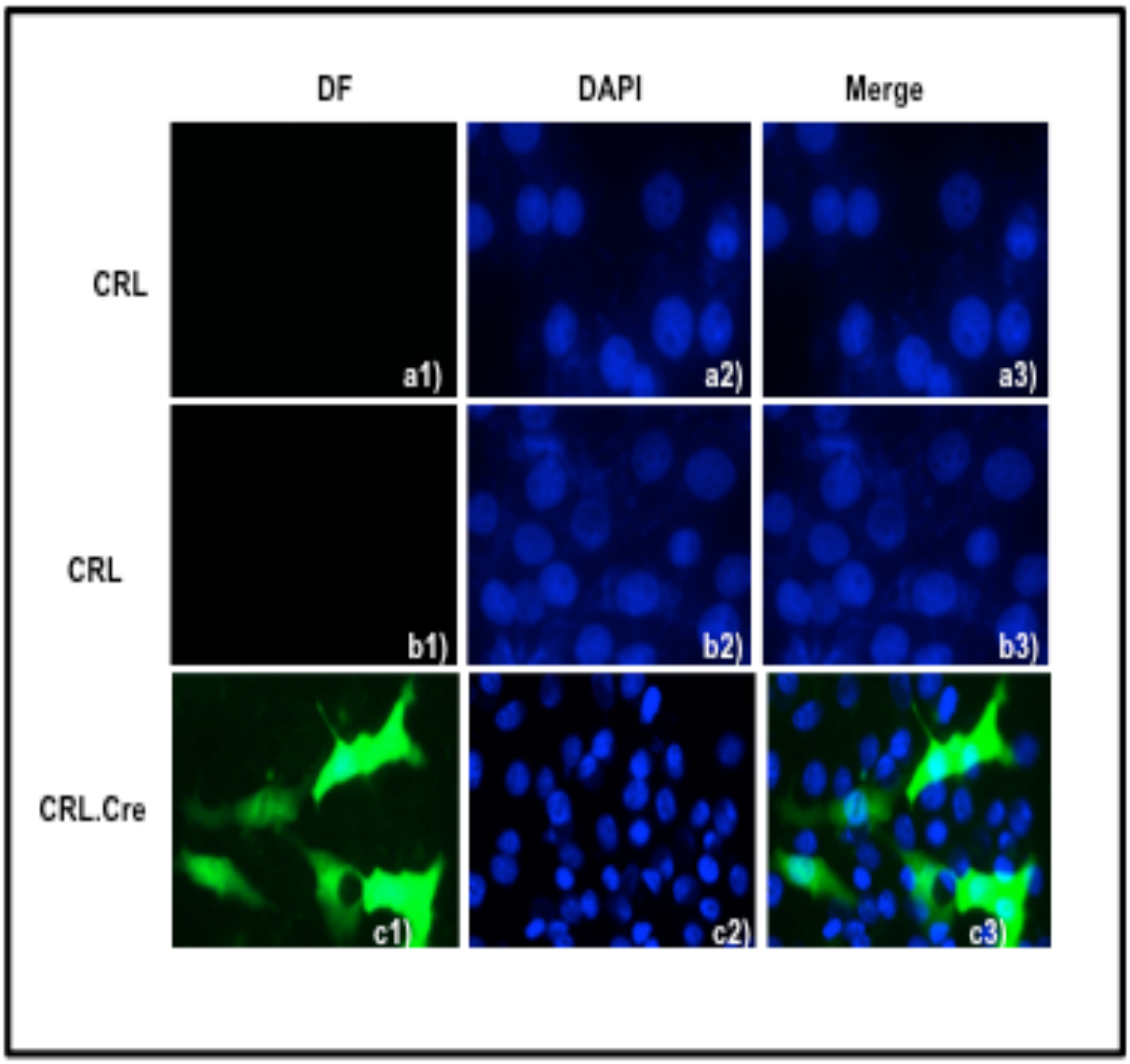

Fig. 7.5 Isolation of cre expressing cell line (CRL.Cre). *Direct fluorescence*. Monolayers of CRL cells mock-transfected (a1-a3) or transfected with pCALNL-GFP (GFP expressing plasmid whose Orf contains a transcription stop flanked by loxP sequence) (b1-b3). Similarly, monolayers of CRL.Cre cells (c1-c3) transfected with pCALNL-GFP. After 36 hrs of transfection, cells processed and observed for the expression of GFP using fluorescent microscope TCS SP5 (Leica).

Although EYFP expressing cells observed after 3 days (Fig. 7.6b), repeated transfection did not induce the development of cytopathic effects in 22 days post-transfection (Fig. 7.6b).

7.4. Discussion

Viral proteins are involved in different steps of the viral replication cycle leading to the production of progeny virions. Though most viral genomes encode proteins which appear essential for the efficient virus replication (den Boon et al., 2010; Le Rouzic and Benichou, 2005; Moss, 2013; Narayanan et al., 2003), viral genomes also encode proteins, which are not essentialfor the efficient replication of virus (Van Vliet et al., 2009).

Like other viruses, the adenovirus genome also encodes proteins that are non-essential or essential for efficient replication of the virus (Reddy et al., 2000; Saha et al., 2014; Zakhartchouk et al., 1998; Zhou and Tikoo, 2001).

Earlier, we demonstrated that core protein pV appears to be essential for the production of infectious BAdV-3 virion (Zhao and Tikoo, 2016). Here, we report that protein IVa2 appears to be critical for the replication of BAdV-3.

Several lines of evidences support that IVa2 is essential for the replication of BAdV-3. First, viable infectious mutant BAdV-3 containing an insertion of an in-frame stop codon or partial deletion of IVa2 could not be isolated in non-complementing CRL cells. Second, no capsid formation could be observed in the cells transfected with plasmid pUC304a.dIVa2 DNA or plasmid pUC304a.IVa2s DNA by TEM. Thirdly, providing IVa2 in-trans (in the cells co-transfected with plasmid pUC304a.dIVa2 DNA and plasmid pC.IVA2 DNA) produced viable mutant BAdV-3.

While CRL cells expressing IVa2 (CRL.IVa2) could be isolated, the use of CRL.IVa2 cells did not lead to the isolation of BAV304a.dIVa2 (IVa2 deleted BAdV-3). It is possible that plasmid pUC304a.dIVa2 contains a mutation in addition to the deletion of IVa2. However, in the complementation assay, viable BAV304a.dIVa2 could be isolated by providing IVa2 in trans. Alternativly, it is possible that the level of IVa2 expressed in CRL.IVa2 is not enough to complement the defect of IVa2 expression in BAV304a.dIVa2. Earlier reports also have concluded that the amount of IVa2 is critical for efficient replication of BAdV-3 (Zhang and Imperiale, 2003). However, the failure of the CRL.IVa2 cells to complement the IVa2 defect of BAV304a.dIVa2 due to the lack of proper folding or absence of any translational modification of IVa2 could not be ruled out.

An earlier report indicated that the substitution of a single amino acid from lysine to arginine or alanine of IVa2 proved lethal for replication of HAdV-5 (Pardo-Mateos and Young, 2004). Insertion of 8 amino acid Strep II tag between amino acids 146-147, 242-243, and after amino acid 448 of IVa2 proved lethal for the replication of BAdV-3 (Chapter 5). Similarly, the addition of loxP sequences between amino acid 373-374 and after amino acid 448 (Chapter 3) and between amino acids 79-80 and after amino acids 448 of BAdV-3 IVa2 also proved lethal for the replication of BAdV-3. Our results confirm earlier observations that adenovirus protein IVa2 appears sensitive to minor insertions or deletions of amino acids (Pardo-Mateos and Young, 2004; Zhang and Imperiale, 2003).

Cre-Lox technology is an important tool for editing genes and studying protein function (Sengupta et al., 2017). It has been employed to analayze the role of viral protein in a virus life cycle (Ostapchuk et al., 2017). Despite the successful generation of CRL.Cre cell line (Cre-expressing cells), the rescue of recombinant BAdV-3 containing a deletion of IVa2 was not

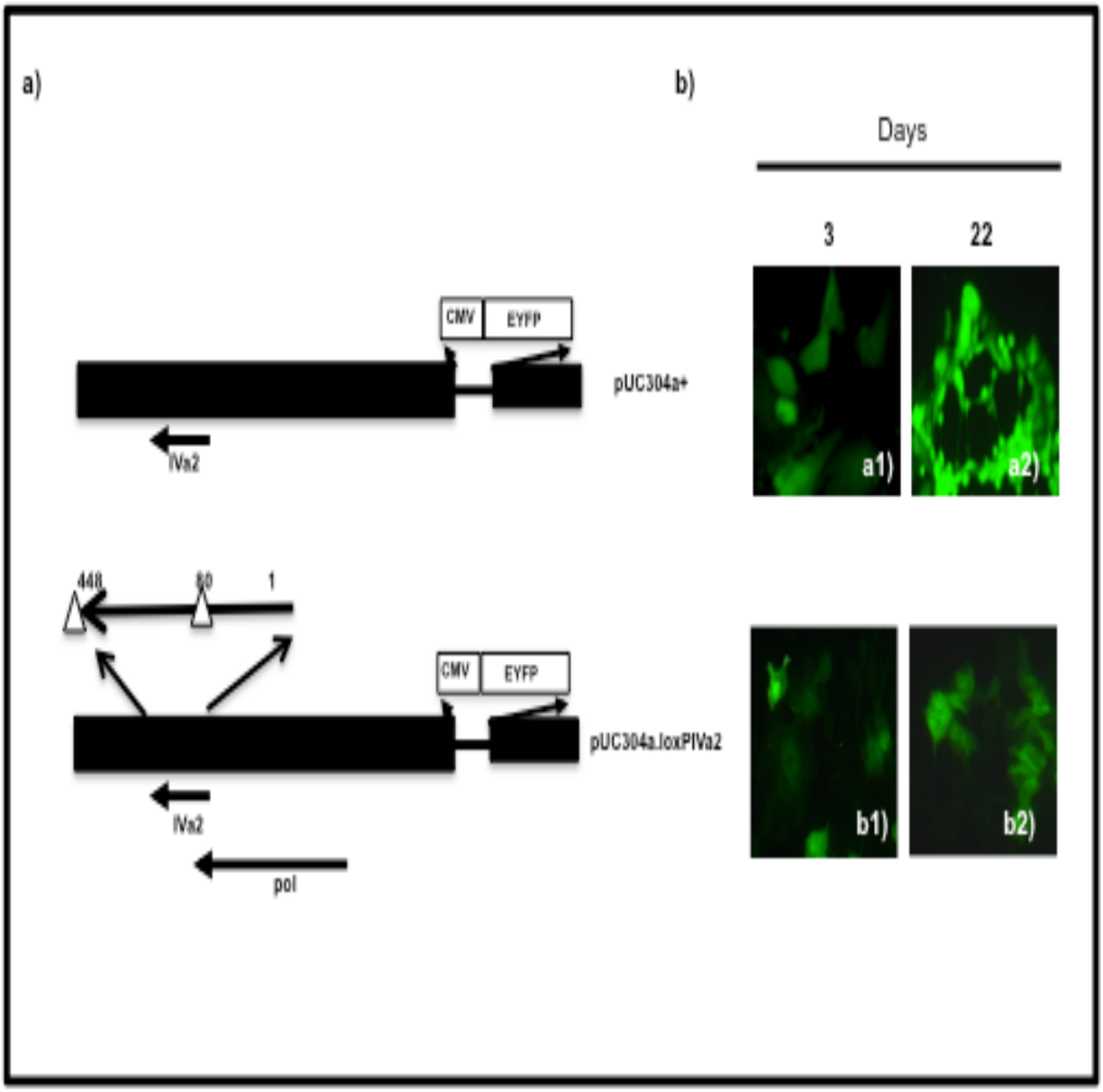

Fig. 7.6 Isolation of recombinant BAdV-3 expressing loxP flanked IVa2. (a) *Schematic diagram of plasmid DNAs.* The name of the plasmids is depicted on the right of the panel. The BAdV-3 sequence is represented by filled box. The thin line represents deleted region. The amino acids numbers of IVa2 are indicated. The arrow show the direction of transcription. Human cytomegalovirus (CMV) immediate early promoter; Enhanced yellow fluorescent protein (EYFP). Ampicillin (Amp). **(b)** *Direct Fluorescence.* Monolayers of CRL cells were transfected indicated plasmid DNA after digested with Pac I and visualized for EYFP expression and development of cytopathic effects at indicated days post transfection using fluorescent microscope TCS SP5 (Leica).

possible as BAV304a.IVa2loxP (IVa2 containing an insertion of loxP sequence) could not be isolated in CRL cells.

8.0 GENERAL DISCUSSION

About 32% of the total clinical trials for gene delivery currently conducted around the world are using adenovirus vectors (Goswami et al., 2019). Interestingly, human adenoviruses are used widely as a viral vector for both vaccinations as well as gene therapy (Wold et al., 2013). Despite the greater share of human adenoviruses as a viral vector, there are limitations associated with their use (Appaiahgari et al., 2015). To overcome limitations associated with the use of human adenoviral vectors, non-human adenoviral vectors are considered as potential alternatives (Bangari and Mittal 2006; Lopez-Gordo et al., 2014). More importantly, there is a need to make use of species-specific adenoviruses as a viral vector for veterinary vaccination where cost and maintenance of cold chains are some of the limiting factors for the currently used veterinary vaccines (Ayalew et al., 2015; Baron et al., 2018; Ndi et al., 2013).

Earlier reports on the use of bovine adenovirus-3 (BAdV-3) as a viral vector have demonstrated the potential of the BAdV-3 as a viral vector for animal vaccination (reviewed in Ayalew et al., 2015). However, the development of improved BAdV-3 vectors needs more detailed knowledge about the structure and function of BAdV-3 proteins. Earlier, analysis of the intermediate region of BAdV-3 predicted to encode protein pIX and IVa2. The objective of this work was to portray BAdV-3 IVa2, identify the interaction of IVa2 with other viral proteins, and determine the role of the IVa2 protein in BAdV-3 life cycle.

Many viral proteins synthesized in the cytoplasm localize to the nucleus and \or nucleolus to perform their function in the production of progeny virus, including in viral mRNA transcription, capsid formation, and genome encapsidation (Li et al., 2019). Antiserum raised in rabbits against GST-IVa2 fusion protein detected a protein of 50 kDa in plasmid DNA transfected cells and BAdV-3 infected cells, which localized to nucleus\nucleolus. Sub cellular

localization of IVa2 in transfected cells suggested that other viral proteins are not involved in the nuclear\nucleolar localization of IVa2. Deletion analysis identified amino acids 4-18 and amino acids 373-448 to be involved in the nuclear and the nucleolar localization of the IVa2 protein, respectively suggesting that IVa2 contains non-overlapping NLS\NoLS. Like other BAdV-3 proteins (Ayalew et al., 2014; Kulshrestha et al., 2014; Makadiya et al., 2015; Paterson, 2012; Said et al., 2018; Zhao, 2016) IVa2 also utilizes importin α\β transport pathway preferentially using importin α-1 as a nuclear receptor for transport to the nucleus.

Earlier, it was demonstrated that ribosomal RNA processing is affected at late times post BAdV-3 infection (Paterson, 2010). Ribosomal RNA processing occurs in the nucleolus (Boisvert et al., 2007). We speculate that like BAdV-3 pV (Zhao, 2016), nucleolar IVa2 may be involved in modulating ribosomal RNA processing. Further work should prove or disprove our speculation.

Earlier reports have demonstrated that nuclear (Brock et al., 2013) or nucleolar (Zhao, 2016) localization of a protein is required for efficient viral replication. Although substitution of a cluster of basic residues ^{6}RRK^{8} showed no significant effect on the localization of IVa2 to nucleus\nucleolus and BAdV-3 replication, it will be interesting to determine the importance of other residues of NLS and NoLs(s) in BAdV-3 replication by creating and evaluating recombinant BAdV-3 expressing IVa2 containing substitutions\mutations in NLS\NoLs.

A better understanding of basic virology is crucial to exploit viruses for different applications, including using as vaccine delivery vehicles (Enquist, 2009). Although adenoviruses encode 23 to 46 proteins, the various functions performed by each protein require protein-protein interactions (Arnberg, 2012; Gustin et al., 1996; Matthews and Russell, 1994; Ostapchuk et al., 2005). Earlier report regarding mass spectrophotometry analysis of purified

proteins from BAdV-3 infected cells detected interaction of BAdV-3 pV with IVa2. We confirmed the interaction of BAdV-3 IVa2 with pV using different assays in plasmid DNA transfected cells and BAdV-3 infected cells. Recently, it has been shown that BAdV-3 pV plays a role in maintaining the stability of BAdV-3 virions (Zhao and Tikoo, 2016). We postulate that the interaction of IVa2 with pV may also be associated with the maintenance of capsid integrity. Since BAdV-3 IVa2 amino acids 121-140 are involved in the interaction with pV, isolation and characterization of recombinant BAdV-3 containing substitution \deletion of the interacting domain should help in determining the biological function of IVa2-pV interaction in BAdV-3 replication.

While the deletion of HAdV-5 IVa2 did not produce progeny virions, there was no effect on the formation of empty capsids (Ostapchuk et al., 2011). However, repeated attempts to rescue recombinant BAdV-3 containing a deletion of IVa2 proved futile with the absence of any potential capsid formation in plasmid pUC304a.dIVa2 DNA transfected cells. Similarly, while introduction of a stop codon at HAdV-5 IVa2 amino acids 17, 19, or 86 did not result in the isolation of a viable virus, insertion of a stop codon at HAdV-5 amino acid 6 resulted in the isolation of a viable HAdV-5. However, the inclusion of a stop codon at BAdV-3 IVa2 amino acid 12 shown to be lethal for the replication of BAdV-3 in plasmid pUC304a.IVa2s DNA transfected cells. It is possible that IVa2 may be functionally different from HAdV-5 IVa2; alternatively, it is possible that this could be due to differences in the cells used to isolate recombinant adenoviruses. Further studies are required to settle this issue.

9.0. REFERENCES

Abida, W. M., Nikolaev, A., Zhao, W., Zhang, W., & Gu, W. (2007). FBXO11 promotes the Neddylation of p53 and inhibits its transcriptional activity. *J Biol Chem, 282*(3), 1797-1804. doi: 10.1074/jbc.M609001200

Ablack, J. N., Cohen, M., Thillainadesan, G., Fonseca, G. J., Pelka, P., Torchia, J., & Mymryk, J. S. (2012). Cellular GCN5 is a novel regulator of human adenovirus E1A-conserved region 3 transactivation. J Virol, 86(15), 8198-8209. doi: 10.1128/JVI.00289-12

Ahi, Y. S., Hassan, A. O., Vemula, S. V., Li, K., Jiang, W., Zhang, G. J., & Mittal, S. K. (2017). Adenoviral E4 34K protein interacts with virus packaging components and may serve as the putative portal. Sci Rep, 7(1), 7582. doi: 10.1038/s41598-017-07997-w

Ahi, Y. S., & Mittal, S. K. (2016). Components of Adenovirus Genome Packaging. Front Microbiol, 7, 1503. doi: 10.3389/fmicb.2016.01503

Ahi, Y. S., Vemula, S. V., Hassan, A. O., Costakes, G., Stauffacher, C., & Mittal, S. K. (2015). Adenoviral L4 33K forms ring-like oligomers and stimulates ATPase activity of IVa2: implications in viral genome packaging. Front Microbiol, 6, 318. doi: 10.3389/fmicb.2015.00318

Ahi, Y. S., Vemula, S. V., & Mittal, S. K. (2013). Adenoviral E2 IVa2 protein interacts with L4 33K protein and E2 DNA-binding protein. J Gen Virol, 94(Pt 6), 1325-1334. doi: 10.1099/vir.0.049346-0

Ahmad, Y., Boisvert, F. M., Gregor, P., Cobley, A., & Lamond, A. I. (2009). NOPdb: Nucleolar Proteome Database--2008 update. Nucleic Acids Res, 37(Database issue), D181-184. doi: 10.1093/nar/gkn804

Akusjarvi, G. (2008). Temporal regulation of adenovirus major late alternative RNA splicing. Front Biosci, 13, 5006-5015. doi: 10.2741/3059

Ali, H., LeRoy, G., Bridge, G., & Flint, S. J. (2007). The adenovirus L4 33-kilodalton protein binds to intragenic sequences of the major late promoter required for late phase-specific stimulation of transcription. J Virol, 81(3), 1327-1338. doi: 10.1128/JVI.01584-06

Alonso-Padilla, J., Papp, T., Kajan, G. L., Benko, M., Havenga, M., Lemckert, A., Baker, A. H. (2016). Development of Novel Adenoviral Vectors to Overcome Challenges Observed With HAdV-5-based Constructs. Mol Ther, 24(1), 6-16. doi: 10.1038/mt.2015.194

Anand, S. K., Singh, J., Gaba, A., & Tikoo, S. K. (2014). Effect of bovine adenovirus 3 on mitochondria. Vet Res, 45, 45. doi: 10.1186/1297-9716-45-45

Anderson, C. W., Young, M. E., & Flint, S. J. (1989). Characterization of the adenovirus 2 virion protein, mu. Virology, 172(2), 506-512. doi: 10.1016/0042-6822(89)90193-1

Anderson, D. J., & Hetzer, M. W. (2007). Nuclear envelope formation by chromatin-mediated reorganization of the endoplasmic reticulum. Nat Cell Biol, 9(10), 1160-1166. doi: 10.1038/ncb1636

Appaiahgari, M. B., & Vrati, S. (2015). Adenoviruses as gene/vaccine delivery vectors: promises and pitfalls. Expert Opin Biol Ther, 15(3), 337-351. doi: 10.1517/14712598.2015.993374

Arnberg, N. (2012). Adenovirus receptors: implications for targeting of viral vectors. Trends Pharmacol Sci, 33(8), 442-448. doi: 10.1016/j.tips.2012.04.005

Arnberg, N., Edlund, K., Kidd, A. H., & Wadell, G. (2000). Adenovirus type 37 uses sialic acid as a cellular receptor. J Virol, 74(1), 42-48.

Arnold, M., Nath, A., Hauber, J., & Kehlenbach, R. H. (2006). Multiple importins function as nuclear transport receptors for the Rev protein of human immunodeficiency virus type 1. J Biol Chem, 281(30), 20883-20890. doi: 10.1074/jbc.M602189200

Avitabile, D., Bailey, B., Cottage, C. T., Sundararaman, B., Joyo, A., McGregor, M., .Sussman, M. A. (2011). Nucleolar stress is an early response to myocardial damage involving nucleolar proteins nucleostemin and nucleophosmin. *Proc Natl Acad Sci U S A, 108*(15), 6145-6150. doi: 10.1073/pnas.1017935108

Ayalew, L. E., Gaba, A., Kumar, P., & Tikoo, S. K. (2014). Conserved regions of bovine adenovirus-3 pVIII contain functional domains involved in nuclear localization and packaging in mature infectious virions. J Gen Virol, 95(Pt 8), 1743-1754. doi: 10.1099/vir.0.065763-0

Ayalew, L. E., Kumar, P., Gaba, A., Makadiya, N., & Tikoo, S. K. (2015). Bovine adenovirus-3 as a vaccine delivery vehicle. Vaccine, 33(4), 493-499. doi: 10.1016/j.vaccine.2014.11.055

Ayalew, L. E., Patel, A. K., Gaba, A., Islam, A., & Tikoo, S. K. (2016). Bovine Adenovirus-3 pVIII Suppresses Cap-Dependent mRNA Translation Possibly by Interfering with the Recruitment of DDX3 and Translation Initiation Factors to the mRNA Cap. Front Microbiol, 7, 2119. doi: 10.3389/fmicb.2016.02119

Backstrom, E., Kaufmann, K. B., Lan, X., & Akusjarvi, G. (2010). Adenovirus L4-22K stimulates major late transcription by a mechanism requiring the intragenic late-

specific transcription factor-binding site. Virus Res, 151(2), 220-228. doi: 10.1016/j.virusres.2010.05.013

Bangari, D. S., & Mittal, S. K. (2006a). Current strategies and future directions for eluding adenoviral vector immunity. Curr Gene Ther, 6(2), 215-226. doi: 10.2174/156652306776359478

Bangari, D. S., & Mittal, S. K. (2006b). Development of nonhuman adenoviruses as vaccine vectors. Vaccine, 24(7), 849-862. doi: 10.1016/j.vaccine.2005.08.101

Barlev, N. A., Liu, L., Chehab, N. H., Mansfield, K., Harris, K. G., Halazonetis, T. D., & Berger, S. L. (2001). Acetylation of p53 activates transcription through recruitment of coactivators/histone acetyltransferases. *Mol Cell, 8*(6), 1243-1254. doi: 10.1016/s1097-2765(01)00414-2

Baron, M. D., Iqbal, M., & Nair, V. (2018). Recent advances in viral vectors in veterinary vaccinology. Curr Opin Virol, 29, 1-7. doi: 10.1016/j.coviro.2018.02.002

Bartha, A. (1969). Proposal for subgrouping of bovine adenoviruses. Acta Vet Acad Sci Hung, 19(3), 319-321.

Baxi, M. K., Reddy, P. S., Zakhartchouk, A. N., Idamakanti, N., Pyne, C., Babiuk, L. A., & Tikoo, S. K. (1998). Characterization of bovine adenovirus type 3 early region 2B. Virus Genes, 16(3), 313-316.

Baxi, M. K., Robertson, J., Babiuk, L. A., & Tikoo, S. K. (2001). Mutational analysis of early region 4 of bovine adenovirus type 3. Virology, 290(1), 153-163. doi: 10.1006/viro.2001.1176

Bayley, S. T., & Mymryk, J. S. (1994). Adenovirus e1a proteins and transformation (review). Int J Oncol, 5(3), 425-444. doi: 10.3892/ijo.5.3.425

Benko, M., Elo, P., Ursu, K., Ahne, W., LaPatra, S. E., Thomson, D., & Harrach, B. (2002). First molecular evidence for the existence of distinct fish and snake adenoviruses. J Virol, 76(19), 10056-10059. doi: 10.1128/jvi.76.19.10056-10059.2002

Bergelson, J. M., Cunningham, J. A., Droguett, G., Kurt-Jones, E. A., Krithivas, A., Hong, J. S., Finberg, R. W. (1997). Isolation of a common receptor for Coxsackie B viruses and adenoviruses 2 and 5. Science, 275(5304), 1320-1323. doi: 10.1126/science.275.5304.1320

Berk, Arnold. J. (2013). Adenoviridae. In D. M. K. Bernard N F, Peter M H. (Ed.), Field's Virology (6th ed., pp. 1704-1731). Philadelphia Wolters Kluwer Health/Lippincott Williams & Wilkins

Bertwistle, D., Sugimoto, M., & Sherr, C. J. (2004). Physical and functional interactions of the Arf tumor suppressor protein with nucleophosmin/B23. Mol Cell Biol, 24(3), 985-996. doi: 10.1128/mcb.24.3.985-996.2004

Biasiotto, R., & Akusjarvi, G. (2015). Regulation of human adenovirus alternative RNA splicing by the adenoviral L4-33K and L4-22K proteins. Int J Mol Sci, 16(2), 2893-2912. doi: 10.3390/ijms16022893

Bischoff, F. R., Krebber, H., Smirnova, E., Dong, W., & Ponstingl, H. (1995). Co-activation of RanGTPase and inhibition of GTP dissociation by Ran-GTP binding protein RanBP1. EMBO J, 14(4), 705-715.

Blackford, A. N., & Grand, R. J. (2009). Adenovirus E1B 55-kilodalton protein: multiple roles in viral infection and cell transformation. J Virol, 83(9), 4000-4012. doi: 10.1128/JVI.02417-08

Blanchette, P., Wimmer, P., Dallaire, F., Cheng, C. Y., & Branton, P. E. (2013). Aggresome formation by the adenoviral protein E1B55K is not conserved among adenovirus species and is not required for efficient degradation of nuclear substrates. J Virol, 87(9), 4872-4881. doi: 10.1128/JVI.03272-12

Boisvert, F. M., van Koningsbruggen, S., Navascues, J., & Lamond, A. I. (2007). The multifunctional nucleolus. Nat Rev Mol Cell Biol, 8(7), 574-585. doi: 10.1038/nrm2184

Bonnet, A., & Palancade, B. (2014). Regulation of mRNA trafficking by nuclear pore complexes. Genes (Basel), 5(3), 767-791. doi: 10.3390/genes5030767

Both, G. W. (2011.). Atadenovirus. Adenoviridae. In Tidona CA & D. G (Eds.), The Springer index of viruses. (pp. 1–12). New York, NY.: Springer.

Boulon, S., Westman, B. J., Hutten, S., Boisvert, F. M., & Lamond, A. I. (2010). The nucleolus under stress. Mol Cell, 40(2), 216-227. doi: 10.1016/j.molcel.2010.09.024

Bremner, K. H., Scherer, J., Yi, J., Vershinin, M., Gross, S. P., & Vallee, R. B. (2009). Adenovirus transport via direct interaction of cytoplasmic dynein with the viral capsid hexon subunit. Cell Host Microbe, 6(6), 523-535. doi: 10.1016/j.chom.2009.11.006

Brock, I., Kruger, M., Mertens, T., & von Einem, J. (2013). Nuclear targeting of human cytomegalovirus large tegument protein pUL48 is essential for viral growth. J Virol, 87(10), 6005-6019. doi: 10.1128/JVI.03558-12

Burckhardt, C. J., Suomalainen, M., Schoenenberger, P., Boucke, K., Hemmi, S., & Greber, U. F. (2011). Drifting motions of the adenovirus receptor CAR and immobile integrins initiate virus uncoating and membrane lytic protein exposure. Cell Host Microbe, 10(2), 105-117. doi: 10.1016/j.chom.2011.07.006

Bursac, S., Brdovcak, M. C., Pfannkuchen, M., Orsolic, I., Golomb, L., Zhu, Y., Volarevic, S. (2012). Mutual protection of ribosomal proteins L5 and L11 from degradation is essential for p53 activation upon ribosomal biogenesis stress. *Proc Natl Acad Sci U S A, 109*(50), 20467-20472. doi: 10.1073/pnas.1218535109

Caly, Leon, Ghildyal, Reena, & Jans, David A. (2015). Respiratory virus modulation of host nucleocytoplasmic transport; target for therapeutic intervention? Front Microbiol, 6(848). doi: 10.3389/fmicb.2015.00848

Cassany, A., Ragues, J., Guan, T., Begu, D., Wodrich, H., Kann, M., Gerace, L. (2015). Nuclear import of adenovirus DNA involves direct interaction of hexon with an N-terminal domain of the nucleoporin Nup214. J Virol, 89(3), 1719-1730. doi: 10.1128/JVI.02639-14

Caswell, J.L., & Williams, K. J. (2016). Pathology of Domestic Animals. In K. P. s. Jubb (Ed.), Pathology of Domestic Animals (Sixth Edition ed., Vol. 2).

Chartier, C., Degryse, E., Gantzer, M., Dieterle, A., Pavirani, A., & Mehtali, M. (1996). Efficient generation of recombinant adenovirus vectors by homologous recombination in Escherichia coli. J Virol, 70(7), 4805-4810.

Chatterjee, P. K., Vayda, M. E., & Flint, S. J. (1985). Interactions among the three adenovirus core proteins. J Virol, 55(2), 379-386.

Chen, J. (2016). The Cell-Cycle Arrest and Apoptotic Functions of p53 in Tumor Initiation and Progression. *Cold Spring Harb Perspect Med, 6*(3), a026104. doi: 10.1101/cshperspect.a026104

Cheng, G., Brett, M. E., & He, B. (2002). Signals that dictate nuclear, nucleolar, and cytoplasmic shuttling of the gamma(1)34.5 protein of herpes simplex virus type 1. J Virol, 76(18), 9434-9445. doi: 10.1128/jvi.76.18.9434-9445.2002

Cheng, P. H., Rao, X. M., McMasters, K. M., & Zhou, H. S. (2013). Molecular basis for viral selective replication in cancer cells: activation of CDK2 by adenovirus-induced cyclin E. PLoS One, 8(2), e57340. doi: 10.1371/journal.pone.0057340

Chinnadurai, G. (2009). The transcriptional corepressor CtBP: a foe of multiple tumor suppressors. Cancer Res, 69(3), 731-734. doi: 10.1158/0008-5472.CAN-08-3349

Chiocca, S., Kurzbauer, R., Schaffner, G., Baker, A., Mautner, V., & Cotten, M. (1996). The complete DNA sequence and genomic organization of the avian adenovirus CELO. J Virol, 70(5), 2939-2949.

Christensen, J. B., Byrd, S. A., Walker, A. K., Strahler, J. R., Andrews, P. C., & Imperiale, M. J. (2008). Presence of the adenovirus IVa2 protein at a single vertex of the mature virion. J Virol, 82(18), 9086-9093. doi: 10.1128/JVI.01024-08

Christensen, J. B., Ewing, S. G., & Imperiale, M. J. (2012). Identification and characterization of a DNA binding domain on the adenovirus IVa2 protein. Virology, 433(1), 124-130. doi: 10.1016/j.virol.2012.07.013

Christie, M., Chang, C. W., Rona, G., Smith, K. M., Stewart, A. G., Takeda, A. A., Kobe, B. (2016). Structural Biology and Regulation of Protein Import into the Nucleus. J Mol Biol, 428(10 Pt A), 2060-2090. doi: 10.1016/j.jmb.2015.10.023

Christophe, D., Christophe-Hobertus, C., & Pichon, B. (2000). Nuclear targeting of proteins: how many different signals? Cell Signal, 12(5), 337-341. doi: 10.1016/s0898-6568(00)00077-2

Chuikov, S., Kurash, J. K., Wilson, J. R., Xiao, B., Justin, N., Ivanov, G. S., Reinberg, D. (2004). Regulation of p53 activity through lysine methylation. *Nature, 432*(7015), 353-360. doi: 10.1038/nature03117

Ciganda, M., & Williams, N. (2011). Eukaryotic 5S rRNA biogenesis. Wiley Interdiscip Rev RNA, 2(4), 523-533. doi: 10.1002/wrna.74

Cohen, M. J., King, C. R., Dikeakos, J. D., & Mymryk, J. S. (2014). Functional analysis of the C-terminal region of human adenovirus E1A reveals a misidentified nuclear localization signal. Virology, 468-470, 238-243. doi: 10.1016/j.virol.2014.08.014

Colombo, E., Marine, J. C., Danovi, D., Falini, B., & Pelicci, P. G. (2002). Nucleophosmin regulates the stability and transcriptional activity of p53. *Nat Cell Biol, 4*(7), 529-533. doi: 10.1038/ncb814

Condezo, G. N., Marabini, R., Ayora, S., Carazo, J. M., Alba, R., Chillon, M., & San Martin, C. (2015). Structures of Adenovirus Incomplete Particles Clarify Capsid Architecture and Show Maturation Changes of Packaging Protein L1 52/55k. J Virol, 89(18), 9653-9664. doi: 10.1128/JVI.01453-15

Condezo, G. N., & San Martin, C. (2017). Localization of adenovirus morphogenesis players, together with visualization of assembly intermediates and failed products, favor a model where assembly and packaging occur concurrently at the periphery of the replication center. PLoS Pathog, 13(4), e1006320. doi: 10.1371/journal.ppat.1006320

Cook, H. V., Doncheva, N. T., Szklarczyk, D., von Mering, C., & Jensen, L. J. (2018). Viruses.STRING: A Virus-Host Protein-Protein Interaction Database. Viruses, 10(10). doi: 10.3390/v10100519

Cros, J. F., Garcia-Sastre, A., & Palese, P. (2005). An unconventional NLS is critical for the nuclear import of the influenza A virus nucleoprotein and ribonucleoprotein. Traffic, 6(3), 205-213. doi: 10.1111/j.1600-0854.2005.00263.x

Crosby, C. M., & Barry, M. A. (2014). IIIa deleted adenovirus as a single-cycle genome replicating vector. Virology, 462-463, 158-165. doi: 10.1016/j.virol.2014.05.030

Cuconati, A., Degenhardt, K., Sundararajan, R., Anschel, A., & White, E. (2002). Bak and Bax function to limit adenovirus replication through apoptosis induction. J Virol, 76(9), 4547-4558. doi: 10.1128/jvi.76.9.4547-4558.2002

Dai, M. S., Sun, X. X., & Lu, H. (2008). Aberrant expression of nucleostemin activates p53 and induces cell cycle arrest via inhibition of MDM2. *Mol Cell Biol, 28*(13), 4365-4376. doi: 10.1128/MCB.01662-07

D'Angelo, M. A., & Hetzer, M. W. (2008). Structure, dynamics and function of nuclear pore complexes. Trends Cell Biol, 18(10), 456-466. doi: 10.1016/j.tcb.2008.07.009

Daniely, Y., Dimitrova, D. D., & Borowiec, J. A. (2002). Stress-dependent nucleolin mobilization mediated by p53-nucleolin complex formation. *Mol Cell Biol, 22*(16), 6014-6022. doi: 10.1128/mcb.22.16.6014-6022.2002

D'Halluin, J. C., Milleville, M., Boulanger, P. A., & Martin, G. R. (1978). Temperature-sensitive mutant of adenovirus type 2 blocked in virion assembly: accumulation of light intermediate particles. J Virol, 26(2), 344-356.

Darbyshire, J. H., Dawson, P. S., Lamont, P. H., Ostler, D. C., & Pereira, H. G. (1965). A new adenovirus serotype of bovine origin. J Comp Pathol, 75(3), 327-330. doi: 10.1016/0021-9975(65)90038-1

Davison, A. J., Benko, M., & Harrach, B. (2003). Genetic content and evolution of adenoviruses. J Gen Virol, 84(Pt 11), 2895-2908. doi: 10.1099/vir.0.19497-0

de Jong, R. N., van der Vliet, P. C., & Brenkman, A. B. (2003). Adenovirus DNA replication: protein priming, jumping back and the role of the DNA binding protein DBP. Curr Top Microbiol Immunol, 272, 187-211.

Debbas, M., & White, E. (1993). Wild-type p53 mediates apoptosis by E1A, which is inhibited by E1B. Genes Dev, 7(4), 546-554. doi: 10.1101/gad.7.4.546

Dechecchi, M. C., Melotti, P., Bonizzato, A., Santacatterina, M., Chilosi, M., & Cabrini, G. (2001). Heparan sulfate glycosaminoglycans are receptors sufficient to mediate the initial binding of adenovirus types 2 and 5. J Virol, 75(18), 8772-8780. doi: 10.1128/jvi.75.18.8772-8780.2001

Deisenroth, C., & Zhang, Y. (2010). Ribosome biogenesis surveillance: probing the ribosomal protein-Mdm2-p53 pathway. *Oncogene, 29*(30), 4253-4260. doi: 10.1038/onc.2010.189

Dekker, J., Kanellopoulos, P. N., Loonstra, A. K., van Oosterhout, J. A., Leonard, K., Tucker, P. A., & van der Vliet, P. C. (1997). Multimerization of the adenovirus DNA-binding protein is the driving force for ATP-independent DNA unwinding during strand displacement synthesis. EMBO J, 16(6), 1455-1463. doi: 10.1093/emboj/16.6.1455

den Boon, J. A., Diaz, A., & Ahlquist, P. (2010). Cytoplasmic viral replication complexes. Cell Host Microbe, 8(1), 77-85. doi: 10.1016/j.chom.2010.06.010

Denning, D., Bennett, S., Mullen, T., Moyer, C., Vorselen, D., Wuite, G.J.L., Nemerow, G., Roos, W.H., 2019. Maturation of adenovirus primes the protein nano-shell for successful endosomal escape. Nanoscale 11, 4015-4024.

Ding, Q., Zhao, L., Guo, H., & Zheng, A. C. (2010). The nucleocytoplasmic transport of viral proteins. Virol Sin, 25(2), 79-85. doi: 10.1007/s12250-010-3099-z

Donati, G., Brighenti, E., Vici, M., Mazzini, G., Trere, D., Montanaro, L., & Derenzini, M. (2011). Selective inhibition of rRNA transcription downregulates E2F-1: a new p53-independent mechanism linking cell growth to cell proliferation. *J Cell Sci, 124*(Pt 17), 3017-3028. doi: 10.1242/jcs.086074

Donati, G., Peddigari, S., Mercer, C. A., & Thomas, G. (2013). 5S ribosomal RNA is an essential component of a nascent ribosomal precursor complex that regulates the Hdm2-p53 checkpoint. *Cell Rep, 4*(1), 87-98. doi: 10.1016/j.celrep.2013.05.045

Doszpoly, A., Wellehan, J. F., Jr., Childress, A. L., Tarjan, Z. L., Kovacs, E. R., Harrach, B., & Benko, M. (2013). Partial characterization of a new adenovirus lineage discovered in testudinoid turtles. Infect Genet Evol, 17, 106-112. doi: 10.1016/j.meegid.2013.03.049

Du, E., & Tikoo, S. K. (2010). Efficient replication and generation of recombinant bovine adenovirus-3 in nonbovine cotton rat lung cells expressing I-SceI endonuclease. J Gene Med, 12(10), 840-847. doi: 10.1002/jgm.1505

Elo, P., Farkas, S. L., Dan, A. L., & Kovacs, G. M. (2003). The p32K structural protein of the atadenovirus might have bacterial relatives. J Mol Evol, 56(2), 175-180. doi: 10.1007/s00239-002-2391-4

Enders, J. F., Bell, J. A., Dingle, J. H., Francis, T., Jr., Hilleman, M. R., Huebner, R. J., & Payne, A. M. (1956). Adenoviruses: group name proposed for new respiratory-tract viruses. Science, 124(3212), 119-120. doi: 10.1126/science.124.3212.119

Enquist, L. W. (2009). Recognizing the top 20 peer reviewers for the Journal of Virology. J Virol, 83(23), 12007. doi: 10.1128/JVI.02016-09

Ewing, S. G., Byrd, S. A., Christensen, J. B., Tyler, R. E., & Imperiale, M. J. (2007). Ternary complex formation on the adenovirus packaging sequence by the IVa2 and L4 22-kilodalton proteins. J Virol, 81(22), 12450-12457. doi: 10.1128/JVI.01470-07

Farkas, S. L., & Gal, J. (2009). Adenovirus and mycoplasma infection in an ornate box turtle (Terrapene ornata ornata) in Hungary. Vet Microbiol, 138(1-2), 169-173. doi: 10.1016/j.vetmic.2009.03.016

Farley, D. C., Brown, J. L., & Leppard, K. N. (2004). Activation of the early-late switch in adenovirus type 5 major late transcription unit expression by L4 gene products. J Virol, 78(4), 1782-1791. doi: 10.1128/jvi.78.4.1782-1791.2004

Fax, P., Carlson, C. R., Collas, P., Tasken, K., Esche, H., & Brockmann, D. (2001). Binding of PKA-RIIalpha to the Adenovirus E1A12S oncoprotein correlates with its nuclear translocation and an increase in PKA-dependent promoter activity. Virology, 285(1), 30-41. doi: 10.1006/viro.2001.0926

Fessler, S. P., & Young, C. S. (1999). The role of the L4 33K gene in adenovirus infection. Virology, 263(2), 507-516. doi: 10.1006/viro.1999.9951

Finnen, R. L., Biddle, J. F., & Flint, J. (2001). Truncation of the human adenovirus type 5 L4 33-kDa protein: evidence for an essential role of the carboxy-terminus in the viral infectious cycle. Virology, 289(2), 388-399. doi: 10.1006/viro.2001.1130

Flatt, J. W., & Butcher, S. J. (2019). Adenovirus flow in host cell networks. Open Biol, 9(2), 190012. doi: 10.1098/rsob.190012

Fonseca, G. J., Cohen, M. J., & Mymryk, J. S. (2014). Adenovirus E1A recruits the human Paf1 complex to enhance transcriptional elongation. J Virol, 88(10), 5630-5637. doi: 10.1128/JVI.03518-13

Fonseca, G. J., Cohen, M. J., Nichols, A. C., Barrett, J. W., & Mymryk, J. S. (2013). Viral retasking of hBre1/RNF20 to recruit hPaf1 for transcriptional activation. PLoS Pathog, 9(6), e1003411. doi: 10.1371/journal.ppat.1003411

Frey, S., Rees, R., Schunemann, J., Ng, S. C., Funfgeld, K., Huyton, T., & Gorlich, D. (2018). Surface Properties Determining Passage Rates of Proteins through Nuclear Pores. Cell, 174(1), 202-217 e209. doi: 10.1016/j.cell.2018.05.045

Frost, J. R., Mendez, M., Soriano, A. M., Crisostomo, L., Olanubi, O., Radko, S., & Pelka, P. (2018). Adenovirus 5 E1A-Mediated Suppression of p53 via FUBP1. J Virol, 92(14). doi: 10.1128/JVI.00439-18

Furcinitti, P. S., van Oostrum, J., & Burnett, R. M. (1989). Adenovirus polypeptide IX revealed as capsid cement by difference images from electron microscopy and crystallography. EMBO J, 8(12), 3563-3570.

Gaba, A., Ayalew, L. E., Patel, A., Kumar, P., & Tikoo, S. K. (2018). Bovine adenovirus-3 protein VIII associates with eukaryotic initiation factor-6 during infection. Cell Microbiol, 20(8), e12842. doi: 10.1111/cmi.12842

Gaba, A., Ayalew, L., Makadiya, N., & Tikoo, S. (2017). Proteolytic Cleavage of Bovine Adenovirus 3-Encoded pVIII. J Virol, 91(10). doi: 10.1128/JVI.00211-17

Gaggar, A., Shayakhmetov, D. M., & Lieber, A. (2003). CD46 is a cellular receptor for group B adenoviruses. Nat Med, 9(11), 1408-1412. doi: 10.1038/nm952

Ghebremedhin, B. (2014). Human adenovirus: Viral pathogen with increasing importance. Eur J Microbiol Immunol (Bp), 4(1), 26-33. doi: 10.1556/EuJMI.4.2014.1.2

Glenewinkel, F., Cohen, M. J., King, C. R., Kaspar, S., Bamberg-Lemper, S., Mymryk, J. S., & Becker, W. (2016). The adaptor protein DCAF7 mediates the interaction of the adenovirus E1A oncoprotein with the protein kinases DYRK1A and HIPK2. Sci Rep, 6, 28241. doi: 10.1038/srep28241

Goldfarb, D. S., Corbett, A. H., Mason, D. A., Harreman, M. T., & Adam, S. A. (2004). Importin alpha: a multipurpose nuclear-transport receptor. *Trends Cell Biol, 14*(9), 505-514. doi: 10.1016/j.tcb.2004.07.016

Gorlich, D., Pante, N., Kutay, U., Aebi, U., & Bischoff, F. R. (1996). Identification of different roles for RanGDP and RanGTP in nuclear protein import. EMBO J, 15(20), 5584-5594.

Gorlich, D., Vogel, F., Mills, A. D., Hartmann, E., & Laskey, R. A. (1995). Distinct functions for the two importin subunits in nuclear protein import. Nature, 377(6546), 246-248. doi: 10.1038/377246a0

Gorman, J. J., Wallis, T. P., Whelan, D. A., Shaw, J., & Both, G. W. (2005). LH3, a "homologue" of the mastadenoviral E1B 55-kDa protein is a structural protein of atadenoviruses. Virology, 342(1), 159-166. doi: 10.1016/j.virol.2005.07.020

Goswami, R., Subramanian, G., Silayeva, L., Newkirk, I., Doctor, D., Chawla, K., Betapudi, V. (2019). Gene Therapy Leaves a Vicious Cycle. Front Oncol, 9, 297. doi: 10.3389/fonc.2019.00297

Graham, D. A., Calvert, V., Benko, M., Curran, W., Wylie, M., Snodden, D. A., Smyth, J. A. (2005). Isolation of bovine adenovirus serotype 6 from a calf in the United Kingdom. Vet Rec, 156(3), 82-86. doi: 10.1136/vr.156.3.82

Greber, U. F., Arnberg, N., Wadell, G., Benko, M., & Kremer, E. J. (2013). Adenoviruses - from pathogens to therapeutics: a report on the 10th International Adenovirus Meeting. Cell Microbiol, 15(1), 16-23. doi: 10.1111/cmi.12031

Greber, U. F., & Flatt, J. W. (2019). Adenovirus Entry: From Infection to Immunity. Annu Rev Virol. doi: 10.1146/annurev-virology-092818-015550

Grgic, H., Krell, P. J., & Nagy, E. (2014). Comparison of fiber gene sequences of inclusion body hepatitis (IBH) and non-IBH strains of serotype 8 and 11 fowl adenoviruses. Virus Genes, 48(1), 74-80. doi: 10.1007/s11262-013-0995-y

Grgic, H., Yang, D. H., & Nagy, E. (2011). Pathogenicity and complete genome sequence of a fowl adenovirus serotype 8 isolate. Virus Res, 156(1-2), 91-97. doi: 10.1016/j.virusres.2011.01.002

Griffin, B. D., & Nagy, E. (2011). Coding potential and transcript analysis of fowl adenovirus 4: insight into upstream ORFs as common sequence features in adenoviral transcripts. J Gen Virol, 92(Pt 6), 1260-1272. doi: 10.1099/vir.0.030064-0

Guan, H., & Ricciardi, R. P. (2012). Transformation by E1A oncoprotein involves ubiquitin-mediated proteolysis of the neuronal and tumor repressor REST in the nucleus. J Virol, 86(10), 5594-5602. doi: 10.1128/JVI.06811-11

Guimet, D., & Hearing, P. (2013). The adenovirus L4-22K protein has distinct functions in the posttranscriptional regulation of gene expression and encapsidation of the viral genome. J Virol, 87(13), 7688-7699. doi: 10.1128/JVI.00859-13

Gustin, K. E., & Imperiale, M. J. (1998). Encapsidation of viral DNA requires the adenovirus L1 52/55-kilodalton protein. J Virol, 72(10), 7860-7870.

Gustin, K. E., Lutz, P., & Imperiale, M. J. (1996). Interaction of the adenovirus L1 52/55-kilodalton protein with the IVa2 gene product during infection. J Virol, 70(9), 6463-6467.

Hafner, A., Bulyk, M. L., Jambhekar, A., & Lahav, G. (2019). The multiple mechanisms that regulate p53 activity and cell fate. *Nat Rev Mol Cell Biol, 20*(4), 199-210. doi: 10.1038/s41580-019-0110-x

Halehalli, R. R., & Nagarajaram, H. A. (2015). Molecular principles of human virus protein-protein interactions. Bioinformatics, 31(7), 1025-1033. doi: 10.1093/bioinformatics/btu763

Hammarskjold, M. L., & Winberg, G. (1980). Encapsidation of adenovirus 16 DNA is directed by a small DNA sequence at the left end of the genome. Cell, 20(3), 787-795. doi: 10.1016/0092-8674(80)90325-6

Harrach, B. (2014). Adenoviruses: General Features☆. In R. M. M. Caplan, R. Bradshaw & L. McManus. (Ed.), Reference Module in Biomedical Sciences, (pp. 1-9). Amsterdam: Elsevier.

Harrach, B., Benkö, M., Both, G.W., Brown, M., Davison, A.J., Echavarría, M., Wadell, G. . (2012). Adenoviridae. . In M. J. A. Andrew M.Q. King, Eric B. Carstens, and Elliot J. Lefkowitz (Ed.), Virus taxonomy: ninth report of the international committee on taxonomy of viruses (pp. 125-141). London.

Haupt, Y., Maya, R., Kazaz, A., & Oren, M. (1997). Mdm2 promotes the rapid degradation of p53. *Nature, 387*(6630), 296-299. doi: 10.1038/387296a0

Henras, A. K., Plisson-Chastang, C., O'Donohue, M. F., Chakraborty, A., & Gleizes, P. E. (2015). An overview of pre-ribosomal RNA processing in eukaryotes. Wiley Interdiscip Rev RNA, 6(2), 225-242. doi: 10.1002/wrna.1269

Hernandez-Verdun, D., Roussel, P., Thiry, M., Sirri, V., & Lafontaine, D. L. (2010). The nucleolus: structure/function relationship in RNA metabolism. Wiley Interdiscip Rev RNA, 1(3), 415-431. doi: 10.1002/wrna.39

Hilleman, M. R., & Werner, J. H. (1954). Recovery of new agent from patients with acute respiratory illness. Proc Soc Exp Biol Med, 85(1), 183-188. doi: 10.3181/00379727-85-20825

Hindley, C. E., Lawrence, F. J., & Matthews, D. A. (2007). A role for transportin in the nuclear import of adenovirus core proteins and DNA. Traffic, 8(10), 1313-1322. doi: 10.1111/j.1600-0854.2007.00618.x

Hoeben, R. C., & Uil, T. G. (2013). Adenovirus DNA replication. Cold Spring Harb Perspect Biol, 5(3), a013003. doi: 10.1101/cshperspect.a013003

Hoelz, A., Debler, E. W., & Blobel, G. (2011). The structure of the nuclear pore complex. Annu Rev Biochem, 80, 613-643. doi: 10.1146/annurev-biochem-060109-151030

Hohlweg, U., Dorn, A., Hosel, M., Webb, D., Buettner, R., & Doerfler, W. (2004). Tumorigenesis by adenovirus type 12 in newborn Syrian hamsters. Curr Top Microbiol Immunol, 273, 215-244. doi: 10.1007/978-3-662-05599-1_7

Hong, S. S., Szolajska, E., Schoehn, G., Franqueville, L., Myhre, S., Lindholm, L., Chroboczek, J. (2005). The 100K-chaperone protein from adenovirus serotype 2 (Subgroup C) assists in trimerization and nuclear localization of hexons from subgroups C and B adenoviruses. J Mol Biol, 352(1), 125-138. doi: 10.1016/j.jmb.2005.06.070

Horwitz, M. S. (2004). Function of adenovirus E3 proteins and their interactions with immunoregulatory cell proteins. J Gene Med, 6 Suppl 1, S172-183. doi: 10.1002/jgm.495

Hsia, K. C., Stavropoulos, P., Blobel, G., & Hoelz, A. (2007). Architecture of a coat for the nuclear pore membrane. Cell, 131(7), 1313-1326. doi: 10.1016/j.cell.2007.11.038

Hsieh, J. C., Yoo, S. K., & Ito, J. (1990). An essential arginine residue for initiation of protein-primed DNA replication. Proc Natl Acad Sci U S A, 87(21), 8665-8669. doi: 10.1073/pnas.87.21.8665

Huang, W., Kiefer, J., Whalen, D., & Flint, S. J. (2003). DNA synthesis-dependent relief of repression of transcription from the adenovirus type 2 IVa(2) promoter by a cellular protein. Virology, 314(1), 394-402. doi: 10.1016/s0042-6822(03)00431-8

Hung, G., & Flint, S. J. (2017). Normal human cell proteins that interact with the adenovirus type 5 E1B 55kDa protein. Virology, 504, 12-24. doi: 10.1016/j.virol.2017.01.013

Hunter, E. (2012). Virus Assembly. In D. M. K. a. P. M. Howley (Ed.), Fields Virology Philadelphia Wolters Kluwer Health/Lippincott Williams & Wilkins

Idamakanti, N., Reddy, P. S., Babiuk, L. A., & Tikoo, S. K. (1999). Transcription mapping and characterization of 284R and 121R proteins produced from early region 3 of bovine adenovirus type 3. Virology, 256(2), 351-359. doi: 10.1006/viro.1999.9626

Iftode, C., & Flint, S. J. (2004). Viral DNA synthesis-dependent titration of a cellular repressor activates transcription of the human adenovirus type 2 IVa2 gene. Proc Natl Acad Sci U S A, 101(51), 17831-17836. doi: 10.1073/pnas.0407786101

Inturi, R., Thaduri, S., & Punga, T. (2013). Adenovirus precursor pVII protein stability is regulated by its propeptide sequence. PLoS One, 8(11), e80617. doi: 10.1371/journal.pone.0080617

Isobe, T., Hattori, T., Kitagawa, K., Uchida, C., Kotake, Y., Kosugi, I., Kitagawa, M. (2009). Adenovirus E1A inhibits SCF(Fbw7) ubiquitin ligase. J Biol Chem, 284(41), 27766-27779. doi: 10.1074/jbc.M109.006809

Isobe, T., Uchida, C., Hattori, T., Kitagawa, K., Oda, T., & Kitagawa, M. (2006). Ubiquitin-dependent degradation of adenovirus E1A protein is inhibited by BS69. Biochem Biophys Res Commun, 339(1), 367-374. doi: 10.1016/j.bbrc.2005.11.028

James, A., Wang, Y., Raje, H., Rosby, R., & DiMario, P. (2014). Nucleolar stress with and without p53. *Nucleus, 5*(5), 402-426. doi: 10.4161/nucl.32235

Jarnik, M., & Aebi, U. (1991). Toward a more complete 3-D structure of the nuclear pore complex. J Struct Biol, 107(3), 291-308. doi: 10.1016/1047-8477(91)90054-z

Javier, R. T. (1994). Adenovirus type 9 E4 open reading frame 1 encodes a transforming protein required for the production of mammary tumors in rats. J Virol, 68(6), 3917-3924.

Johnson, J. S., Osheim, Y. N., Xue, Y., Emanuel, M. R., Lewis, P. W., Bankovich, A., Engel, D. A. (2004). Adenovirus protein VII condenses DNA, represses transcription, and associates with transcriptional activator E1A. J Virol, 78(12), 6459-6468. doi: 10.1128/JVI.78.12.6459-6468.2004

Jung, R., Radko, S., & Pelka, P. (2016). The Dual Nature of Nek9 in Adenovirus Replication. J Virol, 90(4), 1931-1943. doi: 10.1128/JVI.02392-15

Kajan, G. L., Davison, A. J., Palya, V., Harrach, B., & Benko, M. (2012). Genome sequence of a waterfowl aviadenovirus, goose adenovirus 4. J Gen Virol, 93(Pt 11), 2457-2465. doi: 10.1099/vir.0.042028-0

Kajan, G. L., Stefancsik, R., Ursu, K., Palya, V., & Benko, M. (2010). The first complete genome sequence of a non-chicken aviadenovirus, proposed to be turkey adenovirus 1. Virus Res, 153(2), 226-233. doi: 10.1016/j.virusres.2010.08.006

Kallsten, M., Gromova, A., Zhao, H., Valdes, A., Konzer, A., Pettersson, U., & Lind, S. B. (2017). Temporal characterization of the non-structural Adenovirus type 2 proteome and phosphoproteome using high-resolving mass spectrometry. Virology, 511, 240-248. doi: 10.1016/j.virol.2017.08.032

Karen, K. A., & Hearing, P. (2011). Adenovirus core protein VII protects the viral genome from a DNA damage response at early times after infection. J Virol, 85(9), 4135-4142. doi: 10.1128/JVI.02540-10

Kerppola, T. K. (2009). Visualization of molecular interactions using bimolecular fluorescence complementation analysis: characteristics of protein fragment complementation. Chem Soc Rev, 38(10), 2876-2886. doi: 10.1039/b909638h

Kim, T. H., Leslie, P., & Zhang, Y. (2014). Ribosomal proteins as unrevealed caretakers for cellular stress and genomic instability. *Oncotarget, 5*(4), 860-871. doi: 10.18632/oncotarget.1784

King, C. R., Cohen, M. J., Fonseca, G. J., Dirk, B. S., Dikeakos, J. D., & Mymryk, J. S. (2016). Functional and Structural Mimicry of Cellular Protein Kinase A Anchoring Proteins by a Viral Oncoprotein. PLoS Pathog, 12(5), e1005621. doi: 10.1371/journal.ppat.1005621

King, C. R., Gameiro, S. F., Tessier, T. M., Zhang, A., & Mymryk, J. S. (2018). Mimicry of Cellular A Kinase-Anchoring Proteins Is a Conserved and Critical Function of E1A across Various Human Adenovirus Species. J Virol, 92(8). doi: 10.1128/JVI.01902-17

King, C. R., Zhang, A., Tessier, T. M., Gameiro, S. F., & Mymryk, J. S. (2018). Hacking the Cell: Network Intrusion and Exploitation by Adenovirus E1A. MBio, 9(3). doi: 10.1128/mBio.00390-18

Kitchingman, G. R. (1985). Sequence of the DNA-binding protein of a human subgroup E adenovirus (type 4): comparisons with subgroup A (type 12), subgroup B (type 7), and subgroup C (type 5). Virology, 146(1), 90-101. doi: 10.1016/0042-6822(85)90055-8

Klein, M., Earley, E., & Zellat, J. (1959). Isolation from cattle of a virus related to human adenovirus. Proc Soc Exp Biol Med, 102, 1-4. doi: 10.3181/00379727-102-25123

Kohler, A., & Hurt, E. (2010). Gene regulation by nucleoporins and links to cancer. Mol Cell, 38(1), 6-15. doi: 10.1016/j.molcel.2010.01.040

Komoriya, A., Green, L. J., Mervic, M., Yamada, S. S., Yamada, K. M., & Humphries, M. J. (1991). The minimal essential sequence for a major cell type-specific adhesion site (CS1) within the alternatively spliced type III connecting segment domain of fibronectin is leucine-aspartic acid-valine. J Biol Chem, 266(23), 15075-15079.

Kosugi, S., Hasebe, M., Matsumura, N., Takashima, H., Miyamoto-Sato, E., Tomita, M., & Yanagawa, H. (2009a). Six classes of nuclear localization signals specific to different binding grooves of importin alpha. *J Biol Chem, 284*(1), 478-485. doi: 10.1074/jbc.M807017200

Kosugi, S., Hasebe, M., Tomita, M., & Yanagawa, H. (2009b). Systematic identification of cell cycle-dependent yeast nucleocytoplasmic shuttling proteins by prediction of composite motifs. Proc Natl Acad Sci U S A, 106(25), 10171-10176. doi: 10.1073/pnas.0900604106

Kovacs, E. R., & Benko, M. (2009). Confirmation of a novel siadenovirus species detected in raptors: partial sequence and phylogenetic analysis. Virus Res, 140(1-2), 64-70. doi: 10.1016/j.virusres.2008.11.005

Kovacs, G. M., LaPatra, S. E., D'Halluin, J. C., & Benko, M. (2003). Phylogenetic analysis of the hexon and protease genes of a fish adenovirus isolated from white sturgeon (Acipenser transmontanus) supports the proposal for a new adenovirus genus. Virus Res, 98(1), 27-34.

Koyuncu, O. O., & Dobner, T. (2009). Arginine methylation of human adenovirus type 5 L4 100-kilodalton protein is required for efficient virus production. J Virol, 83(10), 4778-4790. doi: 10.1128/JVI.02493-08

Kulshreshtha, V. (2009). Molecular characterization of 33K protein of bovine adenovirus type 3. (PhD thesis), University of Saskatchewan, Saskatoon, Sk, Canada.

Kulshreshtha, V., Ayalew, L. E., Islam, A., & Tikoo, S. K. (2014). Conserved arginines of bovine adenovirus-3 33K protein are important for transportin-3 mediated transport and virus replication. PLoS One, 9(7), e101216. doi: 10.1371/journal.pone.0101216

Kulshreshtha, V., Babiuk, L. A., & Tikoo, S. K. (2004). Role of bovine adenovirus-3 33K protein in viral replication. Virology, 323(1), 59-69. doi: 10.1016/j.virol.2004.02.024

Kulshreshtha, V., Islam, A., Ayalew, L. E., & Tikoo, S. K. (2015). Leucine residues in conserved region of 33K protein of bovine adenovirus - 3 are important for binding to major late promoter and activation of late gene expression. Virology, 483, 174-184. doi: 10.1016/j.virol.2015.04.010

Kulshreshtha, V., & Tikoo, S. K. (2008). Interaction of bovine adenovirus-3 33K protein with other viral proteins. Virology, 381(1), 29-35. doi: 10.1016/j.virol.2008.08.015 Kruse, J. P., & Gu, W. (2008). SnapShot: p53 posttranslational modifications. *Cell, 133*(5), 930-930 e931. doi: 10.1016/j.cell.2008.05.020

Kubbutat, M. H., Jones, S. N., & Vousden, K. H. (1997). Regulation of p53 stability by Mdm2. *Nature, 387*(6630), 299-303. doi: 10.1038/387299a0

Kurki, S., Peltonen, K., Latonen, L., Kiviharju, T. M., Ojala, P. M., Meek, D., & Laiho, M. (2004). Nucleolar protein NPM interacts with HDM2 and protects tumor suppressor protein p53 from HDM2-mediated degradation. *Cancer Cell, 5*(5), 465-475.

Lai, M. C., Lin, R. I., & Tarn, W. Y. (2001). Transportin-SR2 mediates nuclear import of phosphorylated SR proteins. Proc Natl Acad Sci U S A, 98(18), 10154-10159. doi: 10.1073/pnas.181354098

Lam, Y. W., Lamond, A. I., Mann, M., & Andersen, J. S. (2007). Analysis of nucleolar protein dynamics reveals the nuclear degradation of ribosomal proteins. *Curr Biol, 17*(9), 749-760. doi: 10.1016/j.cub.2007.03.064

Lane, D. P. (1992). Cancer. p53, guardian of the genome. *Nature, 358*(6381), 15-16. doi: 10.1038/358015a0

Lang, S. E., & Hearing, P. (2003). The adenovirus E1A oncoprotein recruits the cellular TRRAP/GCN5 histone acetyltransferase complex. Oncogene, 22(18), 2836-2841. doi: 10.1038/sj.onc.1206376

Lange, A., Mills, R. E., Devine, S. E., & Corbett, A. H. (2008). A PY-NLS nuclear targeting signal is required for nuclear localization and function of the Saccharomyces cerevisiae mRNA-binding protein Hrp1. *J Biol Chem, 283*(19), 12926-12934. doi: 10.1074/jbc.M800898200

Lange, A., Mills, R. E., Lange, C. J., Stewart, M., Devine, S. E., & Corbett, A. H. (2007). Classical nuclear localization signals: definition, function, and interaction with importin alpha. *J Biol Chem, 282*(8), 5101-5105. doi: 10.1074/jbc.R600026200

Le Rouzic, E., & Benichou, S. (2005). The Vpr protein from HIV-1: distinct roles along the viral life cycle. Retrovirology, 2, 11. doi: 10.1186/1742-4690-2-11

Ledl, A., Schmidt, D., & Muller, S. (2005). Viral oncoproteins E1A and E7 and cellular LxCxE proteins repress SUMO modification of the retinoblastoma tumor suppressor. Oncogene, 24(23), 3810-3818. doi: 10.1038/sj.onc.1208539

Lee, J. B., Baxi, M. K., Idamakanti, N., Reddy, P. S., Zakhartchouk, A. N., Pyne, C., Tikoo, S. K. (1998). Genetic organization and DNA sequence of early region 4 of bovine adenovirus type 3. Virus Genes, 17(1), 99-100. doi: 10.1023/a:1008017404513

Lehmkuhl, H. D., & Hobbs, L. A. (2008). Serologic and hexon phylogenetic analysis of ruminant adenoviruses. Arch Virol, 153(5), 891-897. doi: 10.1007/s00705-008-0063-4

Lehmkuhl, H. D., Smith, M. H., & Dierks, R. E. (1975). A bovine adenovirus type 3: isolation, characterization, and experimental infection in calves. Arch Virol, 48(1), 39-46. doi: 10.1007/bf01320564

Lenman, A., Liaci, A. M., Liu, Y., Frangsmyr, L., Frank, M., Blaum, B. S., Arnberg, N. (2018). Polysialic acid is a cellular receptor for human adenovirus 52. Proc Natl Acad Sci U S A, 115(18), E4264-E4273. doi: 10.1073/pnas.1716900115

Leopold, P. L., Kreitzer, G., Miyazawa, N., Rempel, S., Pfister, K. K., Rodriguez-Boulan, E., & Crystal, R. G. (2000). Dynein- and microtubule-mediated translocation of adenovirus serotype 5 occurs after endosomal lysis. Hum Gene Ther, 11(1), 151-165. doi: 10.1089/10430340050016238

Levin, A., Armon-Omer, A., Rosenbluh, J., Melamed-Book, N., Graessmann, A., Waigmann, E., & Loyter, A. (2009). Inhibition of HIV-1 integrase nuclear import and replication by a peptide bearing integrase putative nuclear localization signal. Retrovirology, 6, 112. doi: 10.1186/1742-4690-6-112

Li, G., Qi, X., Hu, Z., & Tang, Q. (2019). Mechanisms Mediating Nuclear Trafficking Involved in Viral Propagation by DNA Viruses. Viruses, 11(11). doi: 10.3390/v11111035

Li, M., Brooks, C. L., Wu-Baer, F., Chen, D., Baer, R., & Gu, W. (2003). Mono- versus polyubiquitination: differential control of p53 fate by Mdm2. *Science, 302*(5652), 1972-1975. doi: 10.1126/science.1091362

Li, M., Luo, J., Brooks, C. L., & Gu, W. (2002). Acetylation of p53 inhibits its ubiquitination by Mdm2. *J Biol Chem, 277*(52), 50607-50611. doi: 10.1074/jbc.C200578200

Li, X., Bangari, D. S., Sharma, A., & Mittal, S. K. (2009). Bovine adenovirus serotype 3 utilizes sialic acid as a cellular receptor for virus entry. Virology, 392(2), 162-168. doi: 10.1016/j.virol.2009.06.029

Lichtenstein, D. L., Toth, K., Doronin, K., Tollefson, A. E., & Wold, W. S. (2004). Functions and mechanisms of action of the adenovirus E3 proteins. Int Rev Immunol, 23(1-2), 75-111.

Lin, D. H., & Hoelz, A. (2019). The Structure of the Nuclear Pore Complex (An Update). Annu Rev Biochem, 88, 725-783. doi: 10.1146/annurev-biochem-062917-011901

Lindstrom, M. S. (2011). NPM1/B23: A Multifunctional Chaperone in Ribosome Biogenesis and Chromatin Remodeling. *Biochem Res Int, 2011*, 195209. doi: 10.1155/2011/195209

Lion, T. (2014). Adenovirus infections in immunocompetent and immunocompromised patients. Clin Microbiol Rev, 27(3), 441-462. doi: 10.1128/CMR.00116-13

Liu, Y., Deisenroth, C., & Zhang, Y. (2016). RP-MDM2-p53 Pathway: Linking Ribosomal Biogenesis and Tumor Surveillance. *Trends Cancer, 2*(4), 191-204. doi: 10.1016/j.trecan.2016.03.002

Liu, H., Jin, L., Koh, S. B., Atanasov, I., Schein, S., Wu, L., & Zhou, Z. H. (2010). Atomic structure of human adenovirus by cryo-EM reveals interactions among protein networks. Science, 329(5995), 1038-1043. doi: 10.1126/science.1187433

Liu, Y., Tavana, O., & Gu, W. (2019). p53 modifications: exquisite decorations of the powerful guardian. *J Mol Cell Biol, 11*(7), 564-577. doi: 10.1093/jmcb/mjz060

Lopez-Gordo, E., Podgorski, II, Downes, N., & Alemany, R. (2014). Circumventing antivector immunity: potential use of nonhuman adenoviral vectors. Hum Gene Ther, 25(4), 285-300. doi: 10.1089/hum.2013.228

Lott, K., & Cingolani, G. (2011). The importin beta binding domain as a master regulator of nucleocytoplasmic transport. *Biochim Biophys Acta, 1813*(9), 1578-1592. doi: 10.1016/j.bbamcr.2010.10.012

Lupas, A., Van Dyke, M., & Stock, J. (1991). Predicting coiled coils from protein sequences. Science, 252(5009), 1162-1164. doi: 10.1126/science.252.5009.1162

Lutz, P., & Kedinger, C. (1996). Properties of the adenovirus IVa2 gene product, an effector of late-phase-dependent activation of the major late promoter. J Virol, 70(3), 1396-1405.

Lutz, P., Puvion-Dutilleul, F., Lutz, Y., & Kedinger, C. (1996). Nucleoplasmic and nucleolar distribution of the adenovirus IVa2 gene product. J Virol, 70(6), 3449-3460.

Lutz, P., Rosa-Calatrava, M., & Kedinger, C. (1997). The product of the adenovirus intermediate gene IX is a transcriptional activator. J Virol, 71(7), 5102-5109.

Ma, H. C., & Hearing, P. (2011). Adenovirus structural protein IIIa is involved in the serotype specificity of viral DNA packaging. J Virol, 85(15), 7849-7855. doi: 10.1128/JVI.00467-11

Maclachlan, N. J., Dubovi, E. J., Barthold, S. W., Swayne, D. E., & Winton, J. R. (2016). Virus replication. In: Fenners's Veterinary Vriology (pp. 17-45): Elsevier.

Maier, O., Galan, D. L., Wodrich, H., & Wiethoff, C. M. (2010). An N-terminal domain of adenovirus protein VI fragments membranes by inducing positive membrane curvature. Virology, 402(1), 11-19. doi: 10.1016/j.virol.2010.03.043

Makadiya, N. (2013). Functional characterization of 100k protein of Bovine adenovirus type 3. (PhD), University of Saskatchewan.

Makadiya, N., Gaba, A., & Tikoo, S. K. (2015). Cleavage of bovine adenovirus type 3 non-structural 100K protein by protease is required for nuclear localization in infected cells but is not essential for virus replication. J Gen Virol, 96(9), 2749-2763. doi: 10.1099/vir.0.000205

Mangel, W. F., McGrath, W. J., Toledo, D. L., & Anderson, C. W. (1993). Viral DNA and a viral peptide can act as cofactors of adenovirus virion proteinase activity. Nature, 361(6409), 274-275. doi: 10.1038/361274a0

Mangel, W. F., & San Martin, C. (2014). Structure, function and dynamics in adenovirus maturation. Viruses, 6(11), 4536-4570. doi: 10.3390/v6114536

Marechal, V., Elenbaas, B., Piette, J., Nicolas, J. C., & Levine, A. J. (1994). The ribosomal L5 protein is associated with mdm-2 and mdm-2-p53 complexes. *Mol Cell Biol, 14*(11), 7414-7420. doi: 10.1128/mcb.14.11.7414

Marek, A., Nolte, V., Schachner, A., Berger, E., Schlotterer, C., & Hess, M. (2012). Two fiber genes of nearly equal lengths are a common and distinctive feature of Fowl adenovirus C members. Vet Microbiol, 156(3-4), 411-417. doi: 10.1016/j.vetmic.2011.11.003

Marshall, K. S., Cohen, M. J., Fonseca, G. J., Todorovic, B., King, C. R., Yousef, A. F., Mymryk, J. S. (2014). Identification and characterization of multiple conserved nuclear localization signals within adenovirus E1A. Virology, 454-455, 206-214. doi: 10.1016/j.virol.2014.02.020

Martin, D. E., Powers, T., & Hall, M. N. (2006). Regulation of ribosome biogenesis: where is TOR? Cell Metab, 4(4), 259-260. doi: 10.1016/j.cmet.2006.09.002

Marttila, M., Persson, D., Gustafsson, D., Liszewski, M. K., Atkinson, J. P., Wadell, G., & Arnberg, N. (2005). CD46 is a cellular receptor for all species B adenoviruses except types 3 and 7. J Virol, 79(22), 14429-14436. doi: 10.1128/JVI.79.22.14429-14436.2005

Matera, A. G., Terns, R. M., & Terns, M. P. (2007). Non-coding RNAs: lessons from the small nuclear and small nucleolar RNAs. Nat Rev Mol Cell Biol, 8(3), 209-220. doi: 10.1038/nrm2124

Matsuura, Y. (2016). Mechanistic Insights from Structural Analyses of Ran-GTPase-Driven Nuclear Export of Proteins and RNAs. J Mol Biol, 428(10 Pt A), 2025-2039. doi: 10.1016/j.jmb.2015.09.025

Matthews, D. A., & Russell, W. C. (1994). Adenovirus protein-protein interactions: hexon and protein VI. J Gen Virol, 75 (Pt 12), 3365-3374. doi: 10.1099/0022-1317-75-12-3365

Matthews, D. A., & Russell, W. C. (1998). Adenovirus core protein V is delivered by the invading virus to the nucleus of the infected cell and later in infection is associated with nucleoli. J Gen Virol, 79 (Pt 7), 1671-1675. doi: 10.1099/0022-1317-79-7-1671

Meek, D. W., & Anderson, C. W. (2009). Posttranslational modification of p53: cooperative integrators of function. *Cold Spring Harb Perspect Biol, 1*(6), a000950. doi: 10.1101/cshperspect.a000950

Meier, O., Boucke, K., Hammer, S. V., Keller, S., Stidwill, R. P., Hemmi, S., & Greber, U. F. (2002). Adenovirus triggers macropinocytosis and endosomal leakage together with its clathrin-mediated uptake. J Cell Biol, 158(6), 1119-1131. doi: 10.1083/jcb.200112067

Meier, O., & Greber, U. F. (2004). Adenovirus endocytosis. J Gene Med, 6 Suppl 1, S152-163. doi: 10.1002/jgm.553

Meszaros, N., Cibulka, J., Mendiburo, M. J., Romanauska, A., Schneider, M., & Kohler, A. (2015). Nuclear pore basket proteins are tethered to the nuclear envelope and can regulate membrane curvature. Dev Cell, 33(3), 285-298. doi: 10.1016/j.devcel.2015.02.017

Mittal, S. K., Prevec, L., Babiuk, L. A., & Graham, F. L. (1993). Sequence analysis of bovine adenovirus type 3 early region 3 and fibre protein genes. J Gen Virol, 74 (Pt 12), 2825. doi: 10.1099/0022-1317-74-12-2825

Mittal, S. K., Tikoo, S. K., Van Donkersgoed, J., Beskorwayne, T., Godson, D. L., & Babiuk, L. A. (1999). Experimental inoculation of heifers with bovine adenovirus type 3. Can J Vet Res, 63(2), 153-156.

Miyamoto, Y., Imamoto, N., Sekimoto, T., Tachibana, T., Seki, T., Tada, S., Yoneda, Y. (1997). Differential modes of nuclear localization signal (NLS) recognition by three distinct classes of NLS receptors. J Biol Chem, 272(42), 26375-26381. doi: 10.1074/jbc.272.42.26375

Miyamoto, Y., Yamada, K., & Yoneda, Y. (2016). Importin alpha: a key molecule in nuclear transport and non-transport functions. *J Biochem, 160*(2), 69-75. doi: 10.1093/jb/mvw036

Miyata, Y., & Nishida, E. (2011). DYRK1A binds to an evolutionarily conserved WD40-repeat protein WDR68 and induces its nuclear translocation. Biochim Biophys Acta, 1813(10), 1728-1739. doi: 10.1016/j.bbamcr.2011.06.023

Moll, U. M., & Petrenko, O. (2003). The MDM2-p53 interaction. *Mol Cancer Res, 1*(14), 1001-1008.

Morin, N., & Boulanger, P. (1986). Hexon trimerization occurring in an assembly-defective, 100K temperature-sensitive mutant of adenovirus 2. Virology, 152(1), 11-31. doi: 10.1016/0042-6822(86)90367-3

Moroianu, J., Blobel, G., & Radu, A. (1996). Nuclear protein import: Ran-GTP dissociates the karyopherin alphabeta heterodimer by displacing alpha from an overlapping binding site on beta. Proc Natl Acad Sci U S A, 93(14), 7059-7062. doi: 10.1073/pnas.93.14.7059

Morris, S. J., & Leppard, K. N. (2009). Adenovirus serotype 5 L4-22K and L4-33K proteins have distinct functions in regulating late gene expression. J Virol, 83(7), 3049-3058. doi: 10.1128/JVI.02455-08

Moss, B. (2013). Poxvirus DNA replication. Cold Spring Harb Perspect Biol, 5(9). doi: 10.1101/cshperspect.a010199

Mysiak, M. E., Bleijenberg, M. H., Wyman, C., Holthuizen, P. E., & van der Vliet, P. C. (2004). Bending of adenovirus origin DNA by nuclear factor I as shown by scanning force microscopy is required for optimal DNA replication. J Virol, 78(4), 1928-1935. doi: 10.1128/jvi.78.4.1928-1935.2004

Naim, B., Zbaida, D., Dagan, S., Kapon, R., & Reich, Z. (2009). Cargo surface hydrophobicity is sufficient to overcome the nuclear pore complex selectivity barrier. EMBO J, 28(18), 2697-2705. doi: 10.1038/emboj.2009.225

Nakada, R., Hirano, H., & Matsuura, Y. (2015). Structure of importin-alpha bound to a non-classical nuclear localization signal of the influenza A virus nucleoprotein. *Sci Rep, 5*, 15055. doi: 10.1038/srep15055

Nakielny, S., & Dreyfuss, G. (1999). Transport of proteins and RNAs in and out of the nucleus. Cell, 99(7), 677-690. doi: 10.1016/s0092-8674(00)81666-9

Narayanan, K., Chen, C. J., Maeda, J., & Makino, S. (2003). Nucleocapsid-independent specific viral RNA packaging via viral envelope protein and viral RNA signal. J Virol, 77(5), 2922-2927. doi: 10.1128/jvi.77.5.2922-2927.2003

Ndi, Olasumbo L., Barton, Mary D., & Vanniasinkam, Thiru. (2013). Adenoviral Vectors in Veterinary Vaccine Development: Potential for Further Development. World Journal of Vaccines, 03(03), 111-121. doi: 10.4236/wjv.2013.33016

Nicolas, E., Parisot, P., Pinto-Monteiro, C., de Walque, R., De Vleeschouwer, C., & Lafontaine, D. L. (2016). Involvement of human ribosomal proteins in nucleolar structure and p53-dependent nucleolar stress. *Nat Commun, 7*, 11390. doi: 10.1038/ncomms11390

Oka, M., & Yoneda, Y. (2018). Importin alpha: functions as a nuclear transport factor and beyond. *Proc Jpn Acad Ser B Phys Biol Sci, 94*(7), 259-274. doi: 10.2183/pjab.94.018

Oliner, J. D., Pietenpol, J. A., Thiagalingam, S., Gyuris, J., Kinzler, K. W., & Vogelstein, B. (1993). Oncoprotein MDM2 conceals the activation domain of tumour suppressor p53. *Nature, 362*(6423), 857-860. doi: 10.1038/362857a0

Ostapchuk, P., Almond, M., & Hearing, P. (2011). Characterization of Empty adenovirus particles assembled in the absence of a functional adenovirus IVa2 protein. J Virol, 85(11), 5524-5531. doi: 10.1128/JVI.02538-10

Ostapchuk, P., Anderson, M. E., Chandrasekhar, S., & Hearing, P. (2006). The L4 22-kilodalton protein plays a role in packaging of the adenovirus genome. J Virol, 80(14), 6973-6981. doi: 10.1128/JVI.00123-06

Ostapchuk, P., & Hearing, P. (2005). Control of adenovirus packaging. J Cell Biochem, 96(1), 25-35. doi: 10.1002/jcb.20523

Ostapchuk, P., & Hearing, P. (2008). Adenovirus IVa2 protein binds ATP. J Virol, 82(20), 10290-10294. doi: 10.1128/JVI.00882-08

Ostapchuk, P., Suomalainen, M., Zheng, Y., Boucke, K., Greber, U. F., & Hearing, P. (2017). The adenovirus major core protein VII is dispensable for virion assembly but is essential for lytic infection. PLoS Pathog, 13(6), e1006455. doi: 10.1371/journal.ppat.1006455

Ostapchuk, P., Yang, J., Auffarth, E., & Hearing, P. (2005). Functional interaction of the adenovirus IVa2 protein with adenovirus type 5 packaging sequences. J Virol, 79(5), 2831-2838. doi: 10.1128/jvi.79.5.2831-2838.2005

Pagliara, V., Saide, A., Mitidieri, E., d'Emmanuele di Villa Bianca, R., Sorrentino, R., Russo, G., & Russo, A. (2016). 5-FU targets rpL3 to induce mitochondrial apoptosis via cystathionine-beta-synthase in colon cancer cells lacking p53. *Oncotarget, 7*(31), 50333-50348. doi: 10.18632/oncotarget.10385

Palmero, I., Pantoja, C., & Serrano, M. (1998). p19ARF links the tumour suppressor p53 to Ras. *Nature, 395*(6698), 125-126. doi: 10.1038/25870

Papp, Z., Middleton, D. M., Mittal, S. K., Babiuk, L. A., & Baca-Estrada, M. E. (1997). Mucosal immunization with recombinant adenoviruses: induction of immunity and protection of cotton rats against respiratory bovine herpesvirus type 1 infection. J Gen Virol, 78 (Pt 11), 2933-2943. doi: 10.1099/0022-1317-78-11-2933

Pardo-Mateos, A., & Young, C. S. (2004). Adenovirus IVa2 protein plays an important role in transcription from the major late promoter in vivo. Virology, 327(1), 50-59. doi: 10.1016/j.virol.2004.06.011

Parks, R. J. (2005). Adenovirus protein IX: a new look at an old protein. Mol Ther, 11(1), 19-25. doi: 10.1016/j.ymthe.2004.09.018

Paterson, C. P. (2010). Molecular characterization of 52K protein of bovine adenovirus type 3. (PhD thesis), University of Saskatchewan, Saskatoon, Sk, Canada.

Paterson, C. P., Ayalew, L. E., & Tikoo, S. K. (2012). Mapping of nuclear import signal and importin alpha3 binding regions of 52K protein of bovine adenovirus-3. Virology, 432(1), 63-72. doi: 10.1016/j.virol.2012.05.021

Pelka, P., Ablack, J. N., Torchia, J., Turnell, A. S., Grand, R. J., & Mymryk, J. S. (2009). Transcriptional control by adenovirus E1A conserved region 3 via p300/CBP. Nucleic Acids Res, 37(4), 1095-1106. doi: 10.1093/nar/gkn1057

Pelka, P., Miller, M. S., Cecchini, M., Yousef, A. F., Bowdish, D. M., Dick, F., Mymryk, J. S. (2011). Adenovirus E1A directly targets the E2F/DP-1 complex. J Virol, 85(17), 8841-8851. doi: 10.1128/JVI.00539-11

Pelka, P., Scime, A., Mandalfino, C., Joch, M., Abdulla, P., & Whyte, P. (2007). Adenovirus E1A proteins direct subcellular redistribution of Nek9, a NimA-related kinase. J Cell Physiol, 212(1), 13-25. doi: 10.1002/jcp.20983

Perez-Berna, A. J., Mangel, W. F., McGrath, W. J., Graziano, V., Flint, J., & San Martin, C. (2014). Processing of the l1 52/55k protein by the adenovirus protease: a new substrate and new insights into virion maturation. J Virol, 88(3), 1513-1524. doi: 10.1128/JVI.02884-13

Perez-Berna, A. J., Marion, S., Chichon, F. J., Fernandez, J. J., Winkler, D. C., Carrascosa, J. L., San Martin, C. (2015). Distribution of DNA-condensing protein complexes in the adenovirus core. Nucleic Acids Res, 43(8), 4274-4283. doi: 10.1093/nar/gkv187

Perez-Romero, P., Tyler, R. E., Abend, J. R., Dus, M., & Imperiale, M. J. (2005). Analysis of the interaction of the adenovirus L1 52/55-kilodalton and IVa2 proteins with the packaging sequence in vivo and in vitro. J Virol, 79(4), 2366-2374. doi: 10.1128/JVI.79.4.2366-2374.2005

Perez-Vargas, J., Vaughan, R. C., Houser, C., Hastie, K. M., Kao, C. C., & Nemerow, G. R. (2014). Isolation and characterization of the DNA and protein binding activities of adenovirus core protein V. J Virol, 88(16), 9287-9296. doi: 10.1128/JVI.00935-14

Pestov, D. G., Strezoska, Z., & Lau, L. F. (2001). Evidence of p53-dependent cross-talk between ribosome biogenesis and the cell cycle: effects of nucleolar protein Bop1 on G(1)/S transition. *Mol Cell Biol, 21*(13), 4246-4255. doi: 10.1128/MCB.21.13.4246-4255.2001

Pied, N., & Wodrich, H. (2019). Imaging the adenovirus infection cycle. FEBS Lett, 593(24), 3419-3448. doi: 10.1002/1873-3468.13690

Radko, S., Jung, R., Olanubi, O., & Pelka, P. (2015). Effects of Adenovirus Type 5 E1A Isoforms on Viral Replication in Arrested Human Cells. PLoS One, 10(10), e0140124. doi: 10.1371/journal.pone.0140124

Reddy, P. S., Chen, Y., Idamakanti, N., Pyne, C., Babiuk, L. A., & Tikoo, S. K. (1999). Characterization of early region 1 and pIX of bovine adenovirus-3. Virology, 253(2), 299-308. doi: 10.1006/viro.1998.9510

Reddy, P. S., Idamakanti, N., Chen, Y., Whale, T., Babiuk, L. A., Mehtali, M., & Tikoo, S. K. (1999). Replication-defective bovine adenovirus type 3 as an expression vector. J Virol, 73(11), 9137-9144.

Reddy, P. S., Idamakanti, N., Zakhartchouk, A. N., Baxi, M. K., Lee, J. B., Pyne, C., Tikoo, S. K. (1998). Nucleotide sequence, genome organization, and transcription map of bovine adenovirus type 3. J Virol, 72(2), 1394-1402.

Reddy, P. S., Idamakanti, N., Zakhartchouk, L. N., Babiuk, L. A., Mehtali, M., & Tikoo, S. K. (2000). Optimization of bovine coronavirus hemagglutinin-estrase glycoprotein expression in E3 deleted bovine adenovirus-3. Virus Res, 70(1-2), 65-73. doi: 10.1016/s0168-1702(00)00209-4

Reddy, V. S., & Nemerow, G. R. (2014). Structures and organization of adenovirus cement proteins provide insights into the role of capsid maturation in virus entry and infection. Proc Natl Acad Sci U S A, 111(32), 11715-11720. doi: 10.1073/pnas.1408462111

Reed, M. L., Dove, B. K., Jackson, R. M., Collins, R., Brooks, G., & Hiscox, J. A. (2006). Delineation and modelling of a nucleolar retention signal in the coronavirus nucleocapsid protein. Traffic, 7(7), 833-848. doi: 10.1111/j.1600-0854.2006.00424.x

Reed, S. M., & Quelle, D. E. (2014). p53 Acetylation: Regulation and Consequences. *Cancers (Basel), 7*(1), 30-69. doi: 10.3390/cancers7010030

Rexach, M., & Blobel, G. (1995). Protein import into nuclei: association and dissociation reactions involving transport substrate, transport factors, and nucleoporins. Cell, 83(5), 683-692. doi: 10.1016/0092-8674(95)90181-7

Ribbeck, K., Lipowsky, G., Kent, H. M., Stewart, M., & Gorlich, D. (1998). NTF2 mediates nuclear import of Ran. EMBO J, 17(22), 6587-6598. doi: 10.1093/emboj/17.22.6587

Ritterhoff, S., Farah, C. M., Grabitzki, J., Lochnit, G., Skurat, A. V., & Schmitz, M. L. (2010). The WD40-repeat protein Han11 functions as a scaffold protein to control HIPK2 and MEKK1 kinase functions. EMBO J, 29(22), 3750-3761. doi: 10.1038/emboj.2010.251

Rivera, S., Wellehan, J. F., Jr., McManamon, R., Innis, C. J., Garner, M. M., Raphael, B. L., Frasca, S., Jr. (2009). Systemic adenovirus infection in Sulawesi tortoises (Indotestudo forsteni) caused by a novel siadenovirus. J Vet Diagn Invest, 21(4), 415-426. doi: 10.1177/104063870902100402

Roelvink, P. W., Lizonova, A., Lee, J. G., Li, Y., Bergelson, J. M., Finberg, R. W., Wickham, T. J. (1998). The coxsackievirus-adenovirus receptor protein can function as a cellular attachment protein for adenovirus serotypes from subgroups A, C, D, E, and F. J Virol, 72(10), 7909-7915.

Romanova, L., Grand, A., Zhang, L., Rayner, S., Katoku-Kikyo, N., Kellner, S., & Kikyo, N. (2009). Critical role of nucleostemin in pre-rRNA processing. *J Biol Chem, 284*(8), 4968-4977. doi: 10.1074/jbc.M804594200

Roos, W. H., Ivanovska, I. L., Evilevitch, A., & Wuite, G. J. (2007). Viral capsids: mechanical characteristics, genome packaging and delivery mechanisms. Cell Mol Life Sci, 64(12), 1484-1497. doi: 10.1007/s00018-007-6451-1

Rosa-Calatrava, M., Grave, L., Puvion-Dutilleul, F., Chatton, B., & Kedinger, C. (2001). Functional analysis of adenovirus protein IX identifies domains involved in capsid stability, transcriptional activity, and nuclear reorganization. J Virol, 75(15), 7131-7141. doi: 10.1128/JVI.75.15.7131-7141.2001

Rosa-Calatrava, M., Puvion-Dutilleul, F., Lutz, P., Dreyer, D., de The, H., Chatton, B., & Kedinger, C. (2003). Adenovirus protein IX sequesters host-cell promyelocytic leukaemia protein and contributes to efficient viral proliferation. EMBO Rep, 4(10), 969-975. doi: 10.1038/sj.embor.embor943

Rosenbluh, J., Hayouka, Z., Loya, S., Levin, A., Armon-Omer, A., Britan, E., Loyter, A. (2007). Interaction between HIV-1 Rev and integrase proteins: a basis for the development of anti-HIV peptides. J Biol Chem, 282(21), 15743-15753. doi: 10.1074/jbc.M609864200

Rowe, W. P., Huebner, R. J., Gilmore, L. K., Parrott, R. H., & Ward, T. G. (1953). Isolation of a cytopathogenic agent from human adenoids undergoing spontaneous degeneration in tissue culture. Proc Soc Exp Biol Med, 84(3), 570-573. doi: 10.3181/00379727-84-20714

Rubbi, C. P., & Milner, J. (2003). Disruption of the nucleolus mediates stabilization of p53 in response to DNA damage and other stresses. *EMBO J, 22*(22), 6068-6077. doi: 10.1093/emboj/cdg579

Russell, W. C. (2009). Adenoviruses: update on structure and function. J Gen Virol, 90(Pt 1), 1-20. doi: 10.1099/vir.0.003087-0

Saha, B., Wong, C. M., & Parks, R. J. (2014). The adenovirus genome contributes to the structural stability of the virion. Viruses, 6(9), 3563-3583. doi: 10.3390/v6093563

Said, A., Wang, W., Woldermariam, T., & Tikoo, S. K. (2018). Domains of bovine adenovirus-3 protein 22K involved in interacting with viral protein 52K and cellular importins alpha-5/alpha-7. Virology, 522, 209-219. doi: 10.1016/j.virol.2018.07.015

Said, A., Woldemariam, T. A., & Tikoo, S. K. (2018). Porcine Adenovirus Type 3 E3 Encodes a Structural Protein Essential for Capsid Stability and Production of Infectious Progeny Virions. J Virol, 92(20). doi: 10.1128/JVI.00680-18

Sambrook, J.E , & Russell, D.W. (2000). Molecular Cloning: A Laboratory Manual. New York: Cold Spring Harbor Laboratory Press, Cold Spring Harbor

Samudram, A., Mangalassery, B. M., Kowshik, M., Patincharath, N., & Varier, G. K. (2016). Passive permeability and effective pore size of HeLa cell nuclear membranes. Cell Biol Int, 40(9), 991-998. doi: 10.1002/cbin.10640

San Martin, C. (2012). Latest insights on adenovirus structure and assembly. Viruses, 4(5), 847-877. doi: 10.3390/v4050847

Saxena, A., Rorie, C. J., Dimitrova, D., Daniely, Y., & Borowiec, J. A. (2006). Nucleolin inhibits Hdm2 by multiple pathways leading to p53 stabilization. *Oncogene, 25*(55), 7274-7288. doi: 10.1038/sj.onc.1209714

Schachner, A., Matos, M., Grafl, B., & Hess, M. (2018). Fowl adenovirus-induced diseases and strategies for their control - a review on the current global situation. *Avian Pathol, 47*(2), 111-126. doi: 10.1080/03079457.2017.1385724

Schmidt, T. G., & Skerra, A. (2007). The Strep-tag system for one-step purification and high-affinity detection or capturing of proteins. Nat Protoc, 2(6), 1528-1535. doi: 10.1038/nprot.2007.209

Schreiner, S., Kinkley, S., Burck, C., Mund, A., Wimmer, P., Schubert, T., Dobner, T. (2013). SPOC1-mediated antiviral host cell response is antagonized early in human adenovirus type 5 infection. PLoS Pathog, 9(11), e1003775. doi: 10.1371/journal.ppat.1003775

Schreiner, S., Martinez, R., Groitl, P., Rayne, F., Vaillant, R., Wimmer, P., Wodrich, H. (2012). Transcriptional activation of the adenoviral genome is mediated by capsid protein VI. PLoS Pathog, 8(2), e1002549. doi: 10.1371/journal.ppat.1002549

Schreiner, S., Wimmer, P., Sirma, H., Everett, R. D., Blanchette, P., Groitl, P., & Dobner, T. (2010). Proteasome-dependent degradation of Daxx by the viral E1B-55K protein in human adenovirus-infected cells. J Virol, 84(14), 7029-7038. doi: 10.1128/JVI.00074-10

Schumacher, V. L., Innis, C. J., Garner, M. M., Risatti, G. R., Nordhausen, R. W., Gilbert-Marcheterre, K., Frasca, S., Jr. (2012). Sulawesi tortoise adenovirus-1 in two impressed tortoises (Manouria impressa) and a Burmese star tortoise (Geochelone platynota). J Zoo Wildl Med, 43(3), 501-510. doi: 10.1638/2011-0228R.1

Schwartz, T. U. (2016). The Structure Inventory of the Nuclear Pore Complex. J Mol Biol, 428(10 Pt A), 1986-2000. doi: 10.1016/j.jmb.2016.03.015

Scott, M. S., Boisvert, F. M., McDowall, M. D., Lamond, A. I., & Barton, G. J. (2010). Characterization and prediction of protein nucleolar localization sequences. Nucleic Acids Res, 38(21), 7388-7399. doi: 10.1093/nar/gkq653

Sheng, Z., Lewis, J. A., & Chirico, W. J. (2004). Nuclear and nucleolar localization of 18-kDa fibroblast growth factor-2 is controlled by C-terminal signals. J Biol Chem, 279(38), 40153-40160. doi: 10.1074/jbc.M400123200

Sibley, S. D., Goldberg, T. L., & Pedersen, J. A. (2011). Detection of known and novel adenoviruses in cattle wastes via broad-spectrum primers. Appl Environ Microbiol, 77(14), 5001-5008. doi: 10.1128/AEM.00625-11

Singh, M., Shmulevitz, M., & Tikoo, S. K. (2005). A newly identified interaction between IVa2 and pVIII proteins during porcine adenovirus type 3 infection. Virology, 336(1), 60-69. doi: 10.1016/j.virol.2005.03.003

Singh, Shakti, Kumar, Rakesh, & Agrawal, Babita. (2019). Adenoviral Vector-Based Vaccines and Gene Therapies: Current Status and Future Prospects. doi: 10.5772/intechopen.79697

Sloan, K. E., Bohnsack, M. T., & Watkins, N. J. (2013). The 5S RNP couples p53 homeostasis to ribosome biogenesis and nucleolar stress. *Cell Rep, 5*(1), 237-247. doi: 10.1016/j.celrep.2013.08.049

Smyth, J. A., Benko, M., Moffett, D. A., & Harrach, B. (1996). Bovine adenovirus type 10 identified in fatal cases of adenovirus-associated enteric disease in cattle by in situ hybridization. J Clin Microbiol, 34(5), 1270-1274.

Stephens, C., & Harlow, E. (1987). Differential splicing yields novel adenovirus 5 E1A mRNAs that encode 30 kd and 35 kd proteins. EMBO J, 6(7), 2027-2035.

Stewart, M. (2006). Structural basis for the nuclear protein import cycle. *Biochem Soc Trans, 34*(Pt 5), 701-704. doi: 10.1042/BST0340701

Stilwell, J. L., McCarty, D. M., Negishi, A., Superfine, R., & Samulski, R. J. (2003). Development and characterization of novel empty adenovirus capsids and their impact on cellular gene expression. J Virol, 77(23), 12881-12885. doi: 10.1128/jvi.77.23.12881-12885.2003

Stracker, T. H., Lee, D. V., Carson, C. T., Araujo, F. D., Ornelles, D. A., & Weitzman, M. D. (2005). Serotype-specific reorganization of the Mre11 complex by adenoviral E4orf3 proteins. J Virol, 79(11), 6664-6673. doi: 10.1128/jvi.79.11.6664-6673.2005

Strunze, S., Engelke, M. F., Wang, I. H., Puntener, D., Boucke, K., Schleich, S., Greber, U. F. (2011). Kinesin-1-mediated capsid disassembly and disruption of the nuclear pore complex promote virus infection. Cell Host Microbe, 10(3), 210-223. doi: 10.1016/j.chom.2011.08.010

Strunze, S., Trotman, L. C., Boucke, K., & Greber, U. F. (2005). Nuclear targeting of adenovirus type 2 requires CRM1-mediated nuclear export. Mol Biol Cell, 16(6), 2999-3009. doi: 10.1091/mbc.e05-02-0121

Stuwe, T., Correia, A. R., Lin, D. H., Paduch, M., Lu, V. T., Kossiakoff, A. A., & Hoelz, A. (2015). Nuclear pores. Architecture of the nuclear pore complex coat. Science, 347(6226), 1148-1152. doi: 10.1126/science.aaa4136

Subramanian, T., Zhao, L. J., & Chinnadurai, G. (2013). Interaction of CtBP with adenovirus E1A suppresses immortalization of primary epithelial cells and enhances virus replication during productive infection. Virology, 443(2), 313-320. doi: 10.1016/j.virol.2013.05.018

Sundararajan, R., Cuconati, A., Nelson, D., & White, E. (2001). Tumor necrosis factor-alpha induces Bax-Bak interaction and apoptosis, which is inhibited by adenovirus E1B 19K. J Biol Chem, 276(48), 45120-45127. doi: 10.1074/jbc.M106386200

Suomalainen, M., Luisoni, S., Boucke, K., Bianchi, S., Engel, D. A., & Greber, U. F. (2013). A direct and versatile assay measuring membrane penetration of adenovirus in single cells. J Virol, 87(22), 12367-12379. doi: 10.1128/JVI.01833-13

Tajrishi, M. M., Tuteja, R., & Tuteja, N. (2011). Nucleolin: The most abundant multifunctional phosphoprotein of nucleolus. *Commun Integr Biol, 4*(3), 267-275. doi: 10.4161/cib.4.3.14884

Takagi, M., Absalon, M. J., McLure, K. G., & Kastan, M. B. (2005). Regulation of p53 translation and induction after DNA damage by ribosomal protein L26 and nucleolin. *Cell, 123*(1), 49-63. doi: 10.1016/j.cell.2005.07.034

Taylor, L. A., & Rose, R. E. (1988). A correction in the nucleotide sequence of the Tn903 kanamycin resistance determinant in pUC4K. Nucleic Acids Res, 16(1), 358. doi: 10.1093/nar/16.1.358

Taylor, S. S., Zhang, P., Steichen, J. M., Keshwani, M. M., & Kornev, A. P. (2013). PKA: lessons learned after twenty years. Biochim Biophys Acta, 1834(7), 1271-1278. doi: 10.1016/j.bbapap.2013.03.007

Tessier, T. M., Dodge, M. J., Prusinkiewicz, M. A., & Mymryk, J. S. (2019). Viral Appropriation: Laying Claim to Host Nuclear Transport Machinery. Cells, 8(6). doi: 10.3390/cells8060559

Thanbichler, M., Iniesta, A. A., & Shapiro, L. (2007). A comprehensive set of plasmids for vanillate- and xylose-inducible gene expression in Caulobacter crescentus. Nucleic Acids Res, 35(20), e137. doi: 10.1093/nar/gkm818

Thomson, G.R. (1994). Adenovirus infections. In G. R. T. J. A. W. Coetzer, and R. C. Tustin (Ed.), Infectious Diseases of Livestock, with Special Reference to Southern Africa. (pp. 901–908.). Cape Town, South Africa.: Oxford University Press.

Tormanen, H., Backstrom, E., Carlsson, A., & Akusjarvi, G. (2006). L4-33K, an adenovirus-encoded alternative RNA splicing factor. J Biol Chem, 281(48), 36510-36517. doi: 10.1074/jbc.M607601200

Tormanen Persson, H., Aksaas, A. K., Kvissel, A. K., Punga, T., Engstrom, A., Skalhegg, B. S., & Akusjarvi, G. (2012). Two cellular protein kinases, DNA-PK and PKA, phosphorylate the adenoviral L4-33K protein and have opposite effects on L1 alternative RNA splicing. PLoS One, 7(2), e31871. doi: 10.1371/journal.pone.0031871

Tribouley, C., Lutz, P., Staub, A., & Kedinger, C. (1994). The product of the adenovirus intermediate gene IVa2 is a transcriptional activator of the major late promoter. J Virol, 68(7), 4450-4457.

Tyler, R. E., Ewing, S. G., & Imperiale, M. J. (2007). Formation of a multiple protein complex on the adenovirus packaging sequence by the IVa2 protein. J Virol, 81(7), 3447-3454. doi: 10.1128/JVI.02097-06

Ugai, H., Dobbins, G. C., Wang, M., Le, L. P., Matthews, D. A., & Curiel, D. T. (2012). Adenoviral protein V promotes a process of viral assembly through nucleophosmin 1. Virology, 432(2), 283-295. doi: 10.1016/j.virol.2012.05.028

Ulfendahl, P. J., Linder, S., Kreivi, J. P., Nordqvist, K., Sevensson, C., Hultberg, H., & Akusjarvi, G. (1987). A novel adenovirus-2 E1A mRNA encoding a protein with transcription activation properties. EMBO J, 6(7), 2037-2044.

Umlauf, D., Bonnet, J., Waharte, F., Fournier, M., Stierle, M., Fischer, B., Tora, L. (2013). The human TREX-2 complex is stably associated with the nuclear pore basket. J Cell Sci, 126(Pt 12), 2656-2667. doi: 10.1242/jcs.118000

van Olphen, A. L., Tikoo, S. K., & Mittal, S. K. (2002). Characterization of bovine adenovirus type 3 E1 proteins and isolation of E1-expressing cell lines. Virology, 295(1), 108-118. doi: 10.1006/viro.2002.1389

Van Vliet, K., Mohamed, M.R., Zhang, L., Villa, N.Y., Werden, S.J., Liu, J., McFadden, G., 2009. Poxvirus proteomics and virus-host protein interactions. Microbiology and molecular biology reviews : MMBR 73, 730-749.

Vellinga, J., Van der Heijdt, S., & Hoeben, R. C. (2005). The adenovirus capsid: major progress in minor proteins. J Gen Virol, 86(Pt 6), 1581-1588. doi: 10.1099/vir.0.80877-0

Vijayalingam, S., & Chinnadurai, G. (2013). Adenovirus L-E1A activates transcription through mediator complex-dependent recruitment of the super elongation complex. J Virol, 87(6), 3425-3434. doi: 10.1128/JVI.03046-12

Wang, H., Li, Z. Y., Liu, Y., Persson, J., Beyer, I., Moller, T., Lieber, A. (2011). Desmoglein 2 is a receptor for adenovirus serotypes 3, 7, 11 and 14. Nat Med, 17(1), 96-104. doi: 10.1038/nm.2270

Waye, M. , & Sing, W.(2010). Anti-Viral Drugs for Human Adenoviruses. . Pharmaceuticals. 3. 10.3390/ph3103343.

Weber, J. D., Taylor, L. J., Roussel, M. F., Sherr, C. J., & Bar-Sagi, D. (1999). Nucleolar Arf sequesters Mdm2 and activates p53. *Nat Cell Biol, 1*(1), 20-26. doi: 10.1038/8991

Wente, S. R., & Rout, M. P. (2010). The nuclear pore complex and nuclear transport. Cold Spring Harb Perspect Biol, 2(10), a000562. doi: 10.1101/cshperspect.a000562

White, E. (2006). Mechanisms of apoptosis regulation by viral oncogenes in infection and tumorigenesis. Cell Death Differ, 13(8), 1371-1377. doi: 10.1038/sj.cdd.4401941

Wiethoff, C. M., Wodrich, H., Gerace, L., & Nemerow, G. R. (2005). Adenovirus protein VI mediates membrane disruption following capsid disassembly. J Virol, 79(4), 1992-2000. doi: 10.1128/JVI.79.4.1992-2000.2005

Wimmer, P., Schreiner, S., & Dobner, T. (2012). Human pathogens and the host cell SUMOylation system. J Virol, 86(2), 642-654. doi: 10.1128/JVI.06227-11

Wodrich, H., Cassany, A., D'Angelo, M. A., Guan, T., Nemerow, G., & Gerace, L. (2006). Adenovirus core protein pVII is translocated into the nucleus by multiple import receptor pathways. J Virol, 80(19), 9608-9618. doi: 10.1128/JVI.00850-06

Wodrich, H., Guan, T., Cingolani, G., Von Seggern, D., Nemerow, G., & Gerace, L. (2003). Switch from capsid protein import to adenovirus assembly by cleavage of nuclear transport signals. EMBO J, 22(23), 6245-6255. doi: 10.1093/emboj/cdg614

Wohl, B. P., & Hearing, P. (2008). Role for the L1-52/55K protein in the serotype specificity of adenovirus DNA packaging. J Virol, 82(10), 5089-5092. doi: 10.1128/JVI.00040-08

Wold, W. S., Tollefson, A. E., & Hermiston, T. W. (1995). E3 transcription unit of adenovirus. Curr Top Microbiol Immunol, 199 (Pt 1), 237-274. doi: 10.1007/978-3-642-79496-4_13

Wold, W. S., & Toth, K. (2013). Adenovirus vectors for gene therapy, vaccination and cancer gene therapy. Curr Gene Ther, 13(6), 421-433. doi: 10.2174/15665232136661311250950 46

Wolfrum, N., & Greber, U. F. (2013). Adenovirus signalling in entry. Cell Microbiol, 15(1), 53-62. doi: 10.1111/cmi.12053

Woods, L. W., Schumaker, B. A., Pesavento, P. A., Crossley, B. M., & Swift, P. K. (2018). Adenoviral hemorrhagic disease in California mule deer, 1990-2014. *J Vet Diagn Invest, 30*(4), 530-537. doi: 10.1177/1040638718766036

Wu, K., Guimet, D., & Hearing, P. (2013). The adenovirus L4-33K protein regulates both late gene expression patterns and viral DNA packaging. J Virol, 87(12), 6739-6747. doi: 10.1128/JVI.00652-13

Wu, K., Orozco, D., & Hearing, P. (2012). The adenovirus L4-22K protein is multifunctional and is an integral component of crucial aspects of infection. J Virol, 86(19), 10474-10483. doi: 10.1128/JVI.01463-12

Wu, Q., Chen, Y., Kulshreshtha, V., & Tikoo, S. K. (2004). Characterization and nuclear localization of the fiber protein encoded by the late region 7 of bovine adenovirus type 3. Arch Virol, 149(9), 1783-1799. doi: 10.1007/s00705-004-0323-x

Wu, Q., & Tikoo, S. K. (2004). Altered tropism of recombinant bovine adenovirus type-3 expressing chimeric fiber. Virus Res, 99(1), 9-15. doi: 10.1016/j.virusres.2003.09.009

Xing, L., & Tikoo, S. K. (2006). E1A promoter of bovine adenovirus type 3. J Gen Virol, 87(Pt 12), 3539-3544. doi: 10.1099/vir.0.82108-0

Xing, L., & Tikoo, S. K. (2007). Bovine adenovirus-3 E1A coding region contain cis-acting DNA packaging motifs. Virus Res, 130(1-2), 315-320. doi: 10.1016/j.virusres.2007.06.015

Xing, L., Zhang, L., Van Kessel, J., & Tikoo, S. K. (2003). Identification of cis-acting sequences required for selective packaging of bovine adenovirus type 3 DNA. J Gen Virol, 84(Pt 11), 2947-2956. doi: 10.1099/vir.0.19418-0

Xu, D., Farmer, A., & Chook, Y. M. (2010). Recognition of nuclear targeting signals by Karyopherin-beta proteins. Curr Opin Struct Biol, 20(6), 782-790. doi: 10.1016/j.sbi.2010.09.008

Yang, T. C., & Maluf, N. K. (2012). Cooperative heteroassembly of the adenoviral L4-22K and IVa2 proteins onto the viral packaging sequence DNA. Biochemistry, 51(7), 1357-1368. doi: 10.1021/bi201580f

Yang, K., Wang, M., Zhao, Y., Sun, X., Yang, Y., Li, X., Yi, J. (2016). A redox mechanism underlying nucleolar stress sensing by nucleophosmin. *Nat Commun, 7*, 13599. doi: 10.1038/ncomms13599

Yousef, A. F., Fonseca, G. J., Pelka, P., Ablack, J. N., Walsh, C., Dick, F. A., Mymryk, J. S. (2010). Identification of a molecular recognition feature in the E1A oncoprotein that

binds the SUMO conjugase UBC9 and likely interferes with polySUMOylation. Oncogene, 29(33), 4693-4704. doi: 10.1038/onc.2010.226

Zakhartchouk, A., Connors, W., van Kessel, A., & Tikoo, S. K. (2004). Bovine adenovirus type 3 containing heterologous protein in the C-terminus of minor capsid protein IX. Virology, 320(2), 291-300. doi: 10.1016/j.virol.2003.12.007

Zakhartchouk, A. N., Godson, D. L., Babiuk, L. A., & Tikoo, S. K. (2001). 121R protein from the E3 region of bovine adenovirus-3 inhibits cytolysis of mouse cells by human tumor necrosis factor. Intervirology, 44(1), 29-35. doi: 10.1159/000050027

Zakhartchouk, A. N., Reddy, P. S., Baxi, M., Baca-Estrada, M. E., Mehtali, M., Babiuk, L. A., & Tikoo, S. K. (1998). Construction and characterization of E3-deleted bovine adenovirus type 3 expressing full-length and truncated form of bovine herpesvirus type 1 glycoprotein gD. Virology, 250(1), 220-229. doi: 10.1006/viro.1998.9351

Zemke, N. R., & Berk, A. J. (2017). The Adenovirus E1A C Terminus Suppresses a Delayed Antiviral Response and Modulates RAS Signaling. Cell Host Microbe, 22(6), 789-800 e785. doi: 10.1016/j.chom.2017.11.008

Zhang, A., Tessier, T. M., Galpin, K. J. C., King, C. R., Gameiro, S. F., Anderson, W. W., .Mymryk, J. S. (2018). The Transcriptional Repressor BS69 is a Conserved Target of the E1A Proteins from Several Human Adenovirus Species. Viruses, 10(12). doi: 10.3390/v10120662

Zhang, W., & Arcos, R. (2005). Interaction of the adenovirus major core protein precursor, pVII, with the viral DNA packaging machinery. Virology, 334(2), 194-202. doi: 10.1016/j.virol.2005.01.048

Zhang, W., & Imperiale, M. J. (2000). Interaction of the adenovirus IVa2 protein with viral packaging sequences. J Virol, 74(6), 2687-2693. doi: 10.1128/jvi.74.6.2687-2693.2000

Zhang, W., & Imperiale, M. J. (2003). Requirement of the adenovirus IVa2 protein for virus assembly. J Virol, 77(6), 3586-3594. doi: 10.1128/jvi.77.6.3586-3594.2003

Zhang, Y., & Lu, H. (2009). Signaling to p53: ribosomal proteins find their way. *Cancer Cell, 16*(5), 369-377. doi: 10.1016/j.ccr.2009.09.024

Zhang, C., & Zhou, D. (2016). Adenoviral vector-based strategies against infectious disease and cancer. *Hum Vaccin Immunother, 12*(8), 2064-2074. doi: 10.1080/21645515.2016.1165908

Zhao, H., Chen, M., & Pettersson, U. (2014). A new look at adenovirus splicing. Virology, 456-457, 329-341. doi: 10.1016/j.virol.2014.04.006

Zhao, L. J., Loewenstein, P. M., & Green, M. (2017). Adenovirus E1A TRRAP-targeting domain-mediated enhancement of MYC association with the NuA4 complex activates a panel of MYC target genes enriched for gene expression and ribosome biogenesis. Virology, 512, 172-179. doi: 10.1016/j.virol.2017.08.010

Zhao, L. J., & Padmanabhan, R. (1988). Nuclear transport of adenovirus DNA polymerase is facilitated by interaction with preterminal protein. Cell, 55(6), 1005-1015. doi: 10.1016/0092-8674(88)90245-0

Zhao, X. (2016). The Role of Bovine Adenovirus-3 Protein V (pV) in Virus Replication. (PhD thesis), University of Saskatchewan, Saskatoon, Sk, Canada.

.

Zhao, X., & Tikoo, S. K. (2016). Deletion of pV affects integrity of capsid causing defect in the infectivity of bovine adenovirus-3. J Gen Virol, 97(10), 2657-2667. doi: 10.1099/jgv.0.000570

Zheng, B., Mittal, S. K., Graham, F. L., & Prevec, L. (1994). The E1 sequence of bovine adenovirus type 3 and complementation of human adenovirus type 5 E1A function in bovine cells. Virus Res, 31(2), 163-186. doi: 10.1016/0168-1702(94)90002-7

Zhou, Y., & Tikoo, S. K. (2001). Analysis of early region 1 of porcine adenovirus type 3. Virology, 291(1), 68-76. doi: 10.1006/viro.2001.1219

APPENDIX

Appendix 1

Plasmid Construction

pC.IVa2 and pHA.IVa2. A 1364 bp DNA fragment was amplified by PCR using primers *Kpn*I FP (including 13 nucleotide splice sequence) and XhoI RP (Table 1) and plasmid pUC304a+ (Du and Tikoo, 2010). DNA as a template The PCR product was digested with *Kpn*I-*Xho*I and ligated to *Kpn*I-*Xho*I digested plasmid pCDNA3 Invitrogen) creating plasmid pC.IVa2. A 1365 bp DNA fragment was amplified by PCR using primers EcoRI FP and NotI RP (Table 1), and plasmid pC.IVa2 DNA as a template. The PCR product was digested using *Eco*RI and *Not*I and ligated to *Eco*RI and *Not*I digested plasmid pC3HA (plasmid pCDNA3 containing HA tag obtained from Dr. Joyce Wilson) creating plasmid pHA.IVa2.

pC.IVa2d25. A 1288 bp DNA fragment was amplified by PCR using primers EcorIΔN25 FP and XhoI RP (Table 1), and plasmid pC.IVa2 DNA as a template. The PCR product was digested with *Eco*RI-*Xho*I and ligated to *Eco*RI-*Xho*I digested plasmid pCDNA3 DNA creating plasmid pC.IVa2d25 plasmid (*N-terminus 25 amino acid truncated IVa2*).

pDR.IVa2. A1363bbp DNA fragment was amplified using primers SacI FP and KpnI RP (Table 1), and plasmiud pC.IVa2 DNA as a template. The PCR product was digested with *Sac*I-*Kpn*I and ligated to *Sac*I-*Kpn*I digested plasmid pDsRed-monomer-C1 (pDR) (Clontech, 632466) DNA, creating plasmid pDR.IVa2.

pDR.IVa2d1. A 1272bp DNA fragment amplified using primers SacI FP and RPΔ25C (Table 1) and plasmid pDR-IVa2 DNA as a template. The PCR product was digested with *Sac*I-*Kpn*I and ligated to *Sac*I-*Kpn*I digested plasmid pDR DNA creating plasmid pDR.IVa2d1 (*containing deletion of IVa2 amino acid 424-448).*

pDR-IVa2d2. A1219-bp DNA fragment was amplified by PCR using primers SacI FP and RPΔ50C (Table 1), and plasmid pDR-IVa2 DNA as a template. The PCR product was digested with *Sac*I-*Kpn*I and ligated to *Sac*I-*Kpn*I digested plasmid pDR DNA creating plasmid pDR.IVa2d2 (*containing deletion of IVa2 amino acid 398-448*).

pDR.IVa2d3. A 1288bp DNA fragment amplified using primers FPΔN25 and KpnI RP (Table 1), and plasmid pDR-IVa2 DNA as a template. The PCR product was digested with *Sac*I-*Kpn*I and ligated to *Sac*I-*Kpn*I digested plasmid pDR DNA creating plasmid pDR.IVa2d3 (*containing deletion of IVa2 amino acid 2-25).*

pDR.IVa2d4. A 1138 bp DNA fragment was amplified by PCR using primers FPΔN75 and *KpnI* RP2 (Table 1), and plasmid pDR-IVa2 DNA as a template. The PCR product was digested with *Sac*I-*Kpn*I and ligated to *Sac*I-*Kpn*I digested plasmid pDR DNA creating plasmid pDR.IVa2d4 (*containing a deletion of IVa2 amino acid 2-75*).

pGFP/β gal.NLS. Using primers *Not*I FP and *Apa*I RP (Table 1), and plasmid pC-IVa2 DNA as a template, a 96 bp DNA fragment was amplified by PCR digested with *Not*I-*Apa*I and ligated to *Not*I-*Apa*I digested plasmid pCMVGFP/βgal (Wu and Tikoo, 2004) DNA creating plasmid pGFP/βgal1.NLS (*GFP/Bgal fused with N-terminus 25 amino acids of IVa2*).

pGFP/βgal1.NLS1. A 1116bp PCR product amplified using primers *Not*I 4-18FP and *AVRII* RP (Table 1), and plasmid pGFP/β gal.NLS DNA as template. The 1116 bp DNA fragment digested with NotI 4-18-AVRII and ligated to *NotI-AvrII* pCMV_GFP/βgal (Wu and Tikoo, 2004) creating plasmid pGFP/βgal1.NLS1 (*GFP/Bgal fused with N-terminus 4-18 amino acids of IVa2*).

pDR.IVa2d3.1. A 1373 bp DNA fragment was amplified by PCR using primers FPΔ6-8 and *Bam*HI RP (Table 1), and plasmid pDR-IVa2 DNA as a template. The PCR product was digested with *Xho*I-*Bam*HI and ligated to *Xho*I-*Bam*HI digested plasmid pDR DNA creating plasmid pDR.IVa2d3.1 (*containing a deletion of IVa2 amino acid 6-8*).

pDR.IVa2d3.2. A 1367 bp DNA fragment amplified by PCR using primers FPΔ4-8 and BamHI RP (Table 1), and plasmid pDR-IVa2 DNA as a template was digested with *Xho*I-*Bam*HI and ligated to *Xho*I-*Bam*HI digested plasmid pDR DNA creating plasmid pDR.IVa2d3.2 (*containing a deletion of IVa2 amino acid 4-8)*.

pDR.IVa2d3.3. A 1358 bp DNA fragment amplified by PCR using primers FPΔ4-11 and BamHI RP (Table 1), and plasmid pDR-IVa2 DNA as a template was digested with *Xho*I-*Bam*HI and ligated to *Xho*I-*Bam*HI digested plasmid pDR DNA creating plasmid pDR.IVa2d3.3 (*containing a deletion of IVa2 amino acid 4-11).*

pDR.IVa2d3.4. A 1346 bp DNA fragment amplified by PCR using primers FPΔ4-15 and BamHI RP (Table 1) and plasmid pDRIVa2 DNA as a template was digested with *Xho*I-*Bam*HI and ligated to *Xho*I-*Bam*HI digested plasmid pDR DNA creating plasmid pDR.IVa2d3.4 (*containing a deletion of IVa2 amino acid 4-15).*

pDR.IVa2d3.5. A 1382 bp DNA fragment amplified by PCR using primers FPΔ4-18 and BamHI RP (Table 1), and plasmid pDR-IVa2 DNA as a template was digested with *Xho*I-*Bam*HI and ligated to *Xho*I-*Bam*HI digested plasmid pDR DNA creating plasmid pDR.IVa2d3.5 (*containing a deletion of IVa2 amino acid 4-18).*

pDIVa2.M1. Using primers FP6M and KpnI RP2 (Table 1), and plasmid pDR-IVa2 DNA as a template a 1364 bp DNA fragment was amplified by PCR, digested with SacI-KpnI and ligated to SacI-KpnI digested plasmid pDR DNA creating plasmid pDIVa2.M1 (containing substitution of 6th amino acid of IVa2 in pDR-IVa2 from R to G).

pDIVa2.M2. Using primers FP7M and KpnI RP2 (Table 1), and plasmid pDR-IVa2 DNA as a template, a 1364 bp DNA fragment was amplified by PCR, digested with SacI-KpnI and ligated to SacI-KpnI digested plasmid pDR DNA creating plasmid pDIVa2.R2M (containing substitution of 7th amino acid of IVa2 in pDR.IVa2 from R to G).

pDIVa2.M3. Using primers FP8M and KpnI RP2 (Table 1), and plasmid pDR-IVa2 DNA as a template, a 1364 bp DNA fragment was amplified by PCR, digested with SacI-KpnI and ligated to SacI-KpnI digested plasmid pDR DNA creating plasmid pDIVa2.KM (containing substitution of 8th amino acid of IVa2 in pDR.IVa2 from K to G)

pDIVa2.M4. Using primers FP6-8M and KpnI RP2 (Table 1), plasmid pDR-IVa2 DNA as a template, a 1364 bp DNA fragment was amplified, digested with SacI-KpnI and ligated to SacI-KpnI digested plasmid pDR DNA creating plasmid pDIVa2.RRKM (containing substitution of 6 to 8 amino acid of IVa2 in pDR.IVa2 from RRK to GGG).

pDR.IVa2d3.1a. A 1382 bp DNA fragment amplified by PCR using primers FPM6-8, and BamHI RP (Table 1), and plasmid pDR-IVa2 DNA as a template was digested with *Xho*I-*Bam*HI and ligated to *Xho*I-*Bam*HI digested plasmid pDR DNA creating plasmid pDR.IVa2d3a (*containing substitution of IVa2 amino acid 6-8 from RRK to AAA).*

pDR.IVa2d3.2a. A 1382 bp DNA fragment amplified by PCR using primers FPM4-8 and BamHI RP (Table 1), and plasmid pDR-IVa2 DNA as a template was digested with *Xho*I-*Bam*HI and ligated to *Xho*I-*Bam*HI digested plasmid pDR DNA creating plasmid pDR.IVa2d3.2a (*containing a substitution of IVa2 amino acid 4-8 from RGRRK to AAAAA).*

pDR.IVa2d3.3a. A 1382 bp DNA fragment amplified by PCR using primers FPM4-11 and BamHI RP (Table 1), and plasmid pDR-IVa2 DNA as a template was digested with *Xho*I-*Bam*HI and ligated to *Xho*I-*Bam*HI digested plasmid pDR DNA creating plasmid pDR.IVa2d3.3a (*containing a substitution of IVa2 amino acid 4-11 from RGRRKVRH to AAAAAAAA).*

pDR.IVa2d3.4a. A 1382 bp DNA fragment amplified by PCR using primers FPM4-15 and BamHI RP (Table 1), and plasmid pDR-IVa2 DNA as a template was digested with *Xho*I-*Bam*HI and ligated to *Xho*I-*Bam*HI digested plasmid pDR DNA creating plasmid pDR.IVa2d3.4a (*containing a substitution of IVa2 amino acid 4-15 from RGRRKVRHQQAQ to AAAAAAAAAAAA).*

pDR.IVa2d3.5a. Using primers NheI FP and IRP M4-18 (Table 1), and plasmid pDR-IVa2 DNA as a template a 775 bp DNA fragment (P1) was amplified by PCR. Similarly, using primers IFPM4-18 and BamHI RP (Table 1), and plasmid pDR-IVa2 DNA as a template a 1362 bp DNA Fragment (P2) was amplified by PCR. The P1 and P2 DNA fragments were annealed and a 2094 bp DNA fragment was amplified by PCR using primers NheI-FP and BamHI-RP (Table 1). The 2094 bp DNA fragment was digested with *Nhe*I-*Bam*HI and ligated to *Nhe*I-*Bam*HI digested plasmid pDR DNA creating a plasmid pDR.IVa2d3.5a (*containing a substitution of IVa2 amino acid 4-18 from RGRRKVRHQQAQPEA to AAAAAAAAAAAAAAA*).

pDR.IVa2d5. A 1144 bp DNA fragment amplified by PCR using primers SacI FP and RPΔ75C (Table 1), and plasmid pDR.IVa2 DNA as a template was digested with *Sac*I-*Kpn*I and ligated to *Sac*I-*Kpn*I digested plasmid pDR DNA creating plasmid pDR.IVa2d5 (*containing a deletion of IVa2 amino acid 373-448).*

pDR.IVa2d5.1. A 1150 bp DNA fragment (P1) was amplified by PCR using primers XhoI FP and IRP10-75 (Table 1), and plasmid pDR.IVa2 DNA as a template. Similarly, a 327 bp DNA fragment (P2) was amplified by PCR using primers IFP10-75 and MluI RP (Table 1), and plasmid pDR.IVa2 DNA as a template. The P1 and P2 DNA fragments were annealed and a 1437 bp DNA fragment was amplified by PCR using primers XhoI FP and MluI RP (Table 1). The 1437 bp DNA fragment was digested with *Xho*I-*Mlu*I and ligated to *Xho*I-*Mlu*I digested plasmid pDR DNA creating plasmid pDR.IVa2d5.1 (*containing a deletion of IVa2 amino acid 373-438*).

pDR.IVa2d5.2. A 1150 bp DNA fragment (P1) was amplified by PCR using primers *Xho*I FP and IRP20-75 (Table 1), and plasmid pDR.IVa2 DNA as a template. Similarly, a 357 bp DNA fragment (P2) was amplified by PCR using primers IFP20-75 and MluI RP (Table 1), and plasmid pDR-IVa2 DNA as a template. The P1 and P2 DNA fragments were annealed and a 1467 bp DNA fragment was amplified by PCR using primers XhoI FP and Mlu-RP (Table 1). . The 1467 bp DNA fragment was digested with *Xho*I-*Mlu*I and ligated to *Xho*I- *Mlu*I digested plasmid pDR DNA creating plasmid pDR.IVa2d5.2 (*containing a deletion of IVa2 amino acid 373-428*).

pDR.IVa2d5.3. A 1150 bp DNA fragment (P1) was amplified by PCR using primers XhoI FP and IRP30-75 (Table 1), and template and plasmid pDR.IVa2 DNA as a template. Similarly, a 387 bp DNA fragment was (P2) was amplified by PCR using IFP30-75 and MluI RP (Table 1) as primers, and plasmid pDR.IVa2 DNA as a template The P1 and P2 DNA fragments were annealed and a 1497 bp DNA fragment was amplified by PCR , using XhoI FP and MluI RP as primers (Table 1) . The 1497 bp DNA fragment was digested with *Xho*I-*Mlu*I and ligated to *Xho*I- *Mlu*I digested plasmid pDR DNA creating plasmid pDR.IVa2d5.3 (*containing a deletion of IVa2 amino acid 373-418).*

pDR.IVa2d5.4. A 1142 bp DNA fragment (P1) was amplified by PCR using primers XhoI FP and IRP40-75 (Table 1), and plasmid pDR.IVa2 DNA as a template. Similarly, a 417 bp DNA fragment (P2) was amplified by PCR using IFP40-75 and MluI RP (Table 1) as primers, and plasmid pDR-IVa2 DNA as a template. The P1 and P2 DNA fragments were annealed and a 1527 bp DNA fragment was amplified using XhoI FP and MluI RP as primers. The 1527 bp DNA fragment was digested withg *Xho*I-*Mlu*I and ligated to *Xho*I-*Mlu*I digested plasmid pDR DNA creating plasmid pDR.IVa2d5.4 (*containing a deletion of IVa2 amino acid 373-408).*

pDR.IVa2d5.5. A 1150 bp PCR product (P1) was amplified by PCR using primers XhoI FP and IRP53-75 (Table 1), and plasmid pDR.IVa2 DNA as a template. Similarly, a 456 bp DNA fragment (P2) was amplified by PCR using primers IFP53-75 and MluI RP (Table 1), and plasmids pDR.IVa2 DNA as a template. The P1 and P2 DNA fragments were annealed and a 1566 bp DNA fragment was amplified by PCR using XhoI FP and MluI RP as primers (Table 1)(The 1566 bp DNA fragment was digested with and ligated to *Xho*I-*Mlu*I digested plasmid pDR DNA creating plasmid pDR.IVa2d5.4 (*containing a deletion of IVa2 amino acid 373-395).*

pDR.IVa2d5.6. Using plasmid pDR.IVa2.DNA as a template, and primers XhoI FP and RP411-448 (Table 1), a1249 bp DNA fragment amplified by PCR was digested with *Xho*I-

*Bam*HI and ligated *to XhoI-Bam*HI digested plasmid pDR DNA creating plasmid pDR.IVa2d5.6 (*containing a deletion of IVa2 amino acid 411-448).*

Table 1. List of primer

Primer sequence (5'-----3')	Primer name
CGCTCGAGTCAATAAAATTCTTTATTTTTCCTGTGATAATAC	XhoI FP
GACGGTACCATGGACACCCGAGGGCGACGAAAAGTTCGG	KpnI RP
GCGAATTCATGGACACCCGAGGGCGACGAAA	EcorI FP
GCGAATTCATGTCAGCAGCCCTTCACGGTC	EcorIΔN25 FP
GCCTCGAGTCAATAAAATTCTTTATTTTTCCTGTGATAATACCGTGTCCAGCG TGCTCTGTC	XhoI RP
TGGCGGCCGCTCAATAAAATTCTTTATTTTTCCTGTGATAATACC	Not I RP
GCGAGCTCATGGACACCCGAGGGCGACGAAAAG	SacI FP
GCGGTACCTCAATAAAATTCTTTATTTTTCCTGTGATAATAC	KpnI RP2
GCGGTACCCTAAGGGCCTCATATACCATGGCATGAATATTAAGATACATGGG	RPΔ25C
GCGGTACCCTACTGCAGACTTTCGTGGGGAGGTAAGGTGTTG	RPΔ50C
GCGAGCTCATGTCAGCAGCCCTTCACGGTC	FPΔN25
GCGAGCTCATGGATGTACTAGACCACGTCTCTGAG	FPΔN75
GGGCGGCCGCATGGACACCCGAGGGCGACGAAAAG	NotI FP
CGGGGCCCCTCATCAATAAAATTCTTTATTTTTCCTG	ApaI RP
AGGCGGCCG CCGAGGGCGACGAAAAGTTCGGCACCAGCAGGCTCA GCCTGAGGC	NotI 4-18 FP
AAG CCT AGG CCT CCA AAA AAG	AvrII RP
GCGAATTCATGTCAGCAGCCCTTCACGGTC	EcorIΔN25
GGTGGATCCCGGGCCCGCGGTACCTCAATAAAATTC	BamHI RP
CCGCTAGCGCTACCGGTCGCCACCATGGACAA	NheI FP
ATCTCGAGCTCATGGACACCCGAGGGGTTCGGCACCAGCAGGCTCAG	FPΔ6-8
ATCTCGAGCTCATGGACACCGTTCGGCACCAGCAGGCTCAGC	FPΔ 4-8
ATCTCGAGCTCATGGACACCCAGCAGGCTCAGCCTGAG	FPΔ 4-11
ATCTCGAGCTCATGGACACCCCTGAGGCGCTCGCTGGTC	FPΔ 4-15
ATCTCGAGCTCATGGACACCCCTCGCTGGTCAGCAGACAGAC	FPΔ 4-18
GAGCCTGCTGGTGCCGAACTTTTCGTCCCCTAGCTGTTCAGTGGAATAATAACAAG	IFP6M
TATTCCACTGAACAGCTAGGGGACGAAAAGTTCGGCACCAGCAGGCTCA	RP6M
GAGCCTGCTGGTGCCGAACTTTTCCTCGCCTAGCTGTTCAGTGGAATAATAACAAG	IFP7M
TATTCCACTGAACAGCTAGGCGAGGAAAAGTTCGGCACCAGCAGGCTCA	IRP7M
GAGCCTGCTGGTGCCGAACTTCTCGTCGCCTAGCTGTTCAGTGGAATAATAACAAG	IFP8M
TATTCCACTGAACAGCTAGGCGACGAGAAGTTCGGCACCAGCAGGCTCA	IRP8M
GAGCCTGCTGGTGCCGAACTTCTCCTCCCCTAGCTGTTCAGTGGAATAATAACAAG	IFP6-8M
TATTCCACTGAACAGCTAGGGGAGGAGAAGTTCGGCACCAGCAGGCTCA	IFP6-8M
CTCGAGCTCATGGACACCCGAGGGGGACGAAAAGTTCGGCACCAGCAGGCTCAG	FP 6M
CTCGAGCTCATGGACACCCGAGGGCGAGGAAAAGTTCGGCACCAGCAGGCTCAG	FP 7M
CTCGAGCTCATGGACACCCGAGGGCGACGAGAAGTTCGGCACCAGCAGGCTCAGCCTGAG	FP 8M
CTCGAGCTCATGGACACCCAGGGGGGAGGAGAAGTTCGGCACCAGCAGGCTCAGCCTGAG	FP 6-8M
ATCTCGAGCTCATGGACACCCGAGGGGCAGCAGCAGTTCGGCACCAGCAGGCTCAG	FPM6-8
ATCTCGAGCTCATGGACACCGCAGCGGCAGCAGCAGTTCGGCACCAGCAGGCTCAG	FPM4-8
ATCTCGAGCTCATGGACACCGCAGCGGCAGCAGCAGCTGCGGCCCAGCAGGCTCAG CCTGAG	FPM4-11
ATCTCGAGCTCATGGACACCGCAGCGGCAGCAGCAGCTGCGGCCGCGGCGGCTGCG CCTGAGGCGCTCGCTGGTC	FPM4-15
GCAGCGGCCGCCGCAGCTGCCGCAGCCGCAGCTGCCGCTGCGGCGCTCGCTGGTCA GCAGACAGA	IFPM 4-18
CGCCGCAGCGGCAGCTGCGGCTGCGGCAGCTGCGGCGGCCGCTGCGGTGTCCATGA GCTCGAGAT	IRP M4-18
ATCTCGAGCTCATGGACACCCGAGGGCGACGAAAAG	XhoI FP2
GCGGTACCTCAGATGTCTTTTAGAAGAAGGGTGATTGGCAAAGGGAGGCTCTTA	RPΔ75C
TTACGCGTTAAGATACATTGATGAG	MluI RP
CCCTTCTTCTAAAAGACATCTATTATCACAGGAAAAATAAAGAATTTTATT	IFP 10-75
TTATTTTTCCTGTGATAATAGATGTCTTTTAGAAGAAGGGTGATTG	IRP 10-75

CCCTTCTTCTAAAAGACATCACCCTTATTGACAGAGCACGCTGGA	IFP 20-75
CGTGCTCTGTCAATAAGGGTGATGTCTTTTAGAAGAAGGGTGATTGG	IRP 20-75
CCCTTCTTCTAAAAGACATCGTATATGAGGCCCTTCTCAGGATG	IFP 30-75
CTGAGAAGGGCCTCATATACGATGTCTTTTAGAAGAAGGGTGATTGG	IRP 30-75
ATATTAAGATACATGGGCATGATGTCTTTTAGAAGAAGGGTGATTGG	IRP 40-75
CCCTTCTTCTAAAAGACATCATGCCCATGTATCTTAATATTCATGCCATG	IFP 40-75
TCTTCTAAAAGACATCTTTTCCAGTCTGCAGTGGCTCTACCTCAAC	IFP 375-395
TTGAGGTAGAGCCACTGCAGACTGGAAAAGATGTCTTTTAGAAGAAGGGTGATT	IRP 375-395
GTGGATCCGGGCATAAGGCCCTCAGAAGG	RP411-448
TCACCAGCAATAACTTCGTATAATGTATGCTATACGAAGTTATTCAATA AAATTCTTTATTTTTCCTGTGATAA	IFP loxp 448
ATAACTTCGTATAGCATACATTATACGAAGTTATTGCTGGTGACAGCATA ATAAACTGTATGAGTGTATTTTT	IRP loxp 448
GTATAACTTCGTATAATGTATGCTATACGAAGTTATGTCTTTTAGAAGA AGGGTGATTGGCAAAG	IFP loxp373
ATAACTTCGTATAGCATACATTATACGAAGTTATACATCTTTTCC TTCCACGCCCAGCAC	IFP loxp373

Appendix 2

Plasmid Construction

pGN.IVa2. A 1367 bp DNA fragment containing IVa2 coding region was amplified by PCR using primers FP IVa2 and RP IVa2 (Table 2) and plasmid pCIVa2 as DNA template. The 1367 bp DNA fragment was digested with *Sac*I-*Not*I and ligated to SacI and *Not*I plasmid pGN (Levin et al., 2009) DNA creating plasmid pGN-IVa2.

pGC-VII. A 532 bp PCR product containing VII coding region was amplified by PCR using primers FP VII and RP VII (Table 2) and pC-VII (Anand et al., 2014) DNA as a template. The 532 bp DNA fragment was digested with SalI-EcoRI and ligated to SalI-EcoRI plasmid pGC (Levin et al., 2009) DNA creating plasmid pGC- VII.

pGC-VIII. A 664 bp PCR product containing VIII coding region was amplified by PCR using primers FP VIII and RP VIII (Table 2) and pC-VIII (Ayalew et al., 2016) DNA as a template. The 664 bp DNA fragment was digested with SalI-EcoRI and ligated to SalI-EcoRI plasmid pGC DNA creating plasmid pGC-VIII.

pGC-22K. A 841 bp PCR product containing 33K coding region was amplified by PCR using primers FP 22K and RP 22K (Table 2) and pC-22K (Kulshreshtha et al., 2015) DNA as a template. The 841 bp DNA fragment was digested with SalI-SpeI and ligated to SalI-SpeI plasmid pGC DNA creating plasmid pGC-22K.

pGC-52K. A 1145 bp PCR product containing 52K coding region was amplified by PCR using primers FP 52K and RP 52K (Table 2) and pC-52K (Paterson et al., 2012) DNA as a template. The 1145 bp DNA fragment was digested with SacI-EcorI and ligated to SacI-EcorI plasmid pGC DNA creating plasmid pGC-52K.

pGC-Fiber. A 2947 bp PCR product containing Fiber coding region was amplified by PCR using primers FP Fiber, and RP Fiber (Table 2) and pBAV304 (Wu et al., 2004) DNA as a template. The 2947 bp DNA fragment was digested with SalI-SpeI and ligated to SalI-SpeI plasmid pGC DNA creating plasmid pGC-Fiber.

pGC-Hexon. A 2726 bp PCR product containing hexon coding region was amplified by PCR using primers FP hexon and RP hexon (Table 2) and pDR-Hexon (Makadiya et al 2015) DNA as a template. The 2726 bp DNA fragment was digested with SalI-XmaI and ligated to SalI-XmaI plasmid pGC DNA creating plasmid pGC- Hexon.

pGC-DBP. A 1315 bp PCR product containing DBP coding region was amplified by PCR using primers FP DBP and RP DBP (Table 2) and pGADT7-DBP (Kulshreshtha et al., 2008) DNA as a template. The 1315 bp DNA fragment was digested with SalI-SpeI and ligated to SalI-SpeI plasmid pGC DNA creating plasmid pGC-DBP.

pGC-TP. A 1990 bp PCR product containing TP coding region was amplified by PCR using primers FP TP and RP TP (Table 2) and pGADT7-TP (Kulshreshtha et al., 2008) DNA as a

template. The 1990 bp DNA fragment was digested with BglII and EcoRI and ligated to BglII and EcoRI plasmid pGC DNA creating plasmid pGC-TP.

pGC- IIIa. A 1723 bp PCR product containing IIIa coding region was amplified by PCR using primers FP IIIa and RP IIIa (Table 2) and pGADT7-IIIa (Kulshreshtha et al., 2008) DNA as a template. The 1723 bp DNA fragment was digested with SalI-SpeI and ligated to SalI-SpeI plasmid pGC DNA creating plasmid pGC- IIIa.

pGC-X. A 259 bp PCR product containing X (mu) coding region was amplified by PCR using primers FP X and RP X (Table 2) and pGADT7-X (Kulshreshtha et al., 2008) DNA as a template. The 259 bp DNA fragment was digested with SalI-SpeI and ligated to SalI-SpeI plasmid pGC DNA creating plasmid pGC-X.

pGC-Protease. A 631 bp PCR product containing protease coding region was amplified by PCR using primers FP protease and RP protease (Table 2) and pDR.bProt (Makadiya et al., 2015) DNA as a template. The 631 bp DNA fragment was digested with SalI-SpeI and ligated to SalI-SpeI plasmid pGC DNA creating plasmid pGC-Protease.

pGC-33K. A 856 bp PCR product containing 33K coding region was amplified by PCR using primers FP 33K and RP 33K (Table 2) and pC-33K (Kulshreshtha et al., 2015) DNA as a template. The 856 bp DNA fragment was digested with SalI-SpeI and ligated to SalI-SpeI plasmid pGC DNA creating plasmid pGC- 33K.

pGN.IVa2 d6 (Δ151-300). A 480 bp PCR product (P1) amplified using primers SacI FP and IRPM150 (Table 2), and pGN-IVa2 DNA as a template. Similarly, 483 bp PCR product (P2) amplified using primers IFPM150 and NotI RP (Table 2), and pGN-IVa2 DNA as a template. A 913 bp final PCR product (P3) amplified using, primers SacI FP and NotI RP (Table 2) and P1 and P2 DNA mix as a template. The 913 bp bp DNA fragment was digested with SacI-NotI digested and ligated in to SacI-NotI digested pGN creating plasmid pGN-IVa2 d6 (Δ151-300).

pGN.IVa2 d7 (151-448). A 918 bp PCR product (P1) amplified using primers FP ST and NotI RP (Table 2), and pGN-IVa2 DNA as a template. The 918 bp DNA fragment was digested with SacI-NotI and ligated in to SacI-NotI pGN creating plasmid pGN-IVa2 d7 (151-448).

pGN.IVa2d8 (1-150). A 468 bp PCR product amplified using primers SacI FP and RPF150 (Table 2), and pGN-IVa2 DNA as a template. The 468 bp DNA fragment was digested with SacI-NotI and ligated in to SacI-NotI pGN creating pGN. IVa2d8 (1-150).

pGN.IVa2d9 (Δ121-140). A 388 bp PCR product (P1) amplified using primers SacI FP and IRP121-140 (Table 2) and pGN-IVa2 DNA as a template. Likewise, a 957 bp PCR product (P2) amplified using primers IFP121-140 and NotI RP (Table 2) and pGN-IVa2 DNA as a template. A 1305 bp PCR product (P3) amplified using primers SacI FP and NotI RP (Table 2) and The 1305 bp DNA fragment was digested with SacI-NotI and ligated in to SacI-NotI pGN creating plasmid pGN.IVa2d9 (Δ 121-140).

pGN-IVa2d9.1 (Δ 121-130). A 388 bp PCR product (P1) amplified using primers SacI FP and IRP121-130 (Table 2) and pGN-IVa2 DNA as template. Likewise, a 987 bp PCR product (P2) amplified using primers IFP121-130 and NotI RP (Table 2) and pGN-IVa2 DNA as template. A 1335 bp PCR product (P3) amplified using primers SacI FP and NotI RP (Table 2), and P1 and P2 DNA mix as a template. The 1335 bp DNA fragment was digested with SacI-NotI and ligated in to SacI-NotI pGN creating plasmid pGN-IVa2d9.1 (Δ 121-130).

pGN-IVa2d9.2 (Δ 131-140). A 418 bp PCR product (P1) amplified using primers SacI FP and IRP131-140 (table) and pGN-IVa2 DNA as template. Likewise, a 957 bp PCR product (P2) amplified using primers IFP121-140 and NotI RP (table) and pGN-IVa2 DNA as template. A 1335 bp PCR product (P3) amplified using primers SacI FP and NotI RP (table), and P1 and P2 DNA mix as a template. The 1335 bp DNA fragment was digested with SacI-NotI and ligated in to SacI-NotI pGN DNA creating plasmid pGN-IVa2d9.2 (Δ 131-140).

pGN-IVa2d9.3 (Δ d1.d2). A 398 bp PCR product (P1) amplified using primers SacI FP and IRP121-125 (Table 2) and pGN-IVa2 DNA as template. Likewise, 967 bp PCR product (P2) amplified using primers IFP136-140 and NotI RP (Table 2) and pGN-IVa2 DNA as template. 1335 bp PCR product (P3) amplified using primers SacI FP and NotI RP (Table 2) and P1 and P2 DNA mix as a template. The 1335 bp DNA fragment was digested with SacI-NotI and ligated in to SacI-NotI pGN DNA creating plasmid pGN-IVa2d9.2 (Δ 121-125, 136-140).

Table 2. List of primers

Primer sequence (5'-----3')	Primer name
GCGCATGCTAAAATCAAGCTGCTG	SphI FP
GTCCGCGGCTGGAGAGTC	SacII RP
ATATCTGCGCCCTGACGGTCATGATAAATTCCCCAAATGCACAGGCTACTCTGTTTTTGTG	IFPM150
GCATTTGGGGAATTTATCATGACCGTCAGGGCGCAGATATGGCATGG	IRPM150
GGGCGGCCGCTCAGTCAGGGCGCAGATATGGCATGGTG	RPF150
GCGAGCTCATGGGTTCATGCAAATCTTTAAACTTTACC	FP ST
TGGACGAGCTACTGGCTATGGAATGCCACCATGCCATATC	121-140 IFP
GATATGGCATGGTGGCATTCCATAGCCAGTAGCTCGTCCAA	121-140IRP
TGGACGAGCTACTGGCTATGGACTATAATCAGGCGATAAGAGATG	121-130IFP
CTTATCGCCTGATTATAGTCCATAGCCAGTAGCTCGTCCAA	121-130IRP
CCCTACTCAATGCCCTCTCAAATGCCACCATGCCATATCTG	131-140IFP
AGATATGGCATGGTGGCATTTGAGAGGGCATTGAGTAGGG	131-140IRP
CTCAATGCCCTCTCAGACTATAATCAGGCGAATGCCACCATGCCATATCT	IFP121-125, 136-140
CGCCTGATTATAGTCTGAGAGGGCATTGAGCATAGCCAGTAGCTCGTCCAA	IRP121-125, 136-140
GCGAGCTCATGGACACCCGAGGGCGACGAAAAGTT	FP IVa2
GAGCGGCCGCGGGCCCGCGGTACCTCAATAAAATTCTTTATTTTTCC	RP IVA2
GTGTCGACATGAATCGCAGCGGTGACTT	FP DBP
TCACTAGTTTAAAACAAAGAGTCATCTGCATCGTACTGATC	RP DBP
GTGTCGACATGGCCATTCTAATCTCTCC	FP PVII
CTGAATTCTCAAACGGTGTTGCTGAC	RP PVII
ACCCCGGGATGAGCAAAGAAATTCCCACAC	FP PVIII
CTGAATTCCTATAACCGCTCACAGAGTTGCTG	RP PVIII
GTGTCGACATGAAACCCCGCAGCATGTC	FP 22K
TCACTAGTCTATTTTTCACTTTGAGGTGACACCGCTGAGC	RP 22K
TCACTAGTTTAGGCGGGTCCGGATTCGT	RP 33K
GTGTCGACCCCGGGGACCAGTGAGCTCATGCATCCCGCTTTACGGCAAAT	FP 52K
CTGAATTCTCATTCGTCGACTTCATCGT	RP 52K
GTGTCGACATGAGTGATGCGGACCCC	FP IIIa
TCACTAGTTTACCAAAACTGGCGGGGACCC	RP IIIa
GTGTCGACATGAGTCCCCGCGGAAATCT	FP X
TCACTAGTCTATTTGTTGTGGGCCGCCTGA	RP X
GTGTCGACATGGGTTCTCGGGAAGAGG	FP protease
TCACTAGTCTAATTTGTTAACATTTTATCAAAGGCGGTGTCAG	RP protease
GTGTCGACATGAAGAGAAGTGTGCCCCAGGAC	FP Fiber
TCACTAGTTTAAGTCCAGTAAGAAAAAGTAAGTGTAGAG	RP Fiber
GTGTCGACATGGTCCTACTGCACATC	FP Hexon
GATCCCGGGTTATGTGGTAGCGTTGCC	RP Hexon
CCCCGGGGACTAGCGAGCTCTCTAGAAGATCTATGTTTTTTGCAGAGCGCGAGAG	FP TP
CTGAATTCTTAAAGGGGACGTCGAGGG	RP TP
GCATGAACCGTCAGGGCGCAGCTTCTCGAATTGTGGGTGTGACCAATATGGC ATGGTGGCATTCATGG	IFP 146
GAATGCCACCATGCCATATTGGTCACACCCACAATTCGAGAAGCTGC GCCCTGACGGTTCAT	IRP146
TCATACAGTTTATTATGCTGCCTGCAGGCTAGTACATCTC CATCCAGCAT	IFPΔIVa2
GCTGGATGGAGATGTACTAGCCTGCAGGCAGCATAA TAAACTGTATGA	IRPΔIVa2
CATGATCTTTTCGAACTGCGGGTGGCTCCACTTAAAGGCAGGTT TTAGGGTGCTGCTTTG	IRP242
TTTAAGTGGAGCCACCCGCAGTTCGAAAAGATCATGTCCTATGA AGACCTGACCATGGACTAC	IRP242
CTGTCACTTTTCGAACTGCGGGTGGCTCCAATAAAATTCTTTATTTT TCCTGTGATAATAC	IFP448
TTTTATTGGAGCCACCCGCAGTTCGAAAAGGACAG CATAATAAACTGTATGAG	IRP448

Appendix 3

Table 3. List of Primers

Primer Sequence	Name of Primer
GCGCATGCTAAAATCAAGCTGCTG	SphI FP
GTCCGCGGCTGGAGAGTC	SacII RP
CCAGCGAGCGCCTCAGGCTGAGCCTACTGGTGCCGAACTTTTCGTCGCCTAGC	IFPSTC
CTAGGCGACGAAAAGTTCGGCACCAGTAGGCTCAGCCTGAGGCGCTCGCTG	IRP STC
TCACCAGCAATAACTTCGTATAATGTATGCTATACGAAGTTATTCAATAAAATT CTTTATTTTTCCTGTGATAA	IFP loxp 448
ATAACTTCGTATAGCATACATTATACGAAGTTATTGCTGGTGACAGCATA ATAAACTGTATGAGTGTATTTTT	IRP loxp 448
ATAACTTCGTATAATGTATGCTATACGAAGTTATGTCTAGTACATCTCCA TCCAGCATAGC	IFP loxp 79
ACATAACTTCGTATAGCATACATTATACGAAGTTATACCACGTCTCT GAGCTTTGG	RP loxp 79
TCATACAGTTTATTATGCTGCCTGCAGGCTAGTACATCTCCATCCAGCAT	IFPΔIVa2
GCTGGATGGAGATGTACTAGCCTGCAGGCAGCATAATAAACTGTATGA	IRPΔIVa2